DEPARTMENT OF CHEMISTRY, UNIVERSITY OF JYVÄSKYLÄ
RESEARCH REPORT No. 210

SYNTHETIC STUDIES ON 1-AZABICYCLO[5.3.0]DECANE ALKALOIDS

BY

JUHA SIITONEN

Academic Dissertation for the Degree of
Doctor of Philosophy

To be presented, by permission of the Faculty of Mathematics and Science of the University of Jyväskylä, for public examination in Auditorium Kem4, on October 4th, 2018 at 12 noon.

UNIVERSITY OF JYVÄSKYLÄ

Jyväskylä, Finland
ISBN 978-951-39-7550-0 (print)
ISBN 978-951-39-7551-7 (electronic)
ISSN 0357-346X

ABSTRACT

Siitonen, Juha
Synthetic Studies on 1-Azabicyclo[5.3.0]decane Alkaloids
Jyväskylä: University of Jyväskylä, 2018, 143 p.
Department of Chemistry, University of Jyväskylä Research Report Series
ISSN 0357-346X
ISBN 978-951-39-7550-0 (print) 978-951-39-7551-7 (electronic)

The first chapter introduces the reader to the concept of natural product total synthesis and its importance to chemistry, other sciences, and society.

The second chapter reviews the chemistry of natural products containing 1-azabicyclo[5.3.0]decane motifs. This bicyclic motif and the natural products related to it, have been a continuous source of synthetic inspiration over the last decades. The second chapter of the thesis reviews the strategies and tactics developed.

The third chapter covers the author's total synthesis of stemoamide, a 1-azabicyclo[5.3.0]decane motif containing alkaloid. Additionally, two diastereomers of stemoamide were synthesized, allowing their structural reassignment. Tentative studies towards a divergent route to other stemona alkaloids from a key precursor were also carried out.

The fourth chapter targets another 1-azabicyclo[5.3.0]decane alkaloid, cephalotaxine. These are the results of a four-month exchange to the group of Prof. Peter Somfai at Lund University. After various challenges, a short and facile formal total synthesis relying on a cascade cyclization was developed.

The fifth chapter briefly restates the main conclusions of chapters two, three and four, and contemplates on the future of the field.

Chapters six and seven contain experimental and computational details, respectively.

Keywords: total synthesis, natural products, alkaloids, stemona, cephalotaxus

Author's address

Juha Siitonen
Department of Chemistry
P.O. Box 35
FI-40014 University of Jyväskylä
Finland
juha.h.siitonen@jyu.fi

Supervisor

Prof. Petri Pihko
Department of Chemistry
P.O. Box 35
FI-40014 University of Jyväskylä
Finland

Reviewers

Prof. Edgars Suna
Latvian Institute of Organic Synthesis
Aizkraukles 21
LV-1006, Riga
Latvia

Prof. Trond Vidar Hansen
Department of Pharmaceutical Chemistry
University of Oslo
Sem Sælands vei 3
Famarsibygningen
0371, Oslo
Norway

Opponent

Prof. Anette Bayer
Department of Chemistry
University of Tromsø - The Arctic University of Norway
N-9037, Tromsø
Norway

ACKNOWLEDGEMENTS

The research reported in chapter three was carried out at the Department of Chemistry, University of Jyväskylä, Finland, during 9/2014–5/2018. The research reported in chapter four was carried out at Lund University, Sweden, during 5/2017–9/2017.

Financial support from the Academy of Finland, Wihuri foundation, Alfred Kordelin foundation (Komppa trust), and the University of Jyväskylä is gratefully acknowledged.

Many thanks, in no particular order, to all the people involved: family, friends, mentors (Prof. Petri Pihko and Prof. Peter Somfai) and co-workers. You have kept me afloat. Kiitos.

Jyväskylä, September 7th, 2018
Juha Siitonen

AUTHOR CONTRIBUTIONS

For research described in chapter three, the author has planned the synthesis routes, as well as designed and carried out all experiments. Single crystal X-ray structures were measured and solved by M.Sc. Sami Kortet. The computational work was done by the author with helpful insights from M.Sc. Roman Gritcenko and Dr. Akseli Mansikkamäki.

For research described in chapter four, the author co-planned the synthesis routes with Prof. Peter Somfai, and designed and carried out all the experiments, excluding those mentioned below. Synthesis of **4.009** and **4.019** was established by M.Sc. Giovanni Di Gregorio. Final screening experiments for conversion of **4.032** → **4.010**, including the sodium methoxide modification were made by Dr. Jakob Danielsson. Completion of the racemic synthesis of **4.010** and er determination, as well as the sodium methoxide control experiment, were carried out by M.Sc. Lu Yu.

ACRONYMS, ABBREVIATIONS, SYMBOLS, AND DEFINITIONS

[H]	hydrogenation, reduction
[O]	oxidation
°	degree
μW	microwave
4-NBA	4-nitrobenzoic acid
AB	strongly coupled two-spin-½ system
ABCN	1,1'-diazene-1,2-diyldicyclohexanecarbonitrile
Ac	acetyl
ACN	acetonitrile
AIBN	2,2′-azobis(2-methylpropionitrile)
All	allyl
Alpine borane	9-(2,6,6-trimethylbicyclo[3.1.1]hept-3-yl)-9-bora-bicyclo[3.3.1]nonane
anti	alignment of two substituents on the opposite sides/faces of a molecule
app.	apparent
BINOL	[1,1'-binaphthalene]-2,2'-diol
Bn	benzyl
Boc	*tert*-butoxycarbonyl
BSSE	basis set superposition error
Bu	butyl
Bz	benzoyl
cal	calorie, 4.184 joules
calcd.	calculated
Cbz	carboxybenzyl
CC-PD	creative commons - public domain
CMD	cyclohexyl-3-(2-morpholinoethyl)-carbodiimide methoxy-*p*-toluenesulfonate
CSA	chlorosulfonic acid
d	doublet
Da	Dalton, unit of mass equal to the unified atomic mass unit
dba	dibenzalacetone, (1*E*,4*E*)-1,5-diphenylpenta-1,4-dien-3-one
DBU	1,8-diazabicyclo[5.4.0]undec-7-ene
DCE	1,2-dichloroethane
DCM	dichloromethane

DEAD	diethyl azodicarboxylate
DFT	density functional theory
DIAD	diisopropyl azodicarboxylate
DIBAL-H	diisobutylaluminium hydride
DIPEA	*N*,*N*-diisopropylethylamine, Hüning's base
Disamyl borane	bis(1,2-dimethylpropyl)borane
DMAP	4-dimethylaminopyridine
DMDO	3,3-dimethyldioxirane, Murray's reagent
DME	1,2-dimethoxyethane, glyme
DMP	Dess–Martin periodinane, 1,1,1-triacetoxy-1,1-dihydro-1,2-benziodoxol-3(1*H*)-one
DMPU	*N*,*N*′-dimethylpropyleneurea
DMSO	dimethyl sulfoxide
dppf	1,1′-ferrocenediyl-bis(diphenylphosphine)
dr	diastereomeric ratio
DTBMP	benzyloxy carbamate
E	stereodescriptor for alkenes, groups of highest CIP priority lie on the same side of a reference plane
EDC	1-ethyl-3-(3-dimethylaminopropyl)carbodiimide
ee	enantiomeric excess
endo	oriented away from the highest numbered bridge in a bicyclo[x.y.z]alkane
epi	diastereomer having opposite configuration at only one stereogenic center
equiv.	molar equivalent
er	enantiomeric ratio
ESI	electronspray ionization
Et	ethyl
exo	oriented towards the highest numbered bridge in a bicyclo[x.y.z]alkane
FTIR	Fourier transformed infrared spectroscopy
GC	gas chromatography
gCP	geometrical counterpoise correction
HFIP	hexafluoroisopropanol
HMBC	heteronuclear multiple bond coherence
HMPA	hexamethylphosphoramide
HMQC	heteronuclear multiple-quantum coherence
HOBt	hydroxybenzotriazole
Hoveyda-Grubbs	dichloro[1,3-bis(2,4,6-trimethylphenyl)-2-

2nd generation catalyst	imidazolidinylidene](2-isopropoxyphenylmethylene) ruthenium(II)
HPLC	high-performance liquid chromatography
HRMS	high-resolution mass spectrometry
HSQC	heteronuclear single quantum coherence
i-	iso
IBX	2-iodoxybenzoic acid
in vacuo	under reduced pressure
IRC	intrinsic reaction coordinate
Isatonic anhydride	3,1-benzoxazine-2,4(1*H*)-dione
J	coupling constant
Jones reagent	oxidant, solution of chromium trioxide in aqueous sulfuric acid
Lawesson reagent	thiation reagent, 2,4-bis(4-methoxyphenyl)-2,4-dithioxo-1,3,2,4-dithiadiphosphetane
LC	liquid chromatography
LDA	lithium diisopropylamide
LiHMDS	litrium bis(trimethylsilyl)amide
LRMS	low-resolution mass spectrometry
L-Selectride	lithium tri-*sec*-butylborohydride
m	multiplet
M	molarity, $mol \cdot l^{-1}$
m/z	mass-to-charge ratio
Me	methyl
MEM	2-methoxyethoxymethyl
Mesityl	1,3,5-trimethylphenyl
MM	molecular mechanics
MP	melting point
MS	molecular sieves
n-	"normal", linear chain
NaHMDS	sodium bis(trimethylsilyl) amide
NMM	*N*-methylmorpholine
NMO	*N*-methylmorpholine *N*-oxide
NMR	nuclear magnetic resonance spectroscopy
nOe	nuclear Overhauser effect
NOESY	nuclear Overhauser effect spectroscopy
Ohira-Bestmann reagent	dimethyl (1-diazo-2-oxopropyl)phosphonate

p.a.	puriss analysis
Ph	phenyl
Piv	pivalyl, trimethylacetyl
ppm	parts-per-million
Pr	propyl
rac	racemic
RCM	ring closing metathesis
R_f	retardation factor
rt	room temperature
s	singlet
syn	alignment of two substitutens on the same sides/faces of a molecule
t	triplet
t-	tert
TBAF	*tert*-butylammonium fluoride
TBDPS	*tert*-butyldiphenylsilyl
TBS	*tert*-butyldimethylsilyl
tet	tetragonal
Tf	triflate
TFA	trifluoroacetic acid
TFAA	trifluoroacetic acid anhydride
THF	tetrahydrofuran
TIPS	triisopropylsilyl
TLC	thin-layer chromatography
TMEDA	tetramethyletyhlenediamine
TMS	trimethylsilyl
t_R	retention time
trig	trigonal
Ts	tosyl
UV	ultraviolet
Wilkinson's catalyst	chloridotris(triphenylphosphane)rhodium(I)
Xphos	2-dicyclohexylphosphino-2′,4′,6′-triisopropylbiphenyl
Z	stereodescriptor for alkenes, groups of highest CIP priority lie on the opposite side of a reference plane.
Zhan catalyst	dichloro(1,3-bis(2,4,6-trimethylphenyl)-2-imidazolidinylidene)((5-((dimethylamino)sulfonyl)-2-(1-methylethoxy-O)phenyl)methylene-C)ruthenium(II)
Å	Ångström, 10^{-10} m

CONTENTS

1 INTRODUCTION TO NATURAL PRODUCT TOTAL SYNTHESIS

"One must from time to time attempt things that are beyond one's capacity"

– Pierre-Auguste Renoir

Tens of thousands of natural products have been isolated from a diverse set of organisms including bacteria, marine sponges, fungi, and plants.[1] Many of these natural products have also been synthesized in the laboratory. This effort, the synthesis of naturally occurring molecules in the laboratory from simpler starting materials, is known as total synthesis. The field has two main standpoints. First, to see synthesis as an enabling technology and, second, as a framework to ask questions about the nature of molecules and their behavior.[2,3]

As a framework for asking questions, total synthesis of natural products enables us to probe fundamental (bio)chemical questions, helping advance our understanding of the natural world. To properly study compounds only isolatable in miniscule amounts, we have to synthesize them. Such has been the case for many natural products such as inflammatory hormones prostaglandins, avermectin pesticides, the "last-line-of-defence" antibiotic vancomycin, the chemotherapy agent paclitaxel, the erythromycin antibiotics, and many steroids such as estrogen which led to oral contraceptives.[4] In cases where structural elucidation is uncertain, total synthesis can also be a useful tool.[5]

As an enabling technology, total synthesis efforts have had a major impact on fields of chemistry relying on preparation of new molecules. One of the major fields being benefited by total synthesis is the medicinal industry. Of the 1562 new drugs discovered and launched between 1981 and 2014, 4% are natural products, 21% modified natural products, and 25% mimic natural products in some way. Half of all drugs are related to natural products and our ability to synthesize them.[6] Total synthesis efforts are also a question of pragmatism: analogues of natural products for testing are not available directly from Nature, and very rarely does isolation provide access to multi-gram quantities of the compounds of interest. The demands for scalability and for diversity forces syn-

thesis to be practical. To tackle this challenge, chemists need to be trained to construct complex molecules. In achieving the above-mentioned goals, natural product total synthesis still remains as a major contributor.

In the past, as only a handful of reactions were at chemists' disposal, total synthesis efforts were labor intensive, and in many cases, wasteful. Since mid-1990s the field's focus has changed to how good the synthesis route to the target molecule is. The seemingly objective "goodness" of a synthetic route is typically measured by the route's conicity (convergency) and efficiency. A route with lower step-count, high yields and less waste is considered superior.[7]

Total synthesis has, throughout its history, led to discovery of new synthetic methods. Methods originally developed to streamline natural product syntheses have since proven useful in other areas of chemistry as well. Also, our understanding of reactivity and physical chemistry is strengthened by natural product synthesis. The list of fundamental discoveries fueled by total synthesis is near-endless but to mention a few: the concept of "life-force" was disproven with the total synthesis of urea by Wöhler, leaps of progress in stereochemistry were made by Fischer's sugar syntheses, introduction of curved arrows by Sir Robert Robinson, introduction of conformational analysis by Barton, development of retrosynthesis by Corey, and the introduction of the Woodward–Hoffmann rules as an application of molecular orbital theory.[4]

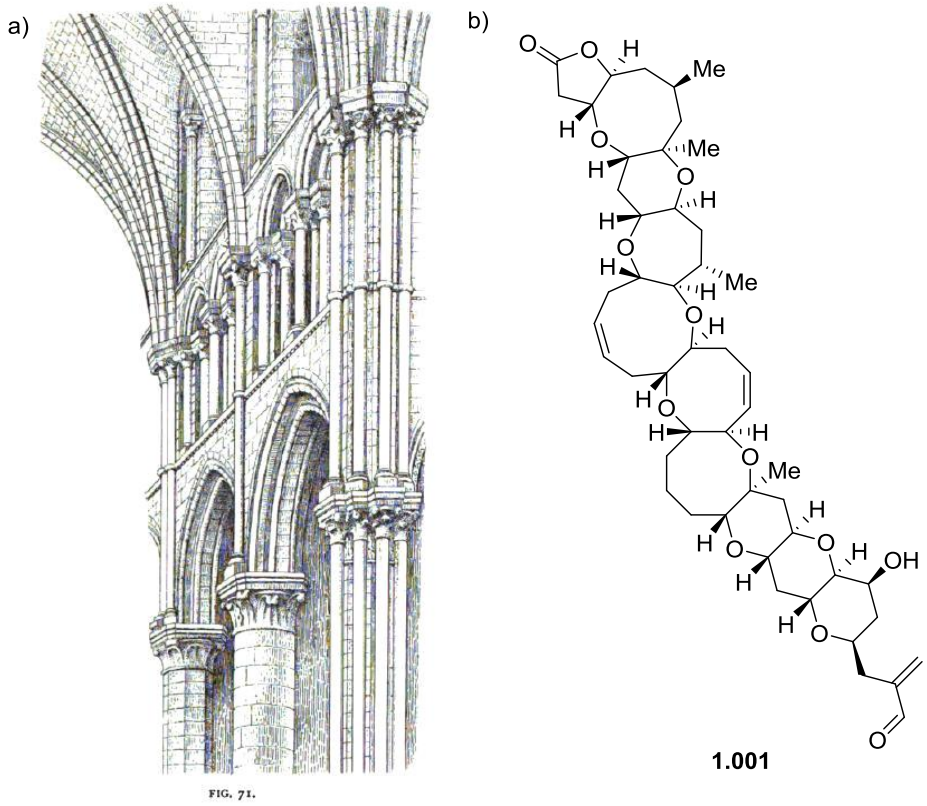

Figure 1: Total synthesis can be compared to other creative human endeavors, such as architecture a) Interior detail of the Canterbury cathedral (CC-PD) b) Complex marine polyketide Brevetoxin A-1 (**1.001**).

Many natural products have three-dimensional structures which can contain a multitude of diverse functional groups and stereogenic centers densely packed together (Figure 1b). Figuring out how such complex structure could be synthesized means mentally disassembling the target molecule, step-by-step, into smaller units until known molecules are reached. The disassembly, or retrosynthetic analysis, reveals the shortcomings of existing synthetic methods, as often no reaction corresponding to a desired disconnection is available. Creativity is needed to work around such problems, and not surprisingly, synthesis has been compared to other creative human endeavors (Figure 1a).[8,9] It is this creativity that captures the imagination of a synthetic chemist and leads to extraordinary and elegant solutions when planning a synthesis.

Planning leads, almost inevitably, to several feasible routes of making a natural product target. Some routes may be riskier and more challenging than others, making it unsure if the target can ever be reached (Figure 2). On the other hand, playing it too safe will not lead to new discoveries, as only well-established chemical steps are being taken. After choosing a well-balanced route, the work in the laboratory begins.

The disassembly plan is now being traversed in the reverse direction, starting from the simplest materials and building up to the target. Using previous literature and chemical intuition as guides for reaction conditions, commercially available materials are converted into more advanced molecules, which are again used as starting materials in further reactions.

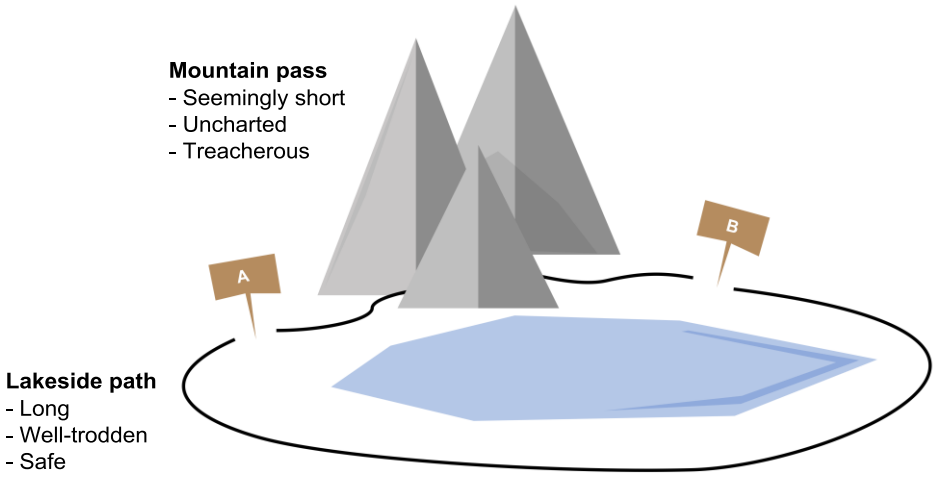

Figure 2: There are many ways to get from **A** to **B**. Choosing a synthesis route is fine a balance between risk and safety. Routes with great risk, analogous to the mountain pass, can lead to new discoveries or great difficulties. On the other hand, traversing known paths such as the lakeside track, are likely to work but with little new to discover.

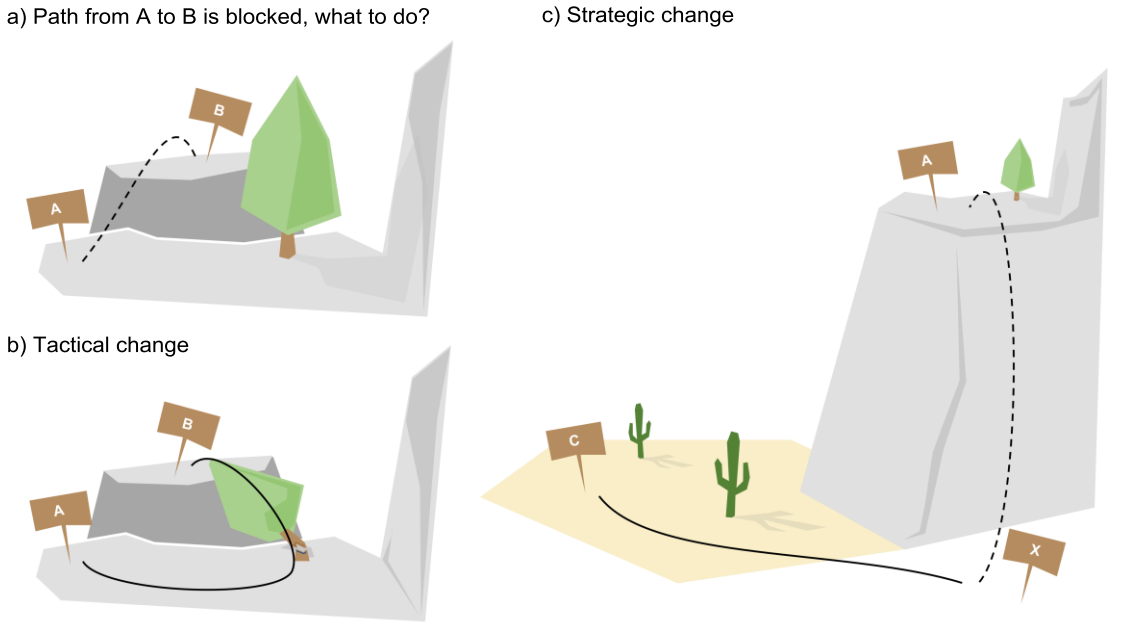

Figure 3: a) Taking the mountain pass has led us to what seems like a dead-end. Designed route taking a step from **A** to **B** is blocked by a ravine. b) Tactical change alters the way point **B** is reached without changing the overall course of the synthesis. This is analogous to chopping down a suitably placed tree to be used as a bridge from **A** to **B** over the ravine. c) Strategic change has us dispatching the **A** to **B** route entirely, backtracking to a previous point **X**, and attempt taking another path. This changes the key intermediates of the synthetic route, analogous to crossing a dessert from **X** to **C** instead of following the originally planned mountaintop route of **X** to **A** to **B**.

In the laboratory, total synthesis projects can be divided into two major efforts. The first effort is the supply chain: preparing large amounts of starting materials using already established, be it from literature or established by experimentation, steps. The second major effort is at the end of the supply chain. As the synthesis progresses, the molecule at hand gets incrementally more complex step by step. Literature methods are no longer available for such complex molecules and experimentation is needed. At this stage, at the forefront of the synthetic exploration, the next steps of the plan are being tested in small-scale with the advanced intermediates. These experiments reveal which reactions could work and which synthetic direction should be followed. In the best scenario, the exploratory stage for a given reaction requires only several reiterations to optimize for yield and selectivity, allowing the reaction be moved to the end of the supply chain. However, a campaign to get a specific reaction to work can take anything from hours up to years. In the worst-case scenario, the reaction does not work in the desired way. It is not at all uncommon for a seemingly well-established reaction to malfunction or stall, when used in the setting of complex-molecule synthesis.[10,11]

Because of the uncertainties associated with the synthesis of any complex molecule, the chosen route cannot be static, and has to be subject to change. If a given synthetic approach does not work, changes are made to the plan accord-

ingly. Generally, this means that unexpected reactivity, or the complete lack of reactivity, will force the chemist to modify the route (Figure 3). If problems are faced in the late stages of the synthesis, only a minor tactical change is typically attempted to resolve the issue. Tactical changes do not change the main strategy of the synthesis, as the same key intermediate molecules are still being used. Tactical changes only alter the way in which these intermediates are reached.

If unacceptable problems arise already at early stages, the entire synthetic strategy needs to be re-evaluated. The synthesis route can also be modified for other reasons. Sometimes unexpected yet beneficial reactivity of an intermediate molecule can lead to new discoveries. Typically, these reactions could not have been easily foreseen at the planning stage. Such discoveries can then be used as waypoints in planning a new, more efficient route. The redesign of a route can lead to either shortcuts or *cul-de-sacs*, as will become evident in chapter 2.

2 STRATEGIES AND TACTICS FOR SYNTHESIS OF 1-AZABICYCLO[5.3.0]DECANE ALKALOIDS

"Every picture shows a spot with which the artist has fallen in love"

– Alfred Sisley

2.1 Seven-membered rings in Nature

Organisms use primary metabolites such as carbohydrates, proteins, fats and nucleic acids to live, grow and reproduce. In addition to primary metabolites, a wide range of species specific compounds, called secondary metabolites, are produced by organisms for a variety of uses, e.g. as toxins to protect the organism or as coloring agents to lure in prey.[12] Structurally, both primary and secondary metabolites contain five- and six-membered rings. However, compared to the hundreds of secondary metabolites with seven-membered rings, primary metabolites with seven-membered rings are practically nonexistent. Why does the nature allow greater diversity in the form of seven-membered rings in secondary metabolism?

Five-, six-, and seven-membered rings are almost equal in their thermodynamic stability. Enthalpies of combustion per CH_2 unit for cyclopentane, cyclohexane and cycloheptane are 158.7 kcal/mol, 157.4 kcal/mol, and 158.3 kcal/mol, respectively, with cyclohexane being essentially strain-free.[13] Even though similar in their strain energy, the cyclization rates for five-, six-, and seven-membered rings are entirely different. The relative rate at which five- and six-membered saturated nitrogenous heterocycles are formed from corresponding bromoamines are 10 000 and 100 times faster, respectively, compared to a corresponding seven-membered azepane.[13] The rate difference between five-, six- and seven-membered rings is mainly imposed by entropic factors: ratio of ring-forming microstates to all microstates is higher for five- and six- membered acyclic precursors. It can be argued, the rate at which five- and six-membered

rings form, compared to seven-membered rings, is a contributor to their marked dominance in both primary and secondary metabolites. Additionally, aromatic six- and five-membered rings are prevalent in the nature. Stabilization of seven-membered rings by aromatization is only possible for fairly exotic species, such as the tropylium cation.

In spite of the differences, seven-membered rings are still markedly present in secondary metabolites. Secondary metabolites are needed and produced in significantly lesser quantities than primary ones. As a result, the biosynthetic routes leading to these compounds are less restricted in terms of efficiency. The lack of restriction gives nature's evolutionary processes more freedom to experiment. The experimentation opens up chemical spaces beyond the easy-to-form five- and six-membered ring units, and seven-membered units come into play. Seven-membered rings are especially pronounced in alkaloids, secondary metabolites containing nitrogen, typically as a part of a heterocyclic system.[i,14]

In very rough terms, seven-membered rings in alkaloids are generated from nitrogen-containing amino acid fragments, such as spermines, pyrrolines and pyrrolinium ions.[15] These nitrogenous fragments are biosynthetically extended with (a)cyclic chains, typically derived from other biosynthetic pathways. The extended chains oxidize, and collapse onto nitrogen. The sheer number of possible cyclizing combinations, and concomitant formation of seven-membered rings embedded into polycyclic systems, has led to a wealth of secondary metabolites with seven-membered rings. Their complex structures and intriguing biological activities have, in turn, been a continuous source of inspiration for synthetic chemists.

2.2 Introduction to 1-azabicyclo[5.3.0]decane alkaloids

The thesis focuses on the total synthesis efforts of a subset of 7-membered ring containing alkaloids. This subset of interest has the core motif **2.001**. The core **2.001** consists of a fused 7- and a 5-membered rings and has a tertiary bridgehead nitrogen (Figure 1a). With systematic naming used for bridged compounds, the motif **2.001** can be called 1-azabicyclo[5.3.0]decane.

In total, 638 alkaloids containing the 1-azabicyclo[5.3.0]decane core structure **2.001** are found in the Reaxys® natural product database.[ii] Some of these alkaloids, such as stemoamide (**2.002**), cephalotaxine (**2.003**), and poison dart frog alkaloid 275A (**2.004**) (Figure 1b), have an easily recognizable 7/5 fused ring system as highlighted in grey.[16–18] In other alkaloids, several C–C disconnections are needed to reveal the underlying 7/5 ring system. Examples include

[i] IUPAC definition for alkaloids: Basic nitrogen containing compounds (mostly heterocyclic) occurring mostly in the plant kingdom (but not excluding those of animal origin). Amino acids, peptides, proteins, nucleotides, nucleic acids, amino sugars and antibiotics are not normally regarded as alkaloids. By extension, certain neutral compounds biogenetically related to basic alkaloids are related.[14]

[ii] Search conducted on 25.5.2018 for natural products with **2.001** as the substructure

the alkaloids norsecurine (**2.005**), nominine (**2.006**), and lundurine C (**2.007**) (Figure 1c).[19–21]

Synthetic routes to these alkaloids are as varied in shape and form as the alkaloids themselves. The following subchapters discuss the strategies and tactics developed and utilized in syntheses of such 7/5 azabicyclic 1-azabicyclo[5.3.0]decane alkaloids.

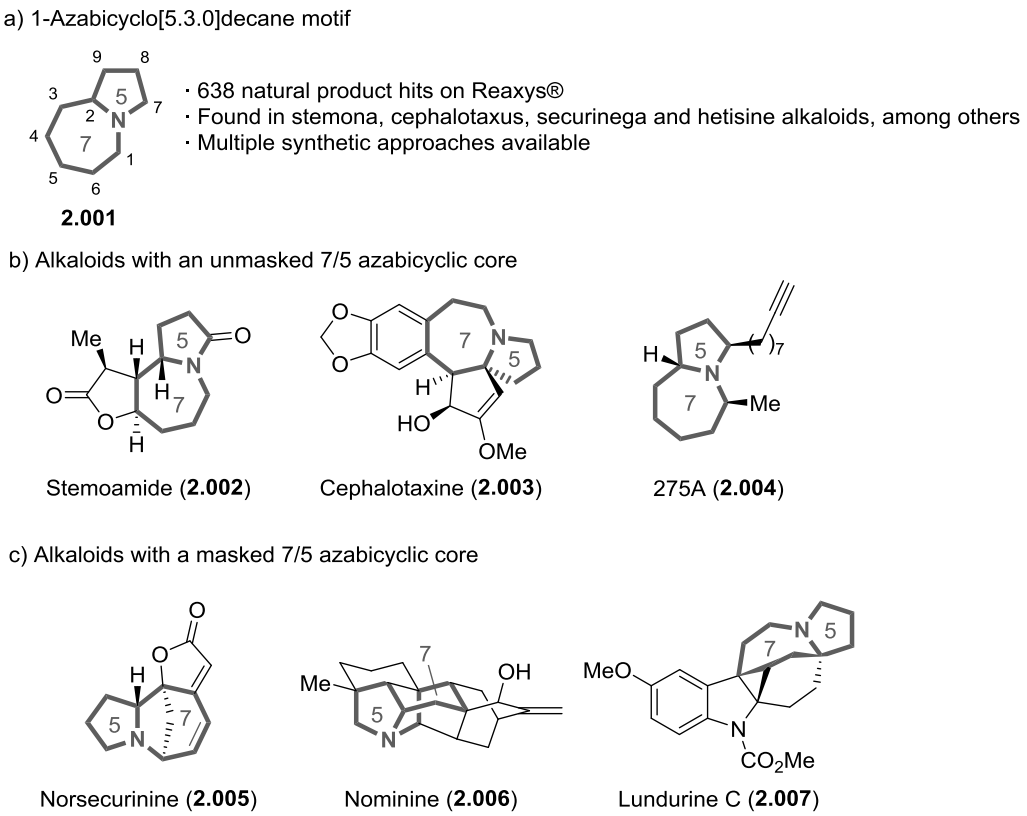

Figure 4: a) 1-Azabicyclo[5.3.0]decane (**2.001**) motif b) and c) Related alkaloids with their 7/5 system highlighted.

2.3 Strategies relying on intramolecular annulation

2.3.1 Disconnections at C1–N

The straight forward disconnection at C1–N can be implemented in many different ways (Figure 5). The issue with the otherwise tempting C1–N disconnection becomes evident when the corresponding synthetic reaction –the cyclization– is analyzed. Cyclisation precursors of the type **2.008** must undergo a 7-*exo-tet* cyclization. These reactions are allowed by Baldwin's rules, but the precursor's substituents can significantly hinder the cyclization.[22] Additionally, low-dilution conditions (in the range of 0.01 M) are typically needed to suppress intermolecular side reactions, as the formation of 7-membered rings is relatively slow.[23–26] Despite these drawbacks, the C1–N disconnection remains as one of

the key bond disconnection in the synthesis of 1-azabicyclo[5.3.0]decane alkaloids.

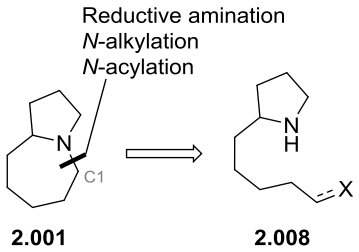

Figure 5: C1–N disconnection leads to substituted pyrrolidines of the type **2.008**.

The Martin group successfully used a C1–N bond forming step in their short total synthesis of (+)-croomine (**2.017**) (Scheme 1).[27] The target molecule (+)-croomine (**2.017**) is pentacyclic, but intriguingly only a single cyclization step is used in the synthesis. This single cyclization step is used to form the azepane ring. All other ring units are brought in as cyclic building blocks.

The synthesis begins with butenolide **2.009**, which was converted into an intermediate silyloxyfuran. The silylation serves two purposes, as will become evident in the two upcoming steps. First, the intermediate silyloxyfuran was lithiated and treated with 1,4-bromobutane to form bromide **2.011**. Second, the still remaining silyloxyfuran motif of **2.011** was used as a vinylogous Mukaiyama-type nucleophile, which reacted with (*S*)-pyroglutamic acid derivative **2.012** in a Mannich reaction to give bicyclic lactone-lactam **2.013**. The bicyclic precursor **2.013** had two of the four rings of the target (+)-croomine in place and the C9–C9a stereochemistry correctly set *anti*.[27] In preparation for the azepane formation, bicycle **2.013** was *N*-deprotected and hydrogenated to yield amine **2.014** with the desired C11 stereochemistry.

The stage was now set for the key C1–N bond formation. Intramolecular *N*-alkylation of **2.014** with NMM as the base uneventfully closed the 7-membered azepane ring. The cyclization product was isolated as the hydrobromide salt (**2.015**). The cyclization rate of the bromide **2.014** is likely increased by the Thorpe–Ingold effect resulting from the butenolide.[28] To install the final butanolide ring unit onto **2.015**, the carboxylic acid **2.015** was decarboxylated with $POCl_3$, and the formed iminium intermediate intercepted by silyloxyfuran **2.016**. Finally, after reduction of the formed butenolide to butanolide, (+)-croomine (**2.017**) was obtained in 9 steps and 5% overall yield.

The extreme efficiency at which the synthesis of (+)-croomine (**2.017**) proceeds can be attributed to the use of prefabricated ring systems, such as **2.009**, **2.012**, and **2.016**, as building blocks. In the key azepane forming step, the *N*-alkylation of **2.014** is likely assisted by Thorpe–Ingold effect, forcing the bromide side-chain to the proximity of the nucleophilic nitrogen. The (+)-croomine synthesis is an example where the C1–N bond formation is implemented synthetically as a 7-*exo*-tet cyclization, and where the implementation works reliably and without issues.

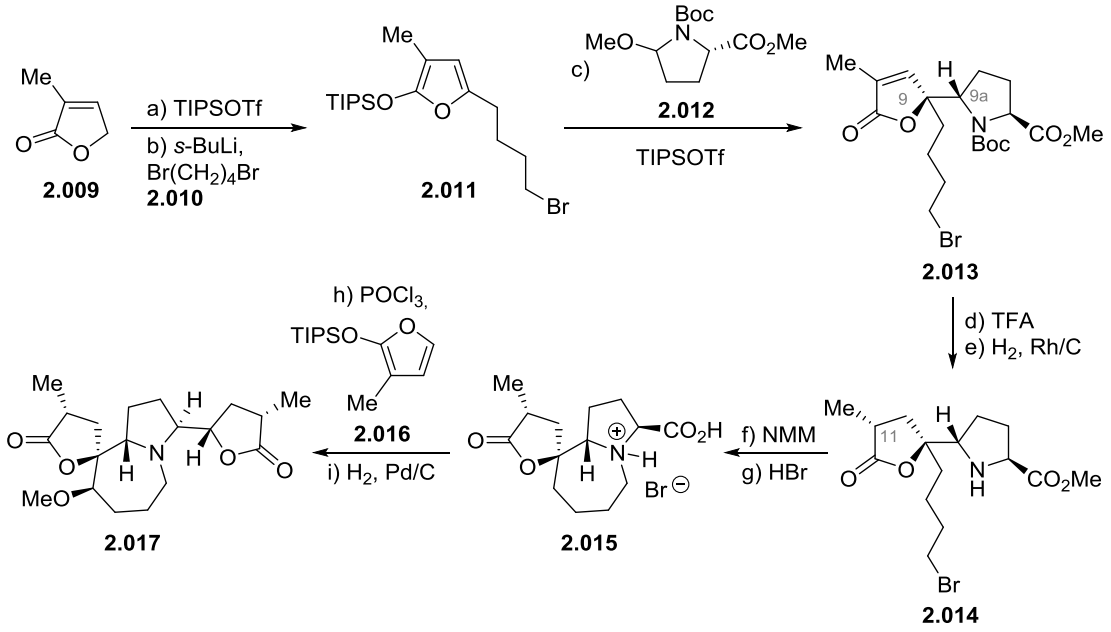

Scheme 1: Total synthesis of (+)-croomine (**2.017**). Reagents and conditions: a) TIPSOTf, Et_3N, DCM, 0 °C to rt, 99%; b) *s*-BuLi, TMEDA, THF, 0 °C, then 1,4-dibromobutane (**2.010**), 83%; c) **2.012**, 5% TIPSOTf, DCM, 0 °C, 32%; d) TFA, DCM, rt; f) H_2, Rh/C, EtOAc–EtOH, 96% over two steps; g) NMM, DMF, reflux; h) aq. HBr (3.0 M), 60 °C, 74% over two steps; i) $POCl_3$, DMF, rt, then **2.017**, 47% (dr 2:1); j) H_2, Pd/C, HCl–EtOH, 85%.

When the C1–N disconnection strategy was applied in the formal synthesis of stemoamide (**2.002**) by the group of Cossy, the disconnection's limitations became obvious (Scheme 2).[24]

The 2,3-dihydrofuran starting material **2.018** was converted into the acyclic bromide precursor **2.024** using a straight forward four-step sequence. The bromide **2.024** was then transhalogenated into a corresponding iodide, in preparation for a radical cyclization. Upon treatment of the intermediate iodide with dilauroyl peroxide, a mixture of inseparable butanolide iodides **2.025** was formed in a 5-*exo*-trig radical cyclization. Since the iodine atom terminated the radical cyclization, it was transposed from C10 to C9a in the process.

The newly formed C9 iodide of **2.025**, was immediately put to use. Treatment of **2.025** with sodium azide, followed by a subsequent reduction to an amine spontaneously closed the 5-membered lactam. The spontaneous cyclization led to the bicyclic intermediate **2.026** as a 1:1 mixture of inseparable epimers.

Tetrahydropyran **2.026** was deprotected and mesylated giving **2.027**, again as an inseparable 1:1 mixture of epimers. With a mesylate leaving group installed, **2.027** was treated with sodium hydride yielding, rather surprisingly, a 3:1 (not 1:1) mixture of tricyclic products **2.028** and **2.029**. Monitoring the cyclization with ^1H NMR showed that the unnatural isomer **2.028** cyclizes faster than the natural isomer: the cyclization rate difference between **2.027** epimers led to kinetic enrichment of the unnatural diastereomer **2.028**. Conversion of

2.029 to stemoamide (**2.002**) has been documented in the literature and was not carried out in this body of work.[25]

The formal synthesis of stemoamide by the Cossy group showcases several problems associated with the C1–N disconnection. Most importantly, when the cyclization precursors are mixtures of diastereomers, such as **2.026**, their separation can be difficult. Using mixtures of diastereomers in the cyclization reaction (**2.026** → **2.027** in this case) can cause issues, as the diastereomers have different cyclization preferences. For example, in the case of stemoamide the cyclization enriched the unnatural epimer **2.028**.

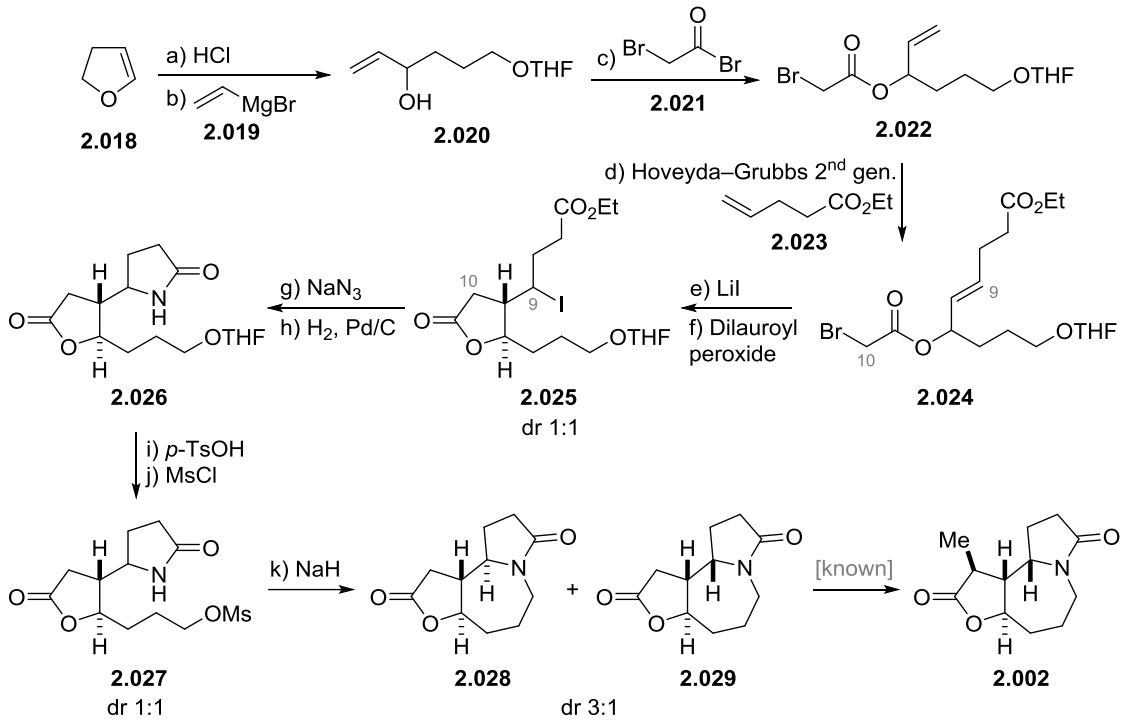

Scheme 2: Formal total synthesis of (±)-stemoamide. Reagents and conditions: a) aq. HCl (0.2 M), 0 °C; b) Vinylmagnesium bromide (**2.019**), THF, 0 °C, 18% over two steps; c) Bromoacetyl bromide (**2.021**), pyridine, DCM, rt, 85%; d) Ethyl pent-4-enoate (**2.023**), Hoveyda–Grubbs 2nd gen. catalyst, DCM, reflux, 54%; e) LiI, DMF, 0 °C to rt, 75%; f) Dilauroyl peroxide, PhH, 65% (dr 1:1); g) NaN_3, DMF, 80 °C; h) H_2, Pd/C, MeOH, rt, 44% over two steps; i) *p*-TsOH, MeOH, rt, 93%; j) MsCl, Et_3N, DCM, 89% (dr 1:1); k) NaH, THF, 0 °C, 60% (dr 3:1).

In both discussed syntheses, the formal synthesis of stemoamide (**2.002**) and the total synthesis of (+)-croomine (**2.017**), the C1–N disconnection was synthetically implemented as an intramolecular *N*-alkylation reaction. Apart from *N*-alkylation, other reactions corresponding to the same disconnection can also be envisaged. For example, the C1–N bond formation can be achieved using reductive amination.

Such an approach is exemplified by Lesma's synthesis of poison dart frog toxin 275A (**2.004**) (Scheme 3).[29] Using pyroglutamic acid derivative **2.012** as the starting point, a side chain is added using the Grignard reagent **2.030** to give pyrrolidone **2.031** as the major diastereomer. Reduction and tosylation of the benzyl ester **2.031** then formed tosylate **2.032**. The tosylate of **2.032** was substi-

tuted with a pendant carbon side derived from iodide **2.033** to yield pyrrolidine **2.034**.

In preparation for the cyclization step, the terminal alkene was extended with a four-carbon unit. The extension was achieved using a cross-metathesis reaction between **2.034** and methyl vinyl ketone (**2.035**) to deliver the enone **2.036**. The intermediate enone **2.036** was now manipulated in preparation for the reductive cyclization. Hydrogenation first reduces the enone **3.026** into a corresponding ketone. Further hydrogenation cleaves the *N*-Cbz protection to liberate the free amine. An intramolecular condensation between the newly formed free amine and ketone at C5 condense to close the 7-membered ring. Finally, the resulting enamine can be hydrogenated with substrate control guiding the forming C5 stereogenic center (dr 5:1). The hydrogenation induced domino process delivered the 1-azabicyclo[5.3.0]decane core **2.037** with the correct stereochemistry in 76% yield.

To complete the synthesis, the silyl protected terminal alcohol **2.037** was deprotected and converted to bromide **2.038**. Alkynylation of the bromide **2.038** with lithium acetylide **2.039** gave the target alkaloid 275A (**2.004**).

The route to 275A allows setting up the otherwise problematic C5 stereogenic center using a face selective hydrogenation **2.036** → **2.037**, in conjunction with the cyclization step. Also, in the route to 275A, all stereochemical information is conveniently induced from L-pyroglutamic acid. The C1–N cyclization approach also allows for reliable, albeit difficult to contorl, stereoinduction.

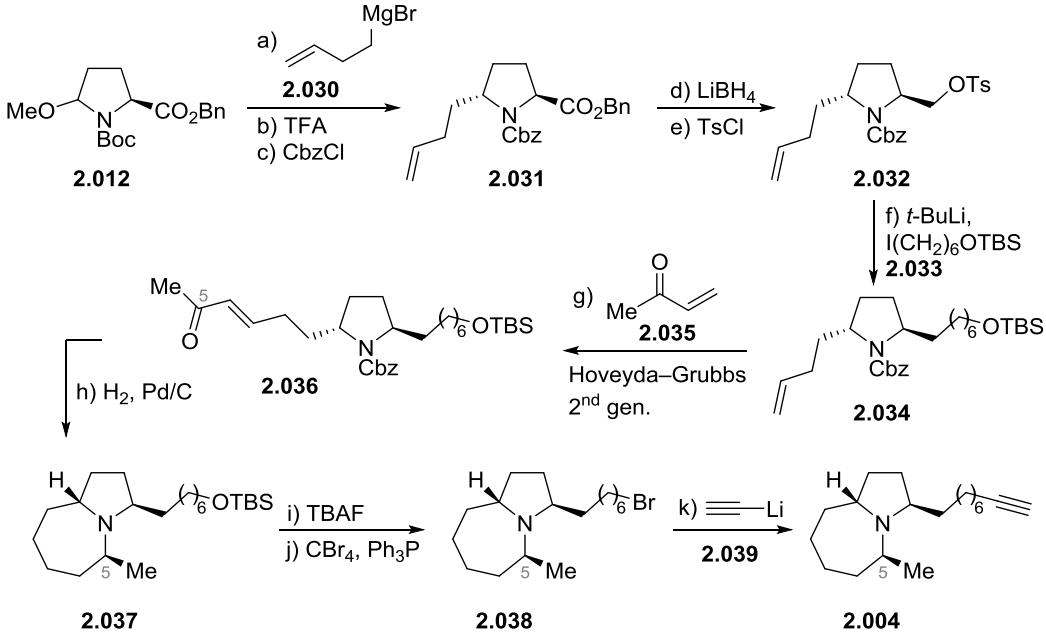

Scheme 3: Total synthesis of 275A (**2.004**). Reagents and conditions: a) But-3-enylmagnesium bromide (**2.030**), CuBr·Me_2S, BF_3·Et_2O, THF, –78 °C to rt, 84%; b) TFA, DCM, rt, 74% (dr 9:1); c) CbzCl, Et_3N, DCM, 96%; d) $LiBH_4$, THF, 0 °C, 84%; e) TsCl, Et_3N, DMAP, DCM, 0 °C to rt, 97%; f) *t*-BuLi, **2.033**, CuI, Et_2O–hexane, –78 °C to –5 °C, 81%; g) Butenone (**2.035**), Hoveyda–Grubbs 2nd gen., PhMe, 40 °C, 90%; h) H_2, Pd/C 10%, MeOH, rt, 76% (dr 5:1); i) TBAF, THF, 0 °C to rt, 62%; j) CBr_4, Ph_3P, DCM, 0 °C to rt, 93%; k) Lithium acetylide (**2.039**) ethylenediamine complex, DMSO, rt, 45%.

In some cases, a direct intramolecular *N*-acylation is also a viable method for such C1–N cyclizations. The acylation reaction was the cyclization method of choice in a straightforward formal synthesis of cephalotaxine (**2.003**) by the Chandrasekhar group (Scheme 4).[30,31]

Their approach began with the chain extension of the proline-derived racemic aldehyde **2.041** (step a), producing β-ketoester **2.043**. The enol form of **2.043** then reacted in a [2+2] cycloaddition reaction with an aryne derived from methylenedioxyarene **2.044**. Rupture of the resulting cyclobutane **2.045** gave the advanced intemediate **2.046**. All the necessary carbons of the cephalotaxine skeleton were now installed in **2.046**, and all but cyclization steps remained.

The first ring to be formed was the 5-membered enone **2.048**. Terminal alkene of **2.026** was oxidized into a corresponding ketone **2.047** using Wacker oxidation. Classic aldol condensation of **2.047** then provided an intermediate enone **2.048**. The enone **2.048** was, without isolation, *N*-deprotected with trifluoroacetic acid. The key cyclization into a 7-membered ring was achieved by a sequential addition of excess DIPEA and EDC/HOBt to the free amine. Intramolecular acylation gave the pentacyclic compound **2.049**, also known as Hanaouka's intermediate, the conversion of which to cephalotaxine is known.[31]

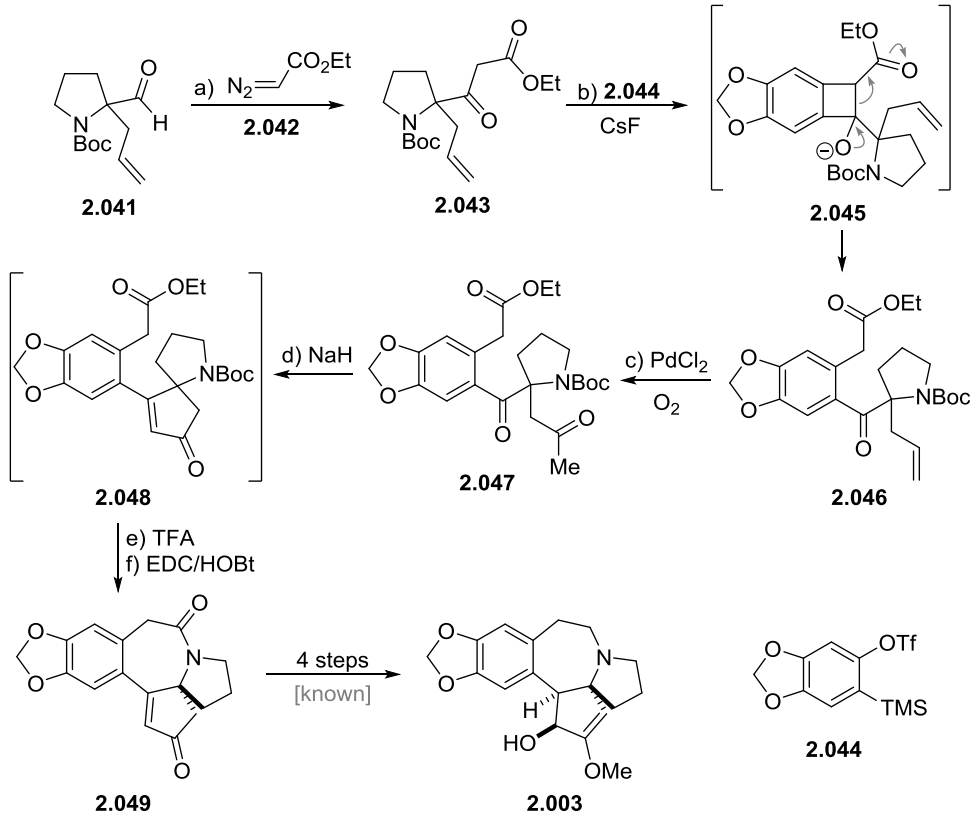

Scheme 4: Formal synthesis of cephalotaxine (**2.003**). Reagents and conditions: a) $SnCl_2$, ethyl diazoacetate (**2.042**), DCM, rt, 80%; b) **2.044**, CsF, MeCN, 80 °C, 72%; c) $PdCl_2$, CuCl, O_2, DMF–H_2O, rt, 70%; d) NaH, PhH–amyl alcohol, rt; e) TFA, EtOAc; f) DIPEA, HOBt, EDC · HCl, 0 °C to rt, 56% over three steps.

The acylation approach suffers from several shortcomings. In a great majority of natural products with azepane rings, the azepane α-carbon is not oxi-

dized. If acylation is used to form the ring, a further deoxygenation stage is needed. Typically, such deoxygenations are carried out using Lawesson's reagent, followed by reductive desulfurisation.[32] Nevertheless, formation of lactams via *N*-acylation is a fairly established method. Lactams are also chemically relatively inert when compared to amines. Because of these reasons, acylation approaches can be very profitable.

Taken together, the C1–N bond is a widely used strategic disconnection in the synthesis of 7/5 ring systems. The necessary precursors for such cyclizations are typically fairly straightforward to prepare. In many cases, readily available 5-membered building blocks (such as butenolides, pyroglutamic acid, proline and other related motifs) can be used as starting materials. These building blocks are extended with suitably long carbon chains, which are ultimately cyclized onto the nitrogen, forming a 7-membered ring. When the molecule is suitably substituted to limit flexibility, such as Thorpe–Ingold effect or aryl substrates, the C1–N bond formation to give a 7-membered ring works the best. In other cases, the cyclization can be hampered due to similar effects working against the cyclization.

2.3.2 Disconnections at C2–C3

Despite the seemingly tempting C2–C3 disconnection, not many syntheses utilize this bond-forming strategy (Figure 6). Synthetic implementations of C2–C3 disconnection rely on C2 being α to a nitrogen. Due to α-nitrogen, the C2 position can harbor either a stabilized radical, or a precursor to an iminium intermediate. In a conceptual retrosynthesis, disconnecting the C2–C3 bond results in precursor of the type **2.050**. In turn, compounds of the type **2.050** could be prepared by *N*-alkylation of prefabricated 5-membered nitrogenous rings.

Forming the C2–C3 bond also forms a new stereogenic center at the C2 position. The C2 stereogenic center is under substrate control, and can be controlled using stereochemical induction or, in some cases using catalytic methods.

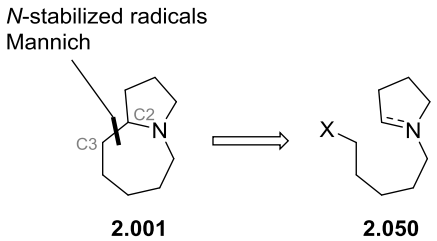

Figure 6: C2–C3 disconnection results in *N*-substituted pyrrolidone of the type **2.050**.

An approach nicely demonstrating the features of C2–C3 disconnection are the efforts aimed towards syntheses of epimers of stemoamide (**2.002**) by Khim and Schultz in 2004 (Scheme 5).[33] Their approach eventually led to 9,10-bis-*epi*-stemoamide (**2.057**).

Starting by hydrolyzing the known iodolactone **2.051** into a butenolide precursor **2.052** gave an acceptable 41% yield. Reduction of the terminal car-

boxylic acid of **2.052** followed by a Mitsunobu reaction with succinimide (**2.053**) provided the cyclic imide **2.054**. At this imide stage, the entire carbon skeleton of the target molecule was already complete.

Proceeding onto the C2–C3 bond forming cyclization stage, imide **2.054** was manipulated to a phenylthiolactam **2.055**. Employing standard radical reaction conditions, the phenylthiolactam **2.054** was treated with tributyl tin hydride and AIBN in a dilute solution. The *N*-stabilized radical formed from **2.055** at C9a facilitated a smooth 7-*exo*-trig cyclization yielding a 1:10 mixture of two diastereomers of stemoamide **2.056** and **2.057**.[22] Stemoamide diastereomers **2.056** and **2.067** have an unnatural *syn* configuration over the butanolide fusion. Such *syn* configuration is not present in any of the natural stemona family members. Equilibration with K_2CO_3 allowed the mixture to be converted to pure 9,10-*epi*-stemoamide (**2.057**) as the final product.

The stereochemical outcome of the C2–C3 cyclization is the most noteworthy lesson learned in the synthesis of 9,10-bis-*epi*-stemoamide. In the stemoamide scaffold, the *N*-stabilized radical always approached the butenolide from the same face as the side chain is attached to. This will always force a *syn* configuration across the ring fusion (**2.055** → **2.056** + **2.057**). As such, the C2–C3 cyclization can be used as an orthogonal tool to introduce *syn* stereochemistry, when compared to other methods, resulting in relative *anti* stereochemistry. If stereochemistry is of no concern, the *N*-stabilized radical approach to construct the C2–C3 bond gives good yields and results in compact syntheses.

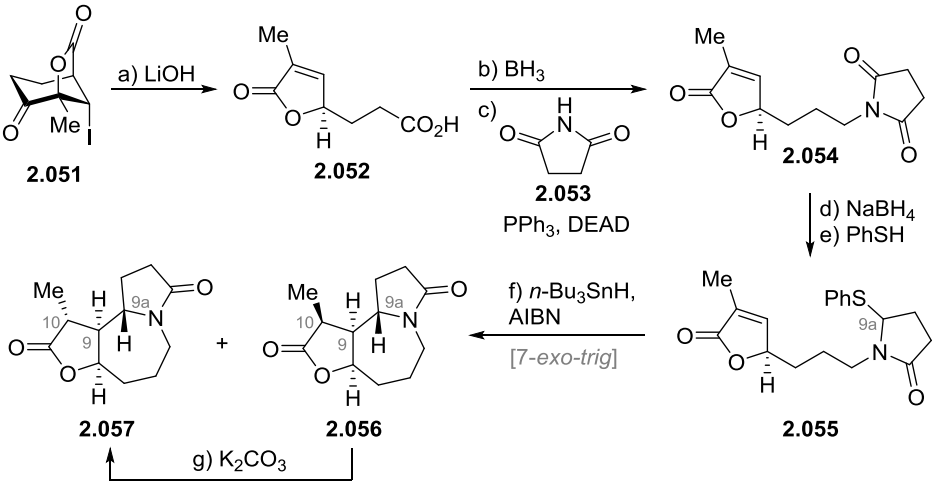

Scheme 5: Total synthesis of 9,10-bis-*epi*-stemoamide (**2.057**). Reagents and conditions: a) LiOH, THF–H_2O, rt, 41%; b) BH_3·THF, THF, –78 °C, 92%; c) Succinimide (**2.053**), Ph_3P, DEAD, THF, rt, 92%; d) $NaBH_4$, MeOH, –10 °C; e) PhSH, *p*-TsOH, PhH, 0 °C, 62% over two steps; f) *n*-Bu_3SnH, AIBN, PhH, reflux, 3.5 mM; g) K_2CO_3, MeOH, rt.

N-acyliminium chemistry has been widely used in alkaloid total synthesis.[34] *N*-acyliminium chemistry has also applications in the construction of 7/5 bicyclic azepine alkaloids, especially in the context of C2–C3 disconnections.

In their total synthesis of a minor cephalotaxus alkaloid desmethoxycephalotaxine (**2.065**), the group of Koley made use of an acyliminium based cyclization (Scheme 6).[35]

Starting with the known aryl iodide **2.058**, a Suzuki coupling with pinacol boronate ester **2.059** gave the allylic silane **2.060**. To **2.060**, succinimide (**2.053**) was introduced using Mitsunobu coupling. Treatment of the intermediate imide with allyl magnesium chloride gave the aminal **2.061**.

Treatment of aminal **2.061** with $TiCl_4$ formed an acyliminium ion **2.062**. This transient species **2.062** underwent a Sakurai-type cyclization with the tethered allylic silane. The domino reaction gave the 7/5 bicyclic product **2.063** in 90% yield and with excellent diastereoselectivity (dr 20:1). Amide **2.063** was reduced with $LiAlH_4$, and the resulting dialkene cyclized to cyclopentene **2.064** using ring closing metathesis. Sequential oxidations gave desmethoxycepalotaxine **2.065**.

Few methods allow the generation of nucleophilic partners under the conditions used for the formation of (acyl)iminiums. The only viable options include acid-catalyzed aldol- or Sakurai reactions. Likely because of these limitations, acyliminium based cyclization reactions are not widely applied in the syntheses of azepane-type alkaloids. However, as shown by the Koley group's synthesis of desmethoxycephalotaxine (**2.065**), good yields and diastereoselectivities are achievable.

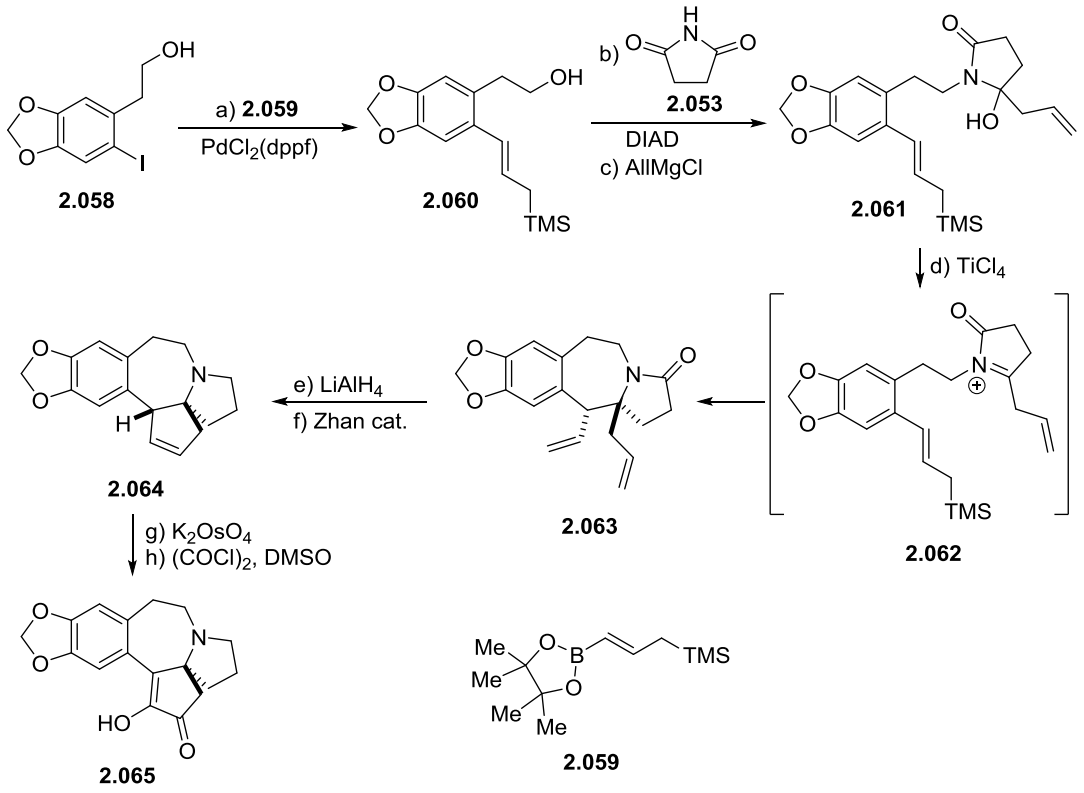

Scheme 6: Total synthesis of desmethoxycephalotaxinone (**2.065**). Reagents and conditions: a) **2.059**, $PdCl_2(dppf)$, K_3PO_4, THF–H_2O, 80 °C, 92%; b) Succinimide (**2.053**), Ph_3P, DIAD, THF, 0 °C, 99%; c) Allyl magnesium chloride, Et_2O, 0 °C, 86%; d) $TiCl_4$, DCM, –60 °C, (dr 20:1), 90%; e) $LiAlH_4$, THF, rt, 89%; f) CSA, Zhan catalyst, PhMe, 90%; g) K_2OsO_4, NMO, *t*-BuOH–H_2O, 84%; h) DMSO, $(COCl)_2$, DCM, –60 °C, 83%.

A noteworthy implementation of the C2–N disconnection stategy, albeit not a total synthesis, is the biomimetic organocatalytic Mannich reaction, developed by the Koley group (Scheme 7).[36] Aminal **2.068** was prepared four steps from readily available bromoalcohol **2.066**. Using MacMillan's imidazolidinone organocatalyst **2.069** the substrate **2.068** readily cyclized, *via* the enamine-iminium intermediate **2.070**, to give a 7/5 ring system **2.071** as a single diastereomer in 91% *ee*. The method is applicable to other ring-sizes and provides a wide range of alkaloid-type scaffolds.

It is likely the Koley method will find use in total syntheses. With the enamine activation mode **2.070**, the nucleophilic partner can be generated under mild conditions, giving control over both relative and absolute configuration of the products. The imine-enamine pairing avoids the complications mentioned above for the C2–C3 bond formation for iminium electrophiles.

The examples covered here show the relative immaturity of C2–C3 disconnection strategies. The route shortening the C2–C3 disconnection offers is very convenient and, in many cases, resembles the precursors resulting from a C1–N disconnection, allowing tethering a readily available 5-membered pyrrolidine derivatives to a long pendant carbon chain from pyrrolidine nitrogen. Such unit then functions as the cyclization precursor. However, as the C2–C3 approach generates a stereogenic center at the C2, unwanted stereochemical outcomes can jeopardize the syntheses.

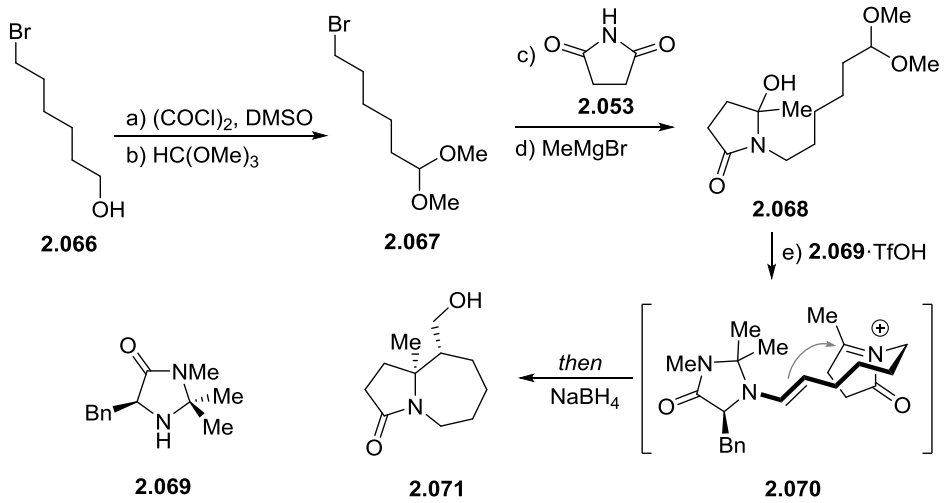

Scheme 7: Biomimetic iminium cyclization. Reagents and conditions: a) DMSO, $(COCl)_2$, DCM, –78 °C; b) $HC(OMe)_3$, MeOH, *p*-TsOH, 0 °C, 87% over two steps; c) Succinimide (**2.053**), K_2CO_3, DMF, 60 °C, 94%; d) MeMgBr, THF, 0 °C, 83%; e) **2.069**·TfOH, ACN, rt, then $NaBH_4$, MeOH, 0 °C, 73%, (dr >20:1, *ee* 91%).

2.3.3 Disconnection at C8–N

Unlike the approaches covered thus far, the C8–N disconnection ruptures the 5-membered ring, leaving behind a 7-membered ring (Figure 7). In stark contrast to the 5-membered pyrrolidine derivatives, the 7-membered azepanes are rarely commercially available, necessitating further synthetic steps for their

preparation. Despite this drawback, such disconnections can prove useful in synthesis planning when the C8 position is further functionalized and cannot readily be accessed otherwise. Also, 5-exo-*tet* cyclizations are very fast, giving safe clearance on more delicate substrates.[13]

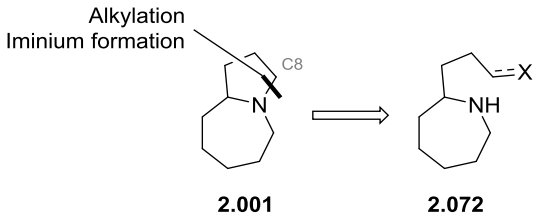

Figure 7: C8–N disconnection results in substituted azepanes **2.072**.

A true *tour de force* in alkaloid total synthesis, the Williams group's stemospironine (**2.088**) synthesis showcases a strategy heavily relying on a C8–N disconnection (Scheme 8).[37] The target molecule **2.088** contains four rings, but the Williams group uses acyclic stereocontrol in the entire sequence.

The synthesis begins with protected ketone **2.073**. Alpine borane reduction, followed by protection and alkyne acylation converts the ketone **2.073** into ynoate **2.075**. Conjugate addition then gives **2.077** stereoselectively. Desilylation and methylation of **2.077** gave an intermediate methyl ether.

Reduction followed by Sharpless epoxidation of the resulting allylic alcohol **2.078** gave an intermediate epoxide, which was converted to enoate **2.079** and then to a differentially protected intermediate **2.080**.

To set the stage for the cyclization sequence, the epoxide **2.080** was opened with lithium azide to give the acyclic azide **2.081**. After this, a C18–C21 fragment was installed *via* a Wittig olefination. At this stage, the cyclization phase of the synthesis was finally initiated. First, using Jones oxidation the butanolide in **2.085** was set in place. Then intramolecular reductive amination was used to close the azepane ring forming **2.086**.

Finally, upon treatment with iodine, **2.086** formed an aziridinium intermediate **2.087**. The liberated iodide ion then demethylated the methyl ester **2.087**, triggering two consecutive ring closures. This impressive synthetic manoeuvre provided (–)-stemospironine **2.088**.

After completing the laborious construction of the acyclic precursor **2.084**, the cyclization phase is a very elegant piece of synthetic chemistry. In the stemospironine case, the chosen strategy of forming the C8–N bond is justified, as it functions as a linchpin for forming the final butanolide in **2.088**. The Williamson approach makes little use of cyclic stereocontrol, though, which is likely partially due to limited availability of suitable azepane starting materials.

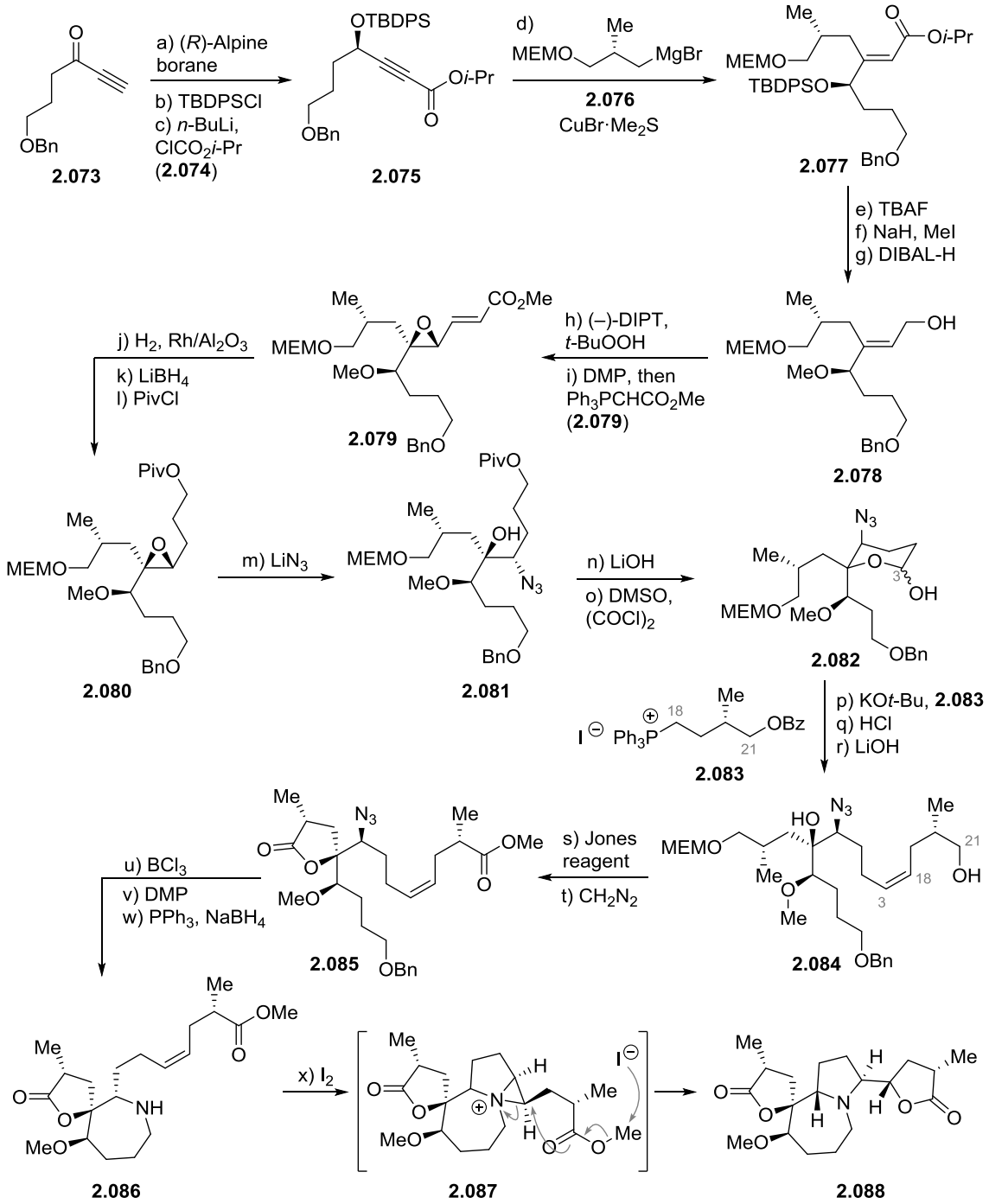

Scheme 8: Total synthesis of (−)-stemospironine. Reagents and conditions a) (*R*)-Alpine borane, THF, –10 °C to rt, 95%, (98% *ee*); b) TBDSCl, imidazole, DCM, rt, 80%; c) *n*-BuLi, $ClCO_2i$-Pr (**2.074**), THF, –78 °C, 90%; d) **2.079**, CuBr · Me_2S, THF, –78 °C to rt, 70%; e) TBAF, THF, rt, 90%; f) NaH, MeI, DMF, rt, 85%; g) DIBAL-H, DCM, –78 °C, 92%; h) Ti(O*i*-Pr)$_4$, CaH_2, SiO_2, (–)-DIPT, *t*-BuOOH, DCM, –20 °C, 90%, (dr 4:1); i) Dess–Martin periodinane, pyridine, DCM, 0 °C to rt, then Ph_3PCHCO_2Me (**2.079**), 0 °C to rt, 60%; j) H_2, Rh/Al_2O_3, THF, rt, 85%; k) $LiBH_4$, MeOH–Et_2O, rt, 90%; l) PivCl, pyridine, DMAP, 91%; m) LiN_3, NH_4Cl, DMPU, 130 °C, 83%; n) LiOH, THF–MeOH–H_2O, rt, 94%; o) DMSO, $(COCl)_2$, Et_3N, DCM, –60 °C, 97%; p) KO*t*-Bu, **2.083**, THF, –10 °C, 77%; q) HCl, THF, rt, 85%; r) LiOH, THF–MeOH–H_2O, rt, 88%; s) Jones reagent, THF, –10 °C; t) CH_2N_2, Et_2O, 0 °C, 80% over two steps; u) BCl_3, DCM, –78 °C to –10 °C, 60%; v) Dess–Martin periodinane, DCM, 80%, rt; w) Ph_3P, THF then $NaBH_4$, MeOH, rt, 60%; x) I_2, DCM–Et_2O, rt, 30%.

The C8–N disconnection approaches have also found use in the synthesis of *Securinega*-type alkaloids, where the 7/5 ring system is embedded into a bridged scaffold. The Weinreb group developed a strategy based on the C8–N disconnection to circumvent epimerization issues faced with other synthetic approaches. Altogether the Weinreb approach led to the enantioselective total syntheses of (+)-14,15-dihydronorsecurinine, (–)-norsecurinine, and phyllathine.[38] The following discussion only covers the norsecurinine route (Scheme 9).

The *N*-tosylated *trans*-4-hydroxy-L-proline (**2.089**) starting material was converted into a silyl protected α,β-unsaturated nitrile **2.091** in three steps. The α,β-unsaturated nitrile was hydrogenated, and the alcohol deprotected and oxidized to deliver ketone **2.092**. Samarium iodide induced radical cyclization of nitrile **2.092** formed the bridged azepane core **2.093**.

The constructed bridged core was then functionalized further. Tertiary alcohol **2.093** was silyl protected and the ketone acetal protected to give the fully protected bridged core **2.094**. The fully protected **2.094** was *N*-deprotected and treated with isatonic anhydride (**2.095**) to give *o*-amino benzamide **2.096**. Diazonation of **2.096** then C–H activated the carbon α to nitrogen to deliver a mixture of α-chloro- and α-methoxy amines **2.097**. The **2.097** mixture was treated with allyl magnesium bromide to install a C8–C10 unit onto the scaffold. The allylated compound was *N*-Boc protected to deliver precursor **2.098**.

The pendant C8–C10 side chain of **2.098** was then utilized to form a fused pyrrolidine ring. In preparation for the C8–N cyclization, **2.098** was hydroborated and oxidized to give an intermediate terminal alcohol, which was tosylated to the tosylate **2.099**. The *N*-Boc amide **2.099** was deprotected with aqueous HCl. The *in situ* generated free amine readily cyclized onto the tosylate, forming the 7/5 ring system in a gratifying 81% yield.

After some unsuccessful attempts at constructing the final butenolide ring, a workaround was developed. A series of manipulations on protected intermediate **2.100** afforded phosphonate **2.102**. An intramolecular Horner–Wadsworth–Emmons cyclization took place forming the final butenolide ring. Finally, the selenoxide was eliminated delivering (–)-norsecurine (**2.005**).

The length of the norsecurine route mostly stems from revising the endgame. Otherwise, the chosen strategy is intriguingly different from the typical synthetic approaches to *Securinega* alkaloids.[39] The Weinreb approach also highlights the utility of the C8–N disconnection. The C8–N bond forming step, the intramolecular substitution reaction **2.099** → **2.100**, takes place after *N*-deprotection with aqueous hydrochloric acid. The pyrrolidine ring forms before the intermediate free amine has time to protonate, underlining how facile the C8–N cyclization truly is.

Taken together, the C8–N disconnection is a curious option for retrosynthesis. It also represents a borderline case of Corey's original rules for retrosynthesis (which recommend to avoid disconnections that generate ≥7 membered rings).[40] Nevertheless it has a *niche* use when the substrate so allows. Suitable substrates are either domino reaction precursors or bridged structures.

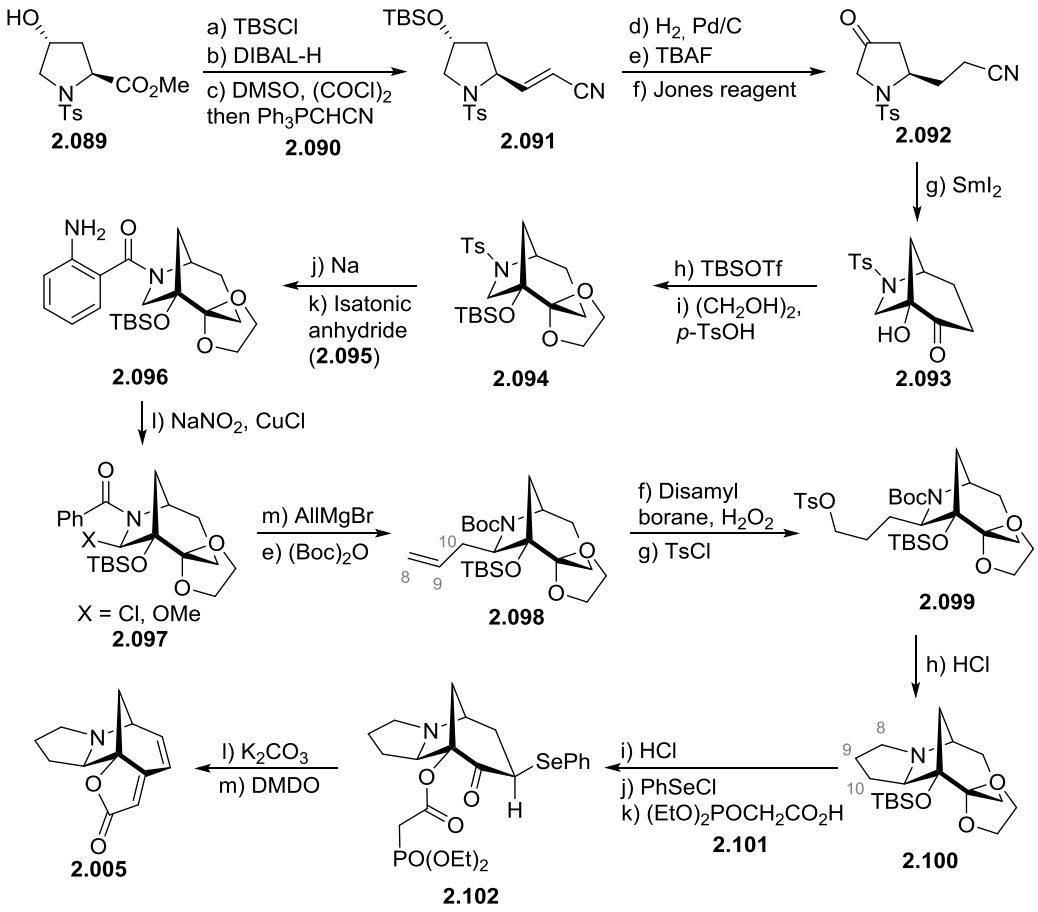

Scheme 9: Total synthesis of (–)-norsecurinine (**2.005**). Reagents and conditions: a) TBSCl, imidazole, DCM, 88%; b) DIBAL-H, PhMe, –78 °C to rt, 98%; c) DMSO, $(COCl)_2$, Et_3N, DCM, –78 °C then Ph_3PCHCN (**2.090**), DCM, –78 °C to rt, 90%, (7:2 *E*/*Z*); d) H_2, Pd/C, EtOAc, rt, 98%; e) TBAF, THF, rt, quant.; f) Jones reagent, acetone, rt, 84%; g) SmI_2, MeOH–THF, –78 °C to rt, 78%; h) TBSOTf, DIPEA, DCM, 0 °C to rt, 91%; i) $(CH_2OH)_2$, *p*-TsOH, PhH, reflux, quant.; j) Na, naphthalene, DME, –78 °C, 88%; k) Isatonic anhydride (**2.095**), DMAP, MeCN, rt, 87%; l) $NaNO_2$, HCl, CuCl, MeOH, rt, 56% combined; m) AllMgBr (14 equiv.), $BF_3 \cdot OEt_2$ (11 equiv.), THF, –78 °C to rt; n) $(Boc)_2O$, Et_3N, DCM, reflux, 68% over two steps; f) Disamyl borane, THF, 0 °C to rt, then H_2O_2, NaOH; g) TsCl, DMAP, Et_3N, DCM, 71% over two steps; h) aq. HCl (3%), MeOH, 60 °C, 81%; i) aq. HCl (3 M), 95 °C, 74%; j) PhSeCl, Et_3N, EtOAc, reflux, 60%; e) $(EtO)_2POCH_2CO_2H$ (**2.101**), CMC, DCM, 0 °C to rt, 88%; f) K_2CO_3, [18]crown-6, PhMe, 0 °C to rt, 95%; g) DMDO, DCM–Acetone, –78 °C, 39%.

2.3.4 Rearrangement and rearrangement-like strategies

Rearrangements and rearrangement-like reactions can significantly simplify and shorten synthetic routes. Rearrangements are, however, difficult to recognize in an initial retrosynthetic analysis. The difficulty stems mostly from the rearrangements' intricate mechanisms, which do not result in direct bond disconnections and subsequent retrons. Neither are rearrangements easily implemented into syntheses as tactical changes.

Despite the difficulties mentioned, when properly recognized in synthesis planning, rearrangement reactions allow fast construction of molecular complexity.[41] Rearrangement processes are thermodynamically driven. Either a small-molecule is expunged in the reaction, or the resulting new isomer is more stable than its parent compound. Typical rearrangement-based synthesis route first constructs a high-energy precursor, which is then rearranged.

The group of Aubé shortened the synthesis of stenine (**2.113**) to just 8 steps using a rearrangement strategy, a truly remarkable feat (Scheme 10).[42] Their approach relies on a highly concise domino Diels–Alder-Schmidt reaction forming rings A and B with correct stereochemistry in just a single step.

Ketophosphonate **2.103** was first elongated with aldehyde **2.014** using a Horner–Wadsworth–Emmons reaction. The elongation was followed by a consecutive silyl enol ether formation to deliver the diene **2.105**. Diene **2.105** was reacted with cyclohexanone **2.016** in the Diels–Alder-Schmidt domino reaction. The domino reaction initiates with a Lewis acid catalyzed *exo*-selective Diels–Alder reaction between diene **2.105** and dienophile **2.106** to give the *cis* decalin **2.107**. Under the same conditions, **2.017** reacts in an intramolecular Schmidt reaction *via* the intermediacy of 6/6/6 ring system **2.018** with rings *pre*-A and *pre*-B rearranging to rings A and B in the 6/5/7 ring system **2.019** in 3:1 diastereomeric ratio. Success of the domino process was very dependent on the Lewis acid used, for example BF_3 favored the wrong diastereomer and gave only a 14% yield.

The tricyclic amide **2.109** formed in the rearrangement process was alkylated at C12 with ethyl bromoacetate (**2.110**) to deliver **2.111**, in preparation for the formation of the D ring butanolide. Diastereoselective reduction of ketone **2.111** then resulted in spontaneous lactonization closing butanolide ring D. Further diastereoselective α-methylation of the newly formed butanolide (LiHMDS, MeI) then gave oxystenine **2.112**. Reduction of oxystenine **2.112** provided stenine (**2.113**) in just 8 steps from **2.103** and 14% overall yield.

The Aubé group's stenine synthesis beautifully exemplifies the power of rearrangement strategies. Rearrangement step from **2.108** to **2.019** allows forming the tricyclic 5/7/6 core of stenine by rearranging a much more easily synthesized 6/6 ring system. The Schmidt approach has since found use in many azepane alkaloid syntheses, further underlining the significance of the method developed.[43,44]

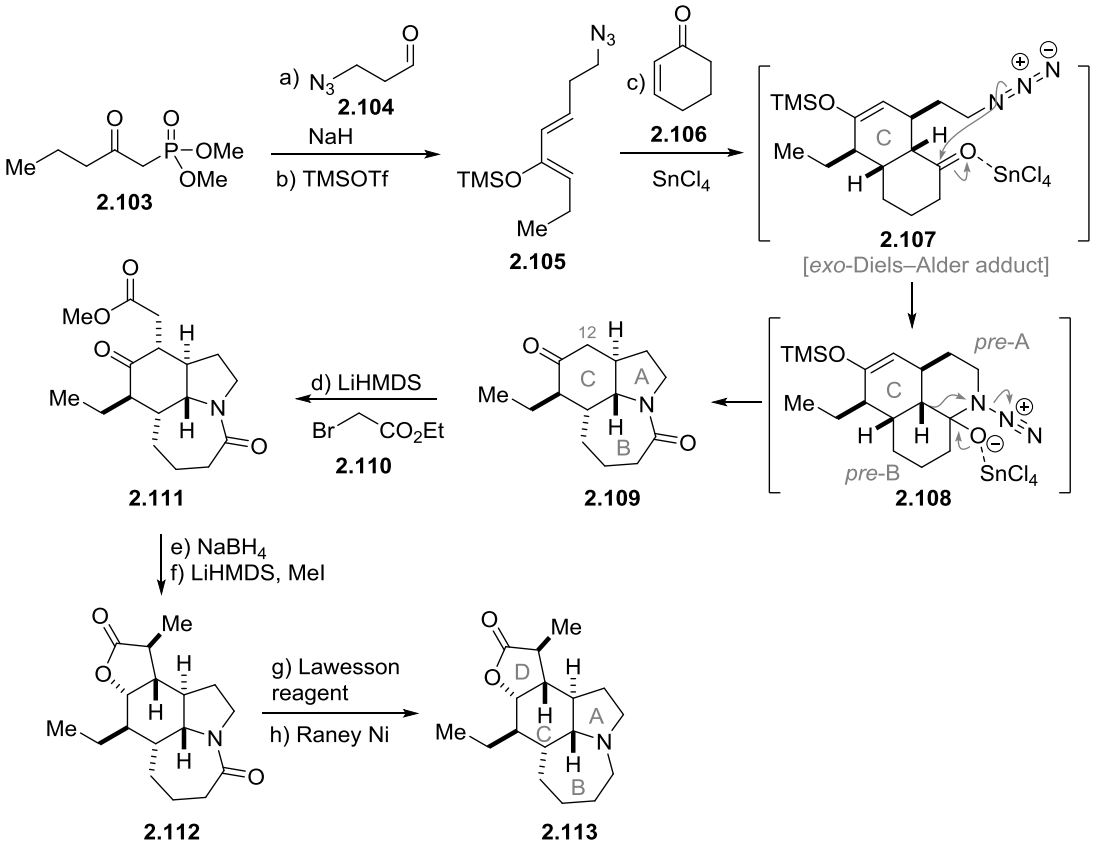

Scheme 10: Total synthesis of (±)-stenine. Reagents and conditions: a) **2.103**, NaH, THF, –78 °C to –25 °C, then **2.104**, 92%; b) TMSOTf, Et_3N, Et_2O, 0 °C, 95%; c) Cyclohex-3-en-1-one (**2.106**), $SnCl_4$, DCM, –78 °C to rt, 52%, (dr 3:1); d) LiHMDS, ethyl-2-bromoacetate (**2.110**), HMPA, –78 °C, 73%; e) $NaBH_4$, MeOH, rt, 64%; f) LiHMDS, MeI, THF, –78 °C, 79%; g) Lawesson reagent, DCM, rt, 93%; h) Raney-Ni, EtOH, rt, 89%.

The landmark synthesis of lundurines by Echaevarren group is an interesting application of rearrangement reactions to access 7/5 azabicyclic cores (Scheme 11).[45] In the lundurine family of natural products, the 7/5 ring system is a part of a larger scaffold containing a cyclopropyl ring (see **2.007**).

Starting with 5-methoxytryptamine (**2.114**) as the indole core, condensation with oxoester **2.115** gave the aldehyde **2.116**. Alkynylation of aldehyde **2.116** using Ohira–Bestmann reagent (**2.117**) delivered **2.118**, and set the stage for an 8-*endo*-dig hydroarylation. With catalytic AuCl the hydroarylation of **2.118** took place giving tetracyclic lactam **2.119** in a 56% yield.

Subsequent manipulations aimed toward constructing the bridging unit onto the tetracyclic scaffold **2.119**. First, the free indole nitrogen of **2.119** was *N*-acylated with methyl chloroformate (**2.120**). Then, a Lemieux–Johnson oxidation of the pendant vinylcyclopentane, carried to **2.119** from starting material **2.115**, resulted in the aldehyde **2.121**. The newly formed aldehyde was converted to a corresponding tosyl hydrazine **2.122**. A BF_3-catalyzed formal [3+2] dipolar cycloaddition then delivered, *via* the intermediacy of pyrazoline **2.123** rearranging to expel nitrogen, the compound **2.124** with the key central cyclopropyl ring in 80% yield. The rearrangement process also formed a 7-membered ring

embedded in the central scaffold. With all of the necessary rings formed, only redox manipulations remained.

Heating alkene **2.124** led to a transannular double-bond migration to form the enamide **2.125**. Sequential reduction of both enamide **2.125** and amide **2.126** led, then, to lundurine C (**2.007**). Lundurines A and B could also be accessed from the key intermediate **2.126**.

In lundurines alkaloids, the 7/5 ring system is masked into a rather complex scaffold with a cyclopropane ring. Using expulsion of nitrogen as an entropic driving force (**2.122** → **2.124**), a transannular cycloaddition and rearrangement allowed access the otherwise difficult-to-form system. Cyclopropanes can be used as points of further functionalization, and the approach could have important future applications.[46]

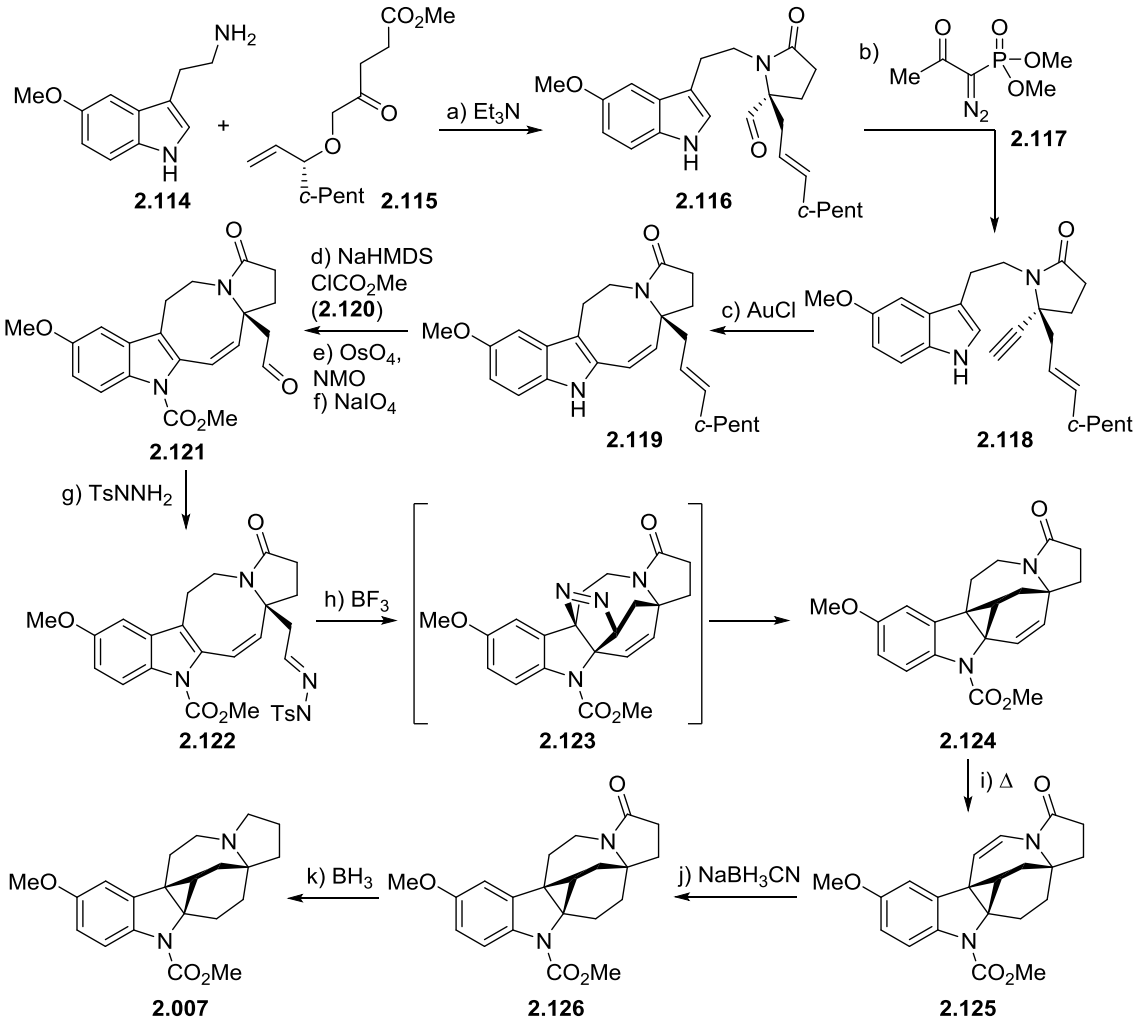

Scheme 11: Total synthesis of lundurine C (**2.007**). Reagents and conditions: a) Et_3N, PhMe, reflux, 84%; b) K_2CO_3, MeOH, Ohira–Bestmann reagent (**2.117**), MeOH, rt, 84%; c) AuCl (0.05 equiv.), DCM, rt, 56%, (er >99:1); d) NaHMDS then $ClCO_2Me$, THF, 0 °C to rt, 88%; e) OsO_4, NMO, acetone–H_2O, rt; f) $NaIO_4$, acetone–H_2O, rt; g) $TsNNH_2$, *p*-TsOH, DCM, rt, 79% over three steps; h) $BF_3 \cdot Et_2O$, DCM, 80 °C, 80%; i) PhMe, 155 °C; j) $NaBH_3CN$, THF–HCO_2H, 2 °C to 40 °C; k) $BH_3 \cdot Me_2S$, THF, rt, 84%.

One of the most efficient syntheses of stemoamide (**2.002**) to date also relies on a rearrangement-like reaction (Scheme 12). Developed by Lee and Jacobi, the synthesis features a Diels–Alder-retro-Diels–Alder sequence.[47]

The key oxazole precursor **2.129** was prepared in two steps from chlorobutyryl chloride (**2.127**) and L-methylalanine (**1.128**). *N*-alkylation of succinimide (**2.053**) with 4-chlorobutyl oxazole **2.129** gave the imide **2.130.** Reduction of imide **2.130** allowed installing alkyne **2.132** using *N*-acyliminium chemistry. The alkyne **2.132** was the needed substrate for the key Diels–Alder-retro-Diels–Alder domino reaction.

Upon heating, a Diels–Alder reaction takes place forming intermediate **2.133**. This is followed by a retro-Diels–Alder reaction, in which **2.133** expels acetonitrile, and yields butenolide **2.134**. Diastereoselective reduction of butenolide **2.134** gave stemoamide (**2.002**). The route could also be rendered enantioselective by using L-pyroglutamic acid in lieu of succinimide (**2.053**).

Jacobi's total synthesis of stemoamide is highly efficient and requires but inexpensive materials. The utilized high-temperature rearrangement method of ring construction would, however, be detrimental to more delicate substrates.

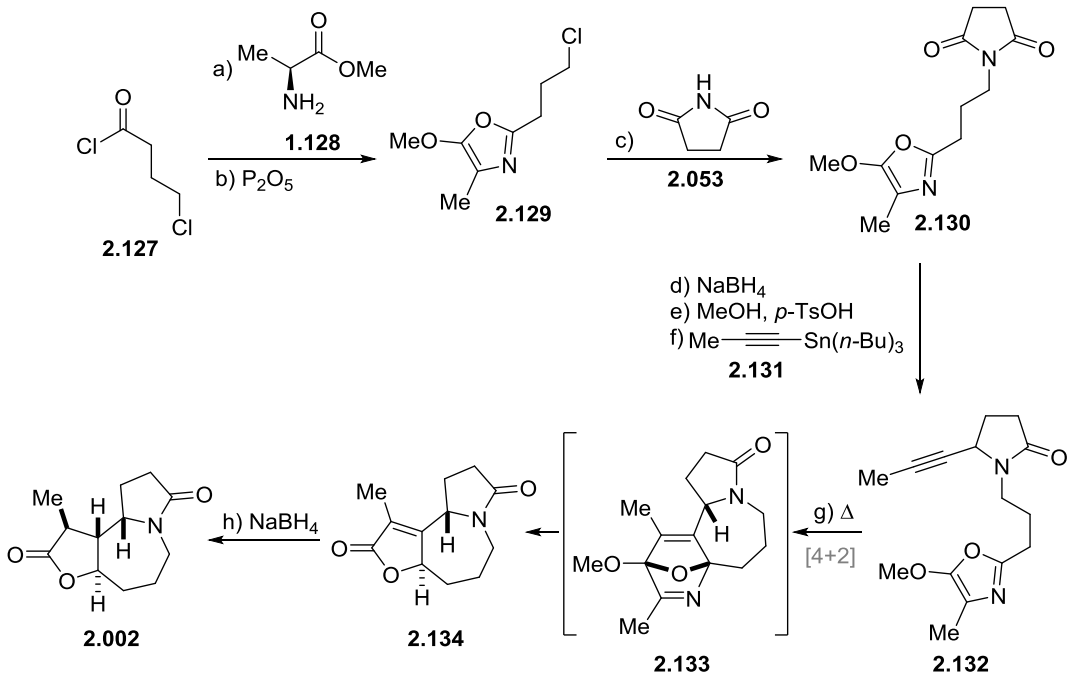

Scheme 12: Total synthesis of stemoamide (**2.002**). Reagents and conditions: a) L-alanine methyl ester hydrochloride (**1.128**·HCl), pyridine, DCM, 0 °C, quant.; b) P_2O_5, $CHCl_3$, reflux, 80%; c) NaH, DMF, 0 °C, 97%; c) $NaBH_4$, MeOH, 0 °C, 78%; e) *p*-TsOH, MeOH, rt, 92%; f) **2.131**, $BF_3 \cdot OEt_2$, DCM, –78 °C, 92%; g) diethylbenzene, reflux, 53%; h) $NaBH_4$, $NiCl_2 \cdot 6H_2O$, MeOH, 65%.

The efficiency of rearrangements is also highlighted in the Li group's formal synthesis of cephalotaxine (**2.003**) (Scheme 13). Li's rearrangement approach relies on a ring-expansion-contraction of a 6/6 ring system to a 7/5 ring system. The rearrangement process bears a resemblance to Aubé's synthesis of stenine (**2.113**, Scheme 10).

The synthesis commences with conversion of amine **2.135** into allylated diester **2.138** using a sequence of five good-yielding manipulations. Diester **2.138** is cyclized to the rearrangement precursor **2.139** using the Dieckmann condensation, followed by a decarboxylation step.

Exposing the thus obtained ketone **2.139** to zinc dust in hot acetic acid resulted in a domino rearrangement-reduction process delivering **2.142**. The rearrangement of **2.139** is thought to proceed *via* a transient aziridinium intermediate **2.140**. The electron rich aromatic system facilitates cleaving the benzylic C–N bond of the intermediate aziridine **2.140**, leading to ring expansion giving **2.141**. After consecutive reductions with metallic zinc **2.141** forms **2.142**. Wacker oxidation of the terminal olefin of **2.142**, followed by a Polonovski–Potier reaction oxizing the amine into enamine, yielded the known intermediate **2.143**.

The rearrangement domino process showcased in the Li's cephalotaxine route is another ring expansion-ring contraction process. The approach proceeds to first prepare 6-membered precursors using well-established carbonyl chemistry. In general, 6-membered carbocycles are easy to prepare with stereo- and regiocontrol when compared to many other ring sizes. When carefully orchestrated, rearrangements of 6/6 ring systems can transpose a methylene unit from one ring to another, resulting in a 5/7 system.

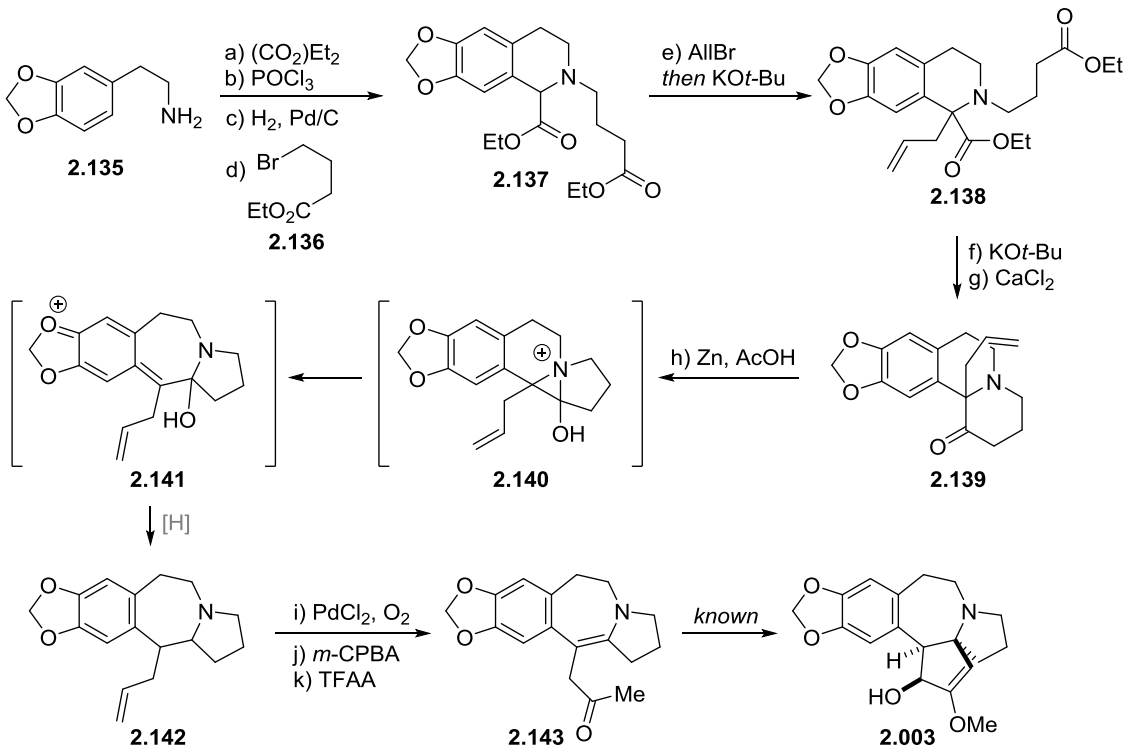

Scheme 13: Formal synthesis of cephalotaxine (**2.003**). Reagents and conditions: a) $(CO_2)Et_2$, PhMe, reflux, 95%; b) $POCl_3$, MeCN, reflux, 74%; c) Pd/C, H_2, rt, 99%; d) Ethyl 4-bromobutyrate (**2.136**), MeCN, reflux, 88%; e) Allyl bromide, DMSO, rt, then KO*t*-Bu, THF, 78%; f) KO*t*-Bu, PhMe, reflux, 75%; g) $CaCl_2$, DMSO, reflux, 78%; h) Zn, HOAc, reflux, 70%; i) $PdCl_2$, $CuCl_2 \cdot 2H_2O$, NaCl, 0.2 M HCl–DMF, 65 °C 74%; j) *m*-CPBA, DCM, 0 °C; k) TFAA, DCM, 0 °C, 70% over two steps.

The Overman laboratory has successfully used rearrangement reactions in the total synthesis of alkaloids for many years. Their approach to stemona alkaloid didehydrostemofoline **2.161** displays a similar inventive rearrangement strategy (Scheme 14).[48]

The group started by constructing a bridged amine **2.146** from functionalized pyrrole **2.144** and nitroacylate **2.145** using a Diels–Alder reaction. Nitro group of **2.146** was then removed in an E1cB elimination, followed by hydrogenation of the resulting α,β-unsaturated ester. Protecting the primary alcohol and subsequent DIBAL-H reduction of the axially disposed ester gave alcohol **2.147**. The alcohol side chain was then truncated to give ketone **2.148**. Vinylation of ketone **2.148** on its convex face, followed by *N*-Boc deprotection provided the hydroiodic acid salt **2.149**.

Treatment of amine **2.149** with paraformaldehyde gave an iminium intermediate **2.150**, initiating an aza-Cope rearrangement to give an enol **2.151**. Enol intermediate **2.151** was primed to undergo an intramolecular Mannich reaction to yield the stemofoline core **2.151** in 94% yield. The rearrangement process also forms the masked 7/5 ring system of interest.

Silylated alcohol of the compound **2.151** was deprotected and oxidized to a corresponding aldehyde. The intermediate aldehyde was reacted with sulfonate **2.152** in a Julia–Kocienski reaction, adding the necessary pendant carbon side chain unit with correct stereochemistry. Further functionalization was achieved as ketone **2.153** was alkylated with iodide **2.154** and equilibrated to the desired diastereomer **2.155**. The added ester functionality would later be used to construct further ring.

To close the southern tetrahydrofuran ring, the methoxy protection of **2.155** was cleaved with BBr_3. The thus obtained intermediate alcohol cyclized onto the central cyclohexanone to form a hemiacetal, which was trapped with TMS. With the tetrahydrofuran ring in place, the ester side chain was α-methylated to yield the polycyclic intermediate **2.156**. Unfortunately, the newly installed methyl stereogenic center on **2.156** had the wrong configuration for didehydrostemofoline. The configuration was corrected with a three-step sequence, leading to an advanced intermediate aldehyde **2.157**.

Synthetic work then continued on the western side of the molecule. A pendant butanolide unit was added to aldehyde **2.157** using a vinylogous aldol reaction with homoenolate generated from butanolide **2.158**. The obtained butanolide **2.159** was oxidized to diol **2.160**. Using a thionocarbonate based dehydration, **2.160** provided didehydrostemofoline **2.161** in two steps.

The Overman approach proceeds towards the ultimate goal in a straight forward manner. The major drawback of the strategy, in this case, is the rather lengthy set of manipulations needed to both construct the rearrangement precursor **2.149** (11 steps), and to reach the target from rearranged **2.151** (15 steps).

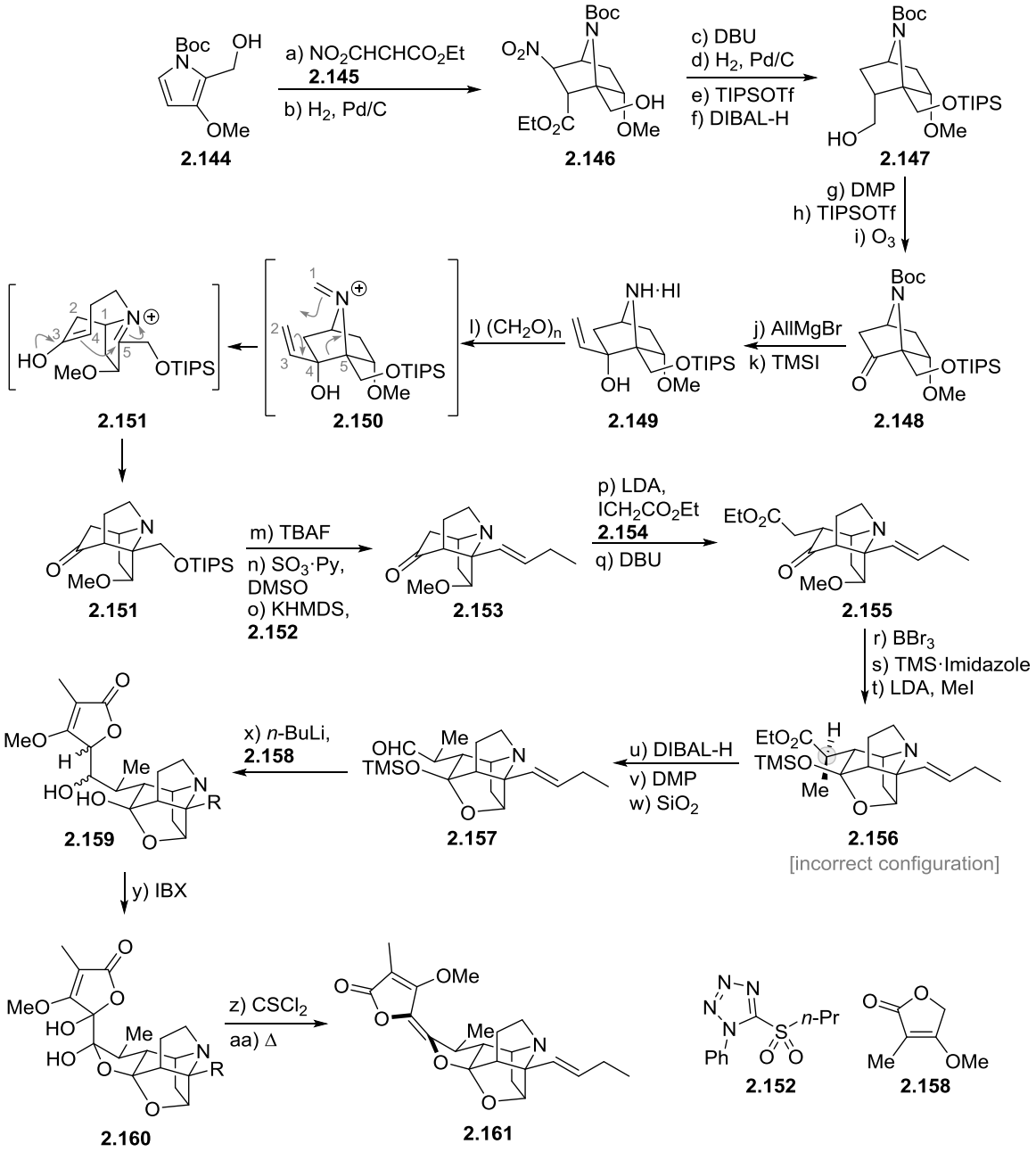

Scheme 14: Total synthesis of didehydrostemofoline (**2.161**). Reagents and conditions: a) (*E*)-3-nitroacrylate (**2.145**), EtOAc, rt; b) H_2, Pd/C, EtOAc, rt, 73% over two steps; c) DBU, DCM, rt; d) H_2, Pd/C, EtOAc, rt; e) TIPSOTf, Et_3N, DCM, –78 °C; f) DIBAL-H, PhMe, –78 °C, 51% over three steps; g) Dess–Martin periodinane, DCM, rt; h) TIPSOTf, Et_3N, DCM, –78 °C; i) O_3, MeOH–DCM, –78 °C, 75% over three steps; j) AllMgBr, $CeCl_3$, THF, –78 °C; k) TMSI, 2,6-lutidine, MeOH, 0 °C to rt, 85% over two steps; l) $(CH_2O)_n$, PhMe–MeCN, 80 °C, 94%; m) TBAF, THF, rt; n) SO_3·Py, Et_3N, DMSO, rt; o) KHMDS, **2.151**, DME, –55 °C, 70% over three steps; p) LDA, THF, ICH_2CO_2Et (**2.154**), –10 °C; q) DBU, PhMe, 130 °C, 67% over two steps; r) BBr_3, DCM, –78 °C to –10 °C then NaOH; s) TMS·Imidazole, 130 °C; t) LDA, MeI, THF–DMPU, –45 °C, 54% over three steps; u) DIBAL-H, DCM, –78 °C, 98%; v) Dess–Martin periodinane, DCM, rt; w) SiO_2, $CHCl_3$, rt, 54% over two steps; x) **2.158**, *n*-BuLi, THF, –78 °C, 93%; y) IBX, DMSO, 55 °C, 55%; z) $CSCl_2$, DMAP, DCM, –50 °C, 68%, (dr 3.5:1); aa) $(MeO)_3P$, 120 °C, 66%.

Taken together, some of the shortest and most efficient total syntheses involving the construction of 7/5 azabicyclic systems rely on using rearrangement reactions. Especially ring expansion or ring contraction rearrangements are particularily useful as they allowing a simpler ring system to be constructed first, and then converted into more complex ones. Rearrangement-based strategies are typically planned around the key rearrangement transformation. This inherent restriction to a key reaction divides the synthesis into two parts: first, making the rearrangement precursor, and second, converting the rearranged material into the penultimate target.

First part, reaching the rearrangement precursor sub-target, can be fairly straight-forward, typically relying on well-established chemistry. However, in cases where the sub-target synthesis is more cumbersome, rearrangement-based strategies lead to lengthy routes.

2.3.5 Peripheral disconnections

Peripheral disconnections are grouped to cover all other bond disconnections of the 7/5 ring system, except those in the near vicinity of the nitrogen atom (Figure 8). Peripheral disconnections are widely used with highly bridged structures containing the 7/5 azabicyclic core. Instead of using the azepane nitrogen as a functional group handle for disconnections, the peripheral disconnections use functionality at the periphery of the structures. In such cases, formation of the 7/5 azabicyclic core is a result of the construction of other motifs.

Figure 8: Disconnections considered peripheral.

Peripheral disconnections allow a great variety of different approaches to be implemented. For example, a radical cyclization leading to a cephalotaxus-like ring system in a cascade fashion was introduced by Ishibashi group in 2004, and has since been used in a 15-step total synthesis of cephalotaxine (Scheme 15).[49,50]

A sugar-derived protected triol **2.162** was triflated and treated with alkynyl lithium derived from phenylacetylene (**2.163**) to give alkyne **2.164**. Bromination of tosylate **2.164**, followed by acetal deprotection delivered diol **2.165**. The bromide **2.165** was cyclized in a radical cyclization to *exo*-olefin **2.166**. Protection of the diol **2.166** followed by ozonolysis of the olefin then provided ketone **2.167**.

Ketone **2.167** was condensed with iodoamine **2.168** to afford an enamine, which was directly *N*-acylated with acroloyl chloride (**2.169**) to give the cyclization precursor **2.170**. Treating iodide **2.170** with tributyl tin hydride and ABCN led to a radical 7-*endo* reaction closing the 7-membered azepane ring. Resulting

N-stabilized radical **2.171** underwent a further 5-*endo* cyclization, delivering pentacyclic amide **2.172** as a single diastereomer.

Deprotection of **2.172** followed by oxidation of the resulting 1,2-diol gave diketone **2.173**. Upon methylation, the diketone formed methyl enol ether **2.174**. Finally, reduction of oxycephalotaxine **2.174** with aluminium hydride gave cephalotaxine (**2.003**).

The approach assembles the cyclization precursor **2.170** in a quick and very convergent fashion. The structure of iodide **2.170** is also near-ideal for forming the 7/5 ring system. The *o*-substitution pattern of iodide in **2.170**, and the side chain of the aromatic unit place the forming *C*-radical in the vicinity of the enamine unit, facilitating smooth cyclization. Without this scaffolding in **2.170** the yield (27%) would be expected to be lower.

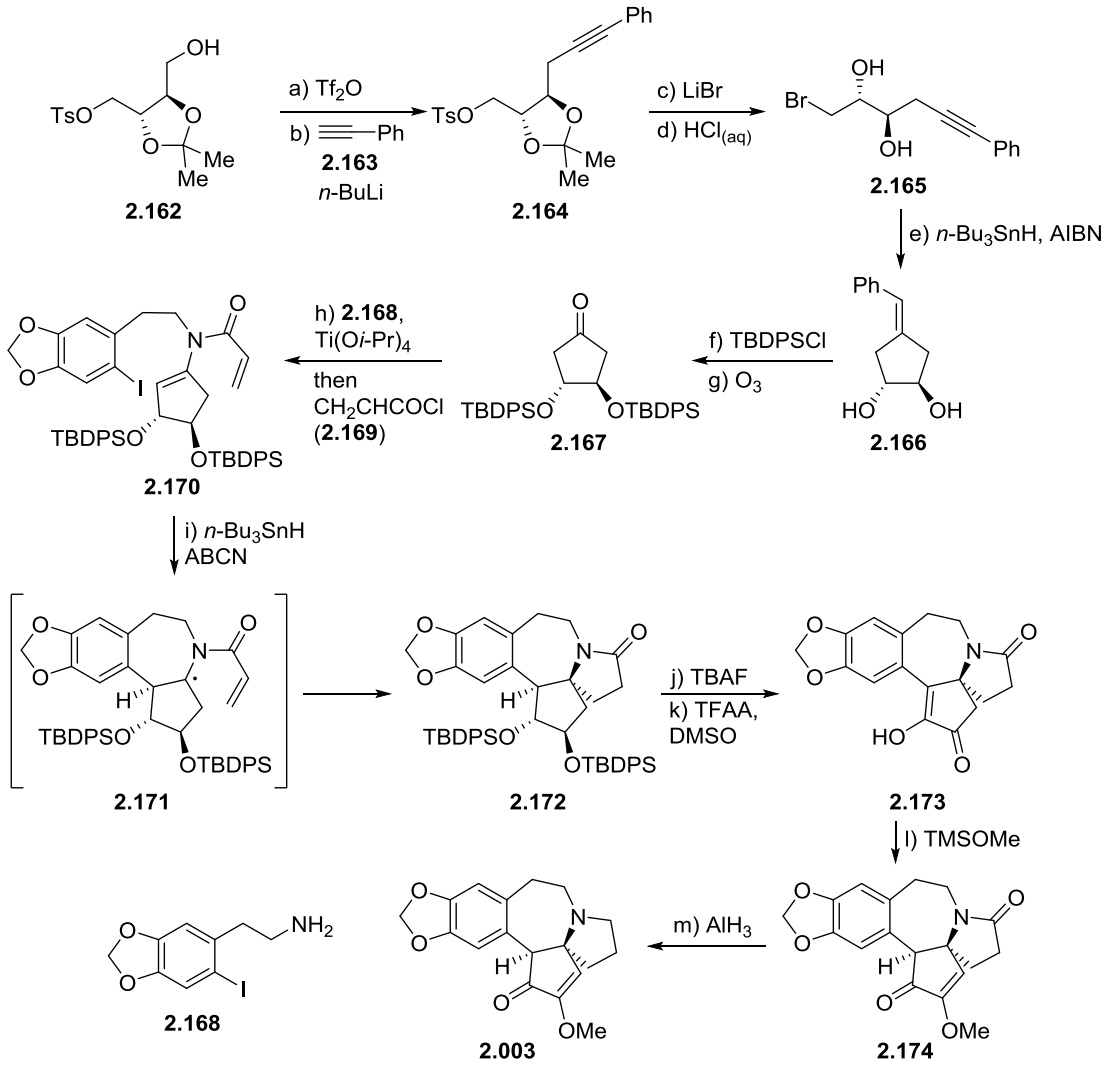

Scheme 15: Total synthesis of cephalotaxine (**2.003**). Reagents and conditions: a) Et_3N, Tf_2O, DCM, –20 °C; b) Phenylacetylene (**2.163**), *n*-BuLi, DMPU, –78 °C to –20 °C; c) LiBr, DMF, 80 °C; d) HCl (10% aq.), THF, reflux; e) *n*-Bu_3SnH, AIBN, PhH, reflux, 53% over 5 steps; f) TBDPSCl, imidazole, DMF, 91%; g) O_3, DCM, –78 °C, 80%; h) **2.168**, $Ti(OiPr)_4$, –78 °C to 0 °C then $PhNEt_2$, acryloyl chloride (**2.169**), –78 °C to 0 °C, 50%; i) *n*-Bu_3SnH, ABCN , PhCl, reflux, 27%; j) TBAF, THF, rt, 96%; k) TFAA, DMSO, –78 °C to –50 °C, 55%; l) TMSOMe, TfOH, DCM, 0 °C to rt, 74%; m) AlH_3, THF, 0 °C, 87%.

Peripheral disconnections are even more convenient to use in bridged structures than fused systems. Such is the case in the total synthesis of vincorine (**2.187**) by the MacMillan group (Scheme 16).[51]

Using protected methoxytryptamine **2.175** as the indole core, **2.175** is *N*-methylated and vinylated to give a masked diene **2.177**. Reacting diene **2.177** with a dienophilic iminium, generated from enal **2.178** and MacMillan's 1st generation catalyst **2.069**, resulted in a Diels–Alder reaction giving enamine **2.179**. The enamine **2.179** then isomerizes to the iminium ion **2.180**. The pendant amine side chain then attacks the resulting iminium ion **2.180**, generating the tetracycle **2.181**. A single dexterous domino reaction converted **2.177** into the advanced intermediate **2.181**.

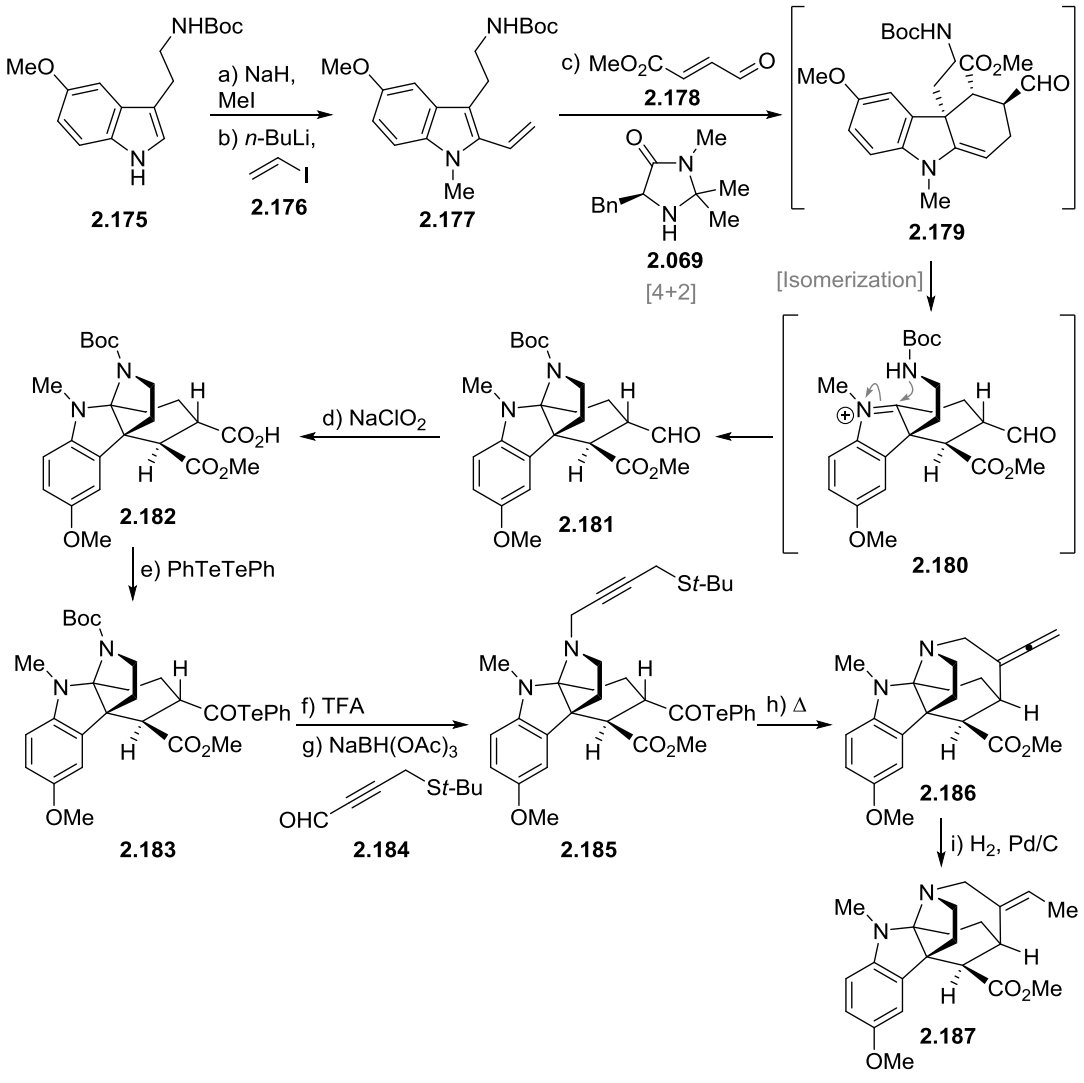

Scheme 16: Total syntheis of vincorine (**2.187**). Reagents and Conditions: a) NaH, DMF, 0 °C, then MeI; b) *n*-BuLi, DME, –40 °C, then $ZnCl_2$, –78 °C to rt then XPhos, vinyl iodide (**2.176**), 67% over two steps; c) **2.178**, 2.**069** · HBF_4, MeCN, –20 °C, 70%, (*ee* 95%); d) $NaClO_2$, 2-methyl-2-butene, THF, *t*-BuOH, H_2O, 0 °C, 84%; e) Isobutyl chloroformate, NMM, THF then PhTeTePh, $NaBH_4$, THF–MeOH, rt, 87%; f) TFA, rt; g) **2.184**, $NaBH(OAc)_3$, DCM, rt, 65% over two steps; h) 1,2-Dichlorobenzene, 200 °C, 51%; i) Pd/C, H_2, THF, –15 °C, 80%.

The following manipulations on **2.181** then aimed to construct the remaining bridging all-carbon unit. Aldehyde **2.181** was oxidized to a corresponding carboxylic acid **2.182** and reacted with diphenylditelluride to deliver an acyl telluride **2.183**. The acyl telluride would serve as a handle when constructing the 7-membered azepane ring. Telluride **2.183** was *N*-deprotected, and the liberated free amine reductively coupled to alkyne aldehyde **2.184**. When heated, telluride **2.185** underwent a radical cyclization with the alkyne, yielding allene **2.186**. Simple hydrogenation of allene **2.186** from the less hindered face provided (–)-vincorine (**2.187**).

Medium-sized rings can be difficult to form. In the vincorine case, the cyclization precursor **2.185** places the alkyne side chain in the proximity of the telluride for the radical cyclization. The vincorine synthesis is an example of a peripheral disconnection relying on a conformational bias to control the cyclization.

A common method in the synthesis of medium- and large sized rings is the ring-closing metathesis reaction (RCM).[52] Therefore, not surprisingly, ring-closing metathesis has also found applications in the synthesis of 7/5 ring systems. In their total synthesis of tuberostemonine, Wipf *et al.* used an RCM approach.[53,54] Chemoselectivity related issues complicated the synthesis, but the convenience of the RCM approach was unquestionable (Scheme 17).

Oxidative cyclization of Cbz-L-Tyrosine (**2.188**) gave a hydroindole derivative **2.189**. In a series of high-yielding transformations hydroindole **2.189** was converted into amine **2.191**. In preparation for the ring-closing metathesis, amine **2.191** was *N*-alkylated with cinnamoyl bromide (**2.192**), and the allylic alcohol oxidized to give the bicyclic enone **2.193**. Enone **2.193** was α-allylated to give **2.194**. The southern part of bicyclic **2.194** was now primed for a ring closing metathesis reaction.

Ring closing metathesis of **2.194** with the ruthenium catalyst **2.195** formed the azepine **2.196** in a 92% yield. Azepine **2.196** was then reduced to azepane **2.197**, while having the enone protected as a thiophenol adduct. The ketone had now served its purpose and was reduced and silylated to the protected vinyl alcohol **2.198**. Work was then initiated to install the last remaining rings.

To this end, ester **2.198** was converted to the corresponding Weinreb amide **2.199**. Lithiated orthoester **2.200** was then added, providing ketone **2.201**. The ketone **2.201** was reduced with L-selectride to an intermediate alcohol. Once the orthoester of this intermediate alcohol was cleaved, the substrate spontaneously cyclized to form butanolide **2.202**. After desilylation of **2.202**, the free allylic alcohol was subjected to Eschenmosher–Clarke rearrangement with *N*,*N*-dimethylacetamide dimethylacetal. The intermediate γ,δ-unsaturated amide was selenolactonized to afford the completed ring assembly **2.203**. Moving forward, selenide **2.203** was allylated with $AllSnPh_3$, and the northern butanolide methylated to give the near-complete tuberostemonine precursor **2.204**. After a four-step sequence truncating the allyl side chain, **2.204** gave tuberospironine **2.206**.

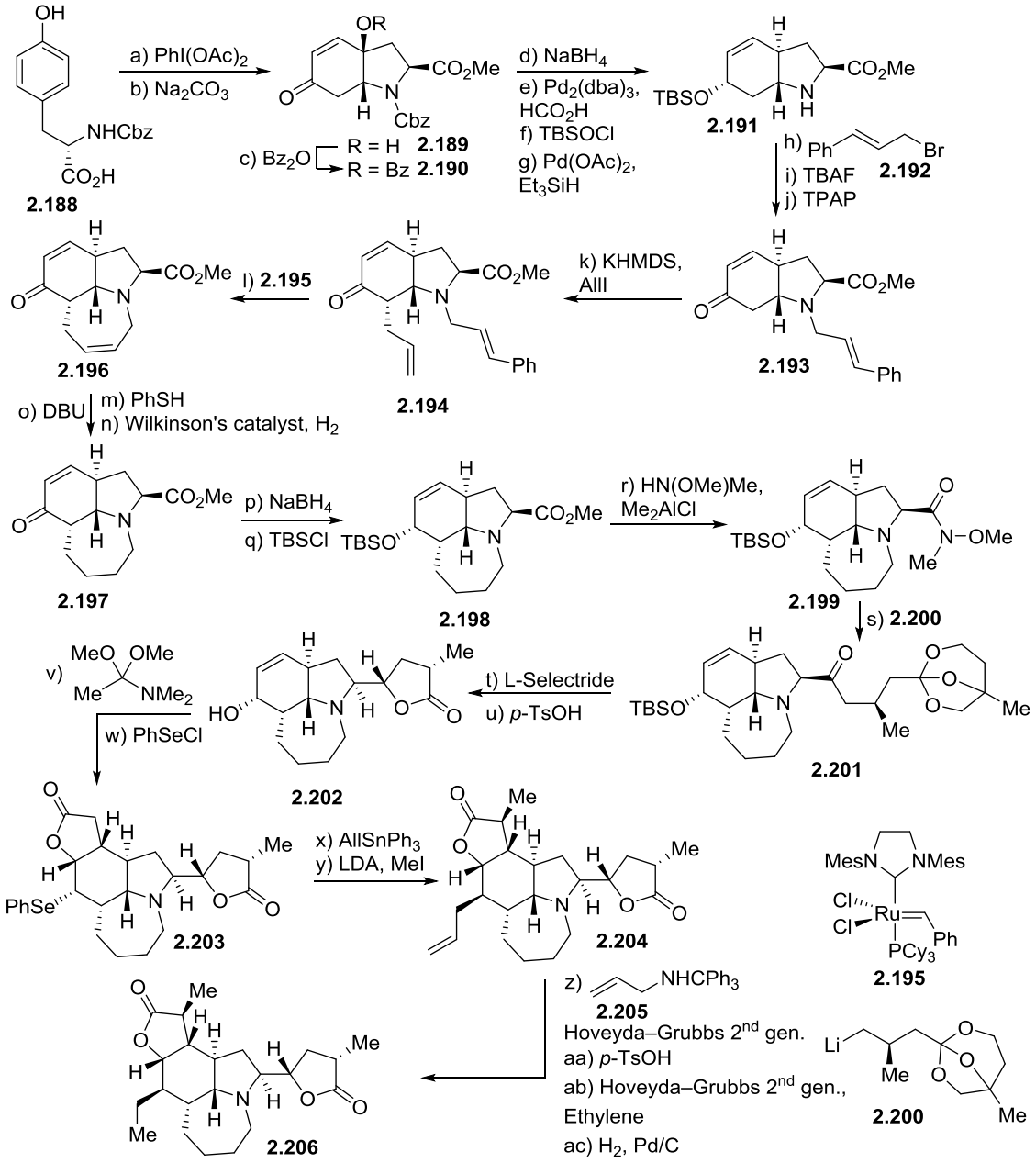

Scheme 17: Total synthesis of tuberostemonine (**2.206**). Reagents and conditions: a) $PhI(OAc)_2$, $MeNO_2$, rt, 35%; b) Na_2CO_3, MeOH, rt; c) Bz_2O, DMAP, pyridine, reflux, 51% over two steps; d) $NaBH_4$, $CeCl_3 \cdot 7H_2O$, MeOH, 0 °C, 97%; e) $Pd_2(dba)_3 \cdot CHCl_3$, Bn_3P, Et_3N, HCO_2H, THF, reflux, 93%; f) TBSCl, DMAP, imidazole, DCM, 0 °C, 97%; g) $Pd(OAc)_2$, Et_3SiH, Et_3N, DCM, rt, 90%; h) Cinnamyl bromide (**2.192**), K_2CO_3, PhMe, 60 °C, 96%; i) TBAF, THF, rt, 96%; j) NMO, TPAP, 4 Å MS, DCM, 0 °C to rt, 88% k) KHMDS, THF, –90 °C then AllI, 66%; l) Cat **2.195**, DCM, reflux, 92%; m) PhSH, DCM, Et_3N, rt; n) Wilkinson's catalyst, DCM, rt; o) DBU, DCM, rt, 89% over three steps; p) $NaBH_4$, $CeCl_3 \cdot 7H_2O$, MeOH, 0 °C, 71%; q) TBSCl, imidazole, DMAP, DCM, 79% over two steps; r) $HN(OMe)Me \cdot HCl$, $AlMe_3$, DCM, 0 °C to rt, 94%; s) 4,4′-di-*tert*-butylbiphenyl, Li, THF, –15 °C to –78 °C, then **2.200,** then **2.199**, 95%; t) L-Selectride, THF, –78 °C; u) *p*-TsOH, MeOH, rt, 70% over two steps; v) *N*,*N*-dimethylpropionamide dimethylacetal, xylenes, 140 °C, 78%; w) PhSeCl, MeCN–H_2O, 0 °C, 67%; x) AIBN, $AllSnPh_3$, THF, reflux, 70%; y) MeI, LDA, THF–HMPA, –78 °C, 59%; z) Hoveyda–Grubbs 2nd gen., allyltritylamine (**2.205**), DIPEA, DCM, reflux, 85%; aa) *p*-TsOH, DCM, DCM, reflux; ab) Hoveyda–Grubbs 2nd gen., ethylene, DCM, reflux, 81% over two steps; ac) H_2, Pd/C, MeOH, rt 97%.

Again, a rigid octahydroindole core is used to assist with the cyclization at **2.194** → **2.196**. As is the case for tuberostemonine (**2.206**), the 7-membered ring is entirely without functionalization, making the peripheral disconnection a rather convenient one. Also, the peripheral cyclization step does not impose any concern over stereochemistry.

Intramolecular Diels–Alder reactions have also led to powerful synthetic strategies. Diels–Alder reactions allow forming six-membered units with full stereofidelity, and when used in an intramolecular fashion, allow concurrent formation of complex fused ring systems.[55] It is not immediately obvious how Diels–Alder reactions could be applied in 7/5 azabicyclic systems. In cases of masked 7/5 azabicyclic systems, however, intramolecular Diels–Alder reactions can offer very tempting approaches. This is demonstrated by the Gin's impressive total synthesis of hestine alkaloid nominine (**2.006**) (Scheme 18).[56]

Despite the target molecule **2.006** being aliphatic, the synthesis commenced with an aromatic starting material, the protected *p*-methoxybenzaldehyde **2.027**. An *o*-lithiation converted the acetal **2.207** into chloroketone **2.209**. Displacing the α-chlorine on **2.209** with azide, followed by an acid-catalyzed rearrangement then generated the azide bisacetal **2.210**.

Reductive amination of azide **2.210** with aldehyde **2.211** formed a 3:3:2:2 mixture of diastereomers of mixed acetal **2.212**. TFA treatment of **2.212** resulted in expulsion of methanol and gave directly the stable cycloaddition precursor **2.213**. This charming sequence allowed key precursor **2.213** to be prepared on scale.

Heating the betaine **2.213** in a sealed tube resulted in an intramolecular 1,3-dipolar cycloaddition between the betaine and the α,β-unsaturated nitrile. The intramolecular cycloaddition formed the intricate polycyclic amine **2.214** in 1:3.6 diastereoselectivity. Ketone **2.214** was then deoxygenated in a three-step sequence leading to the nitrile **2.215**. Nitrile **2.215** was reduced to an aldehyde with DIBAL-H. The intermediate aldehyde was Wittig olefinated to deliver alkene **2.216** to be used in an upcoming Diels–Alder reaction.

Proceeding to the final cyclization phase, the anisol **2.216** was reduced in a Birch type reduction to form a stable β,γ-cyclohexenone **2.217**. Treating ketone **2.217** with pyrrolidine formed an intermediate dienamine **2.218**. An intramolecular Diels–Alder reaction then united the olefin dienophile and dienamine diene to give **2.219**, a compound with the entire polycyclic scaffold of nominine. The final steps on the Diels–Alder adduct **2.219** involved a Wittig olefination, followed by a diastereoselective allylic oxidation to afford nominine (**2.006**).

The Gin synthesis of nominine is an intriguing piece of work, which must have necessitated extensive experimental studies. The use of time-tested Diels–Alder reaction does not, perhaps, seem like the ideal tool for constructing 7/5 ring systems. In cases of highly bridged systems masking the 7/5 ring system, however, using the Diels–Alder reaction can have a profound impact. Also, again, we see a prefabricated ring system assisting in the formation of a more complex core unit.

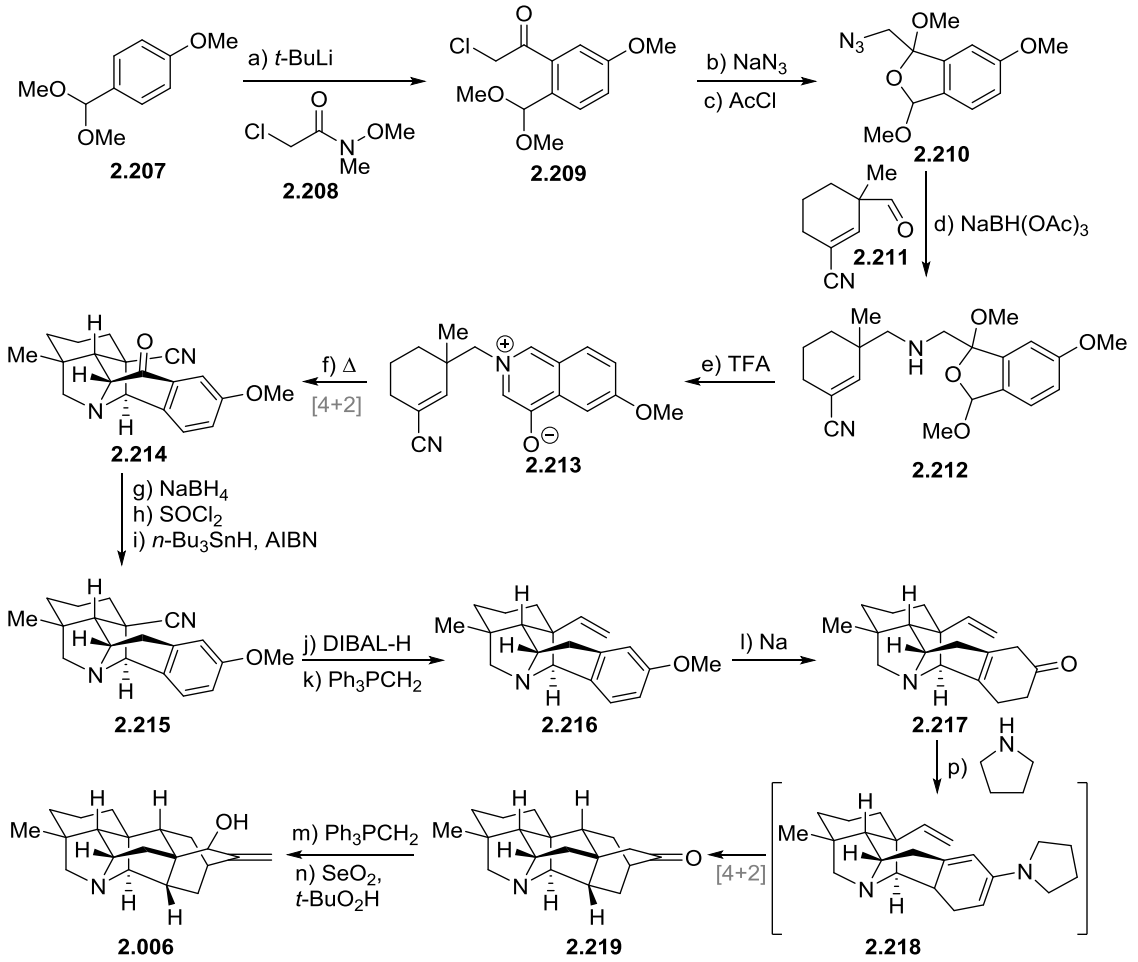

Scheme 18: Total synthesis of (±)-nominine (**2.006**). Reagents and conditions a) *t*-BuLi, Et_2O, –23 °C then **2.208**, 52%; b) NaN_3, acetone, rt, 95%; c) AcCl, MeOH, rt, 99%, (dr 3:2); d) **2.211**, *n*-Bu_3P, $NaBH(OAc)_3$, DCM, rt, 79%, (dr 3:3:2:2); e) TFA, DCM, 0 °C, 93%; f) THF, 180 °C (dr 1:3.6); g) $NaBH_4$, EtOH, rt; h) $SOCl_2$, DCM, reflux; i) *n*-Bu_3SnH, AIBN, PhH, reflux, 68% over four steps; j) Na, *i*-PrOH, THF, –78 °C; j) Pyrrolidine, MeOH, 60 °C, 78%; k) Ph_3PCH_2, THF, 70 °C, 77%; l) SeO_2, *t*-BuO_2H, DCM, rt, 66%, (dr 7:1).

Peripheral disconnections showcase some of the most impressive synthetic approaches to 7/5 ring systems. Their applications are often based on pre-formed rigid backbones. The rigid backbones limit the degrees of freedom for the cyclization precursor, as well as the stereochemical outcomes of the reactions. Peripheral disconnections, when applicable, should thus be considered alongside with the more traditional disconnections made in close proximity to the ring heteroatoms.

2.4 Strategies relying on intermolecular annulation

Few examples of intermolecular annulation strategies exist in the context of 7/5 azepane chemistry (Figure 9). This is not entirely unexpected, as intermolecular

methods impose significant restraints on stereocontrol, and such cyclizations would be expected to be prone to oligomerization side-reactions.

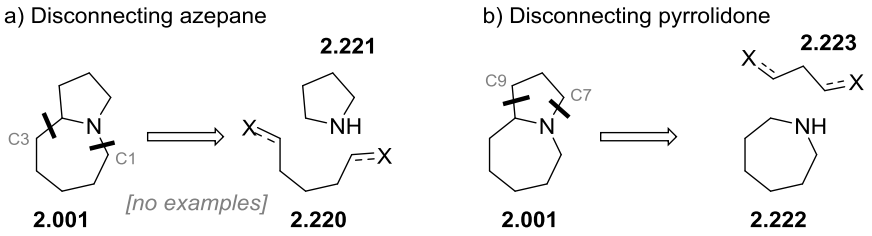

Figure 9: Intermolecular ring annulations a) No examples found for intermolecular annulation using C1 and C3 disconnections (**2.220** + **2.221**) b) Single example found using C9 and C7 disconnections (**2.222** + **2.223**).

The single example of an intramolecular approach is from a 2013 formal synthesis of Cephalotaxine by Zhang *et al* (Scheme 19).[57] The synthesis was initiated with the transannular cyclization reaction. A reaction between a known amine **2.224** and 1,3-dibromopropane afforded the annulation product **2.226** in one step and 79% yield. Further α-allylation of ketone **2.226** delivered amine **2.227** with all the necessary carbon atoms of the target **2.228** in place.

Subsequent Wacker oxidation of **2.227** resulted in the formation of diketone **2.228**, which underwent an intramolecular aldol condensation to yield enone **2.228**. The synthesis campaign was completed by deprotection-protection sequence on **2.228** to deliver the enone **2.228**, from which the synthesis of cephalotaxine is known.[58]

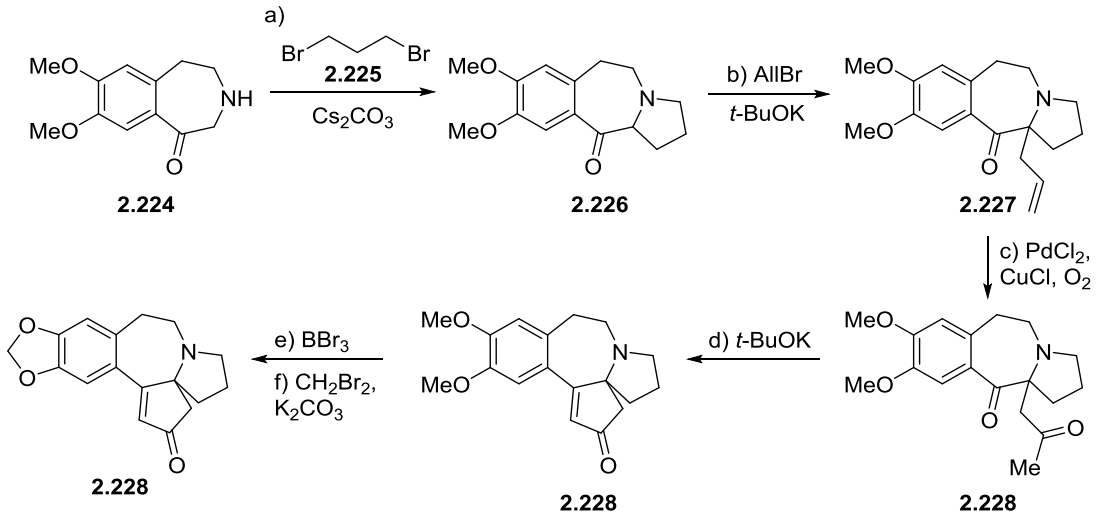

Scheme 19: Formal synthesis of (±)-cephalotaxine. Reagents and conditions: a) 1,3-dibromorpopane (**2.225**), $CsCO_3$, MeCN, reflux, 79%; b) AllBr, *t*-BuOK, THF, –15 °C, 85%; c) $PdCl_2$, $CuCl_2$, NaCl, O_2, DMF–H_2O, 42%; d) *t*-BuOK, *t*-BuOH, 40 °C, 80%; e) BBr_3, DCM, –78 °C; f) K_2CO_3, CH_2Br_2, MeCN, reflux, 50% over two steps.

2.5 Conclusions

The 1-azabicyclo[5.3.0]decane 7/5 ring system has been approached from many synthetic directions. Several key points of interest can be extracted from the rather widespread examples.

First, 5-membered building blocks are widely used as starting materials. Readily available compounds, such as succinimide, proline, and pyroglutamic acid, are represented in almost all syntheses despite the applied ring-forming strategy. Second, as a corollary, the 7-membered azepane ring is typically constructed onto the 5-memebered pyrrolidine unit. As the azepane is typically more functionalized, a rather diverse set of approaches have been applied in their construction, such as *N*-alkylations, rearrangements, acylations and so on. Third, peripheral disconnection strategies, i.e using disconnections not α or β the heterocyclic nitrogen atom, have shown surprising synthetic efficiency. Fourth, in the case of 1-azabicyclo[5.3.0]decane ring systems, intermolecular annulations seem to be very underrepresented.

Even with the ample research literature available on 1-azabicyclo[5.3.0]decane alkaloids, their chemistry is still developing. For example, catalytic enantioselective methods are scarce as opposed to the ample use of chiral pool starting materials.

3 TOWARD A DIVERGENT SYNTHESIS OF STEMONA ALKALOIDS

"Only when one no longer knows what one is doing
does the painter do good things"

– Edgar Degas

3.1 Aim of the study

Stemona is the largest genus within *Stemonaceae* species plants distributed in the subtropical and tropical regions of south-eastern Asia. The plants are deciduous and survive in the hot subtropical regions with their strong storage roots. These roots have been used for thousands of years in folk medicine. In fact, dried roots of stemona plants are still used for their antitussive effects.[59] Many of the alkaloids isolated from the roots of Stemona plants, coined stemona alkaloids, have shown intriguing biological activities, ranging from insecticidal to neuromuscular effects.[60]

Despite extensive synthetic studies, only relatively few divergent syntheses of stemona alkaloids have been studied compared to many other alkaloid families.[59,61,62] As divergent strategies allow comprehensive syntheses of entire natural product families by diverting a late-stage intermediate into a number of natural product targets, such approach could have a lasting effect on stemona alkaloid chemistry.

We focused our divergency study on the stemoamide subfamily of stemona alkaloids. The stemoamide subfamily is built around a central 5/7/5 scaffold, with stemoamide (**3.006**) being the archetypal member (Figure 10a). Intriguingly, this subfamily comprises of a great variety of alkaloids having their lactam rings oxidized or reduced. Notably, alkaloids with more oxidized lactam units have only been tentatively studied.[63,64]

To access the higher oxidized lactam units, we chose the α,β-unsaturated tricyclic lactam **3.003** as our point of divergence (Figure 10a). With the unsatu-

rated lactam unit of **3.003** already at a higher oxidation, accessing other stemona alkaloids, including but not limited to stemoamide **3.006**, bisdehydroneostemoninine **3.004**, parvistemonine A **3.005** and stemona-lactam O **3.007**, should be possible with relative ease (Figure 10a).

To realize this plan, a convenient method for preparing the tricyclic key intermediate **3.003** was needed. Disconnecting the azepane of **3.003** in an *N*-alkylation reveals an intermediate of the type **3.002**, which can be traced to the butanolide aldehyde **3.001**. In turn, aldehyde **3.001** can be synthesized using an organocatalytic Mukaiyama–Michael reaction previously developed in our group by Dr. Eeva Kemppainen (Figure 10b).[65,66] The use of butenolide aldehyde **3.001** was also backed up by literature precedents showing the use of racemic butanolide units of the type **3.001** in total syntheses of stemona alkaloids.[67]

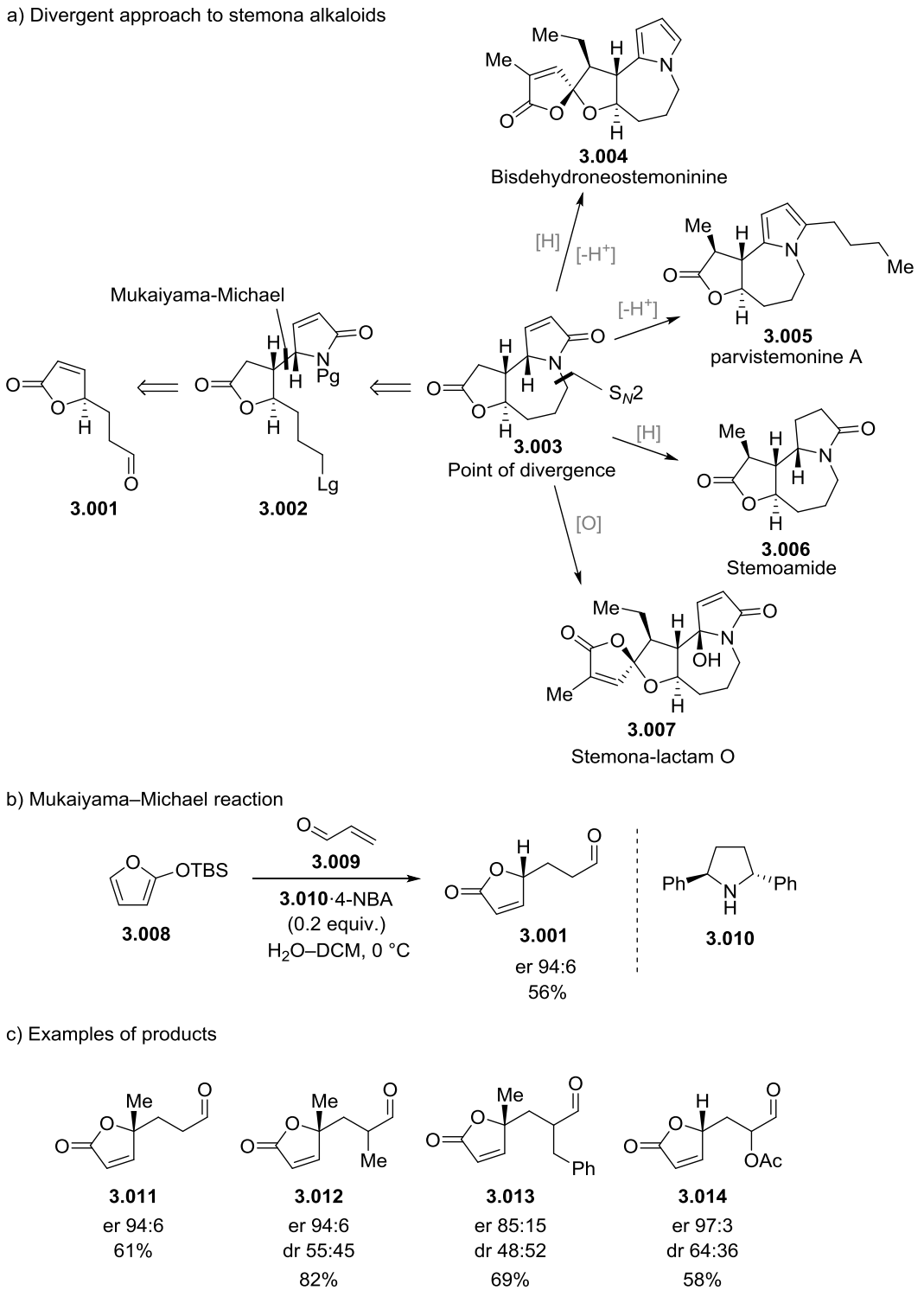

Figure 10: Plan for a divergent synthesis of stemona alkaloids. a) Unsaturated stemona alkaloid core **3.003**, derivable from aldehyde **3.001**, would allow divergent access to many stemona-alkaloids, such as bisdehydroneostemoninine (**3.004**),[68] parvistemonine A (**3.005**),[69] stemoamide (**3.006**),[70] and stemona-lactam O (**3.007**).[71] b,c) Mukaiyama–Michael reaction with a biarylpyrrolidine catalyst **3.010** allows forming enantiopure butanolide aldehydes (**3.011 – 3.014**) in good yields and enantioselectivities.[65]

3.2 Strategy

As delineated in Figure 10, a synthetic route to access **3.003** from a butenolide **3.001** was needed. Disconnecting **3.003** in an *N*-alkylation allowed **3.003** to be traced back to **3.002** (Figure 11a). At this stage, a vinylogous Mukaiyama–Michael reaction would very conveniently form the α,β-unsaturated lactam of **3.002**. Following this line of thought led to a prefabricated nucleophile **3.016** and butenolide **3.015** with a suitable leaving group attached.

Several risks are associated with the strategy (Figure 11b). First, two new stereogenic centers at C9 and C9a are formed as silyloxypyrrole **3.016** reacts with butenolide **3.015**. With our previous experience on Michael additions to butenolides, the C9–C10 stereochemistry would be cleared and set *anti*, as the nucleophile would attack the Michael acceptor from the less hindered face.[72] However, the C9a configuration is dependent on the relative orientation of silyloxypyrrole **3.016** with respect to the Michael-acceptor **3.015** during the attack, and cannot be reliably predicted *a priori*. Second, there is a risk of racemizing the butenolide **3.015** at the relatively acidic hydrogen at the C5 stereogenic center.[72] If the butanolide gets deprotonated at any stage, the enantiopurity of **3.015** could be severely compromised.[72] Third, due to the electrophilic nature of the α,β-unsaturation of **3.002**, possible side reactions could interfere with the synthesis.

We hoped, however, that by alternating the variable units on the starting materials **3.015** and **3.016** (nitrogen protection, silyl group, and leaving group), and with minor tactical changes, the route would work. With this plan at hand, we embarked on the synthesis campaign.

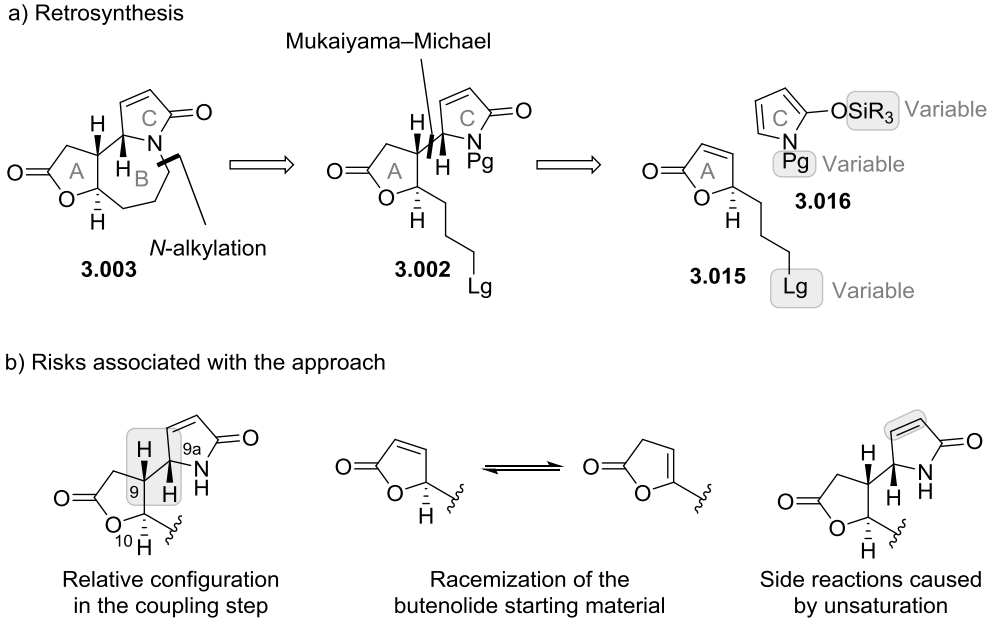

Figure 11: Strategy and retrosynthesis a) Proposed retrosynthesis leads to a highly modular A and C ring units **3.015** and **3.016** b) Several risks are associated with the chosen strategy.

3.3 Initial studies

A Mukaiyama–Michael reaction between silyloxypyrrole **3.018** and butenolides was not known in the literature when the work was initiated. Because of this, we started with a model study to establish conditions for such a reaction. Previous reports for reactions of silyloxypyrroles with acyclic Michael acceptors pointed towards potential Lewis acids, namely $SnCl_4$ and $Sc(OTf)_3$.[73–75]

The starting materials for the synthesis, *N*-Boc silyloxypyrrole **3.018** and γ-butyrolactone (**3.017**) were prepared in multigram scale using literature procedures.[76,77] In the initial screening experiments (Table 1) with γ-butyrolactone (**3.017**) TBSOTf with hexafluoroisopropanol (HFIP) clearly outperformed other Lewis acids. Several modifications, including the addition of 4 Å molecular sieves, improved the yield up to 48%.

Table 1: Initial coupling studies between butenolides and silyloxypyrroles

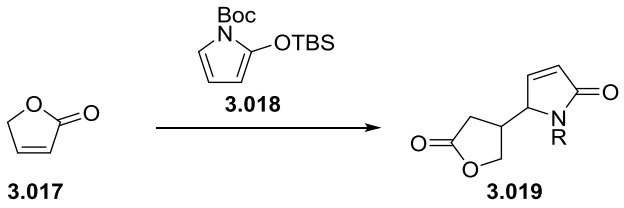

Entry	Conditions	Result
1	$SnCl_4$ (1.0 equiv.), DCM, –78 °C to rt	**3.018** decomposed
2	TBAF (1.0 equiv.), THF, –78 °C	**3.018** decomposed
3	$BF_3 \cdot OEt_2$ (1.0 equiv.), THF, –78 °C	**3.018** decomposed
4	$SnCl_4$ (2.2 equiv.), DCM, –78 °C	Traces of **3.018**
5	$Yb(OTf)_3$ (0.1 equiv.), THF, 0 °C	Traces of **3.018**
6	$Sc(OTf)_3$ (0.1 equiv.), HFIP (5.0 equiv.), DCM, 0 °C	23%
7	$SnCl_4$ (0.1 equiv.), HFIP (5.0 equiv.), DCM, 0 °C	4%
8	TBSOTf (0.1 equiv.), HFIP (5.0 equiv.), DCM, 0 °C	25%
9	TBSOTf (0.1 equiv.), HFIP (5.0 equiv,), 4 Å MS	48%
10	TBSOTf (0.1 equiv.), HFIP (5.0 equiv), 2,6-lutidine (1.0 equiv.), 4 Å MS	**3.018** slowly decomposed
11	TBSOTf (0.1 equiv.), DCM, 0 °C	Traces of **3.018**
12	Tf_2NH (0.1 equiv.), 0 °C	Traces of **3.018**
13	(*R*)-TRIP (0.1 equiv.), 0 °C	**3.018** decomposed

The marked performance of TBSOTf and HFIP led us to hypothesize that instead of Lewis acid catalysis, the reaction might also proceed under Brønsted acid catalysis (Figure 12a). More specifically, two possible activation modes for the butenolide can be envisioned, as the butenolide can either be protonated or silylated (Figure 12b). The role of HFIP would then be three-fold 1) forming a catalytic amount of triflic acid (**3.023**) *in situ* 2) giving rise to a silyl transfer reagent (**3.022**) 3) functioning as an ion-stabilizing solvent.[78] In a control experiment, formation of TfOH (**3.023**) was observed when HFIP (**3.020**) was treated with TBSOTf (**3.021**) in anhydrous $CDCl_3$.[79,80] This result suggests that TfOH might also be the true catalyst.

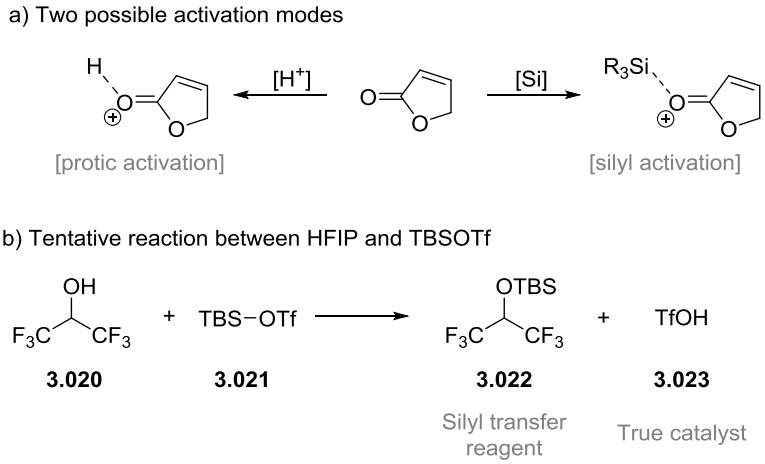

Figure 12: a) Both Brønsted acid activation and silyl-activation modes of butanolide are possible. b) Presumed reaction between hexafluoroisopropanol (**3.020**) and tert-butyldimethyllyltriflate (**3.021**). Tentative confirmation from NMR experiments agree with the formation of silylated hexafluoroisopropanol **3.022** and triflic acid **3.023**.

We also attempted a direct Friedel–Crafts type coupling of γ-butyrolactone (**3.017**) and *N*-methylpyrrole (**3.024**) (Scheme 20). Previous literature examples show pyrrole and indole reacting in Michael additions, but only with highly reactive dicarbonyl Michael-acceptors.[81,82] As butenolides are markedly less reactive than even typical esters, it is highly likely that the pyrrole simply polymerized, and none of the desired product **3.025** was observed.[83]

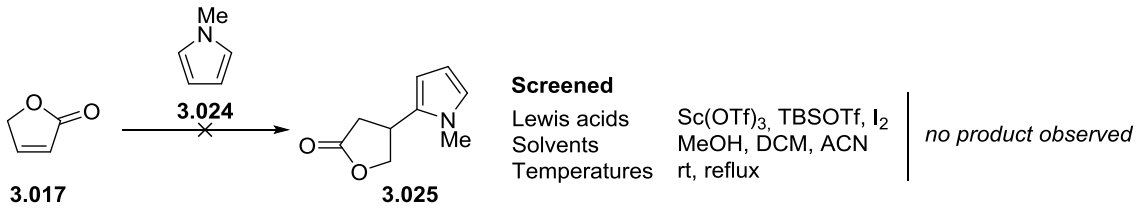

Scheme 20: Direct Friedel–Crafts coupling was not successful.

3.3.1 First approach with bromide

Having identified viable conditions (TBSOTf, HFIP) for the key Mukaiyama–Michael reaction, we then turned our attention to using the real butenolide substrate. To install different leaving groups, the butenolide aldehyde **3.001** was reduced into a corresponding alcohol **3.026**. Initially, the enantioenriched Mukaiyama-Michael product aldehyde **3.001** was reduced under Luche conditions ($CeCl_3 \cdot 7H_2O$, $NaBH_4$). These conditions were chemoselective in providing the desired butenolide alcohol **3.026**, but the product was completely racemized. To resolve the issue, Luche conditions were replaced with a less basic $BH_3 \cdot THF$ as the reductant. This modification suppressed the unwanted epimerization, affording enantioenriched alcohol **3.026** (Scheme 21a).

Several leaving groups could be installed to alcohol **3.026**. We anticipated halide leaving groups to interfere the least, compared to, say, alkynyl sulfonates, with the upcoming Lewis acid catalyzed Mukaiyama–Michael reaction. Thus, the alcohol was brominated under Appel conditions to butenolide bromide **3.027**.

Now, the bromide fragment **3.027** was coupled with silyloxypyrrole **3.018** under the previously established conditions for the model reaction (TBSOTf, HFIP, 4 Å MS). Despite moderate performance with the model system, the yields of the desired adduct **3.028** were low and varied between different batches. Additionally, the little of **3.028** that was obtained had a dr of ~1:1 based on ^{1}H NMR.

With longer reaction times, Mukaiyama–Michael reaction between bromide **3.027** and silyloxypyrrole **3.018** gave an unexpected rearranged product **3.029**. Subsequent NMR kinetics experiments showed how the desired adduct **3.028** rearranges into the undesired butanolide **3.029**. Even before all starting material bromide **3.027** was consumed, **3.029** had already formed to a significant degree based on ^{1}H NMR.

Several reasonable mechanistic options for the rearrangement can be envisioned. One plausible option is presented in Scheme 21b, where the butanolide is first silylated, and deprotonated to form a silyloxyfuran and butyrolactone. These compounds are essentially the starting materials but with the nucleophile and electrophile having changed places.

Screening alternative Lewis acids, additives, addition rates, temperatures and catalyst loadings did not suppress the formation of **3.029**. After extensive experimentation, our attention turned to other leaving group options.

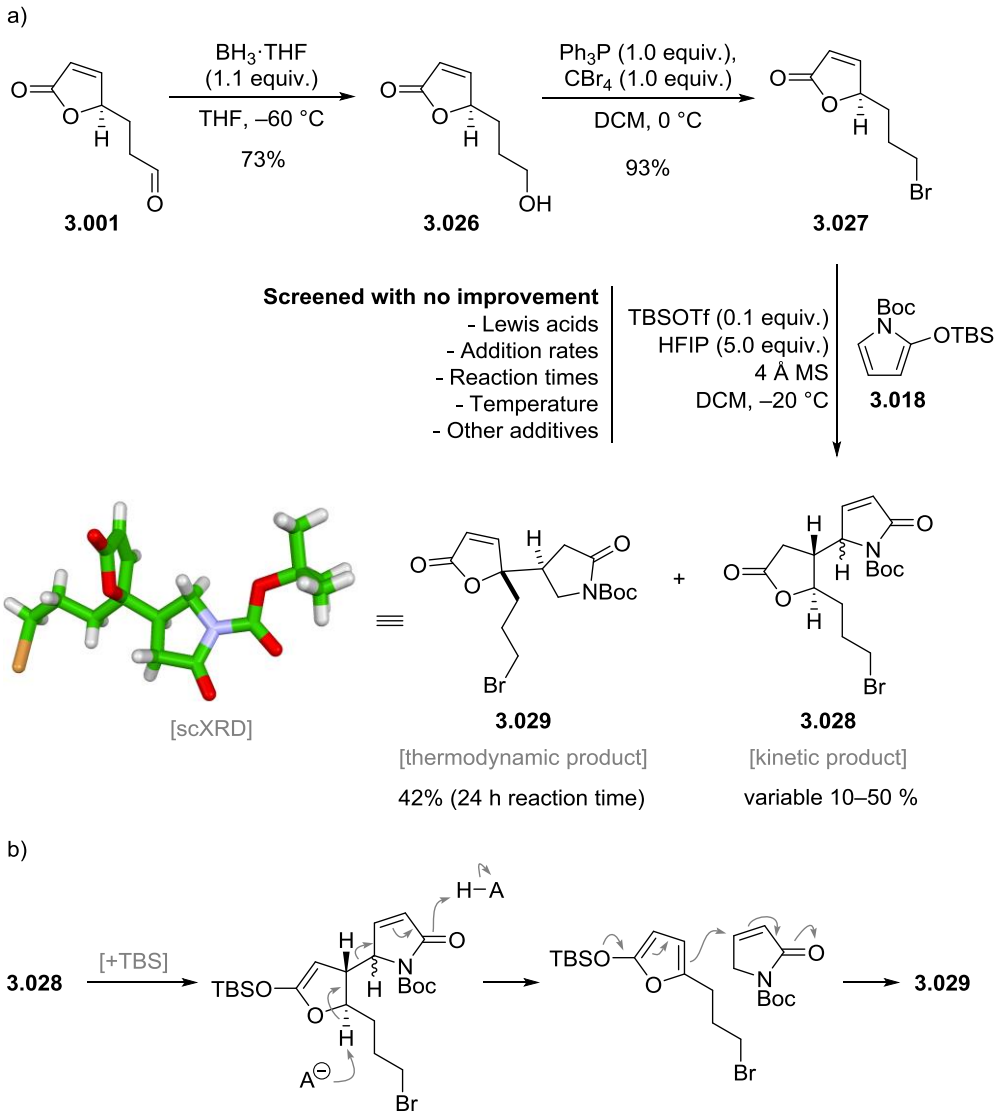

Scheme 21: a) Synthesis of bromobutenolide fragment **3.027** from aldehyde **3.001**. The bromobutenolide adduct **3.027** is not stable and rearranges to give **3.029**. b) Proposed mechanism for the rearrangement reaction.

3.3.2 Revised approach with mesylate

With only mixed success with bromide **3.027**, we switched to mesylate **3.030**, hoping that this change would suppress the rearrangement side reaction (Scheme 22). With mesylate **3.030**, the Mukaiyama–Michael coupling to form **3.031** worked yet again in variable yields, but thankfully the rearrangement pathway was not observed. The exact reason why mesylate suppressed the rearrangement is, at the moment, unknown.

The adduct **3.031** was again formed with dr ~1:1, with some variation between batches. Purification of **3.031** proved very tedious, as hydrolyzed nucleophile **3.032** co-eluted with the product **3.031**. With complications in purification, and the capricious nature of the reaction, a new approach was clearly needed.

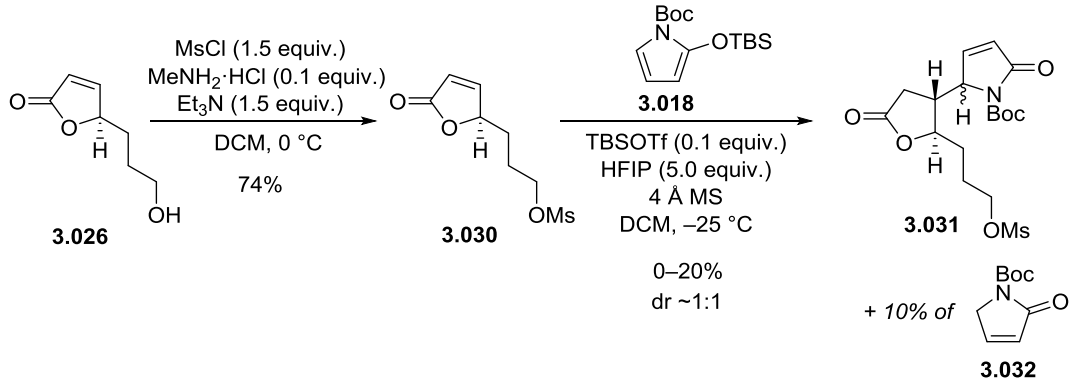

Scheme 22: Preparation of mesylate butenolide **3.030** and formation of adduct **3.031**.

The impure mesylate fragment **3.031** was deprotected with TFA to scout the route further (Scheme 23). Treating **3.031** with trifluoroacetic acid led to a single new spot on TLC. Within minutes, however, this first spot started dissipating, giving way to another new spot. The product was isolated, and shown to be a 1.1:1 mixture double-bond migrated γ,δ-enamides **3.034** and **3.035**. Deducing from this, the initial product of the deprotection reaction is presumably the α,β-unsaturated lactam **3.033**, which then migrates to give the γ,δ-unsaturated enamides **3.034** and **3.035**.[84]

Our initial plan (Figure 10) relied on the cyclization of α,β-unsaturated free amide **3.033** to the tricyclic core. This approach would not work, and instead of cyclization, the free amide would isomerize to the enamide. This problem would have to be solved later on.

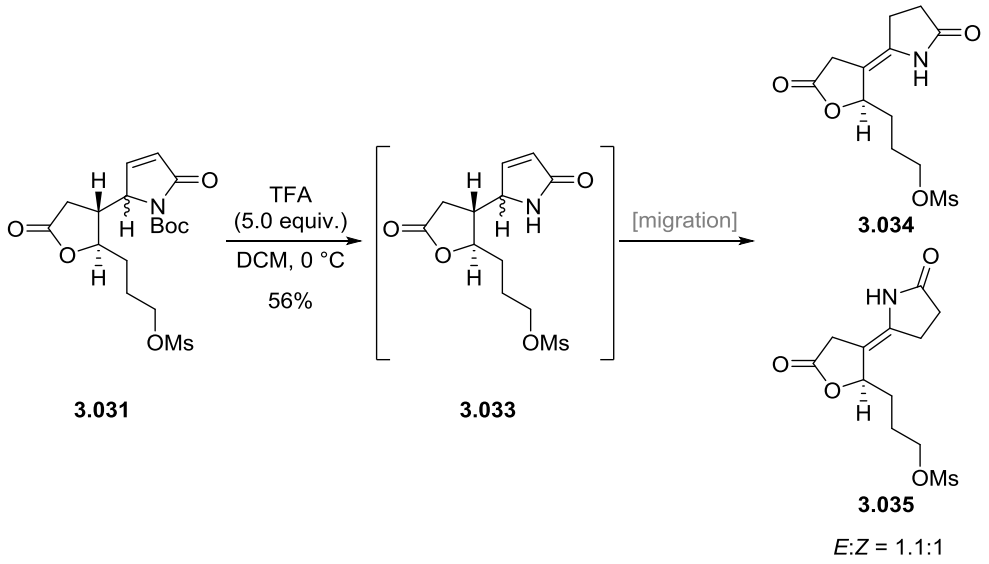

Scheme 23: Deprotection of lactam **3.031** leads to double-bond migration giving a mixture of enamides **3.034** and **3.035**.

3.3.3 Third and final approach with tosylate

Faced with rearrangement side reaction with the bromide **3.027** and scalability issues with mesylate **3.030**, we opted to prepare the corresponding tosylate **3.036** in hopes that the aromatic unit would aid with purification, and the sulfonate group might hinder the rearrangement observed with bromide.

Tosylation of alcohol **3.026** under typical tosylation conditions (TsCl, Et_3N, DMAP) proceeded only very sluggishly over several hours, which gave triethyl amine time to epimerize the butenolide **3.026** (from 94:6 to 90:10 er). Significantly faster tosylation was observed with a method from the Tanabe group, using methylamine hydrochloride as an auxiliary base.[85] This modification gave complete conversion to tosylate **3.036** in minutes without compromising the enantiopurity. When the thus obtained tosylate **3.036** was used in the Mukaiyama–Michael reaction, the yields of **3.037** improved significantly (Scheme 24). Still, the reaction seemed to behave in an erratic way, with varying yields and conversions.

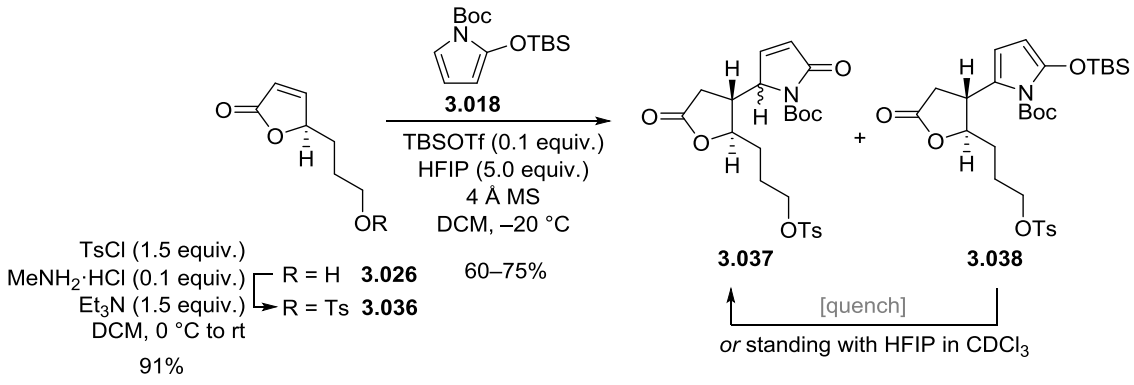

Scheme 24: Using tosylate as the leaving group allows the vinylogous Mukaiyama–Michael reaction with **3.036** to proceed without significant complications.

A surprisingly good yield of the desired adduct **3.037**, 67%, was obtained when the quenched reaction mixture was left in a fridge overnight. This observation sparked further investigations on the reaction.

The Mukaiyama–Michael reaction was very tedious to follow (some 10 spots on TLC, crowded crude ^1H NMR). However, allowing reaction mixtures to stand after aqueous quench, showed on TLC that a very nonpolar compound disappeared and the product **3.037** spot enhanced. Quenched with triethylamine, instead of pH 7.0 buffer used in aqueous quenches, the abovementioned nonpolar compound could be isolated. Structural studies revealed the compound to be a silyloxypyrrole derivative **3.038** of the desired product **3.037** (Scheme 24). Standing in HFIP/$CDCl_3$, the silyloxypyrrole **3.038** slowly hydrolyzed to the lactam product **3.037** with 1:1 dr.

The erratic yields of **3.037** observed for the reaction could now be explained. The exact time the quench and extraction stages took, and the amount of water the HFIP had, altered the ratios of silylated **3.038** and non-silylated **3.038**. This, in turn, translated to a wide yield range of **3.037**, depending on how

much material was trapped in the silylated form **3.038**. The discovery led to an alternative quenching method, where after addition of pH 7.0 buffer, the reaction mixture is stirred until TLC shows all **3.038** is hydrolyzed. With this modification at hand, yields of **3.037** ranging from 60–70% were routinely obtained.

The best conditions found for the reaction are shown in Table 2 and were obtained by trial-and-error. At this point, a robustness screen was carried out by modifying several reaction parameters (Table 2). In these experiments the Mukaiyama–Michael reaction was also observed to proceed with triflic acid as the catalyst, but with a dr of 1:2. The initially recognized addition of molecular sieves was now observed to lower the yield somewhat. All-in-all the reaction performed with a stable 75% yield and a dr of 1:1.

Table 2: Deviation from optimized conditions for the vinylogous Mukaiyama–Michael reaction.

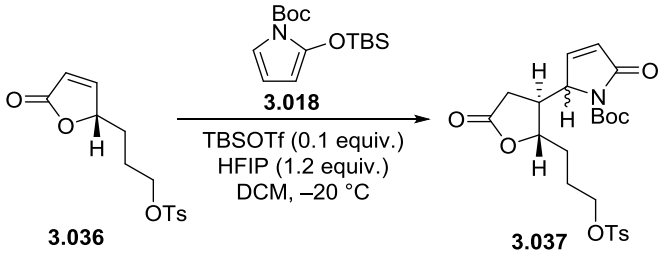

Entry	Change	Yield
1	No change	75%
2	No HFIP	10%
3	4 Å MS (50 wt-%)	65%
4	1.1 equiv. of **3.018**	61%
5	0.5 equiv. of HFIP	48%
6	0.1 equiv. of HFIP	12%
7	No precautions[a]	72%
8	0.1 equiv. of TfOH, no HFIP, no TBSOTf	13%
9	0.1 equiv. of TfOH, no TBSOTf	61%

[a]No rigorous drying or handling under argon.

Scaling the method up to provide grams of **3.037** allowed several other side products to be purified and observed (Figure 13). The complexity of the system was striking. Several over-addition products, hydrolysis and migration products could be isolated. At this point, we accepted the difficulties associated with the reaction and decided not to go into further optimization attempts as the yields of **3.037** were satisfactory for our needs.

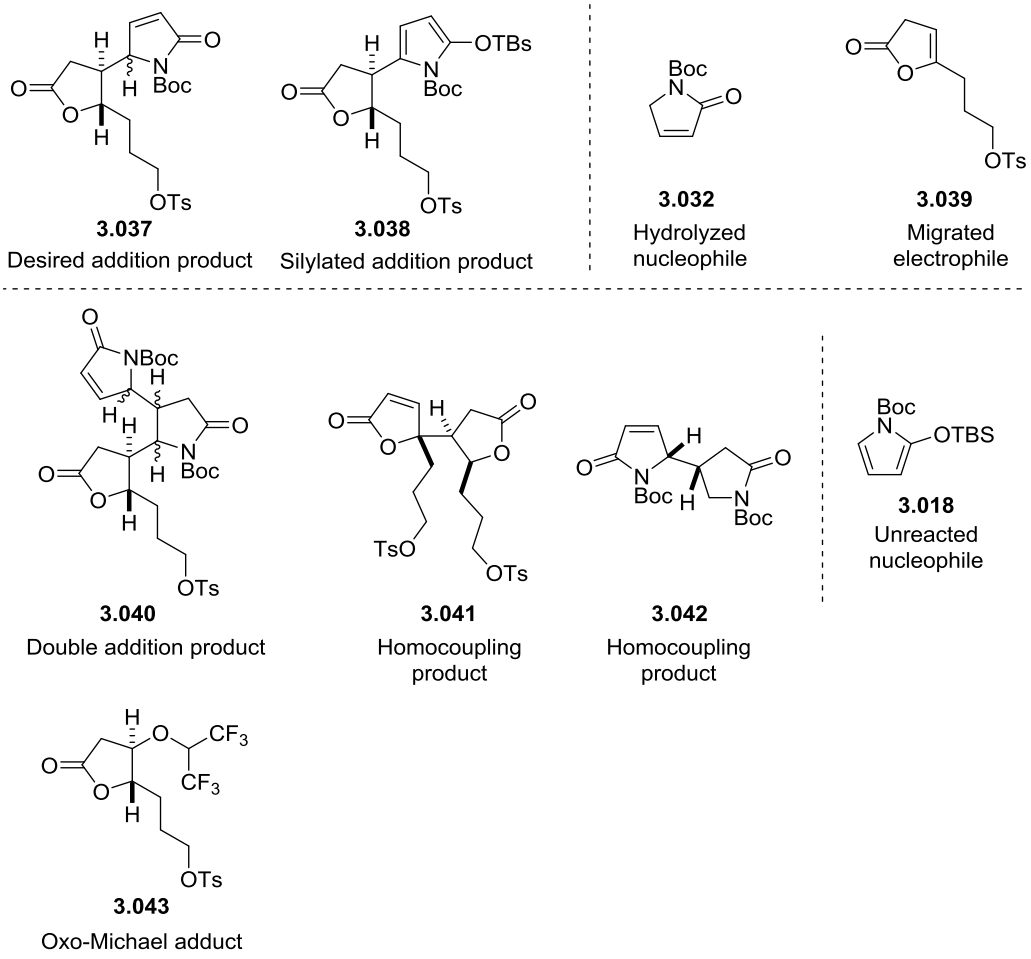

Figure 13: Products isolated from the vinylogous Mukaiyama–Michael reaction between silyloxypyrrole **3.028** and silyloxypyrrole **3.036**, tentative structural assignments.

3.4 Total Synthesis of Stemoamide and 9a,10-bis-*epi*-Stemoamide

3.4.1 Hydrogenation allows separation of 9a-diastereomers

Having access to large amounts of tosylated adduct **3.037**, we proceeded to hydrogenate the α,β-unsaturation before *N*-deprotection. We feared the reverse, deprotection before hydrogenation, would result in double-bond migration as observed with the corresponding mesylate **3.032** (Scheme 23). The hydrogenation of **3.037** proceeded smoothly. Thankfully, the two formed saturated lactams **3.044** and **3.045** were separable using flash chromatography.

At this stage, 2D NMR studies were inconclusive in providing an assignment of relative configuration for either **3.044** or **3.045**. We continued the routes with both diastereomers, knowing that in the upcoming intermediates the configurations could be assigned.

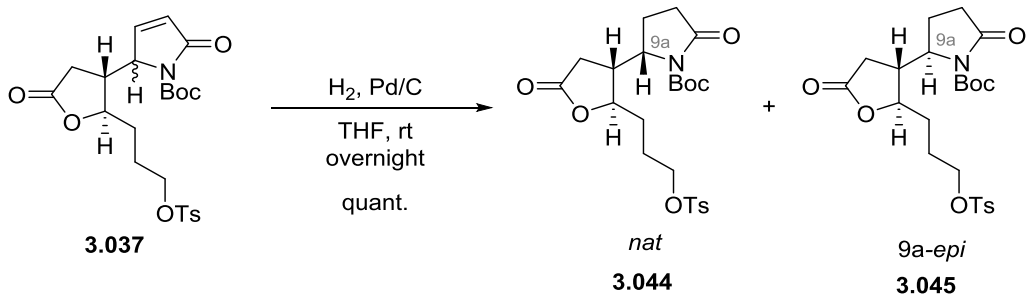

Scheme 25: Hydrogenation of **3.037** allows 9a epimeric lactams **3.044** and **3.045** to be separated.

3.4.2 Epimerization: the fate of the enantioselective version of the synthesis

At this stage a rather worrying observation was made. The optical rotations of **3.044** and **3.045** were near-zero and varied from batch to batch. The troublesome epimerization of the butanolide starting material **3.036** was likely taking place to a variable degree in the key Mukaiyama–Michael reaction (Scheme 26).

This fear was later proven correct as we compared the optical rotation data of our final stage products, such as **3.047** and **3.006**, with identical compounds reported in the literature. The optical rotations of our compounds were close to zero and did not match the reported values. Unfortunately, this forced us to continue the project as a racemic synthesis. From this point onwards, most work described has been carried out with racemic material as denoted by the usage of — instead of ◣ and ····· instead of ····· as the stereochemical descriptors.

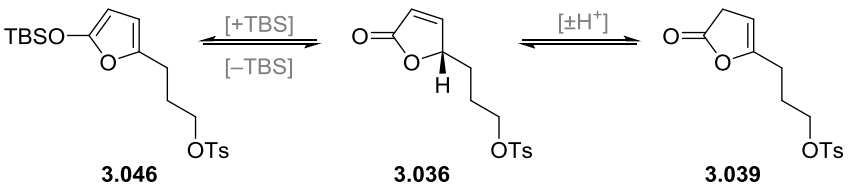

Scheme 26: Racemization processes of **3.036** can take place *via* the formation and hydrolysis of a silyloxyfuran **3.036**, or γ,δ-migration of the double bond to **3.039**.

3.4.3 Synthesis of Stemoamide

As underlined in 3.4.2, all reactions from this point onwards have been carried out with racemic material, unless otherwise mentioned. The *N*-Boc lactam **3.044** was deprotected with trifluoroacetic acid to give **3.047** and cyclized (NaH, THF) to give **3.048** (Scheme 27). Proceeding only sluggishly the cyclization **3.047** → **3.048** took 16 hours to complete and resulted in a significant amount of baseline side-products. At this stage we had reached a known compound, norstemoamide (**3.048**). ^{1}H and ^{13}C NMR data of our synthetic sample matched those reported in the literature.[86] The matching data allowed stereochemical assignment of the two diastereomers **3.044** and **3.045** separated earlier (Scheme 25).

The norstemoamide (**3.048**) was then α-methylated to complete the synthesis of stemoamide (**3.006**). Enolization of **3.048** with LiHMDS and treatment with MeI at –78 °C, allowing the reaction to reach rt over 15 min, was detrimental to diastereoselectivity. In ^{1}H NMR two doublet signals in the 1.5–1.6 ppm region, corresponding to two different methylated products, were observed. The issue was resolved by forming the enolate of **3.048** as before but allowing the reaction to reach completion at –78 °C, giving stemoamide (**3.006**) as the sole product (Scheme 27).

The route was also carried out with **3.044** derived from enantioenriched aldehyde. In this case, the optical rotation of Stemoamide (**3.006**) $[\alpha]_D^{20}$ = –3.8° (c = 0.4, MeOH) was significantly lower than reported $[\alpha]_D^{20}$ = –141 (c 0.3, MeOH), attesting to epimerization taking place under the Mukaiyama–Michael conditions.[86]

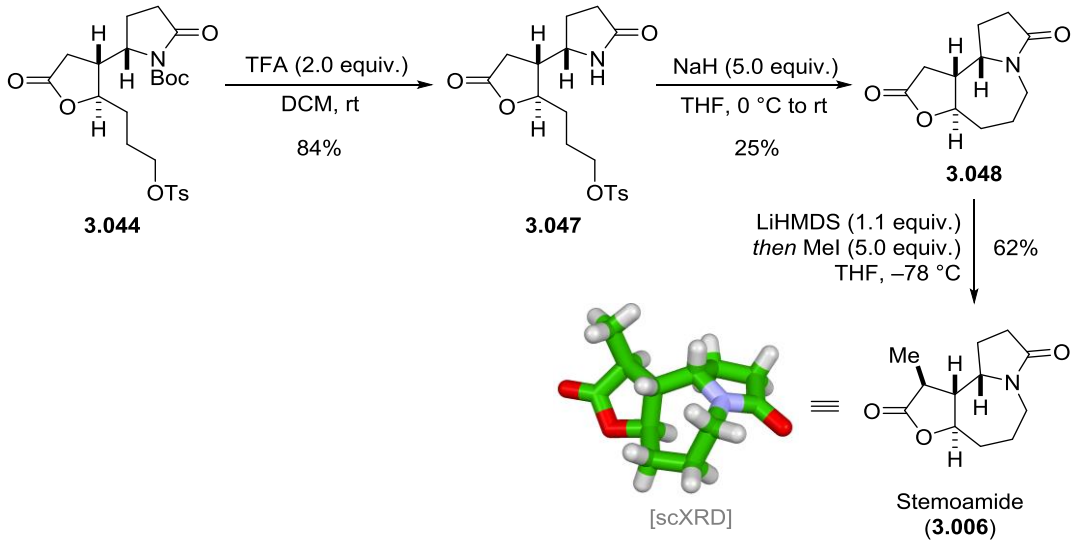

Scheme 27**:** Final stages and completion of (±)-stemoamide (**3.006**).

3.4.4 Synthesis of 10,9a-bis-*epi*-Stemoamide

As in the synthesis of stemoamide (**3.006**) (Scheme 27), the 9a-epimeric tosylate **3.045** was *N*-deprotected with trifluoroacetic acid to yield free amide **3.049**. Unlike the natural free lactam, the 9a-epimeric lactam **3.049** was crystalline (Scheme 28, inset), further proving the relative 9a configuration.

We also attempted to verify the enantiopurity of **3.049** by converting the butanolide into a pair of diastereomers with an enantiopure reagent. This was conveniently done by opening the butanolide of **3.048** with a trimethylaluminium complex of a chiral amine **3.050**. The reaction did not, however, reach completion, and is subject to kinetic enrichment.[87] As such, this approach was not a reliable way to measure the enantiopurity of **3.045**.

Despite this discrepancy, the discovered conversion of butenolide **3.049** to tetrahydrofuran **3.050** is an undocumented domino reaction. As the aluminum amide formed from **3.049** opens the butanolide ring of **3.048**, the newly formed

alkoxide closes onto the tethered tosylate of **3.049**. This will ultimately form a new tetrahydrofuran ring **3.051**. As a way of making tetrahydrofurans, reactions of the type **3.049** → **3.051** could find use in other synthesis efforts.

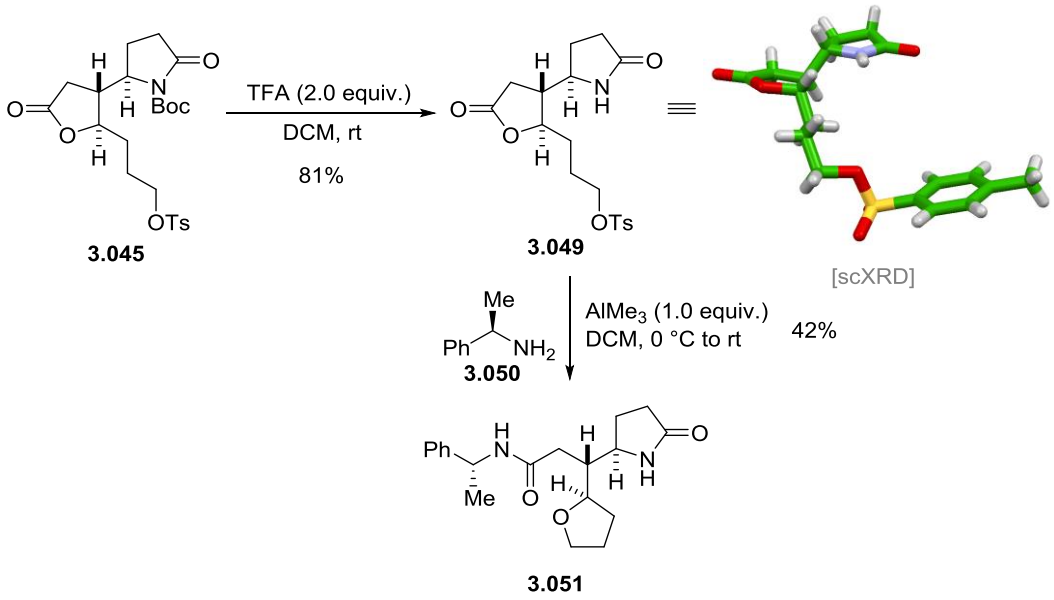

Scheme 28: Accessing the cyclization precursor **3.049** from tosylate **3.045**. Discovered domino reaction produces **3.051**.

In the natural series, compound **3.047** took 16 hours to cyclize. In turn, the cyclization of the 9a-*epi*-isomer **3.049** took only 4 hours to complete, under otherwise identical conditions. Cyclization of **3.049** reaction gave a very satisfactory 73% yield (Scheme 29). For the first time the reaction rate difference in these cyclizations was observed with pure 9a epimers. Previous observations pointing to reaction rate differences were observed for mixtures of natural and 9a-epimeric stemoamides by Cossy *et al*.[24] Preliminary computational studies on the marked difference between **3.047** and **3.049** are presented in more detail in chapter 3.4.6.

The tricyclic lactone **3.049** was then α-methylated to deliver a 1:9 mixture of diastereomers with **3.053** being the major diastereomer (Scheme 29). The lack of diastereoselectivity in the case of 9a-*epi*-nor-stemoamide (**3.052**) was presumably due to the relative flat contour of the molecule.

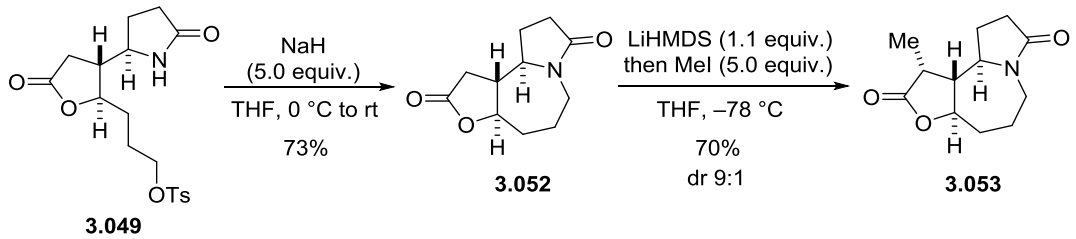

Scheme 29: Final stages and completion of 9a,10-bis-*epi*-stemoamide (**3.053**).

With careful flash purification, the major diastereomer (**3.053**) could be isolated and fully characterized with NMR. The ^{1}H and ^{13}C NMR data of **3.053** matched to those previously reported for 9a-*epi*-stemoamide (**3.054**).[88] However, ^{1}H–^{1}H NOESY data was not in agreement with the proposed structure of 9a-*epi*-stemoamide (**3.054**). Cross-peaks corresponding to unlikely interactions between opposite faces of the tricyclic scaffold of **3.054**, such as C10–Me ↔ C8–H, were observed (Figure 14a, dashed lines).

The ^{1}H–^{1}H NOESY data could be fully accounted for if, instead of 9a-*epi*-stemoamide (**3.054**), the isolated compound was 9a,10-bis-*epi*-stemoamide (**3.053**) with inverted C10 configuration (Figure 14a, solid lines).

In addition to ^{1}H–^{1}H NOESY, vicinal $^{3}J_{HH}$ coupling constants are direct readouts of stereochemical information as the magnitude of a ^{3}J coupling follows the spatial orientation of the two coupled hydrogens. For comparison, in stemoamide (**3.006**) the H10–H9 configuration is locked *trans* and has a ^{3}J = 13.1 Hz (Figure 14b), a typical large value for hydrogen atoms disposed *trans*.[89]

Stemoamide (**3.006**) and 9a-*epi*-stemoamide (**3.054**) have the same *trans* H10–H9 relationship. If the isolated compound was 9a-*epi*-stemoamide (**3.053**), a ^{3}J value close to 13 Hz would be expected. This is not the case, and the isolated compound has a ^{3}J of 7.7 Hz, typical to a *cis* relationship and matching to 9a,10-bis-*epi*-stemoamide (**3.053**).

Both the ^{1}H–^{1}H NOESY and vicinal H–H coupling constant data gave definite proof that the compound previously assigned as 9a-*epi*-stemoamide (**3.054**) was, in fact, 9a,10-bis-*epi*-stemoamide (**3.053**).

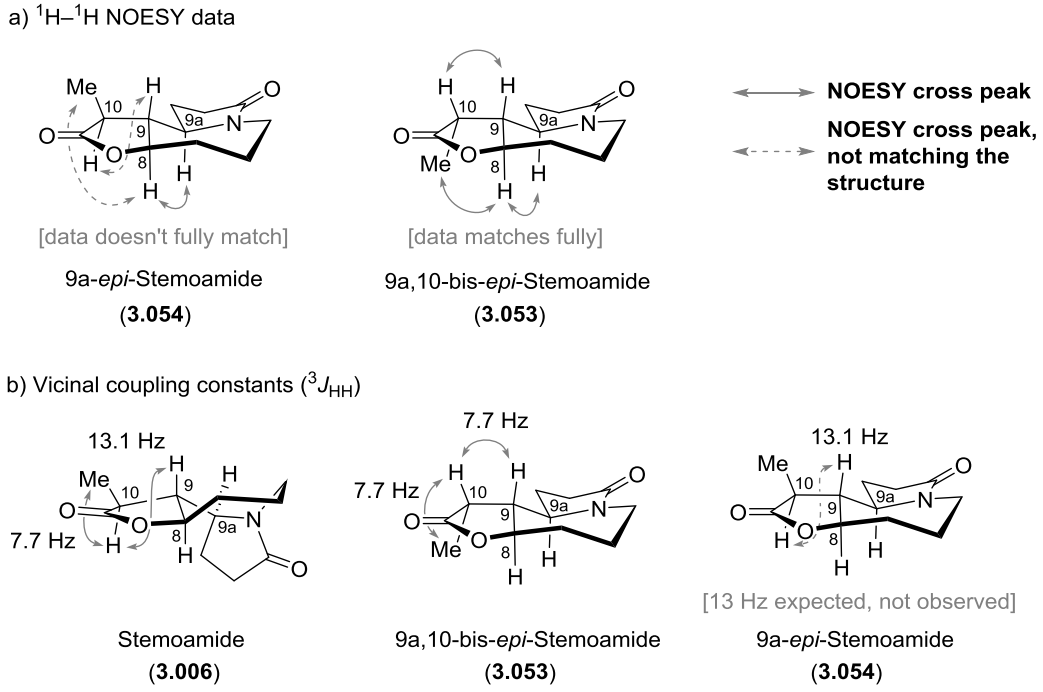

Figure 14: NMR experiments confirming the structure of 9a,10-bis-*epi*-stemoamide (**3.053**). a) ^{1}H–^{1}H NOESY data does not fully match with 9a-*epi*-stemoamide (**3.054**) (discrepancies with dashed arrows) but matches with 9a,10-bis-*epi*-stemoamide (**3.053**) b) Comparison of vicinal $^{3}J_{HH}$ coupling constants also rules out 9a-*epi*-stemoamide (**3.054**).

3.4.5 Combined computational and experimental investigation into the synthesis of 9a-*epi*-stemoamide

9a,10-bis-*epi*-Stemoamide (**3.053**) was the major product when 9a-*epi*-norstemoamide (**3.052**) was α-methylated. It was, however, unclear if it was the kinetic or the thermodynamic product.

To gain further insight into this issue, all possible diastereomers of stemoamide (**3.006**) were optimized and their electronic single-point energies computed at B97D3/DEF2SVP level of theory. The data strongly indicated 9a-*epi*-stemoamide (**3.054**) to be lower in energy than the observed major product 9a,10-bis-*epi*-stemoamide (**3.053**) (Table 3, entries 5 and 6). If this is the case, 9a,10-bis-*epi*-stemoamide is the kinetic methylation product, and 9a-*epi*-stemoamide the thermodynamic product. Also, as a side-note, the computational data showed stemoamide (**3.006**) to be the lowest-energy diastereomer out of all the possible diastereomers.

Table 3: Relative electronic energies of stemoamide diastereomers. Only minimum energy conformers have been taken into account. Computations carried out at B97D3/DEF2SVP level of theory.[90]

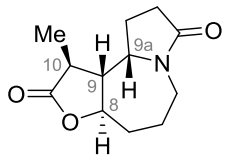

3.006

Entry	Configurations				Energy (kcal mol^{-1})	Notes
	8	**9**	**9a**	**10**		
1	*R*	*S*	*S*	*R*	5.78	
2	*R*	*S*	*S*	*S*	5.62	
3	*R*	*S*	*R*	*R*	8.50	
4	*R*	*S*	*R*	*S*	5.23	
5	*R*	*R*	*S*	*R*	2.42	9a-*epi*-stemoamide (**3.054**)
6	*R*	*R*	*S*	*S*	4.65	9a,10-bis-*epi*-stemoamide (**3.053**)
7	*R*	*R*	*R*	*R*	0.00	stemoamide (**3.006**)[a]
8	*R*	*R*	*R*	*S*	5.12	

With this data at hand, we returned to experiments. When a 9:1 mixture 9,10-bis-*epi*-stemoamide (**3.053**) and 9a-*epi*-stemoamide (**3.054**) was treated with K_2CO_3 equilibration to a 3:1 mixture of 9a-*epi*-stemoamide (**3.054**) and 9,10-bis-*epi*-stemoamide (**3.053**) was noticed (Scheme 30). This concluded our studies on the 9a-*epi* series as both C10 isomers could be made, and 9a-*epi*-stemoamide (**3.053**) is now reported herein for the first time.

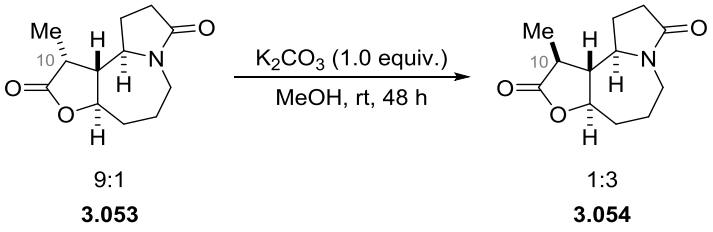

Scheme 30: 9a,10-bis-*epi*-stemoamide (**3.053**) is equilibrated into 9a-*epi*-stemoamide (**3.054**).

3.4.6 Computational details of the cyclization

Given the marked cyclization rate difference observed between the two 9a diastereomeric pairs, we initiated tentative computational studies. These computations were done with a bare anionic amide in gas phase. Admittedly, this scenario is an oversimplification for the energetics, and typically for such computations discrete solvent models would give more reliable energetics, it gives an indication of the nature of the transition states.[91] To analyze the resulting transition states in closer detail, an IRC analysis followed by transition state minimization was carried out at the B97D3/DEF2SVP level of theory.

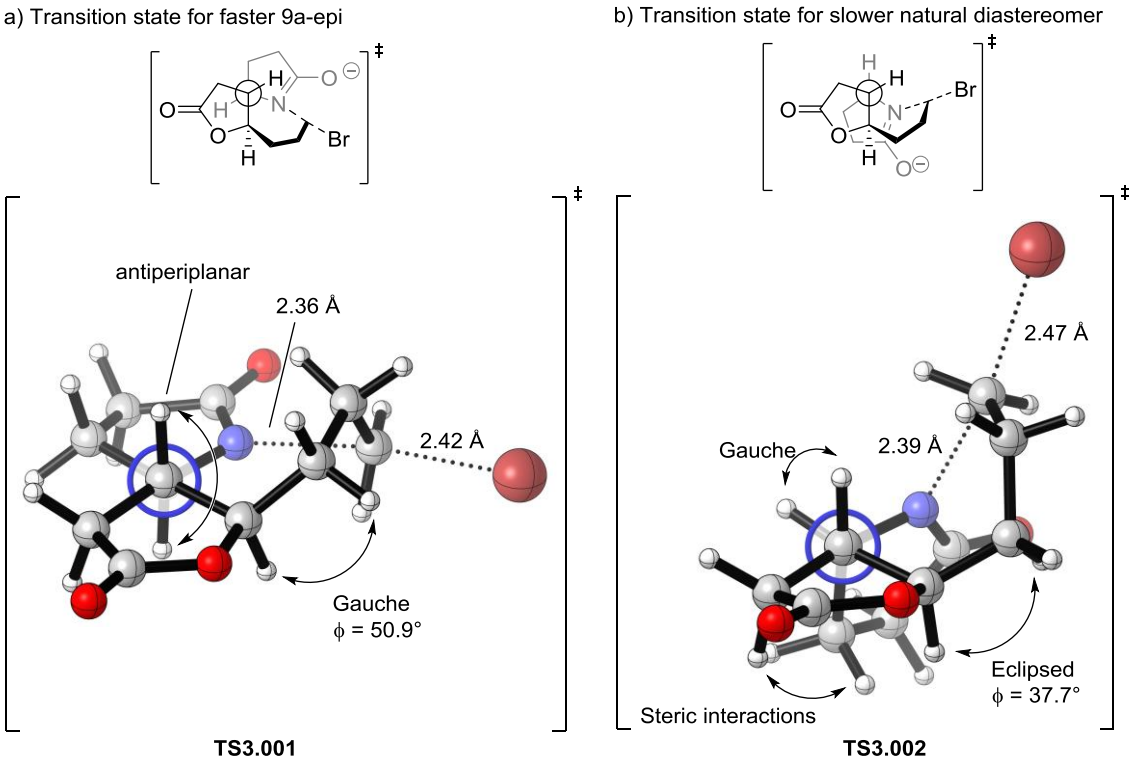

Figure 15: Transition state structures of natural diastereomer **TS3.001** and 9a-*epi* **TS3.002** show marked differences.

In the case of the 9a-*epi*-diastereomer, the cyclization occurs by placing the C9 and C9a hydrogens antiperiplanar (Figure 15a). As a result, the butanolide and lactam rings do not overlap in the transition state **TS3.001**. As the cyclization brings the pendant bromide end closer to the amide nitrogen, the side chain can fold to an all *gauche* form.

This is in stark contrast to the natural stereoisomer cyclizing, which requires significant distortion of the system and has a $\Delta G^{\ddagger}$ difference of 8.5 kcal mol^{-1}. As the cyclization progresses, the butanolide and lactam rings have to overlap causing methylene protons to clash **TS3.002** (Figure 15b). The distortion also forces the bromide side chain to a near-eclipsed conformation. These effects in part explain why cyclization with the natural epimer is indeed so difficult.

3.5 Comparison to the route used by Sato and Chida

During the finalization of our stemona alkaloid project in late 2017, the Sato and Chida group published their approach to stemona alkaloids relying on a similar silyloxypyrrole addition (Scheme 31).[26] The observations made in the Sato–Chida study with bromide **3.027** could be corroborated by our discoveries. In the Sato–Chida synthesis, a one-pot vinylogous Michael addition/reduction process was used without isolation of the intermediate **3.056**. We have earlier shown that isolation of the bromide silyloxypyrrole intermediate **3.056** would likely result in a rearrangement (Chapter 3.3.1).

This direct reduction approach allowed access to intermediate **3.058** *en route* to stemoamide. Interestingly, the Sato–Chida method was not applicable to neither a free amide nor the *N*-Boc protected silyloxypyrrole, both giving a 0% yield. The final approach relied on a PMB protection **3.058** giving good diastereoselectivity and yield. Also, their experiment with OMe protected silyloxypyrrole replicated our poor diastereoselectivity with product **3.057**.

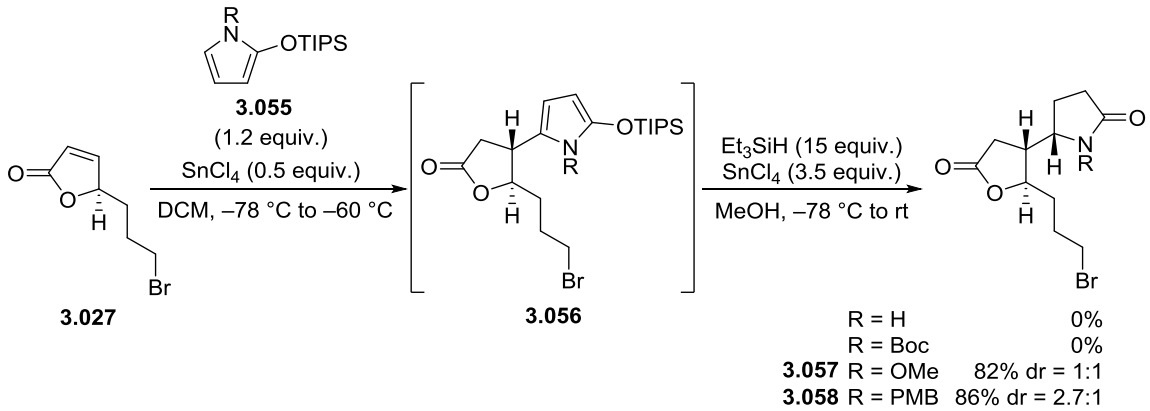

Scheme 31: Approach to stemoamide used by Sato and Chida relies on a similar Mukaiyama-Michael reaction to our route.

3.6 Further experiments on the divergent compound

At this point we had completed the syntheses of stemoamide (**3.006**), 9a-*epi*-stemoamide (**3.054**) and 9a,10-bis-*epi*-stemoamide (**3.053**) from the divergent unit **3.037**. We then initiated studies towards other stemona alkaloid targets.

To access the pyrrol series, we studied first the triflation of **3.037**. After some experimentation the labile triflate **3.059** could be isolated (Scheme 32). Noteworthily, the *N*-Boc deprotection was also simultaneously cleaved. The marked instability of **3.059** allowed characterization only by ^{1}H NMR and IR. Further use of triflate **3.059** in preparative reactions will likely require great care.

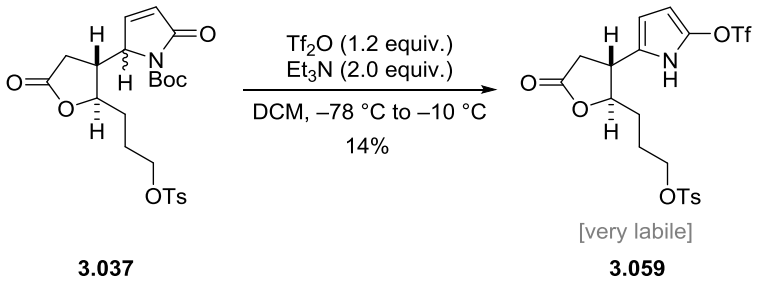

Scheme 32: Fragment **3.037** can be triflated to form a corresponding pyrrole **3.059**

Initial studies were also made towards protecting the double bond of **3.037** in order to prevent it from migrating. These initial studies showed how addition of thiophenol resulted in conjugate addition, giving product **3.060** as a complex mixture of diastereomers (Scheme 33). The *N*-deprotection proceeded cleanly to give free lactam **3.061**, and the progress of the reaction could be followed by LRMS. With these promising preliminary results access to further alkaloids should be within our reach.

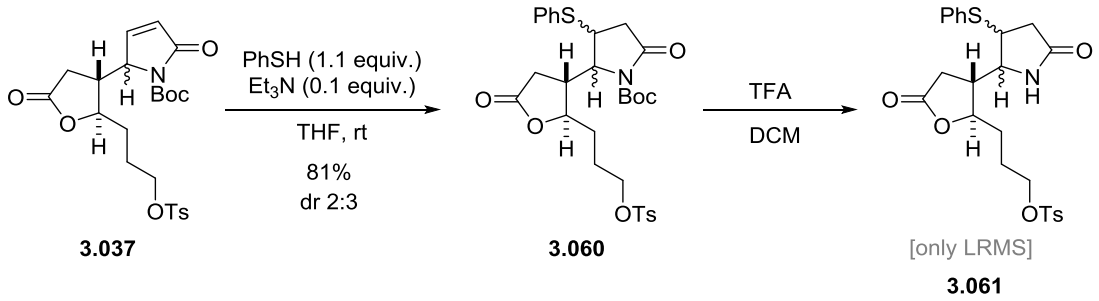

Scheme 33: Tentative experiments show double bond of **3.037** can be masked with thiophenol.

3.7 Conclusions and outlook

We set out to develop a divergent route to stemona alkaloids, which ultimately led to total syntheses of stemoamide (**3.006**), 9a-*epi*-stemoamide (**3.054**) and 9a,10-*bis*-epi-stemoamide (**3.054**) (Figure 10). Several attempts at converting the divergent intermediate into other Stemona alkaloids, including the synthesis of a pyrrole precursor **3.059** were also carried out (Figure 16a). Despite the tentative nature of these experiments, it is very likely that from intermediate **3.059** breakthroughs in synthesis of oxidized stemona alkaloids could ensue.

The route relies on a new type of a vinylogous Mukaiyama–Michael reaction, which allows coupling silyloxypyrroles **3.018** to butenolides using a silyl triflate–hexafluoroisopropanol catalyst system. Further studies towards the substrate scope of this catalyst system, and its performance in other similar transformations would be interesting.

Other, more serendipitous, discoveries made during the project include the migration of α,β-unsaturated lactams into γ,δ-unsaturated enamides upon deprotection (Figure 16b), and the domino reaction forming tetrahydrofurans from butenolides (Figure 16c).

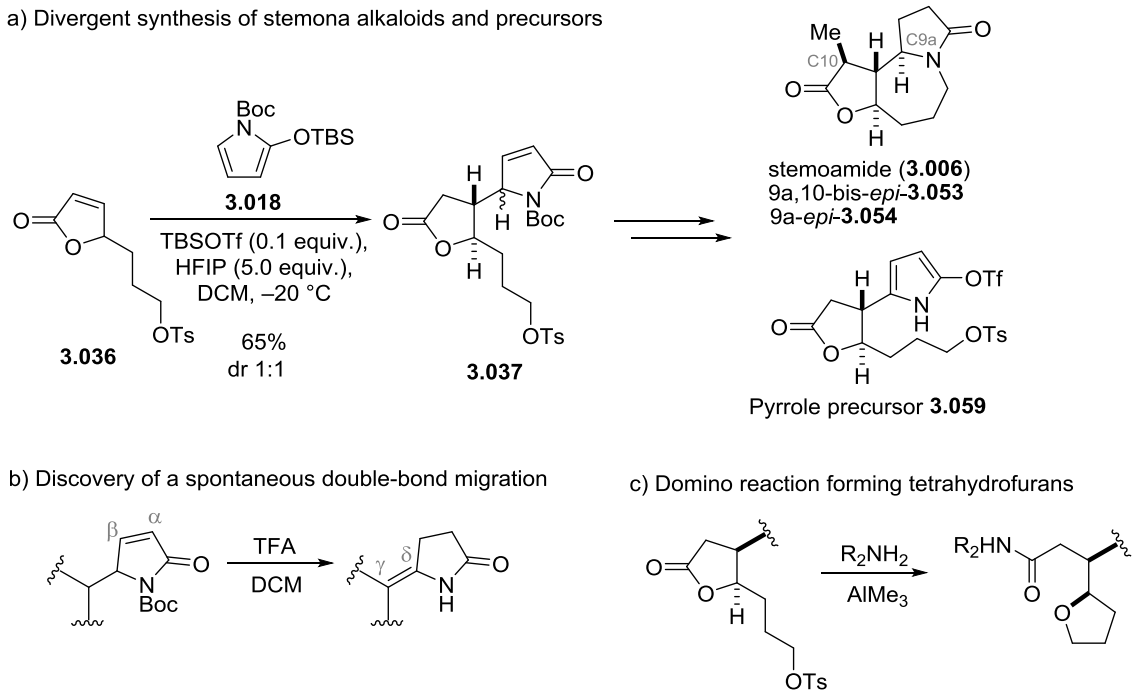

Figure 16: Key discoveries made during studies on stemona alkaloids. a) Using TBSOTf and HFIP as a catalyst system in Mukaiyama–Michael reactions, and the structural reassignment of 9a-epimers of stemoamide c) Spontaneous migration of lactam α,β-unsaturation to γ,δ upon deprotection d) Domino reaction forming tetrahydrofurans.

4 DOMINO APPROACH TO CEPHALOTAXUS ALKALOIDS

"If you hear a voice within you say 'you cannot paint', then by all means paint, and that voice will be silenced"

–Vincent van Gogh

4.1 Aim of the study

Cephalotaxus alkaloids are notably antileukemial (Figure 17a). In fact, homoharringtonine (**4.003**), one of cephalotaxus alkaloids, is an FDA and European medicine agency approved antileukemia drug.[92] Homoharringtonine inhibits protein synthesis by binding to the A-site cleft in the large ribosomal subunit, which affects chain elongation and prevents protein synthesis, ultimately killing fast-dividing cells (Figure 17b and c).[93]

Unfortunately, the main source of homoharringtonine (**4.003**), the Cephalotaxus shurbs, are extremely slow to grow and are mostly endangered and protected species. Additionally, medicinal formulations made from natural extracts can vary with the source of the raw material. The main production route relies on semisynthesis, using a direct esterification of naturally isolated Cephalotaxine (**4.001**).[94] There have been attempts at alleviating the availability problem with the discovery of a fungus capable of biosynthesizing homoharringtonine.[95]

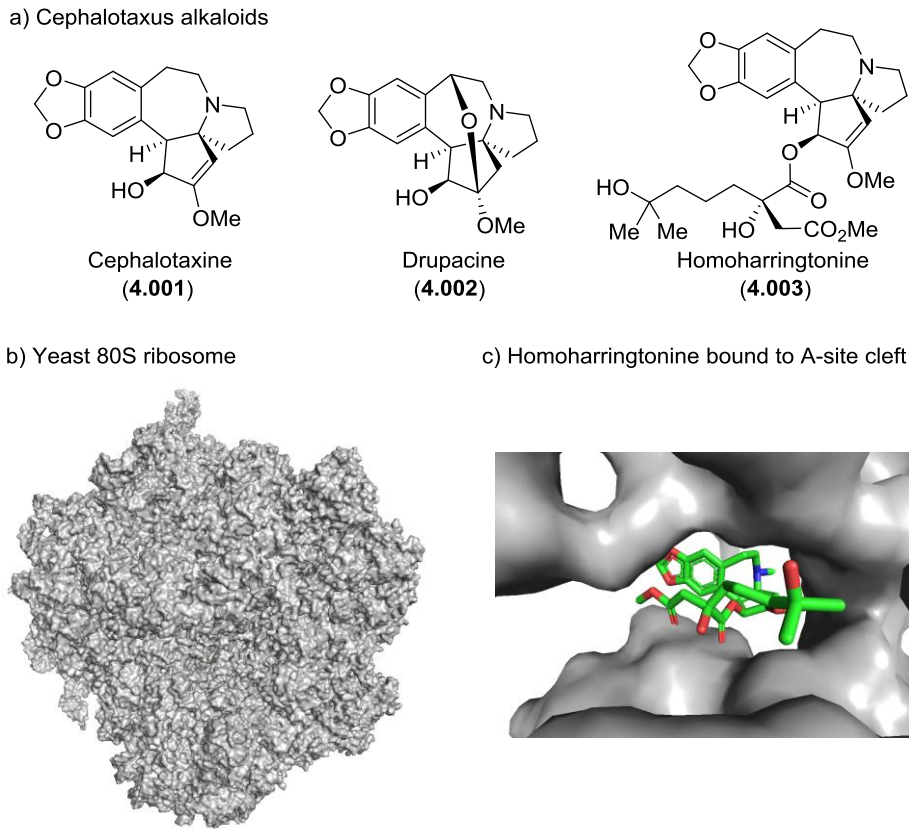

Figure 17: Cephalotaxus alkaloids and their biological importance. a) Cephalotaxine (**4.001**), drupacine (**4.002**) and homoharringtonine (**4.003**) b) Yeast 80S ribosome unit c) Homoharringtonine (**4.003**) bound to mRNA binding A-site cleft of yeast 80S ribosome (PDB: 4U4Q).[96]

In this light, a straight-forward and scalable synthetic access to cephalotaxus alkaloids would be highly desirable. A multitude of synthetic approaches have been published, but unfortunately most of them are not enantioselective nor very short.[97] To address this problem, the Somfai group group had opted to develop a synthetic sequence to access cephalotaxus alkaloids in a more direct fashion.

A versatile [1,2]-Stevens rearrangement to generate α-benzylated amino acid derivatives **4.006** *via* a boronate templated system **4.005** had been previously developed in the Somfai group (Scheme 34a).[98] An extension to [2,3]-rearrangements using *N*-allylated prolineamide **4.007** had also been initially studied and shown to work. Comparing α-allylated proline derivatives **4.009** and cephalotaxine (**4.001**) (Scheme 34c) highlights how the formed quaternary stereogenic center could work as a stepping-stone to access cephalotaxus alkaloids. However, the absolute configurations are the opposite. This would result in the unnatural enantiomer of cephalotaxine when natural L-proline was used.

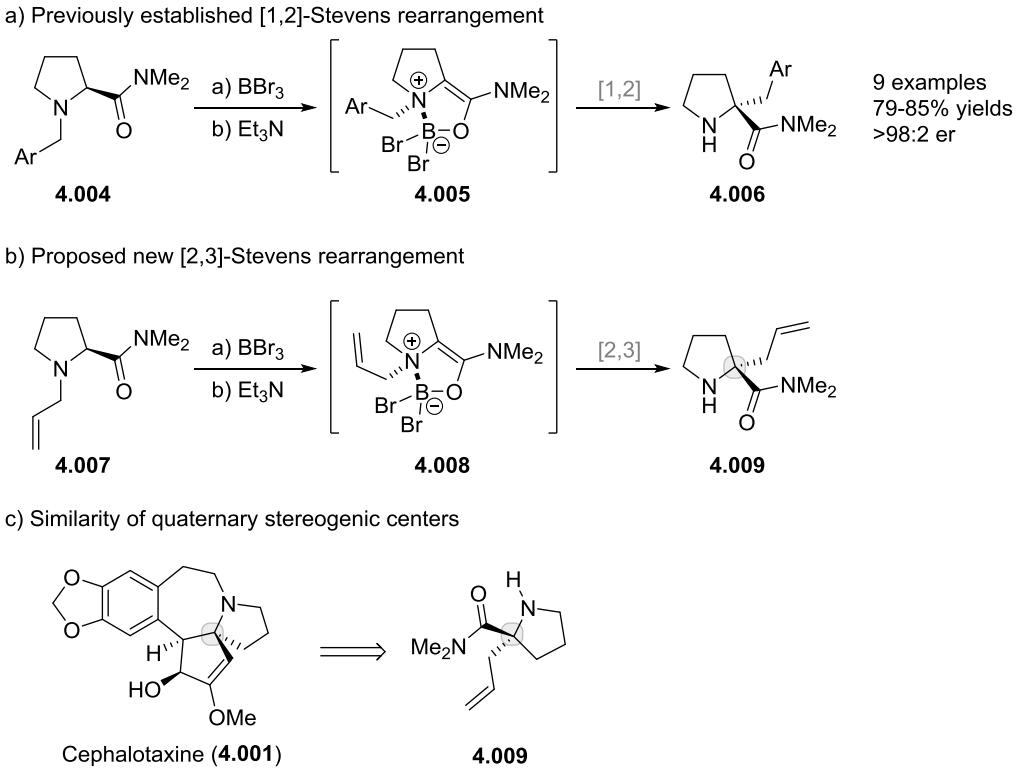

Scheme 34: a) Previously established [1,2]-Stevens rearrangement of *N*-benzyl prolineamides **4.004** [98] b) Proposed [2,3]-Stevens rearrangement of *N*-allyl prolineamide **4.007** c) Comparison of quaternary stereogenic centers in cephalotaxine and rearranged prolineamide **4.009**.

4.2 Strategy

First, we retrosynthetically simplified *ent*-cephalotaxine (*ent*-**4.001**) to enone **4.010**, since the conversion of **4.010** to cephalotaxine is known.[58] Second, the approach was strictly guided by a choice of a structure-goal strategy, keeping the α-allylated proline derivative **4.009** as our starting material regardless of the route taken. With these two premises, several key aspects of a retrosynthesis could already be formulated (Scheme 35).

The electron rich aromatic core of **4.010** was believed to be moderately nucleophilic, allowing a disconnection of the azepane ring. This disconnection would lead to a synthetic equivalent of the type **4.011,** with Z being a leaving group. Further disconnecting the enone of **4.011** reveals a fragment **4.012**, which, when disassembled, leads to compounds **4.013** and **4.009**. With this conceptual roadmap, we ventured into the synthesis by preparing the aromatic fragment **4.013** and prolineamide **4.009**.

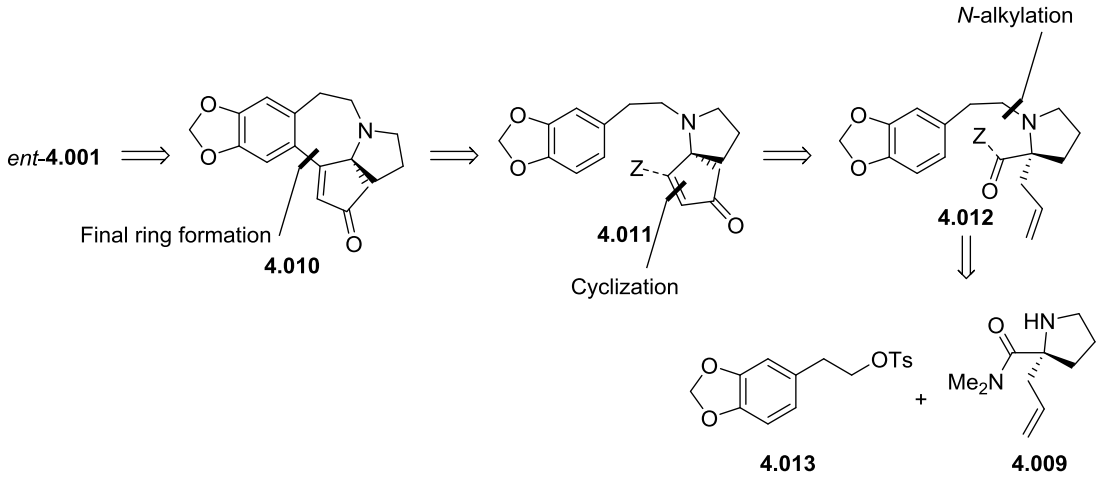

Scheme 35: Conceptual retrosynthesis of enone **4.010** leading to aromatic tosylate **4.013** and prolineamide **4.009**.

4.3 Preparation of starting materials

4.3.1 Synthesis of the aromatic subunit

The aromatic 1,3-benzodioxole fragment **4.013** was prepared according to a literature procedure from commercially available 3,4-(methylenedioxy)phenylacetic acid (**4.014**) *via* borane reduction and tosylation (Scheme 36a).[99] *N*-Allyl prolineamide **4.007** was prepared with direct allylation of commercially available prolineamide **4.016** using allyl bromide (Scheme 36b).

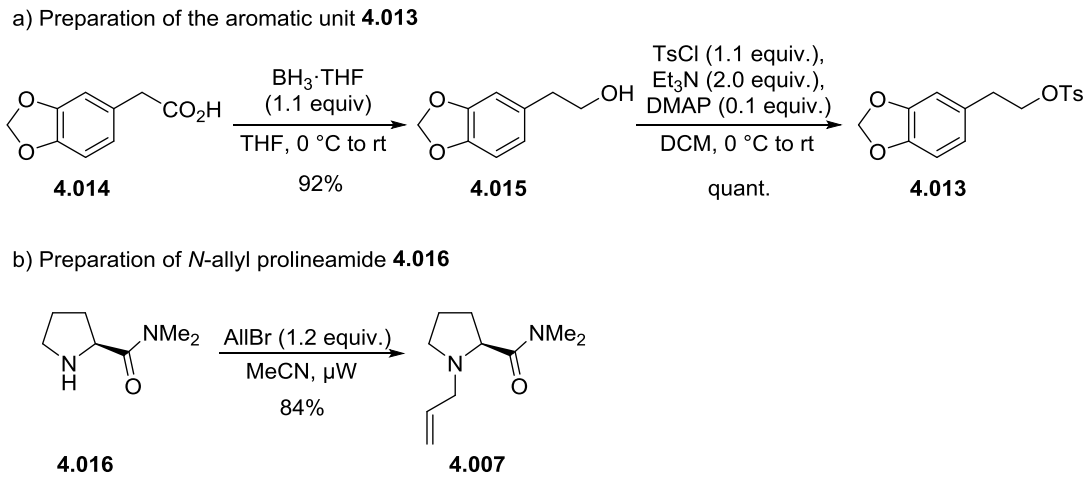

Scheme 36: Preparation of starting materials **4.013** and **4.007**.

4.3.2 Synthesis of allyl amine subunit

The key [2,3]-Stevens rearrangement was optimized by M.Sc. Giovanni Di Gregorio. He had established that using DBU, instead of triethyl amine as the base, gave useful 50–73% yields of the rearranged product **4.009** (Scheme 37).[100]

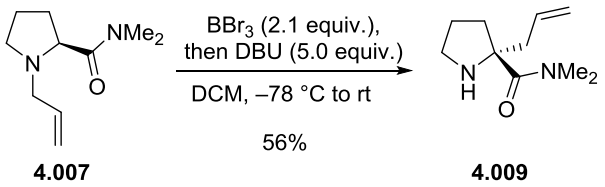

4.007 **4.009**

Scheme 37: Rearrangement of allylated prolineamide to form **4.009**.

4.3.2.1 Mechanistic considerations

When the rearrangement to form **4.009** was scaled up, several modifications were made by the author. Previously the rearrangement had been quenched with 2 M HCl and stirred at room temperature for 2 h. Approaching the step with some trepidation as gram quantities of **4.007** were used, only a 5-minute stirring period was used. With this modification at hand, a fairly nonpolar crystalline solid aminoborane *syn*-AB-**4.008** could be isolated (26%), alongside with the desired product **4.009** (56%) (Scheme 38).

Considering that aminoborane *syn*-AB-**4.008** is stable enough to be isolated, it has to lie reasonably low in energy with respect to other intermediates. One interpretation is, that two isomeric aminoboranes, *syn*-AB-**4.008** and *anti*-AB-**4.008**, are initially formed as the prolineamide **4.009** is treated with boron tribromide. The *syn* and *anti* aminoborane species interconvert only very slowly. If this was not the case, *syn*-AB-**4.008** would not be isolatable and would isomerize to *anti*-AB-**4.008** under the reaction conditions.

The faiths of *syn*-AB-**4.008** and *anti*-AB-**4.008** aminoboranes are different. Isomer *syn*-AB-**4.008** cannot cyclize into a highly strained *trans*-oxazaaminoborane *trans*-OAB-**4.017**. On the contrary, *anti*-AB-**4.008** can readily cyclize to give a *cis*-oxazaaminoborane *cis*-OAB-**4.017**. The *cis*-OAB-**4.017** is then deprotonated by DBU to give enamine **4.018**, which can undergo a [2,3]-rearrangement. The rearrangement forms a trapped product **4.019** which is then fed further downstream to ultimately give the observed rearranged product **4.009** with retention of configuration. Other possibilities for these observations, however, cannot be ruled out at this stage.

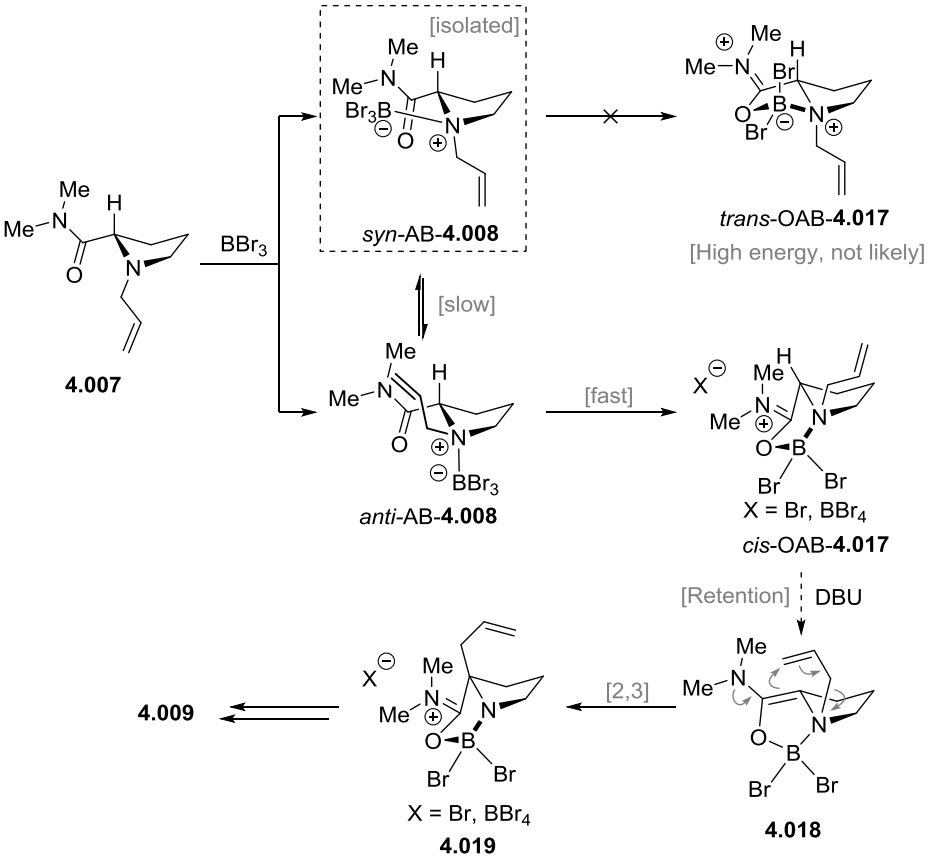

Scheme 38: Isolation of stable adduct *syn*-AB-**4.008** provides insight into the mechanism of the [2,3]-Stevens rearrangement. When boron tribromide forms an adduct with **4.016** two possible aminoboranes, *syn*-AB-**4.008** and *anti*-AB-**4.008** can form. The *syn*-aminoborane, *syn*-AB-**4.008**, is a dead-end intermediate as it cannot close into a strained oxazaaminoborane *trans*-OAB-**4.017**. On the other hand, *anti*-**4.008** can easily cyclize into *cis*-OAB-**4.017** and react further.

4.4 Initial studies

Reaction between prolineamide **4.009** and tosylate **4.013** had been conceived in the initial studies by M.Sc. Giovanni Di Georgio.[100] The preparation was repeated to access gram-quantities of **4.020** (Scheme 39).

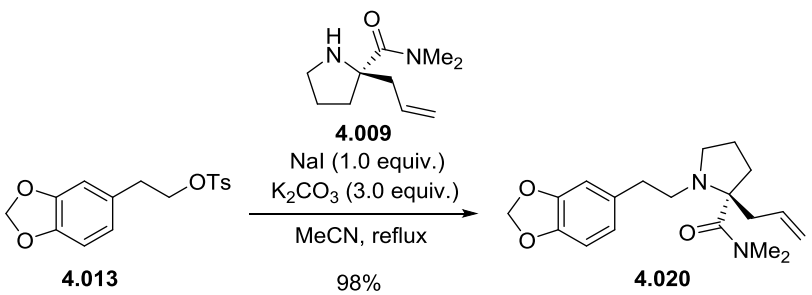

Scheme 39: *N*-alkylation of prolineamide **4.009** with tosylate **4.013** gives **4.020**.

4.4.1 First approach with Wacker oxidation

With intermediate **4.020** at hand, we attempted the first approach, which was to oxidize the terminal alkene into a ketone **4.021** followed by an intramolecular aldol condensation to give **4.022** (Figure 18a). After screening a variety of conditions for the Wacker oxidation, only traces of ketone **4.021** could be observed by LRMS (Figure 18a).

The reluctance of **4.020** to oxidize could be explained by a stable chelate **4.023** (Figure 17b). As deprotonation of this π-allyl complex **4.023** is hindered, a σ-alkyl complex necessary for a Wacker oxidation cannot form. Similar to **4.023** ligation between an amide and alkene has been observed with lithium.[101] Another approach had to be considered.

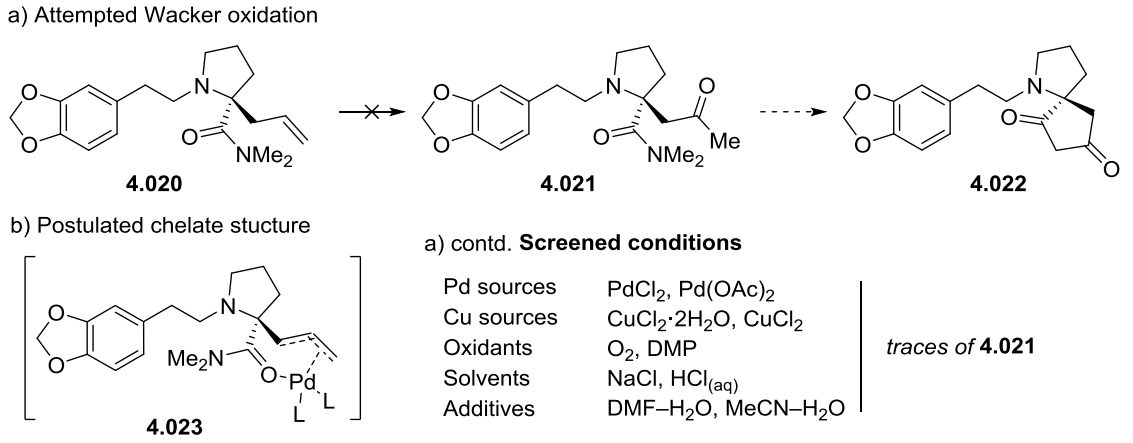

Figure 18: Attempted Wacker oxidation from **4.019** to **4.020** could not be achieved even after extensive screening.

4.4.2 Second approach with amide activation

Regrouping, we then considered an alternative order for the ring formation. In the second approach, the amide of **4.020** would be activated using Vilsmeyer–Haack type chemistry. Tethered to an electron-rich aromatic system, an attack to the highly activated iminium ion should ensue.

Unfortunately, the substrate **4.020** resisted all attempts at such cyclization. Varying temperatures and iminum generating reagents gave no conversion to **4.024** (Table 4). Even a mixture of Tf_2O and DTBMP, reported to work for difficult cases, proved unsuccessful.[102] Previous studies have noted that benzyloxy derivatives are not as nucleophilic as typical phenol ethers, as such the arene might not be nucleophilic enough to facilitate cyclization.[103] The route had to be rethought once more.

Table 4: Attempted Vilsmeyer–Haack cyclizations to form **4.024**.

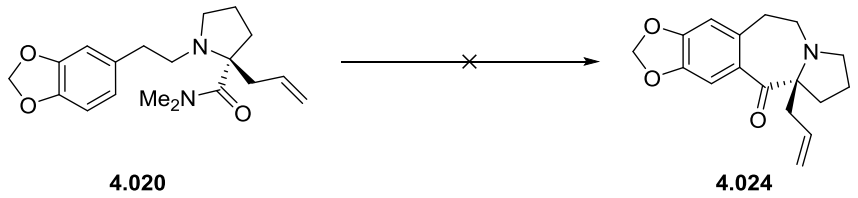

Entry	Conditions	Result
1	$COCl_2$, (1.1 equiv.), DCM, –78 °C to RT	no rxn
2	$C_2O_2Cl_2$ (2.1 equiv.), DCM, –78 °C to reflux	no rxn
3	$POCl_3$ (1.1 equiv.), DCE, reflux	no rxn
4	Tf_2O (1.1 equiv.), DTBMP (0.1 equiv.), DCE, 60 °C	no rxn

4.4.3 Third approach with lithium-halogen exchange

So far, we had established that the allylic double bond of **4.020** resists early-stage oxidation, and that the bare 1,3-benzodioxole core of **4.020** is not very nucleophilic. These observations left us with little choice, but to chemically render the 1,3-benzodioxolone core more nucleophilic.

Following this line of thought, lithium–halogen exchange to form an aryllithium **4.026** would undoubtably attack even the rather unreactive amide to give **4.024** (Scheme 40). This approach, a lithium–halogen exchange induced cyclization, is also known as Parham cyclization.[104]

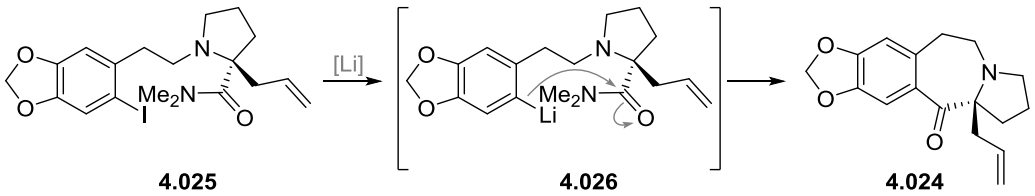

Scheme 40: Revised approach to **4.024** based on lithium-halogen exchange.

Two different options are available to access the needed iodinated precursor **4.025**: aryl group can be iodinated before *N*-alkylation, or the *N*-alkylated fragment **4.020**. The latter option was studied first as the material **4.020** was already available.

Treating **4.020** under the standard CF_3CO_2Ag, I_2 conditions used for iodinating electron rich aryl systems did not result in the desired aryl iodination but rather formed an iodolactone **4.027**, another dead-end (Scheme 41).[105] When forcing with excess of silver trifluoroacetate and iodide, partial iodination of the aromatic core to give the correspondin di-iodide could also be observed.

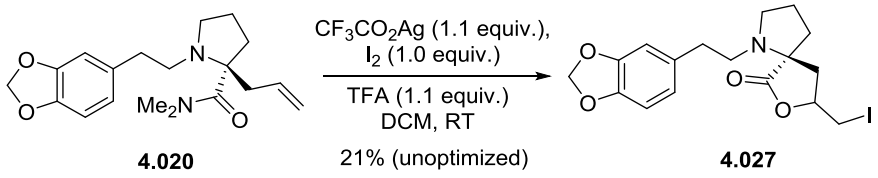

Scheme 41: Compound **4.020** iodolactonizes to form **4.027** instead of aryl iodination.

With this setback, the campaign changed its course to prepare pre-iodinated 1,3-benzodioxole motif. With straight forward literature procedures, both nosyl and tosyl iodides **4.029** and **4.030**, respectively, could be prepared in gram-scale (Scheme 42).[99]

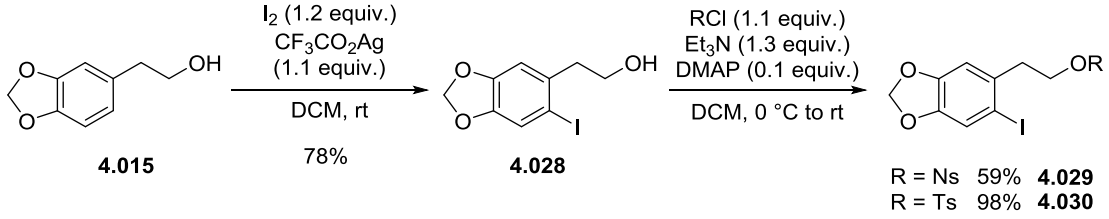

Scheme 42: Preparation of iodinated aryl precursors **4.029** and **4.030**.

N-alkylation of **4.009** with the iodinated fragment was not as straight-forward as we had expected. Using the procedure established for non-iodinated tosylate **4.030** (Table 5, Entry 1), the iodinated compound was only observed to eliminate to give a corresponding styrene. After screening a variety of bases, it became obvious the tosylate **4.030** would not be a suitable leaving group. Additionally, we noticed a competing Ritter-side reaction with the solvent giving acetamide **4.031**. Gratifyingly, in small scale screening, elimination and Ritter side reactions could be avoided with nosylate **4.029** (Table 5, Entries 3–4). In preparative scale, potassium carbonate as the base provided desired product **4.025** in 95% yield in 50 mg scale. In gram scale the yield suffers slightly (71% with 1 g of **4.025**, 83% with 600 mg of **4.025**).

Treating the iodide with *t*-BuLi resulted, based on LC/MS analysis, to the desired cyclization product **4.024** (Scheme 43). At this stage, however, we realized the full potential of our previous iodolactamization discovery (Scheme 41). A new approach was conceived as detailed in the next chapter.

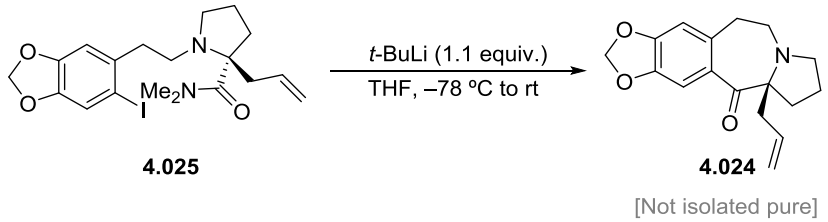

Scheme 43: Tentative success at Parham cyclization of **4.025**.

Table 5: Optimization of the *N*-alkylation of **4.009** with iodoaryls **4.029** and **4.030**.

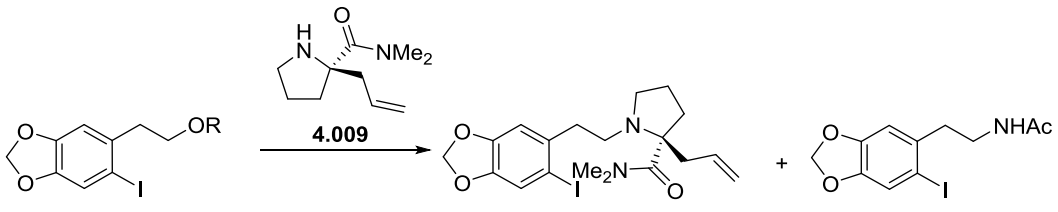

Entry	Conditions	Yield	Notes
1	**4.030** (2.0), NaI (1.0 equiv.), K_2CO_3 (3.0 equiv.), ACN, reflux	21%	Mostly elimination
2	**4.030** (1.2), K_2CO_3 (3.0 equiv.), ACN 50 °C	–[a]	33:66 **4.030** to **4.025**[b]
4	**4.030** (1.2), DIPEA (3.0 equiv.), ACN, 50 °C	–[a]	96:4 **4.030** to **4.025**[b]
3	**4.029** (1.2), K_2CO_3 (3.0 equiv.), ACN, 75 °C, 7 h	–[a]	14:86 **4.029** to **4.025**[b]
4	**4.029** (1.2), DIPEA (3.0 equiv.), ACN, 75 °C, 7 h	–[a]	33:66 **4.029** to **4.025**[b]
5	**4.029** (1.2), K_2CO_3 (3.0 equiv.), ACN, reflux, 2 days	95%	Unreacted **4.029** recovered
6	**4.029** (1.1), K_2CO_3 (3.0 equiv), ACN reflux, 14 h	71%	1 g scale

[a]Small-scale experiment, followed using ^{1}H NMR [b]Tosylate **4.030** was followed despite it not being the limiting reagent as the amine signals were broad and not clearly visible.

4.5 Formal synthesis of Cephalotaxine

Based on the discoveries so far, we re-evaluated our stance. The two stepping-stones were 1) the lithium-halogen exchange induced cyclization of the 7-membered azepane ring (Scheme 43), and 2) amide functionalization with halolactonization (Scheme 41).

A review of literature showed how halolactonization products of type **4.032** can be converted to *exo*-methylene butenolides **4.033** *via* a fairly straightforward dehydrohalogenation (Figure 19a).[106] The dehydrohalogenation is also an indirect way of oxidizing the **4.025**, and circumvents the issues associated with the Wacker process. With back-of-the-envelope mechanistic rationalization, we also found the conversion of *exo*-methylene butenolides **4.034** to enones **4.036** upon nucleophilic attack should be feasible (Figure 19b). Several literature precedents on the transformation were also found, albeit not for systems of this type *per se*.[107–109]

Combining these insights with the lithium-halogen exchange led to a very tempting cascade process (Figure 19c). Treating *exo*-methylene butanolide **4.033**

with a lithium source would result in lithium-halogen exchange. The newly formed aryllithium would undergo a 1,2-attack with the butanolide to form **4.037**. Rupturing the butanolide, as shown in Figure 18b, would result in a spontaneous aldol condensation, giving enone **4.010** in a domino fashion.

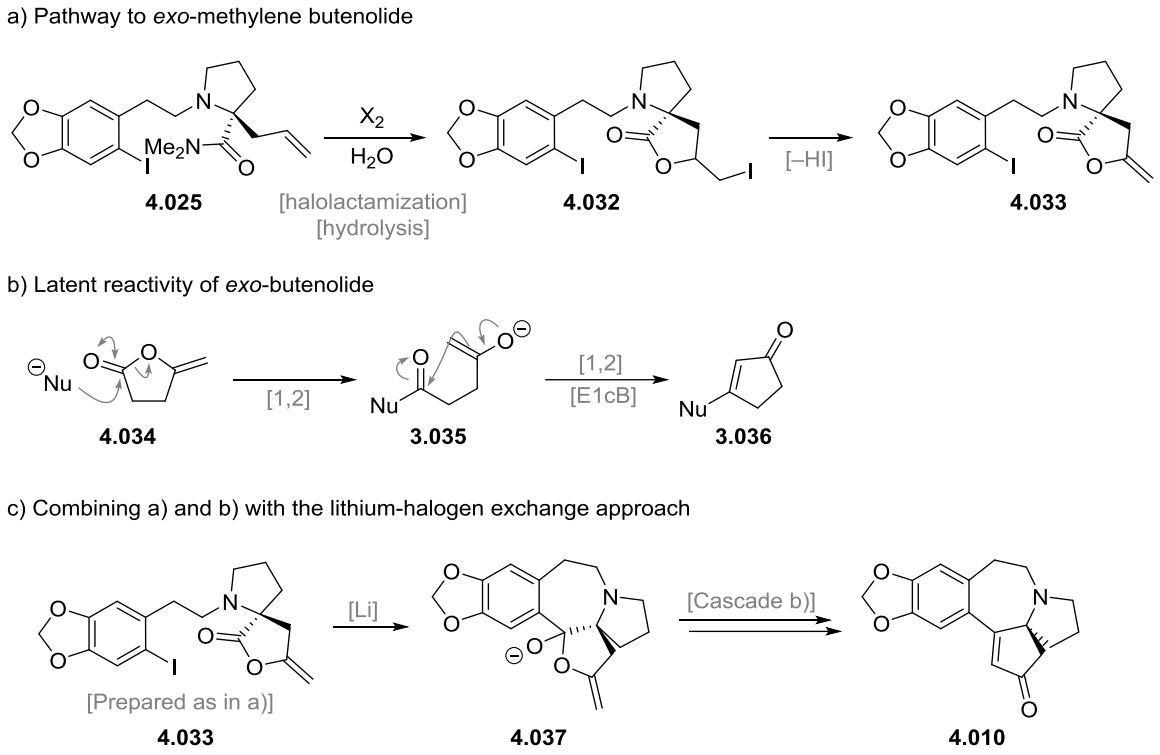

Figure 19: A new approach to **4.010** relying on a domino cyclization of **4.033**.

4.5.1 Accessing the cascade precursor

Pushing forward with the new route, successful iodolactonization of **4.025** to **4.032** was achieved in THF-water (2:1) mixture (Scheme 44). Notably, the typically used 1:1 mixture gave a 14% yield, likely due to solubility issues. Halolactonization of **4.025** to **4.031** proceeds with excellent diastereoselectivity (92:8) but since the subsequent dehydrohalogenation step destroys the newly formed stereogenic center, the relative stereochemistry is naturally unimportant. A short condition screen for elimination of **4.031** showed conventional heating giving lower yields of **4.033** when compared to microwave irradiation, 43% and 65% respectively, taking several days to complete (Scheme 44).

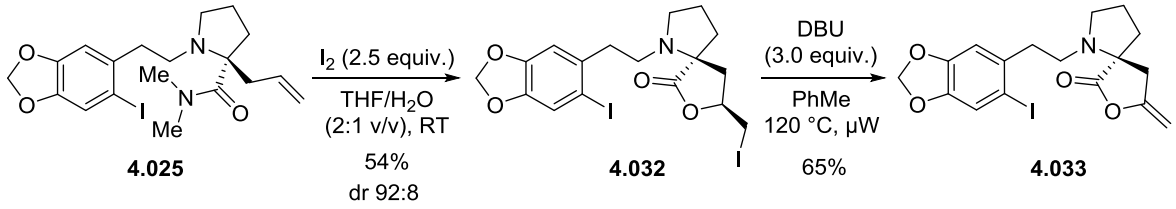

Scheme 44: Preparation of *exo*-methylene butanolide **4.033**.

4.5.2 Parham-Aldol cascade reaction

With the cascade precursor **4.033** at hand, it was treated with a variety of metalating agents (*t*-BuLi, *n*-BuLi, MesitylLi, *i*-PrMgCl·LiCl) at –100 °C in THF. Allowing the reaction mixture to warm to room temperature resulted in near full consumption of **4.033** but yielded complex mixtures with varying amounts of diketone **4.038**, but only traces of desired enone **4.010** (Scheme 45). Attempts at chancing the solvent to heptane/THF led to no improvement, nor did additives such as TMEDA, *t*-BuOH or MeOH.[104,110,111] At best, the desired enone **4.010** was obtained in 9% isolated yield (*n*-BuLi, THF, –78 °C 2 h, warmed to room temperature and heated to 50 °C for 20 min). Furthermore, screening addition rates, reverse addition and reaction temperatures led to no significant improvement. Overall the reaction behavior was seemingly erratic, with side-by-side batches proceeding at different rates, one forming enone **4.010** formation and the other not.

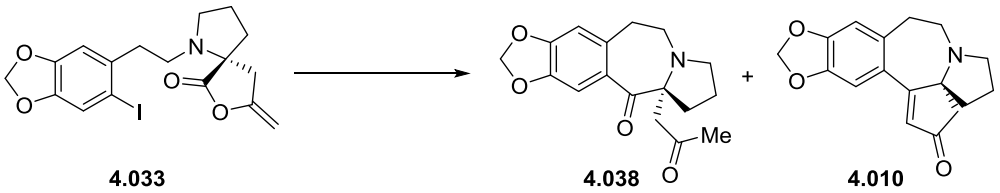

Screened conditions

Metallating agents	*n*-BuLi, *t*-BuLi, MesitylLi, *i*-PrMgCl·LiCl (1.0 to 2.5 equiv.)	*no trend observed*
Solvents	THF, THF–Heptane	
Additives	TMEDA, *t*-BuOH, MeOH, EtOAc	
Misc	Addition rates, reverse addition, temperatures (–100°C to 60°C, variable warming rates)	

Scheme 45: Inconsistent behavior of the domino reaction giving **4.010**.

These setbacks led us to analyze our proposed reaction mechanism in closer detail (Scheme 46). The first step, lithium-halogen exchange of **4.033** to give aryllithium **4.039** was clearly taking place as **4.033** was being consumed. Also, indicative of the Parham cyclization, we could isolate varying amounts of the diketone **4.038**. Yet conversion to enone **4.010** was low.

The difficulty at forming the enone **4.010** led us to speculate that the lithium alkoxide formed after the Parham cyclization does not collapse into enolate **4.041**, but rather chelates with the tertiary nitrogen to form intermediate **4.040**,

which is too stable under the reaction conditions to react further. With this insight at hand, we repeated the most successful reaction sequence (*n*-BuLi, –78 °C 2 h, warmed to room temperature and heated to 50 °C for 20 min) and then added sodium methoxide (1.0 equiv., 0.5 M in methanol) to break the postulated chelate **4.040** to produce the more reactive sodium enolate **4.041** before heating the reaction mixture to 50 °C. Thankfully, with this modification the enone **4.010** was isolated in a 58% yield and 91:9 er completing our formal synthesis campaign.

It can, however, be argued that with the addition of sodium methoxide all **4.040** is initially converted into **4.038**, which then undergoes an aldol condensation *via* **4.041**. To rule out this possibility, neat NaOMe was also used as the additive, delivering a comparable 52% yield of **4.010**. With no protic solvent added, ketone **4.038** cannot form and the reaction occurs *via* transmetalation.

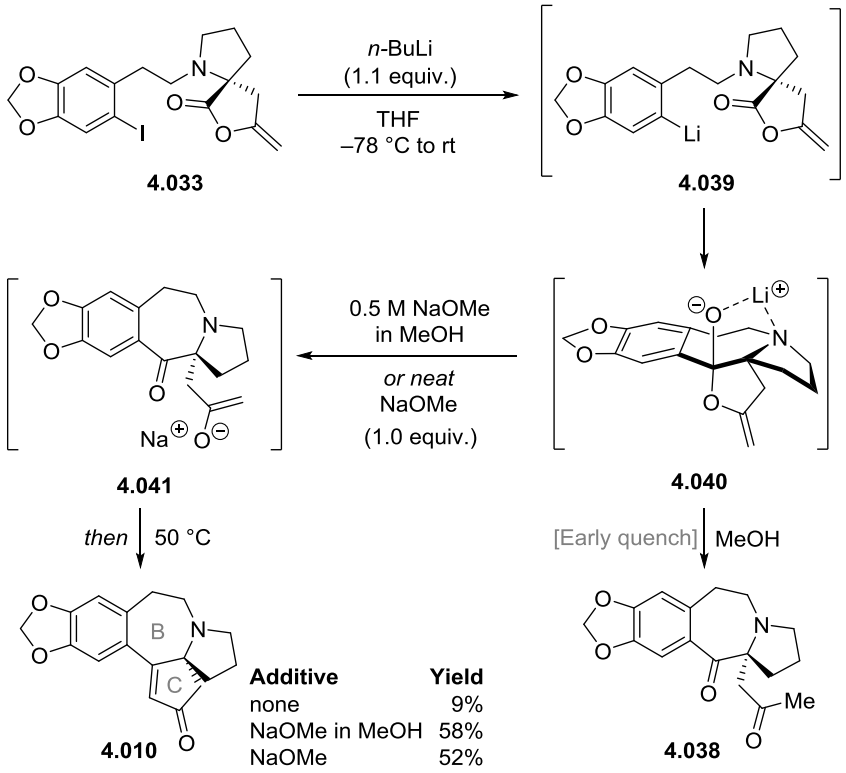

Scheme 46: Completion of the formal synthesis and insight into the domino cyclization with and without the sodium methoxide modification.

4.6 Conclusions and outlook

We set out to develop a concise route to cephalotaxus alkaloids using a new [2,3]-Stevens rearrangement of *N*-allylated prolineamides. Rearranged prolineamide **4.009** was relatively easily elaborated the advanced intermediate **4.025**, with all carbons of the cephalotaxus core in place. Forming the necessary rings onto **4.025** intermediate proved more difficult. Several dead-end ap-

proaches allowed us to gather vital clues on the reactivity of the intermediate: most important being the imidolactonization of **4.025**. This originally unplanned cyclization led to the intriguing cascade process which eventually allowed forming both rings of **4.010** in a one-pot operation. The cephalotaxus project is a prime example of how we have to listen molecules' reactivity preferences, and to follow these trends to arrive to a synthetic route.

During the synthesis efforts, several new reactions and methods were discovered. These include a new Parham–aldol cascade reaction to form enones from *exo*-methylene butenolides (**4.033** → **4.010**), and the establishment of a new [2,3]-rearrangement reaction of *N*-allylated prolineamides (**4.007** → **4.009**). Additionally, several limitations to existing methods were uncovered, most notably the reluctance of certain chelating substrates to react under Wacker oxidation conditions.

In summary, we achieved a 6-step synthesis of the enantiopure pentacyclic core **4.010** of cephalotaxus alkaloids starting from commercially available L-prolineamide **4.016**. The new reactions described herein are a testimony to the usefulness of total synthesis efforts in method development.

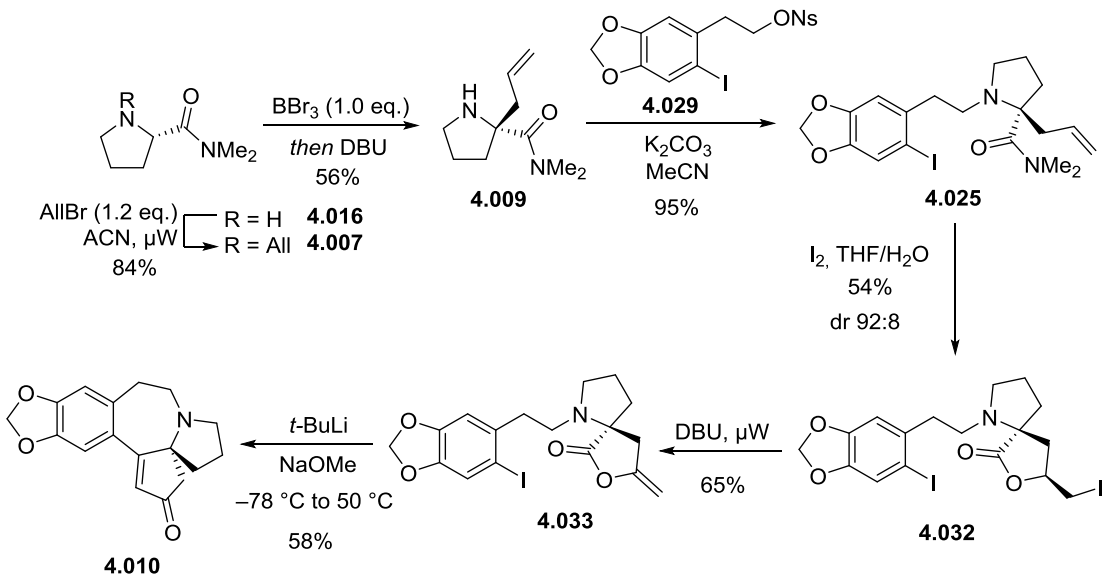

Scheme 47: Developed route to access the *ent*-cephalotaxus alkaloid core **4.010**.

5 CONCLUSIONS AND SUMMARY

"It doesn't make much difference how the paint is put on as long as something has been said. Technique is just a means of arriving at a statement."

– Jackson Pollock

Great turning-points of history have been associated with access to new materials: copper, bronze, iron, oil, plastics, radioactive elements, and semiconductors. In this light, our future lies in our skill to turn existing substances into new ones, our skill to *synthesize*. In this grand picture, the efforts of this thesis have made only infinitesimal improvements to our synthetic skills. Despite new synthetic routes and new reactions discovered, many stones were left unturned: the original divergent plan for stemona alkaloids was not realized in its entirety, nor can the cephalotaxus route compete with semisynthesis. I part with my projects leaving behind more questions than answers.

The two projects highlighted here are examples of how total synthesis develops. Initial rudamentary strategies are only guidelines necessary for exploration. The experimental findings from the first explorations are nessecary to develop new strategies and tactics. Out of this iterative process grows a full-fleshed synthesis, often more intriguing than the one sketched at the early planning stages.

Total synthesis of natural products has faced a lot of criticism in the recent years. There are, however, few other tools that expose and resolve the deep-rooted limitations of our current chemistry. Even seemingly reliable reactions, such as Wacker oxidation or *N*-Boc deprotection, can fail with complex substrates. To be able to streamline the solving of such problems, total synthesis will greatly benefit from fields such as artificial intelligence, cheminformatics, synthesis automatization and synthetic biology.[3]

6 EXPERIMENTAL SECTION

Unless otherwise stated, all reactions were performed with magnetic stirring under a positive pressure of argon gas. Oven- or flame-dried glassware (oven temperature 120 °C) was cooled under vacuum, followed by back-filling with argon, and fitted with rubber septa prior to use. Solids were added under inert gas counter flow or were dissolved and transferred in the appropriate solvent. Solutions and liquid reagents were transferred to reaction vessels by oven-dried stainless-steel cannulas or argon-flushed plastic syringes. Low temperature reactions were carried out in a Dewar vessel filled with isopropanol/liquid nitrogen (–78 °C) or water/ice (0 °C). Prolonged cooling was achieved with Neslab CC 100 immersion cooler. Heated reactions were conducted using a silicon oil bath in reaction vessels equipped with a reflux condenser.

Dry solvents were obtained from a solvent drying system (MBraun SPS-800). Triethylamine was dried by storage over potassium hydroxide pellets. Reactions were monitored by thin-layer-chromatography (TLC) using Merck silica gel F254 pre-coated aluminum plates (230–400 mesh) and visualized by exposure to ultraviolet light (254 nm) or by staining with aqueous potassium permanganate solution [$KMnO_4$ (1 g), K_2CO_3 (6.7 g), NaOH solution (1M aq., 1.7 ml), water (100 ml)], vanillin solution [vanillin (6 g), H_2SO_4 (98%, 5 ml), acetic acid (3 ml), EtOH (250 ml)], or ninhydrin solution [Ninhydrin (0.3 g), acetic acid (1 ml), EtOH (100 ml)], followed by heating with a heat-gun. Flash column chromatography was performed using Merck silica gel 60 (230–400 mesh) with pressurized air using PA grade solvents. Additionally, CombiFlash purification system (CombiFlash® Rf 200, Teledyne ISCO) was used with Redisep Rf Gold® normal phase (400–632 mesh) pre-packaged silica columns.

TBSOTf was prepared using Corey's procedure.[112] 2-furanone **(3.017)** was prepared with Näsman's procedure.[77] *N*-Boc pyrrolam **3.032** was prepared with Curti's procedure.[76] (2*S*,5*S*)-diphenylpyrrolidine (**3.010**) and silyloxyfuran **3.008** were prepared with Pihko's procedure.[65] Molecular sieves were pre-dried in an oven (120 °C) and activated with flame drying under high-vacuum. All other chemicals and reagents were used as received from the supplier without further purification, unless otherwise noted.

NMR spectra were recorded at room temperature on a Bruker Avance III 500, 400 or 300 spectrometers. Proton chemical shifts are expressed in parts-per-million (ppm) and are relative to the residual chloroform in the NMR solvent ($CHCl_3$: 7.26). Carbon chemical shifts are expressed in parts-per-million (ppm) and are relative to the residual chloroform in the NMR solvent ($CDCl_3$: 77.16). Except for complex and overlapping multiplets where a range is given, the chemical shifts of all other multiplets are reported as the center of the signal range. Additionally, other NMR techniques (COSY, HMQC, HMBC, and DEPT) were used to assist with signal assignment. For further elucidation of 3D structure, nuclear Overhouser enhanced spectroscopy (NOESY) was used. Raw FID data was processed and analyzed using MestReNova 10.0.2 from Mestrelab Research R.L.

Mass spectra were recorded with Micromass LCT ESI-TOF Premier mass spectrometer, and with Agilent 6560 Ion Mobility Q-TOF LC-MS.

IR spectra were recorded with Bruker Alpha Platinum ATR single reflector spectrometer and the compound was applied as a thin film directly on the ATR unit (neat or in dichloromethane). Data are represented as the most characteristic absorption frequencies in cm^{-1}.

Optical rotation values were recorded on a Perkin Elmer Model 343 polarimeter at room temperature using the sodium D-line (λ = 589 nm) and a 10 cm cuvette. The sample concentration and solvent are reported in the relevant sections of the experimental part. Specific rotations are given in 10^{-1} deg cm^2 g^{-1}.

The enantiomeric ratios (er) were determined either by GC using Agilent 7820A GC system (SUPELCO Astec CHIRALDEX B-DM column) or by HPLC using Waters 501 pump unit and Waters 486 detector (CHIRALPAL IC ø 0.46 cm × 25 cm) in comparison to the corresponding racemic samples.

Melting points were determined in open capillaries using Gallenkamp melting point apparatus and are uncorrected.

6.1 Stemona alkaloid project

6.1.1 *tert*-Butyl 2-((*tert*-butyldimethylsilyl)oxy)-1*H*-pyrrole-1-carboxylate (3.018)

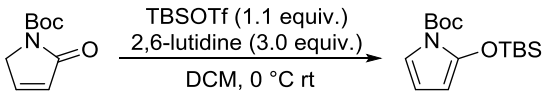

3.032 **3.018**

To a solution of *N*-Boc pyrrolam **3.032** (3.0 g, 16 mmol, 1.0 equiv., recrystallized from hexane, dried in high-vacuum for 1 h) and 2,6-lutidine (5.7 ml, 49 mmol, 3.0 equiv.) in DCM (30 mL) at 0 °C was added TBSOTf (4.0 ml, 4.5 g, 17 mmol, 1.1 equiv.). The reaction mixture was allowed to warm to rt and stirred for 1 h. The reaction was quenched with sat. aq. $NaHCO_3$ (50 mL). The reaction mixture

was extracted with Et_2O (2 × 50 mL). The combined organic layers were dried with Na_2SO_4 and concentrated *in vacuo*. Purification of the residue by flash chromatography (5% EtOAc/hexane to 10% EtOAc/hexane) afforded the desired product **3.018** as light-yellow viscous oil (3.45 g, 71%).

Spectroscopic data matched those reported previously.[76]

***R*f** (50% EtOAc/hexane): 0.40 (Vanillin, dark brown).

^{1}H NMR (300 MHz) δ: 6.59 (dd, *J* = 3.7, 2.0, 1H), 5.80 (t, *J* = 3.7 Hz, 1H), 5.09 (dd, *J* = 3.7, 2.0 Hz, 1H), 1.47 (s, 9H), 0.89 (s, 9H), 0.13 (s, 6H) ppm.

^{13}C NMR (75 MHz) δ: 173.1, 156.4, 121.5, 83.2, 61.8, 29.6, 27.8 ppm.

6.1.2 *tert*-Butyl 2-oxo-5-(5-oxotetrahydrofuran-3-yl)-2,5-dihydro-1*H*-pyrrole-1-carboxylate (3.019)

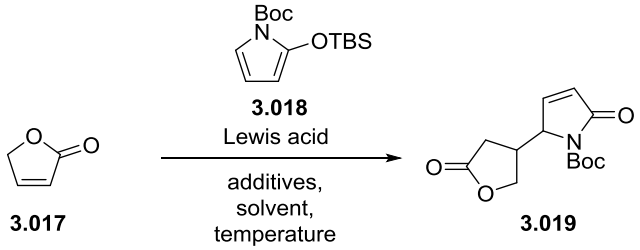

To a solution of butenolide (**3.017**) (1.0 equiv.), Lewis acid (0.1 equiv.) and additives in DCM (0.1 M) at 0 °C silyloxypyrrole **3.018** (1.0–2.0 equiv.) was added in DCM (0.1 M). The reaction mixture was stirred until full consumption of either starting material was observed and quenched with water (1 ml). The mixture was extracted with EtOAc (3 × 1 ml), the combined organic layers were dried with Na_2SO_4 and concentrated *in vacuo*. Purification with flash chromatography (EtOAc) gave the adduct **3.019** as a yellow oil.

^{1}H NMR (300 MHz, $CDCl_3$) δ: 7.34 (d, *J* = 5.6 Hz, 1H), 6.00 (d, *J* = 5.6 Hz, 1H), 5.02 (tdd, *J* = 6.7, 3.0, 1.5 Hz, 1H), 2.20–1.68 (m, 4H), 1.67 (s, 3H), 1.56 (s, 3H), 1.46 (s, 3H) ppm.

^{13}C NMR (75 MHz, $CDCl_3$) δ: 172.8, 160.4, 133.0, 123.2, 120.7, 89.1, 38.6, 25.9, 24.3, 22.8, 18.0 ppm.

6.1.3 (*R*)-5-(3-Hydroxypropyl)furan-2(5*H*)-one (3.026)

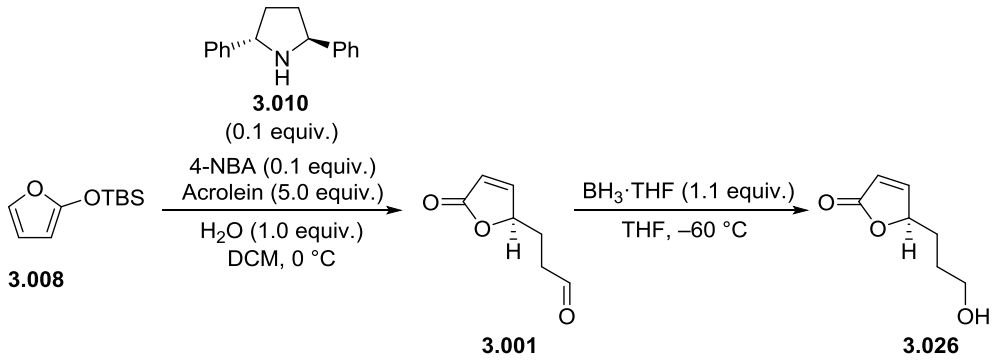

To a stirred solution of 4-nitrobenzoic acid (374 mg, 2.24 mmol, 0.100 equiv.), (2*S*,5*S*)-diphenylpyrrolidine (**3.010**) (500 mg, 2.24 mmol, 0.1 equiv.), water (0.8 ml, 0.8 g, 5 mmol, 2 equiv.) and acrolein (7.5 ml, 6.3 g, 110 mmol, 5.0 equiv.) in DCM (25 mL) at 0 °C was added silyloxyfuran **3.008** (4.6 ml, 4.4 g, 2.4 mmol, 1.0 equiv.). After 5 h the reaction mixture was directly loaded onto a SiO_2 column and eluted with Et_2O to afford the aldehyde **3.001** as a clear oil (2.03 g, 65%).

To a stirred solution of the resulting aldehyde **3.001** (2.03 g, 14.5 mmol, 1.00 equiv., dried as a THF azeotrope) in THF (50 ml) at –60 °C was added BH_3·THF (1.37 g, 15.9 ml, 1.10 equiv., 1.0 M soln. in THF). The mixture was allowed to stir for 30 min, after which time TLC showed full conversion. The reaction was quenched with aq. sat. NH_4Cl (10 ml) and allowed to warm to rt. After effervescence subsided the mixture was further diluted with brine (20 ml) and extracted with EtOAc (6 × 20 ml). The combined organic layers were dried with Na_2SO_4 and concentrated. Purification with flash column (EtOAc) gave the desired alcohol **3.026** as a clear oil (1.51 g, 73%, er = 95:5).

Note: Racemic aldehyde was prepared from (furan-2-yloxy)trimethylsilane according to the following procedure:

To a stirred solution of 4-nitrobenzoic acid (3.26 g, 15.4 mmol, 0.2 equiv.), pyrrolidine (1.3 ml, 3.3 g, 15.4 mmol, 0.2 equiv.), water (2.7 ml, 154 mmol, 2.0 equiv.) and acrolein (15.5 ml, 12.9 g, 230 mmol, 3.0 equiv.) in DCM (300 ml) at –50 °C was added (furan-2-yloxy)trimethylsilane (12.0 g, 77 mmol, 1.0 equiv.). After 5 h the reaction mixture was carefully concentrated to half the volume and directly loaded onto a flash column and eluted with Et_2O to afford the aldehyde *rac*-**3.026** as a clear oil (6.82 g, 64%).

Spectroscopic data matched those reported previously.[66]

R_f (EtOAc): 0.27 (Vanillin, dark blue).

^{1}H NMR (300 MHz, $CDCl_3$) δ: 7.46 (dd, *J* = 5.7, 1.5 Hz, 1H), 6.07 (dd, *J* = 5.7, 2.0 Hz, 1H), 5.09 (app. tdd, *J* = 7.0, 1.8, 5.0 Hz, 1H), 3.67 (t, *J* = 5.9 Hz, 1H), 2.09 (br. s, 1H), 1.91 (m, 1H), 1.70 (m, 3H) ppm.

^{13}C NMR (75 MHz, $CDCl_3$) δ: 173.1, 156.4, 121.5, 83.2, 61.8, 29.6, 27 ppm.

FTIR (film, cm^{-1}) ν: 3402, 3088, 2931, 2873, 1734, 1330, 1162, 1011, 817.

$[\alpha]_D^{20}$ = +67.1° (*c* = 1.0, DCM).

GC (SUPELCO Astec CHIRALDEX B-DM column, 150 °C isothermal): $t_R(R)$ = 8.6 min, $t_R(S)$ = 10.0 min.

6.1.4 (*R*)-3-(5-Oxo-2,5-dihydrofuran-2-yl)propyl 4-methylbenzenesulfonate (3.036)

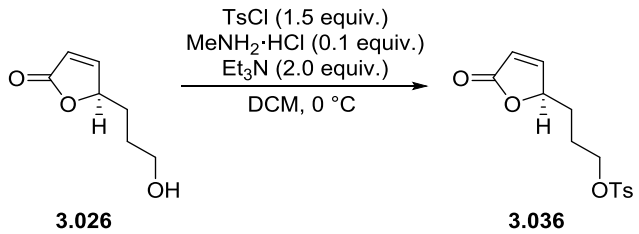

3.026 **3.036**

To a stirred solution of methylamine hydrochloride (170 mg, 1.8 mmol, 0.1 equiv), triethylamine (5.0 mL, 3.6 g, 36 mmol, 2.0 equiv.) and alcohol **3.026** (2.53 g, 17.8 mmol, 1.00 equiv.) in DCM (20 ml) at 0 °C, tosyl chloride (5.09 g, 26.7 mmol, 1.50 equiv.) was added in small portions. The mixture was allowed to stir for 10 min, after which time the reaction was complete as indicated by TLC. The reaction was quenched with 1 M aq. $NaHSO_4$ (10 ml) followed by water (20 ml). The aqueous layer was extracted with dichloromethane (3 × 20 mL), the combined organic layers dried with Na_2SO_4, and concentrated *in vacuo*. Purification of the residue by flash chromatography (30% EtOAc/hexane to 60% EtOAc/hexane) afforded the desired product **3.036** as white solid (4.79 g, 91%, er = 95:5).

R_f (60% EtOAc/hexane): 0.46 (Ninhydrin, orange).

^{1}H NMR (300 MHz, $CDCl_3$) δ: 7.84–7.73 (m, 2H), 7.40 (dd, *J* = 5.7, 1.5 Hz, 1H), 7.38–7.32 (m, 2H), 6.11 (dd, *J* = 5.7, 2.0 Hz, 1H), 5.02 (ddt, *J* = 8.0 Hz, 4.3 Hz, 1.9 Hz, 1H), 4.11 (ddd, *J* = 10.0, 6.7, 5.5 Hz, 1H), 4.05 (ddd, *J* = 10.0, 6.7, 5.5 Hz, 1H), 2.46 (s, 3H), 2.04–1.56 (m, 4H) ppm.

^{13}C NMR (75 MHz, $CDCl_3$) δ: 172.7, 155.8, 145.1, 133.0, 130.1, 128.0, 128.0, 122.0, 83.3, 69.6, 29.4, 24.5, 21.7 ppm.

FTIR (film, cm^{-1}) v: 1748, 1353, 1172, 927, 811, 661, 552.

$[\boldsymbol{\alpha}]_{\boldsymbol{D}}^{\mathbf{20}}$ = +19.1° (*c* = 1.0, DCM).

HRMS (ESI^+): m/z [M+Na] calcd. for [$C_{14}H_{15}NO_5SNa^+$] 319.0611, found 319.0600, Δ = 1.1 mDa.

HPLC: Chiralpak IC, 50% 2-propanol/hexane, 0.5 mL · min^{-1}, rt, λ = 210 nm, t_R(*R*) = 114.2 min, t_R(*S*) = 121.9 min.

6.1.5 *tert*-Butyl (*R**/*S**)-2-oxo-5-((2*R**,3*R**)-5-oxo-2-(3-(tosyloxy)propyl)tetrahydrofuran-3-yl)-2,5-dihydro-1*H*-pyrrole-1-carboxylate (3.037)

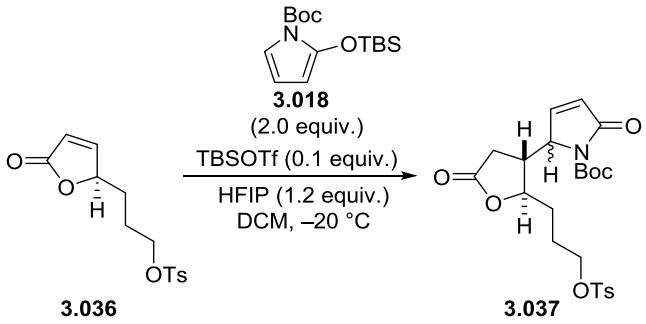

To a stirred solution of tosylate **3.036** (100 mg, 0.34 mmol, 1.0 equiv.) at –20 °C in DCM (10 ml) was added TBSOTf (8 µL, 9 mg, 0.1 equiv.) and HFIP (35 µL, 57 mg, 1.0 equiv.). To this solution was then added silyloxypyrrole **3.018** (201 mg, 0.67 mmol, 2.0 equiv.) in DCM (0.5 ml) and the resulting solution was stirred for 8 h. The reaction was quenched with pH 7.0 buffer (2 ml), and vigorously stirred for 1 h at rt. The resulting mixture was then extracted with EtOAc (5 × 3 ml), the combined organic layers dried with Na_2SO_4, and concentrated *in vacuo*. Purification of the residue by CombiFlash automated chromatography system (10% EtOAc/hexane to 80% EtOAc/hexane) afforded the desired product **3.037** as a white foam (105 mg, 65%, dr 1:1).

$\boldsymbol{R_f}$ (60% EtOAc/hexane): 0.19 (ninhydrin, brown).

^{1}H (300 MHz, $CDCl_3$, diastereomers overlapping): 7.75–7.82 (m, 2H), 7.33–7.39 (m, 2H), 7.04–7.08 (m, 1H), 6.23–6.30 (m, 2H), 4.70–4.77 (m, 2H), 3.37–4.44 (m, 1H), 3.87–4.20 (m, 3H), 3.14–3.28 (m, 1H), 2.83 (dd, *J* = 18.4, 9.9 Hz, 0.5H), 3.36–3.48 (m, 1H), 2.46 (s, 3H), 1.98–2.07 (m, 1H), 1.82–1.94 (m, 2H), 1.57 (s, 9H) ppm.

^{13}C NMR (127 MHz, $CDCl_3$, diastereomers overlapping) δ: 177.82, 177.58, 174.28, 174.07, 83.48, 81.10, 80.53, 62.13, 61.07, 57.82, 55.27, 52.57, 48.97, 40.91, 40.32, 39.93, 38.59, 30.84, 30.36, 30.13, 29.77, 24.94, 23.34, 22.36, 21.77, 15.50, 10.97.

HRMS (ESI$^+$): m/z [M+Na] calcd. for [$C_{23}H_{29}NO_8SNa$] 502.1506, found 502.1511, Δ = –0.5 mDa.

FTIR (film, cm^{-1}) ν: 2978 (weak), 2934 (weak), 1769, 1738, 1771, 1353, 1310, 1172, 1153, 816, 662, 553.

Note: Additional side products observed.

3-(5-Oxo-4,5-dihydrofuran-2-yl)propyl 4-methylbenzenesulfonate (3.039)

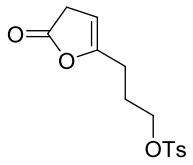

3.039

***R*$_f$** (60% EtOAc/hexane): 0.72 (Vanillin, yellow).

^{1}H NMR (300 MHz, $CDCl_3$) δ: 7.79 (d, *J* = 8.3 Hz, 2H), 7.35 (d, *J* = 8.3 Hz, 2H), 5.13–5.10 (m, 1H), 4.07 (t, *J* = 6.0 Hz, 2H), 3.14 (q, *J* = 3.14 Hz, 2H), 2.45 (s, 3H), 3.41-3.34 (m, 2H), 1.91 (q, *J* = 6.5 Hz, 2H), 1.60–1.55 (m, 2H) ppm.

***tert*-Butyl 2-(1-(*tert*-butoxycarbonyl)-5-oxopyrrolidin-3-yl)-5-oxo-2,5-dihydro-1*H*-pyrrole-1-carboxylate (3.042)**

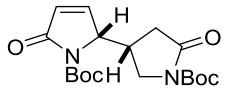

3.042

***R*$_f$** (80% EtOAc/hexane): 0.34 ($KMnO_4$).

^{1}H NMR (300 MHz, $CDCl_3$) δ: 7.10 (dd, *J* = 6.2, 2.0 Hz, 1H), 6.22 (dd, *J* = 6.2, 1.7 Hz, 1H), 4.70 (dt, *J* = 4.0, 1.8 Hz, 1H), 3.63–3.60 (m, 1H), 3.30–3.20 (m, 2H), 8.65 (dd, *J* = 18.0, 9.4 Hz, 1H), 2.50–2.40 (1H, m), 1.57 (9H, s), 1.50 (9H, s) ppm.

^{13}C NMR (75 MHz, $CDCl_3$) δ: 172.1, 168.5, 145.6, 129.2, 84.2, 83.7, 64.0, 54.6, 39.0, 30.7, 28.3, 28.1 ppm.

3-((*R)-5-Oxo-2-((2*S**,3*S**)-5-oxo-2-(3-(tosyloxy)propyl)tetrahydrofuran-3-yl)-2,5-dihydrofuran-2-yl)propyl 4-methylbenzenesulfonate**

Note that the following side product was characterized only after hydrogenation.

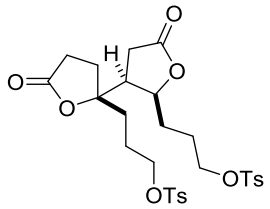

3.041 [reduced]

R_f (10% MeOH/EtOAc): 0.72 (Vanillin, blue).

^{1}H NMR (400 MHz, $CDCl_3$, 1:1.1 dr) δ: 7.75–7.80 (4H, m), 7.34–7.38 (4H, m), 4.40 (td, *J* = 9.2, 3.6 1H), 3.99–4.14 (4H, m), 2.71 (dd, *J* = 18.4, 10.1 Hz, 1H, major) 2.71 (dd, *J* = 18.3, 10.1 Hz, 1H, minor), 2.59–2.66 (m, 2H), 2.55 (1H, td, J = 9.8, 4.7 Hz), 2.46 (s, 3H), 2.45 (s, 2H), 2.36 (dd, *J* = 18.4, 4.9 Hz, 1H, major), 2.35 (dd, *J* = 18.3, 4.9 Hz, 1H, minor), 2.07–2.16 (m, 1H), 1.96–2.04 (m, 1H), 1.61–1.90 (8H, m) ppm.

^{13}C NMR (100 MHz, $CDCl_3$, 1:1.1 dr) δ: 175.2, 174.6, 145.3 (major), 145.2 (minor), 130.2 (major), 130.1 (minor), 128.0, 87.0, 79.7, 69.7 (major), 69.6 (minor), 47.9, 32.7, 32.1, 29.9, 28.6, 28.2, 25.0, 23.0, 21.8 ppm.

FTIR (film, cm^{-1}) v: 2961 (weak), 225, 1767, 1352, 1174, 912, 728, 509.

HRMS (ESI^+): m/z [M+Na] calcd. for [$C_{18}H_{23}NO_6SNa$] 617.1491, found 617.1451, Δ = –0.4 mDa.

6.1.6 *tert*-Butyl 2-((*tert*-butyldimethylsilyl)oxy)-5-((2*R**,3*R**)-5-oxo-2-(3-(tosyloxy)propyl)tetrahydrofuran-3-yl)-1*H*-pyrrole-1-carboxylate (3.038)

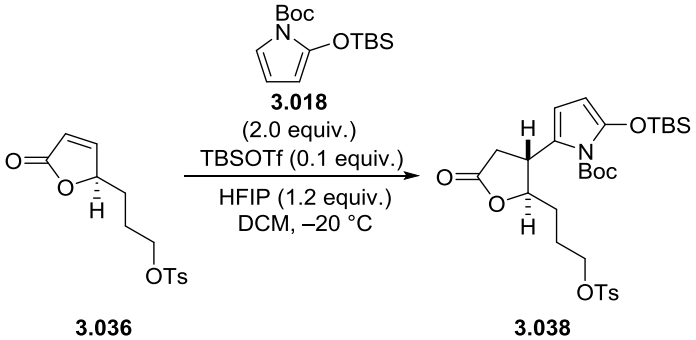

3.036 **3.038**

Carried out according to the procedure in 6.1.5 but quenched with triethylamine (0.5 ml). Purification of the residue by flash chromatography (30% EtOAc/hexane to 60% EtOAc/hexane) afforded the silyloxypyrrole **3.038** as a yellow oil (48 mg, 23%, 10:1 mixture of rotamers).

R_f (30% EtOAc/hexane): 0.33 (Vanillin, dark brown).

^{1}H NMR (300 MHz, $CDCl_3$) δ: 8.30 (d, *J* = 8.3 Hz, 2H), 7.34 (d, *J* = 8.3 Hz, 2H), 5.74 (dd, *J* = 3.7, 0.9 Hz, 1H), 5.12 (d, *J* = 3.7 Hz, 1H), 4.44 (ddd, *J* = 9.2, 6.6, 2.6 Hz, 1H), 4.00–4.13 (m, 2H), 3.68 (app. q, *J* = 8.0 Hz, 2H), 2.90 (dd, *J* = 17.7, 8.6 Hz, 1H), 2.48 (dd, J = 17.7, 7.9 Hz, 1H), 2.44 (s, 3H), 1.67–1.95 (4H, m), 1.58 (s, 9H), 0.97 (s, 9H), 0.25 (s, 6H) ppm.

^{13}C NMR (75 MHz, $CDCl_3$) δ: 175.8, 149.7, 144.9, 144.0, 133.2, 130.0, 128.0, 124.1, 106.5, 90.0, 84.5, 84.0, 70.0, 40.2, 36.5, 30.7, 28.2, 25.9, 25.7, 21.8, 18.6, –4.4 ppm.

FTIR (film, cm^{-1}) v: 2957, 2931, 2859, 1781, 1733, 1596, 1545, 1298, 1174, 816, 743, 663, 553.

HRMS (ESI^+): m/z [M+Na] calcd. for [$C_{29}H_{43}NO_8SSiNa$] 616.2371, found 616.2349, Δ = 2.2 mDa.

6.1.7 *tert*-Butyl (*R*/S**)-2-oxo-5-((2*R**,3*R**)-5-oxo-2-(3-(tosyloxy)propyl)tetrahydrofuran-3-yl)pyrrolidine-1-carboxylate (3.044) and (3.045)

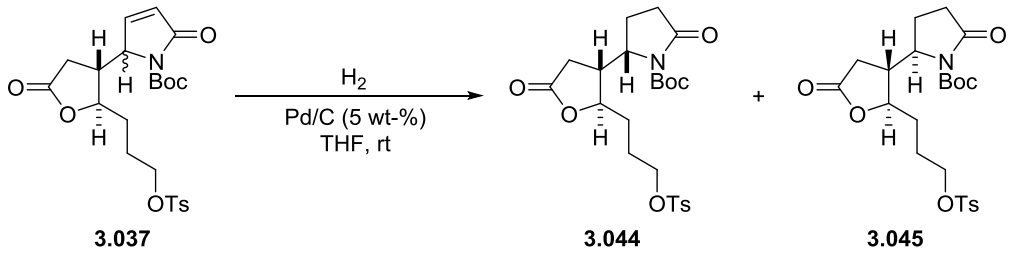

A suspension of Pd/C (20 mg, 5 wt-%, washed with acetone before using) and lactam **3.037** (400 mg, 834 mmol, 1.0 equiv.) in THF (5 ml) was stirred under a balloon pressure of H_2 overnight. The resulting mixture was filtered through a short pad (0.5 cm × 0.6 cm) of alumina, and the pad washed with further THF (3 × 2 ml). Combined filtrates were concentrated. Flash column chromatography (30% EtOAc/hexane to 70% EtOAc/hexane) gave the lactam **3.044** (192 mg, 96%) as a white sticky semisolid and lactam **3.045** (188 mg, 94%) as a white foamy semisolid.

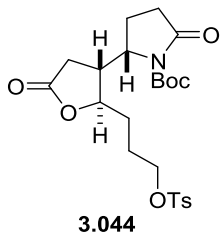

***R*$_f$** (80% EtOAc/hexane): 0.48 ($KMnO_4$).

^{1}H NMR (500 MHz, $CDCl_3$) δ: 7.77 (app. d, *J* = 8.3 Hz, 2H), 7.95 (app. d, *J* = 8.4 Hz, 2H), 4.33 (ddd, *J* = 8.5, 5.0, 3.2 Hz, 1H), 4.24 (ddd, *J* = 8.7, 4.9, 3.5 Hz, 1H), 4.08 (ddd, *J* = 10.0, 6.8, 4.8 Hz, 1H), 4.02 (ddd, *J* = 10.0, 6.6, 5.2 Hz, 1H), 2.75 (tdd, *J* = 9.9, 6.1, 5.0 Hz, 1H), 2.66 (dd, *J* = 17.7, 9.4 Hz, 1H), 2.51–2.55 (m, 2H), 2.45 (s, 3H), 2.38 (dd, *J* = 17.7, 6.2 Hz, 1H), 2.22 (dtd, *J* = 13.7, 9.8, 8.7 Hz, 1H), 1.18–1.88 (m, 1H), 1.71–1.77 (m, 3H), 1.16–1.68 (m, 1H), 1.53 (s, 9H) ppm.

^{13}C NMR (127 MHz, $CDCl_3$) δ: 175.0 (C=O), 173.6 (C=O), 150.6 (C=O), 145.1 (C), 133.0 (C), 130.1 (CH), 128.0 (CH), 84.4 (C), 80.6 (CH), 69.6 (CH_2), 57.5 (CH), 43.6 (CH), 31.8 (CH_2), 31.5 (CH_2), 30.8 (CH_2), 28.1 (CH_3), 25.2 (CH_2), 21.8 (CH_3), 20.7 (CH_2) ppm.

FTIR (film, cm^{-1}) ν: 2977, 2932, 2252, 1772, 1711, 1173, 1511.

HRMS (ESI^+): m/z [M+Na] calcd. for [$C_{23}H_{31}NO_8SNa$] 504.1663, found 504.1656, Δ = 0.7 mDa.

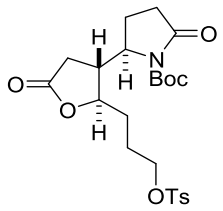

3.045

***R*$_f$** (80% EtOAc/Hexane): 0.39 ($KMnO_4$).

^{1}H NMR (500 MHz, $CDCl_3$) δ: 7.76 (app. d, *J* = 8.2 Hz, 2H), 7.34 (app. d, *J* = 8.2 Hz, 2H), 4.27–4.32 (m, 2H), 4.08 (ddd, *J* = 10.0, 6.8, 4.9 Hz, 1H), 4.00 (ddd, *J* = 10.0, 6.6, 5.1 Hz, 1H), 2.77 (tdd, *J* = 8.9, 6.9, 5.5 Hz, 1H), 2.58 (dd, *J* = 17.7, 8.7 Hz, 1H), 2.51–2.54 (m, 2H), 2.44 (s, 3H), 2.33 (dd, *J* = 17.7, 8.7 Hz, 1H), 2.20 (dtd, *J* = 13.6, 10.1, 8.7 Hz, 1H), 1.85–1.93 (m, 1H), 1.73–1.82 (m, 3H), 1.59–1.65 (m, 1H), 1.52 (s, 9H) ppm.

^{13}C NMR (127 MHz, $CDCl_3$) δ: 174.68 (C=O), 173.19 (C=O), 150.28 (C=O), 145.09 (C), 132.88 (C), 130.06 (CH), 127.97 (CH), 84.13 (C), 81.19 (CH), 69.64 (CH_2), 57.70 (CH), 43.85 (CH), 31.55 (CH_2), 31.54 (CH_2), 30.63 (CH_2), 28.10 (CH_3), 25.49 (CH_2), 21.74 (CH_3), 19.96 (CH_2) ppm.

FTIR (film, cm^{-1}) ν: 2978, 1773, 1710, 1355, 1256, 1172, 1149, 959, 915, 729, 662, 553.

HRMS (ESI^+): m/z [M+Na] calcd. for [$C_{23}H_{31}NO_8SNa$] 504.1663, found 504.1659, Δ = 0.4 mDa.

6.1.8 3-((2*R**,3*R**)-5-Oxo-3-((*R**)-5-oxopyrrolidin-2-yl)tetrahydrofuran-2-yl)propyl 4-methylbenzenesulfonate (3.047)

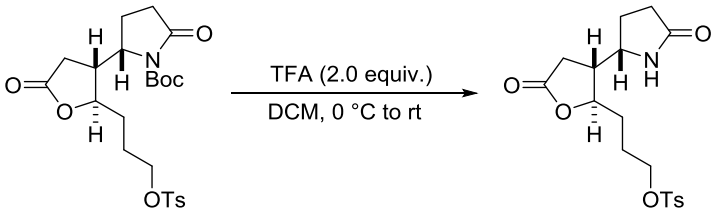

3.044 **3.047**

To a solution of *N*-Boc lactam **3.044** (100 mg, 2.1 mmol, 1.0 equiv) in dry DCM (2 ml) at 0 °C was added trifluoroacetic acid (32 µl, 47 mg, 4.2 mmol, 2.0 equiv) and then allowed to warm to rt. After stirring for 4 h the mixture was diluted with DCM (2 ml) and quenched with 7% aqueous $NaHCO_3$ (2 ml). The aqueous phase was immediately extracted with DCM (4 × 2 ml). Combined organic layers were dried with Na_2SO_4, and concentrated *in vacuo* to give the lactam **3.047** as beige foam (70 mg, 84%).

Note: As an alternative to the extraction protocol, trifluoroacetic acid can also be removed by successive azeotropical distillation, first with toluene (5 × 5 ml) and after that with chloroform (5 × 5 ml).

R_f (10% MeOH/EtOAc): 0.23 ($KMnO_4$).

^{1}H NMR (500 MHz, $CDCl_3$) δ: 7.78 (app. d, *J* = 8.3 Hz, 1H), 7.44 (br. s, 0.85H), 7.36 (app. d, *J* = 8.3 Hz, 1H), 4.29 (ddd, *J* = 9.3, 6.2, 2.6 Hz, 1H), 4.14 (ddd, *J* = 10.0, 6.9, 4.5 Hz, 1H), 4.02 (ddd, *J* = 10.0, 6.5, 4.3 Hz, 1H), 3.87 (app. q, *J* = 7.0 Hz, 1H), 2.67 (dd, *J* = 17.7, 9.0 Hz, 1H), 2.46 (s, 3H), 4.40–2.47 (m, 3H), 2.32–2.38 (m, 2H), 1.67–1.93 (m, 5H) ppm.

^{13}C NMR (127 MHz, $CDCl_3$) δ: 180.0 (C=O), 174.9 (C=O), 145.3 (C), 132.9 (C), 130.1 (CH), 128.00 (CH), 80.7 (CH), 69.6 (CH_2), 55.3 (CH), 45.9 (CH), 31.2 (CH_2), 30.4 (CH_2), 30.2 (CH_2), 25.2 (CH_2), 25.1 (CH_2), 21.8 (CH_3) ppm.

FTIR (film, cm^{-1}) ν: 3225, 2928, 1772, 1690, 1353, 1173, 959, 922, 663, 552.

HRMS (ESI^+): m/z [M+H] calcd. for [$C_{18}H_{23}NO_6SH$] 382.1319, found 382.1314, Δ = 0.5 mDa.

6.1.9 Norstemoamide (3.048)

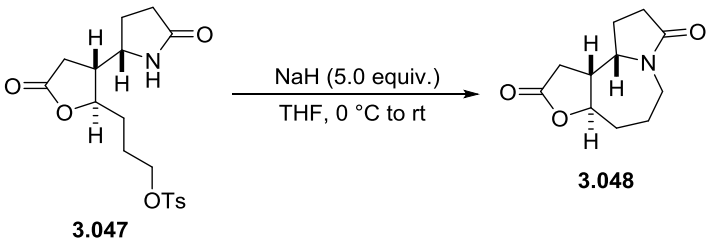

3.047 3.048

To a stirred suspension of NaH (136 mg, 3.41 mmol, 5.0 equiv., 60 wt-% in mineral oil) in THF (15 mL) at 0 °C a solution of tosylate **3.047** (140 mg, 0.367 mmol, 1.0 equiv.) in THF (10 mL) was cannulated dropwise and the flask rinsed with further THF (1 mL). The reaction mixture was allowed to warm to rt. After 17 h of stirring the reaction was quenched at 0 °C with dropwise addition of 2 M HCl (2 ml). The mixture was partitioned into two phases by adding brine (2 ml). THF layer was collected, and the aqueous layer extracted with EtOAc (4 × 8 ml). Combined organic layers were dried with Na_2SO_4 and concentrated *in vacuo*. Flash chromatography (EtOAc to 5% MeOH/EtOAc) gave the free lactam **3.048** as a clear oil (35.7 mg, 25%).

Spectroscopic data matched those reported previously.[23,26,86,113]

R_f (10% MeOH/EtOAc): 0.20 ($KMnO_4$).

^{1}H NMR (500 MHz, $CDCl_3$) δ: 4.28 (td, *J* = 10.2, 2.9 Hz, 1H), 4.15 (td, *J* = 3.0, 13.7 Hz, 1H), 3.99 (dt, *J* = 6.4, 10.5 Hz, 1H), 2.85 (dtd, *J* = 6.8, 9.4, 12.7 Hz, 1H), 2.62–2.70 (m, 2H), 2.51 (dd, *J* = 12.7, 17.3 Hz, 1H), 2.37–2.44 (m, 3H), 2.04–2.10 (m, 1H), 1.83–1.88 (m, 1H), 1.71 (app. p, *J* = 10.5 Hz, 1H), 1.52–1.61 (m, 2H) ppm.

^{13}C NMR (127 MHz, $CDCl_3$) δ: 176.4 (C=O), 175.8 (C=O), 81.5 (CH), 57.7 (CH), 46.6 (CH), 41.9 (CH_2), 36.3 (CH_2), 32.7 (CH_2), 32.3 (CH_2), 27.2 (CH_2), 24.4 (CH_2) ppm.

6.1.10 (±)-Stemoamide (3.006)

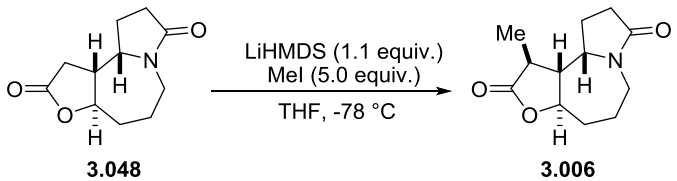

3.048 3.006

To a solution of norstemoamide **3.048** (5.0 mg, 0.024 mmol, 1.0 equiv.) in THF (0.5 ml) LiHMDS (27 µl, 4.4 mg, 0.026 mmol, 1.1 equiv., 1.0 M in THF) was added at –78 °C. After 10 min the reaction mixture was warmed to 0 °C for 10 min and then recooled to –78 °C. To the stirred yellow suspension methyl iodide (7 µl, 17 mg, 0.12 mmol, 5.0 equiv.) was added dropwise. After 3 h the reaction

mixture was quenched with sat. aq. NH_4Cl (0.5 ml) and extracted with EtOAc (5 × 2 ml). Combined organic layers were dried with Na_2SO_4 and concentrated *in vacuo*. Flash chromatography gave (±)-stemoamide (**3.006**) as a white solid (3.3 mg, 62%).

Note: X-Ray quality crystals were obtained upon slow evaporation from ethyl acetate.

Specroscopic data matched those reported previously.[86]

***R*f** (10% MeOH/EtOAc): 0.34 ($KMnO_4$).

^{1}H NMR (500 MHz, $CDCl_3$) δ: 4.19 (app. td, *J* = 4.8, 10.7 Hz, 1H), 4.16 (td partially obstructed, *J* = 3.0, 14.8 Hz, 1H), 4.02 (td, *J* = 10.7, 6.4 Hz, 1H), 2.26–2.68 (m, 1H), 2.60 (dq, *J* = 12.3, 6.9 Hz, 1H), 2.40–2.46 (m, 4H), 2.04–2.10 (m, 1H), 1.87–1.91 (m, 1H), 1.74 (app. dq, *J* = 12.3, 10.7 Hz, 1H), 1.51–1.60 (m, 3H), 1.33 (d, *J* = 6.9 Hz, 3H) ppm.

^{13}C NMR (127 MHz, $CDCl_3$) δ: 177.5, 174.1, 77.6, 56.0, 52.9, 40.4, 37.5, 35.0, 30.8, 25.8, 22.7, 14.3 ppm.

FTIR (film, cm^{-1}) ν: 3501, 2935, 1764, 1676, 1420, 1190, 1008.

HRMS (ESI^+)**:** m/z [M+H] calcd. for [$C_{12}H_{17}NO_3$] 223.1208, found 223.1208, Δ = 0.0 mDa.

ScXRD:

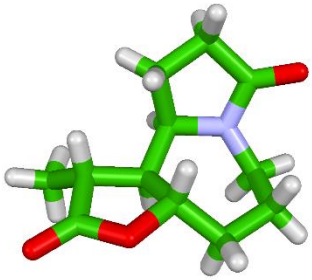

Empirical formula	$C_{12}H_{16}NO_3$
M (g mol^{-1})	223.26
Space group	$P2_1$
Crystal system	monoclinic
a [Å]	7.3465(2)
b [Å]	6.75007(19)
c [Å]	11.6498(4)
α [°]	90
β [°]	102.056(3)
γ [°]	90
V [Å^3]	564.97(3)
Z	2
ρ_{calcd} [mg m^{-3}]	1.312
Wavelength [Å]	0.71073
reflections collected	2585
refined parameters	146
R	0.0522
wR	0.1107
GOF	1.079

6.1.11 3-((2*R**,3*R**)-5-Oxo-3-((*R**)-5-oxopyrrolidin-2-yl)tetrahydrofuran-2-yl)propyl 4-methylbenzenesulfonate (3.048)

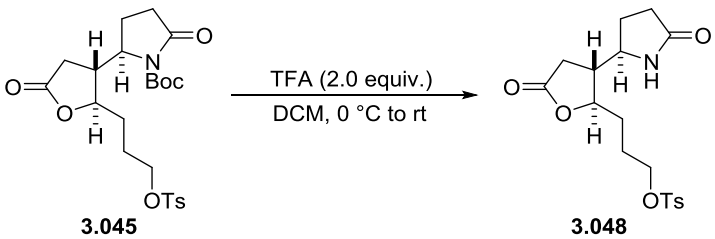

3.045 **3.048**

To a solution of *N*-Boc lactam **3.045** (106 mg, 2.2 mmol, 1.0 equiv) in dry DCM (2 ml) at 0 °C was added trifluoroacetic acid (34 µl, 47 mg, 4.4 mmol, 2.0 equiv) and then allowed to warm to rt. After stirring for 4 h the mixture was diluted with DCM (2 ml) and quenched with 7% aqueous $NaHCO_3$ (2 ml). The aqueous phase was immediately extracted with DCM (4 × 2 ml). Combined organic lay-

ers were dried with Na_2SO_4 and concentrated to give the lactam **3.048** as beige foam (68.1 mg, 81%, 1:4.7 mixture presumed to be rotamers).

Note: Alternative to the extraction trifluoroacetic acid can also be removed by azeotropical distillation with toluene (5 × 5 ml) followed by chloroform (5 × 5 ml).

Note: X-Ray quality crystals were obtained upon slow evaporation from DCM.

MP: 156.5–157.7 °C.

$\boldsymbol{R_f}$ (6% MeOH/DCM): 0.45 (UV or $KMnO_4$).

^{1}H NMR (500 MHz, $CDCl_3$, major rotamer) δ: 7.97 (br. s., N–*H*, 0.75H), 7.77 (d, *J* = 8.2 Hz, 2H), 7.36 (app. d., *J* = 8.2 Hz, 2H), 4.37 (ddd, *J* = 2.5, 4.8, 9.5 Hz, 1H), 4.12 (dt, *J* = 5.7, 10.1 Hz, 1H), 4.01 (dt, *J* = 5.6, 10.1 Hz, 1H), 3.73 (app. q., *J* = 7.7 Hz, 1H), 2.68–2.74 (m, 1H), 2.45 (s, 3H), 2.27–2.44 (m, 5H), 1.80–1.91 (m, 3H), 1.71–1.79 (m, 1H), 1.60–1.68 (m, 1H) ppm.

^{13}C NMR (127 MHz, $CDCl_3$, major rotamer) δ: 179.7, 175.1, 145.2, 132.8, 130.1, 127.0, 82.2, 70.0, 54.8, 46.1, 32.2, 31.2, 30.0, 25.3, 25.1, 21.8 ppm.

FTIR (film, cm^{-1}) ν: 3211.6, 2926.6, 1768.4, 1688.0, 1351.1, 1171.1, 956.8, 917.1, 661.3, 552.6.

HRMS (ESI^+): m/z [M+Na] calcd. for [$C_{18}H_{23}NO_6SNa$] 404.1138, found 404.1154, Δ = –1.6 mDa.

ScXRD:

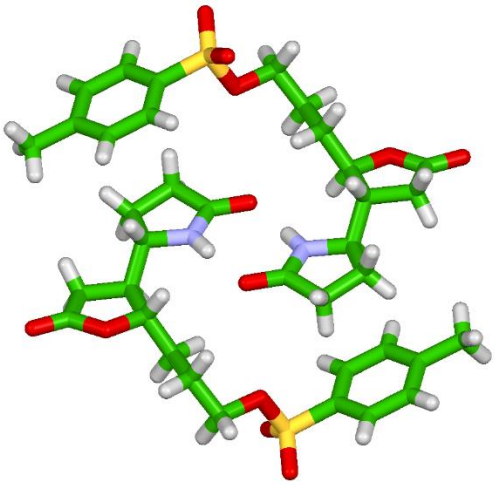

Empirical formula	$C_{18}H_{23}NO_6S$
M (g mol^{-1})	380.42
Space group	P21/n
Crystal system	monoclinic
a [Å]	12.654(3)
b [Å]	5.4874/11)
c [Å]	26.225(5)
α [°]	90
β [°]	97.85(3)
γ [°]	90
V [Å^3]	1804.0(6)
Z	4
ρ_{calcd} [mg m^{-3}]	1.416
Wavelength [Å]	0.71073
μ [mm^{-1}]	0.214
reflections collected	20160
R	0.0595
wR	0.1099
GOF	1.053
max., min. peaks [eÅ^{-3}]	0.985, 0.997

6.1.12 (*R*)-3-((*R*)-5-oxopyrrolidin-2-yl)-*N*-((*S*)-1-phenylethyl)-3-((*R*)-tetrahydrofuran-2-yl)propenamide (3.050)

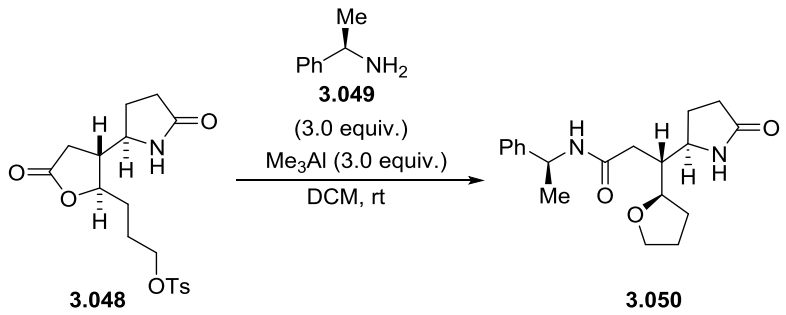

To a solution of (*R*)-1-phenylethan-1-amine (**3.049**) (14 µL, 13 mg, 0.11 mmol, 3.0 equiv.) in DCM (1 mL) at room temperature Me_3Al (55 µL, 0.11 mmol, 3.0 equiv., 1.0 M in PhMe) was added dropwise. The resulting solution was stirred at room temperature for 30 min, after which a solution of lactone **3.048** (14 mg, 0.037 mmol, 1.0 equiv.) in DCM (0.5 mL) was added dropwise. The reaction was allowed to stir at rt for 20 h and quenched with 2 M HCl (3 mL). The resulting mixture was extracted with DCM (4 × 1 mL), the combined organic layers dried with Na_2SO_4, and concentrated *in vacuo*. Flash chromatography (10% to 15% MeOH/EtOAc) gave the amide **3.050** as clear oil (5.1 mg, 42%).

R_f (10% MeOH/EtOAc): 0.15 (Vanillin, red).

^{1}H NMR (300 MHz, $CDCl_3$) δ: 7.40–7.25 (m, 5H), 6.24 (br. s, 1H), 6.05 (br. d, *J* = 8.0 Hz, 1H), 5.10 (p, *J* = 6.8 Hz, 1H), 3.88–3.58 (m, 4H), 2.34 (app. t, *J* = 5.8 Hz, 1H), 2.31–2.20 (m, 3H), 2.09 (dq, *J* = 13.1, 6.5 Hz, 1H), 1.93–1.85 (m, 2H), 1.84–1.72 (m, 3H), 1.65–1.54 (m, 1H), 1.48 (d, *J* = 6.9 Hz, 3H) ppm.

^{13}C NMR (75 MHz, $CDCl_3$) δ: 177.85 (C=O), 170.97 (C=O), 143.21 (C), 128.87 (CH), 127.60 (CH), 126.34 (CH), 79.54 (CH), 67.83 (CH_2), 55.68 (CH), 49.17 (CH), 43.45 (CH), 34.16 (CH_2), 30.26 (CH_2), 29.23 (CH_2), 25.83 (CH_2), 25.39 (CH_2), 21.73 (CH_3) ppm.

FTIR (film, cm^{-1}) ν: 3272 (broad), 3972, 2920, 2871, 1687 (with a shoulder), 1542, 1200, 1135, 761, 565.

HRMS (ESI^+): m/z [M+Na] calcd. for [$C_{19}H_{26}N_2O_3Na$] 353.1841, found 353.1841, Δ = 0.0 mDa.

6.1.13 9a-*epi*-Norstemoamide (3.052)

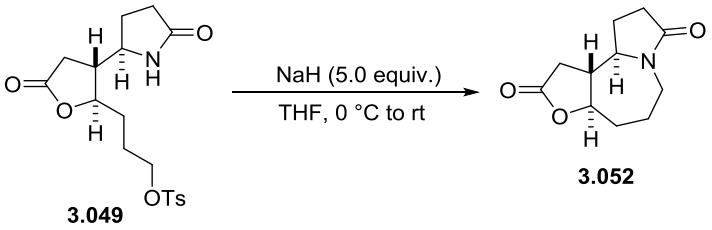

3.049 **3.052**

To a stirred suspension of NaH (74 mg, 1.84 mmol, 60 wt-% in mineral oil, 5.0 equiv.) in THF (10 mL) at 0 °C a solution of tosylate **3.049** (140 mg, 0.36 mmol, 1.0 equiv.) in THF (26 mL) was cannulated dropwise and the flask rinsed with further THF (1 mL). The reaction mixture was allowed to warm to rt for 6 h, after which the reaction was complete (TLC). The reaction mixture was cooled to 0 °C and quenched by dropwise addition of 2 M HCl (2 ml). The mixture was partitioned into two phases by adding brine (2 ml). Organic layer was collected, and the aqueous layer extracted with EtOAc (4 × 8 ml). Combined organic layers were dried with Na_2SO_4 and concentrated *in vacuo*. Flash chromatography (5% MeOH/EtOAc) gave 9a-*epi*-norstemoamide **3.052** as a white solid (54.6 mg, 73%).

Spectroscopic data matched to those reported previously.[24,88]

R_f (10% MeOH/EtOAc): 0.27 ($KMnO_4$).

^{1}H NMR (500 MHz, $CDCl_3$) δ: 4.35 (ddd, *J* = 5.3, 9.6, 11.1 Hz, 1H), 3.82 (ddd, *J* = 3.6, 6.3, 14.7 Hz, 1H), 3.54 (app. dd, *J* = 7.4, 9.2 Hz, 1H), 3.16 (ddd, *J* = 3.9, 8.2, 14.7 Hz, 1H), 2.63 (dd, *J* = 6.9, 16.1 Hz, 1H), 2.26–2.50 (m, 5H), 2.19 (dddd, *J* = 4.3, 7.0, 8.7, 13.0 Hz, 1H), 1.80–1.88 (m, 2H), 1.69–1.77 (m, 1H), 1.60–1.66 (m, 1H) ppm.

^{13}C NMR (127 MHz, $CDCl_3$) δ: 174.5 (C=O), 174.2 (C=O), 83.5 (CH), 61.1 (CH), 48.9 (CH), 40.6 (CH_2), 33.2 (CH_2), 30.6 (CH_2), 30.4 (CH_2), 24.5 (CH_2), 22.4 (CH_2) ppm.

6.1.14 9a,10-bis-*epi*-Stemoamide (3.053)

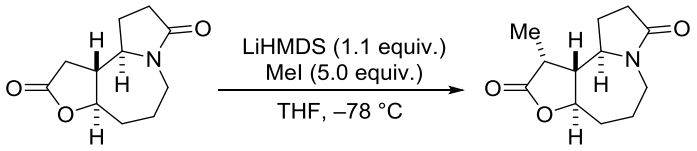

3.052 **3.053**

To a solution of 9a-*epi*-norstemoamide (**3.052**) (16.0 mg, 0.76 mmol, 1.0 equiv.) in THF (1 ml) at –78 °C was added LiHMDS (84 µl, 14 mg, 0.84 mmol, 1.1 equiv., 1.0 M in THF). After 10 min the reaction mixture was warmed to 0 °C for 10 min

and then recooled to –78 °C. To the stirred yellow suspension methyl iodide (38.8 µl, 54 mg, 0.382 mmol, 5.0 equiv.) was added dropwise. After 3 h the reaction mixture was quenched with sat. aq. NH_4Cl (0.5 ml) and extracted with EtOAc (5 × 2 ml). Combined organic layers were dried with Na_2SO_4 and concentrated *in vacuo*. Flash chromatography gave 9a,10-bis-*epi*-stemoamide (**3.053**) as a white solid (12.0 mg, 70%).

MP: 127.3–127.9 °C.

R_f (10% MeOH/EtOAc): 0.32 ($KMnO_4$).

^{1}H NMR (500 MHz, $CDCl_3$) δ: 4.51 (td, *J* = 10.7, 4.8 Hz, 1H), 3.90 (ddd, *J* = 14.6, 6.3, 3.6 Hz, 1H), 3.65 (ddd, *J* = 10.4, 7.3, 6.2 Hz, 1H), 3.04 (ddd, *J* = 14.3, 10.7, 3.1 Hz, 1H), 2.81 (app. pent., *J* = 7.7 Hz, 1H), 2.52–2.41 (3H, m), 2.37–2.29 (1H, m), 2.25 (app. td., *J* = 7.8, 10.4 Hz, 1H), 1.98–1.66 (4H, m), 1.30 (d, *J* = 7.7 Hz, 3H) ppm.

^{13}C NMR (127 MHz, $CDCl_3$) δ: 177.9, 173.9, 80.5, 57.8, 52.5, 40.8, 38.5, 30.2, 30.0, 23.2, 21.7, 10.8 ppm.

FTIR (film, cm^{-1}): 2940, 1773, 1681, 1208, 1005.

HRMS (ESI^+): m/z [M+H] calcd. for [$C_{12}H_{17}NO_3$] 223.1208, found 223.1201, Δ = –0.7 mDa.

^{1}H–^{1}H NOESY ($CDCl_3$):

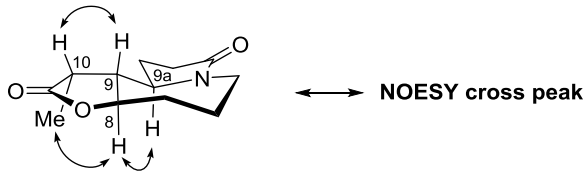

6.1.15 9a-*epi*-Stemoamide (3.054)

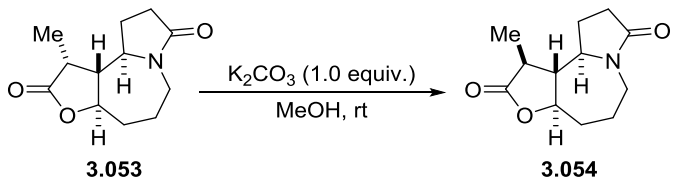

3.053 **3.054**

To a solution of 9a,10-bis-*epi*-stemoamide (**3.053**) (6.0 mg, 2.7 µmol, 1.0 equiv.) in methanol (0.5 ml) was added potassium carbonate (3.7 mg, 2.7 µmol, 1.0 equiv.). The resulting suspension was stirred at rt for 48 h, concentrated *in vacuo* and acidified with 2 M HCl (0.5 ml). The resulting solution was extracted with DCM (5 × 1 ml) and the combined organic layers dried with Na_2SO_4. The sol-

vent was evaporated *in vacuo* to give a 3:1 mixture of 9a-*epi*-stemoamide (**3.054**) and 9,10-*bis*-epistemoamide (**3.054**).

Characteristic data for 9a-*epi*-stemoamide:

^{1}H NMR (500 MHz, $CDCl_3$) δ: 4.33 (ddd, *J* = 11.1, 9.9, 5.2 Hz, 1H), 3.89–3.92 (m, 1H), 3.54–3.63 (m, 1H), 3.12–3.19 (m, 1H), 2.43–2.54 (m, 5H), 1.93–2.00 (m, 1H), 1.81–1.90 (3H, m), 1.70–1.81 (m, 1H), 1.41 (d, *J* = 7.0 Hz, 3H) ppm.

^{13}C NMR (127 MHz, $CDCl_3$) δ: 177.6, 174.3, 81.2, 62.2, 55.4, 40.3, 39.9, 30.9, 30.5, 24.9, 22.4, 15.5 ppm.

Table 6: Comparison of ^{13}C NMR shifts.

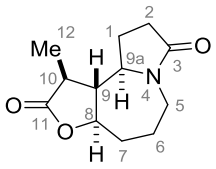

Carbon	9a,10-bis-*epi* (127 MHz, $CDCl_3$)	9a-*epi* (127 MHz, $CDCl_3$)	9a-*epi* (literature)[88] (75 MHz, $CDCl_3$)
11	177.9	177.6	178.0
3	173.9	174.3	174.0
8	80.5	81.2	80.5
9a	57.8	62.2	57.8
9	52.5	55.4	52.3
5	40.8	40.3	40.8
10	38.5	39.9	38.4
7	30.2	30.9	30.2
2	30.0	30.5	30.0
1	23.3	24.9	23.2
6	21.7	22.4	21.6
12	10.8	15.5	10.8

6.1.16 3-((2*R**,3*R**)-5-Oxo-3-(5-(((trifluoromethyl)sulfonyl)oxy)-1*H*-pyrrol-2-yl)tetrahydrofuran-2-yl)propyl 4-methylbenzenesulfonate (3.059)

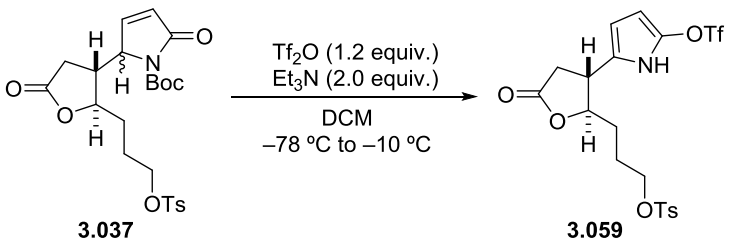

To a solution of lactam **3.037** (40 mg, 0.084 mmol, 1.0 equiv., azeotropically dried with PhMe) and triethylamine (17 mg, 23 µL, 0.17 mmol, 2.0 equiv., distilled over CaH_2) in DCM (1.6 ml) at –78 °C was added trifluoromethanesulfonic anhydride (28 mg, 0.1 mmol, 17 µL, 1.2 equiv.). The resulting solution was allowed to slowly warm to –10 °C over the course of 3 h and kept at this temperature for 12 h. The reaction mixture was quenched with 7% aq. $NaHCO_3$ (1 ml), and extracted with DCM (4 × 1 ml). Combined organic layers were dried with Na_2SO_4 and carefully concentrated (bath 20 °C) *in vacuo*. Flash purification (20% EtOAc/hexane to 90% EtOAc/hexane) gave the triflate **3.059** as a clear oil (6.1 mg, 14%).

***R*f** (80% EtOAc/hexane): 0.76 (Vanillin, dark brown, UV).

^{1}H NMR (300 MHz, $CDCl_3$) δ: 8.89 (br. s, 1H), 7.78 (app. d., J = 8.3 Hz, 2H), 7.35 (app. d., J = 8.3 Hz, 2H), 5.95 (t, J = 3.4 Hz, 1H), 5.91 (t, J = 3.4 Hz, 1H), 4.40 (app. dt, J = 3.8, 3.4 Hz, 1H), 4.12 (t, J = 5.3 Hz, 2H), 3.32 (q, J = 9.3 Hz, 1H), 2.82 (ABX, $|J_{AB}|$ = 17.7 Hz, J_{AX} = 8.68 Hz, J_{BX} = 10.44 Hz, υ_A = 2.92 ppm, υ_A = 2.74 ppm, 2H), 2.45 (s, 3H), 1.96–1.90 (m, 2H), 1.83–1.72 (m, 2H) ppm.

FTIR (film, cm^{-1}) ν: 3305, 2928, 1760, 1427, 1175, 925, 839.

6.1.17 *tert*-Butyl (2*S*/*R**,3*R*/*S**)-5-oxo-2-((2*R**,3*R**)-5-oxo-2-(3-(tosyloxy)propyl)tetrahydrofuran-3-yl)-3-(phenylthio)pyrrolidine-1-carboxylate (3.060)

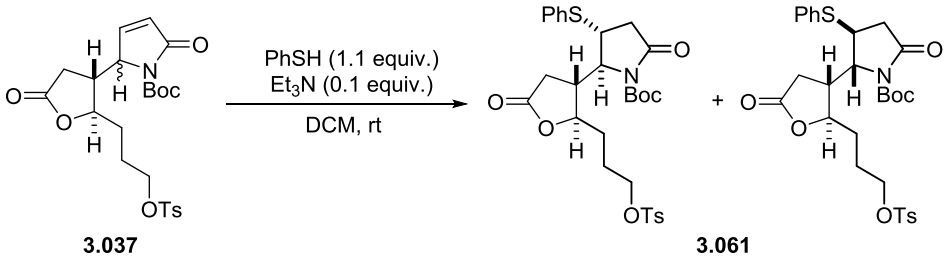

3.037 **3.061**

To a solution of lactam **3.037** (27.2 mg, 0.567 mmol, 1.0 equiv.) and triethyl amine (0.8 µl, 5.76 µmol, 0.1 equiv) in DCM (1 ml) at rt was added thiophenol (6.9 mg, 6.4 µL, 6.24 mmol, 1.1 equiv.). The resulting solution was stirred at rt for 6 h and concentrated *in vacuo*. Crude product was purified using flash column chromatography (50% EtOAc/hexane) to give a mixture of thiophenol adducts **3.061** as a semisolid foam (27.3 mg, 81%, dr 1:1.5).

***R*f** (60% EtOAc/hexane): 0.57 (Ninhydrin, purple).

^{1}H NMR (500 MHz, $CDCl_3$, diastereomers overlapping) δ: 7.74–7.78 (m, 2H), 7.45–7.51 (m, 2H), 7.37–7.42 (m, 3H), 7.34–3.37 (m, 2H), 4.11–4.22 (m, 1H), 3.88–4.06 (m, 4H), 3.38–3.46 (m, 1H), 2.89–3.00 (m, 1H), 2.456–2.59 (m, 4H), 2.45 (s,

3H), 2.18–2.26 (m, 0.5H), 1.96–2.05 (m, 1H), 1.71–1.82 (m, 1H), 1.60–1.69 (m, 1H), 1.54 (s, 9H), 1.37–1.48 (m, 2H) ppm.

^{13}C NMR (127 MHz, $CDCl_3$, signals not assigned) δ: 174.5, 173.9, 171.2, 170.6, 150.5, 150.3, 145.2, 145.1, 134.9, 134.5, 133.0, 131.8, 130.1, 130.1, 123.0, 129.9, 129.8, 129.5, 128.1, 128.0, 84.8, 84.6, 81.1, 80.8, 69.6, 69.5, 63.9, 63.1, 44.4, 44.0, 42.6, 41.9, 38.5, 31.5, 31.3, 31.3, 30.4, 29.8, 28.2, 28.1, 25.8, 25.2, 21.8 ppm.

FTIR (film, cm^{-1}) v: 2978, 2930, 1780, 1714, 1303, 1175, 962, 736, 555.

HRMS (ESI^+): m/z [M+Na] calcd. for major [$C_{29}H_{35}NO_8S_2Na$] 612.1696, found 612.1689, Δ = 0.7 mDa, for minor 612.1692, Δ = 0.4 mDa.

6.1.18 (*R*)-5-(3-Bromopropyl)furan-2(5*H*)-one (3.027)

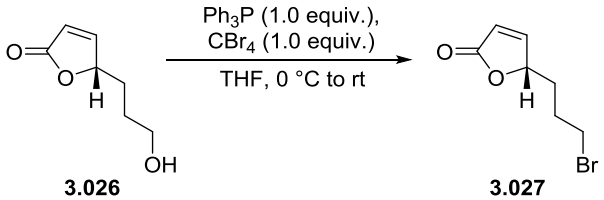

3.026 **3.027**

To a solution of alcohol **3.026** (200 mg, 1.41 mmol, 1.0 equiv., dried as a THF azeotrope 2 × 1 ml) and Ph_3P (467 mg, 1.41 mmol, 1.0 equiv.) in DCM (15 ml) at 0 °C was added a solution of CBr_4 (1.0 equiv.) in DCM (10 mL). The reaction mixture was allowed to warm to rt. After 10 min TLC showed completion. Solvent was evaporated *in vacuo* and the residue purified with flash column chromatography (50% EtOAc/hexane) to give the bromide **3.027** as a clear oil (270 mg, 93%).

R_f (50% EtOAc/hexane): 0.67 (Vanillin, dark green).

^{1}H NMR (300 MHz, $CDCl_3$) δ: 7.45 (dd, *J* = 5.7, 1.5 Hz, 1H), 6.13 (dd, *J* = 5.7, 2.0 Hz, 1H), 5.07 (dp, *J* = 7.6, 1.8 Hz, 1H), 3.44 (m, 2H), 2.03 (m, 3H), 1.74 (m, 1H) ppm.

^{13}C NMR (75 MHz, $CDCl_3$) δ: 172.8, 155.8, 122.1, 82.4, 32.9, 31.8, 28.2 ppm.

FTIR (film, cm^{-1}) v: 3089, 2921, 1743, 1439, 1248, 1204, 814.

HRMS (ESI^+): m/z [M+Na] calcd. for [$C_7H_9BrO_2Na$] 226.9678, found 226.9691, Δ = –1.3 mDa.

6.1.19 *tert*-Butyl (*S*)-4-((*R*)-2-(3-bromopropyl)-5-oxo-2,5-dihydrofuran-2-yl)-2-oxopyrrolidine-1-carboxylate (3.029)

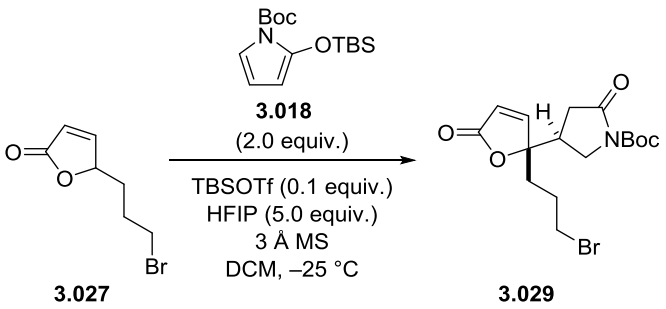

To a solution of bromide **3.027** (50 mg, 0.2 mmol, 1 equiv.) in DCM (1 ml) was added hexafluoroisopropanol (128 µL, 205 mg, 1.22 mmol, 5.00 equiv.), TBSOTf (6 µl, 7 mg, 0.1 equiv.) and 3 Å molecular sieves (70 mg). The resulting solution was cooled to –25 °C and a solution of silyloxypyrrole **3.018** (145 mg, 0.49 mmol, 2.00 equiv.) in DCM (1 ml) was added dropwise. After 25 h the reaction was quenched with triethyl amine (0.1 ml) and extracted with DCM (3 × 2 ml). Combined organic layers were dried with Na_2SO_4 and concentrated *in vacuo*. Purification with flash column chromatography (50% EtOAc/hexane) gave title compound **3.029** as a clear oil which solidified upon standing (40 mg, 42%).

Note: X-Ray quality crystals were obtained upon slow evaporation from DCM.

R_f (50% EtOAc/hexane): 0.15 ($KMnO_4$).

^{1}H NMR (300 MHz, $CDCl_3$) δ: 7.28 (d, *J* = 5.7 Hz, 1H), 6.21 (*J* = 5.67 Hz, 1H), 3.66 (dd, *J* = 8.3, 11.6 Hz, 1H), 3.40 (dt, *J* = 5.9, 10.3 Hz, 1H), 3.32 (dt, *J* = 5.1, 2.9 Hz, 1H), 3.25 (dd, *J* = 11.6 Hz, 8.3 Hz, 1H), 1.55–2.10 (m, 4H), 1.48 (s, 9H) ppm.

^{13}C NMR (75 MHz, $CDCl_3$) δ: 171.2, 171.1, 155.9, 149.8, 123.9, 88.3, 83.7, 46.2, 36.9, 34.2, 33.9, 32.7, 28.1, 26.15 ppm.

FTIR (film, cm^{-1}) ν: 2980, 2921, 2850, 2252, 1761, 1716, 1456, 1293, 1151, 911, 825, 728.

HRMS (ESI^+): m/z [M+Na] calcd. for [$C_{16}H_{22}BrNO_5Na$] 410.0574, found 410.0573, Δ = 0.1 mDa.

scXRD:

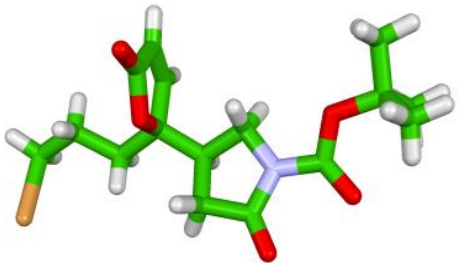

Empirical formula	$C_{16}H_{22}BrNO_5$
M (g mol^{-1})	385.23
Space group	-P1
Crystal system	triclinic
a [Å]	6.18132(18)
b [Å]	8.6154(2)
c [Å]	15.7974(4)
α [°]	101.211(2)
β [°]	93.251(2)
γ [°]	93.251(2)
V [Å^3]	831.64(4)
Z	2
ρ_{calcd} [mg m^{-3}]	1.538
Wavelength [Å]	1.54184
reflections collected	11081
refined parameters	211
R	0.0222
wR	0.0578
GOF	1.050

6.1.20 3-(5-Oxo-2,5-dihydrofuran-2-yl)propyl methanesulfonate (3.030)

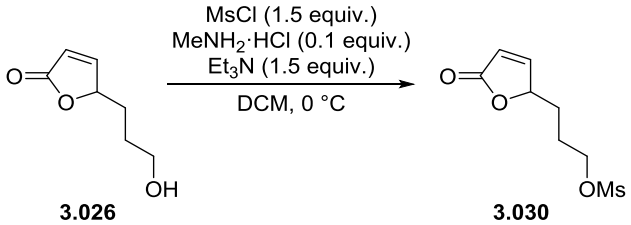

To a solution of alcohol **3.026** (1.40 g, 9.85 mmol, 1.00 equiv), methylamine hydrochloride (14 mg, 0.98 mmol, 0.10 equiv.) and Et_3N (2.1 ml, 1.5 g, 15 mmol, 1.5 equiv) in DCM (15 ml) at 0 °C was dropwise added MsCl (1.1 ml, 1.7 g, 15 mmol, 1.5 equiv) in DCM (5 ml). The mixture was allowed to stir for 30 min, after which time the reaction was diluted with DCM (10 ml) and quenched with sat. aq. NH_4Cl (10 ml). Resulting mixture was extracted with DCM (3 × 10 mL).

The combined organic layers were dried with Na_2SO_4 and concentrated *in vacuo*. Purification of the residue by flash chromatography (50% EtOAc/hexane to 100% EtOAc) afforded the desired product **3.030** as a clear oil which solidifies upon standing (1.6 g, 74%)

R_f (25% hexane/EtOAc): 0.67 (Vanillin stain, brown).

^{1}H NMR (300 MHz, $CDCl_3$) δ: 7.45 (dd, *J* = 1.5, 5.7 Hz, 1H), 6.13 (ddd, *J* = 0.7, 1.9, 5.7 Hz, 1H), 5.08 (ddt, *J* = 1.9, 4.1, 7.7 Hz, 1H), 4.29 (m, 2H), 3.01 (s, 3H), 1.86–2.10 (m, 3H), 1.65–1.78 (m, 4H) ppm.

^{13}C NMR (75 MHz, $CDCl_3$) δ: 172.7, 155.7, 122.1, 82.4, 77.1, 29.4, 25.1 ppm.

FTIR (film, cm^{-1}) ν: 2940, 1743, 1344, 1164, 926, 790, 448.

HRMS (ESI^+): m/z [M+Na] calcd. for [$C_6H_{12}O_5SNa$] 234.0298, found 234.0287, Δ = 1.1 mDa.

6.1.21 *tert*-Butyl (*R**/*S**)-2-((2*S**,3*S**)-2-(3-((methylsulfonyl)oxy)propyl)-5-oxotetrahydrofuran-3-yl)-5-oxo-2,5-dihydro-1*H*-pyrrole-1-carboxylate (3.031)

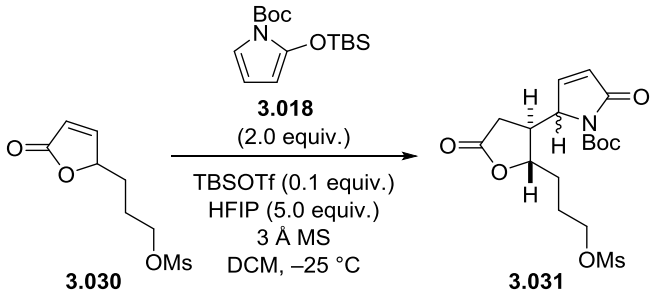

Carried out using the general procedure in **6.4.1** using mesylate **3.030** (50 mg) to give **3.031** (17 mg, 19%).

Note: Product contaminated with hydrolyzed nucleophile:

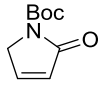

R_f (EtOAc): 0.55 (Diastereomer 1; ninhydrin, brown) 0.63 (Diastereomer 2, ninhydrin, brown).

^{1}H NMR (300 MHz, $CDCl_3$): 7.10 (dd, *J* = 6.2, 2.0 Hz, 1H), 6.28 (dd, *J* = 5.9, 1.7 Hz, 1H), 4.75 (app. td, *J* = 4.0, 1.9 Hz, 1H), 4.23 (dt, *J* = 6.0, 2.2 Hz, 1H), 3.98 (ddd, *J* = 8.3, 5.0, 3.4 Hz, 1H), 3.23 (app. dt, *J* = 9.6, 4.1 Hz, 1H), 3.02 (3H, s), 2.88

(dd, *J* = 18.4, 9.9 Hz, 1H), 2.43 (dd, *J* = 18.4, 4.5 Hz, 1H), 1.62–2.00 (4H, m), 1.57 (9H, s) ppm.

HRMS (ESI$^+$): m/z [M+Na] calcd for [$C_{17}H_{25}NO_8SNa$] 426.1193, found 426.2736, Δ = 0.9 mDa.

6.1.22 (*Z*/*E*)-5-(2-(3-Bromopropyl)-5-oxodihydrofuran-3(2*H*)-ylidene)pyrrolidin-2-one (3.034) and (3.035)

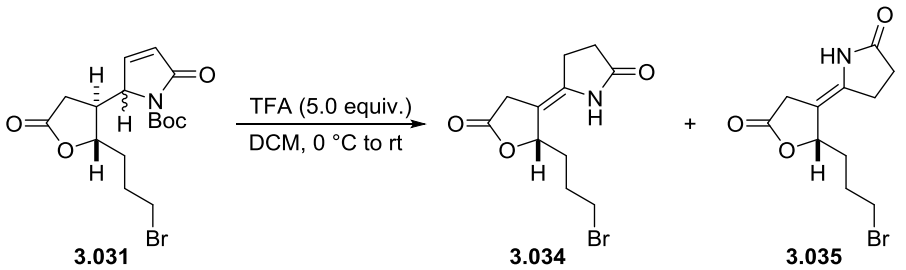

To a solution of lactam **3.031** (10 mg, 0.026 mmol, 1.0 equiv.) in DCM (2 ml) at 0 °C was added trifluoroacetic acid (8 µL, 13 mg, 0.13 mmol, 5.0 equiv.). After stirring overnight the reaction mixture was concentrated *in vacuo* and purified with flash column chromatography (2% MeOH/EtOAc) to afford the γ,δ-unsaturated compounds **3.034** and **3.035** as a yellow oil (4.2 mg, 56%, *E*:*Z* = 1.4:1).

^{1}H NMR (500 MHz, $CDCl_3$) δ: Major: 8.92 (br. s, 0.8 H), 5.08 (app. d, *J* = 9.8 Hz, 1H), 4.20–4.14 (m, overlapping with minor isomer, 2H), 3.06–3.12 (m, 2H), 2.96 (s, 3H), 2.43–2.50 (m, 4H), 1.84–1.90 (m, obstructed by impurities, based on ^{1}H–^{1}H COSY, 2H), 1.56–1.61 (m, 2H); Minor: 8.33 (br. s, 0.8H), 5.02 (app. d, *J* = 8.6 Hz, 1H), 4.32 (dt, *J* = 5.7, 9.9 Hz, 1H), 4.25–4.20 (m, overlapping with major isomer, 1H), 2.92–2.95 (m, 2H), 2.93 (s, 3H), 2.51–2.53 (m, 4H), 1.84–1.90 (m, 2H, obstructed by impurities, based on ^{1}H–^{1}H COSY), 1.64–1.69 (m, 2H), 1.58–1.62 (m, 2H) ppm.

^{13}C NMR (127 MHz, $CDCl_3$) δ: Major: 178.6, 174.8, 131.9, 102.76, 80.2, 69.0, 37.7, 31.4, 30.7, 29.8, 29.17, 24.9; Minor: 178.0, 174.4, 132.6, 103.1, 80.6, 69.38, 37.6, 31.6, 30.9, 29.6, 28.9, 23.2 ppm.

^{1}H–^{13}C HMBC correlations:

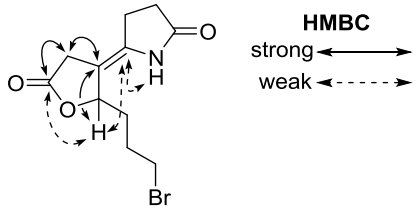

6.2 Cephalotaxus project

General procedures described in section 6.1 were used with the modifications outlined below.

Triethyl amine was dried by storage over potassium hydroxide pellets. Flash column chromatography was performed using silica gel (230–400 mesh) with pressurized air using PA grade solvents.

L-Dimethylprolineamide (**4.009**) was purchased from BACHEM (Product n.o. E-2320.0005). Iodonosylate **4.029** and iodotosylate **4.030** were prepared according to the literature from homopiperonic acid.[114]

NMR spectra were recorded at room temperature on a Bruker Avance II 400 spectrometer equipped with a Bruker BBO probe operating at 400 MHz for proton nuclei and 100 MHz for carbon nuclei. When toluene-d_8 was used proton shifts are relative to residual toluene (2.08) and carbon shifts relative to toluene-d_8 (20.43). Low-resolution mass spectra were recorded with Q-Tof Micromass spectrometer. High resolution mass spectra were measured with Waters QTOF XEVO-G2 mass spectrometer. Optical rotation values were recorded on a Perkin Elmer Model 341 polarimeter at room temperature using the sodium D-line (λ = 589 nm) and a 10 cm cuvette. The enantiomeric ratio of **4.010** was determined by HPLC in comparison to the corresponding racemic samples using Agilent 1260 Infinity HPLC.

Microwave reactions were carried out using Biotage Initiator EXP EU microwave reactor rated at maximum power output of 400 W with the magnetron operating at 2450 MHz. All reactions were done in oven-dried Biotage microwave vials of suitable volume, equipped with a magnetic stir-bar. Reaction temperatures, irradiation times and power limits are reported in the relevant sections of the experimental part.

Kugelrohr distillations were carried out using Büchi GKR-51 bulb-to-bulb distillation unit cooled with dry-ice.

6.2.1 (*S*)-1-Allyl-*N*,*N*-dimethylpyrrolidine-2-carboxamide (4.007)

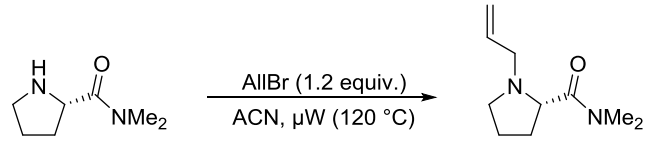

4.016 **4.007**

To a solution of allyl bromide (640 mg, 450 μL, 5.3 mmol, 1.2 equiv.) in acetonitrile (2 ml) *N*,*N*-dimethyl proline amide (**4.016**) (500 mg, 4.38 mmol, 1.0 equiv.) was added at 0 °C. The resulting solution was heated using a microwave reactor (100 W, 120 °C) for 5 min, allowed to cool to rt, and quenched with aqueous 2 M NaOH (10 ml). The resulting biphasic mixture was extracted with EtOAc (3 × 5 ml) and the combined organic layers washed with brine (10 ml), dried

with Na_2SO_4, and concentrated *in vacuo*. The thus obtained crude allyl amine **4.007** is NMR pure (540 mg, 84%).

Note: When scaling up, combined batches of allyl amine **4.007** (2 g) were further purified with Kugelrohr distillation (120 °C, 0.1 mbar) to yield the allyl amine **4.007** as a colorless oil.[iii]

^{1}H NMR (400 MHz, $CDCl_3$) δ: 5.94 (dddd, *J* = 17.2, 10.1, 7.3, 6.1 Hz, 1H), 5.14 (ddd, *J* = 17.1, 3.2, 1.5 Hz, 1H), 5.05 (ddd, *J* = 10.1, 2.1, 1.1 Hz, 1H), 3.40–3.28 (m, 2H), 3.19 (td, *J* = 8.0 Hz, 2.8 Hz, 1H), 3.06 (s, 3H), 3.00 (dd, *J* = 13.1, 7.3 Hz, 1H), 2.94 (s, 3H), 2.33 (dd, *J* = 16.5, 8.7 Hz, 1H), 2.15–2.04 (m, 1H), 2.01–1.89 (m, 1H), 1.87–1.74 (m, 2H) ppm.

^{13}C NMR (100 MHz, $CDCl_3$) δ: 173.3, 136.1, 116.8, 63.9, 57.6, 53.3, 37.0, 36.1, 28.9, 23.0 ppm.

FTIR (film, cm^{-1}) ν: 2945, 2799, 1638, 1418, 1261, 1115, 919.

$[\alpha]_D^{20}$ = –104.6° (*c* = 1.0, DCM).

HRMS (ESI^+): m/z [M+H] calcd. for [$C_{10}H_{19}N_2O$] 183.1497, found 182.1495 Δ = –1.1 mDa.

6.2.2 (*R*)-2-Allyl-*N*,*N*-dimethylpyrrolidine-2-carboxamide (4.009)

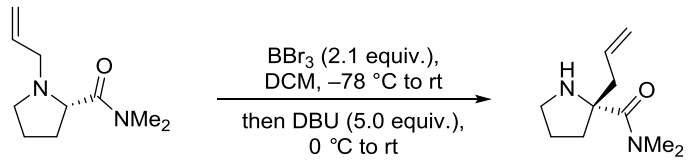

To a solution of allyl amine **4.007** (1.0 g, 5.5 mmol, 1.0 equiv.) in DCM (60 ml) at –78 °C BBr_3 (12.0 ml, 2.89 g, 11.5 mmol, 2.10 equiv., 1.0 M solution in DCM) was added dropwise. The resulting solution was allowed to warm to rt and stirred for 1 h, then cooled to 0 °C followed by dropwise addition of DBU (4.1 ml, 4.2 g, 27 mmol, 5.0 equiv.). The mixture was allowed to warm to rt and stirred for 1 h. The resulting deep orange reaction mixture was quenched with 1 M HCl (10 ml), biphasic mixture separated, and the organic layer washed with 1 M NaOH (20 ml). The basified aqueous layer was further extracted with DCM (3 × 30 ml), and the combined organic layers washed with brine (50 ml), dried with Na_2SO_4 and concentrated *in vacuo*. The crude product was purified by flash column

[iii] The fact that residual NaOH might epimerize the material upon heating during distillation is acknowledged. In this case, however, both distillation and column purification gave the product with identical optical rotations.

chromatography (50% acetone/pentane, 1% *i*-PrNH$_2$) to afford amine **4.009** as a pale-yellow oil (729 mg, 73%, er = 96:4).

Note: In gram scale flash purifications trace amounts of traces of starting material can contaminate the product but do not affect the following reactions.

Note: Enantiopurity determined using Mosher's amide derivative, see section 6.2.8.

R$_f$ (50% acetone/heptane): 0.13 (KMnO$_4$).

^{1}H NMR (400 MHz, CDCl$_3$) δ: 5.81-5.71 (m, 1H), 5.05–5.03 (m, 1H), 5.02–4.99 (m, 1H), 3.09–2.88 (m, 1H), 2.78–2.72 (m, 1H), 1.87–1.81 (m, 1H), 1.80–1.65 (m, 2H) ppm.

^{13}C NMR (100 MHz, CDCl$_3$) δ: 175.5, 134.3, 117.5, 68.5, 46.6, 44.7, 35.3, 26.5 ppm.

FTIR (film, cm^{-1}) ν: 3074, 2942, 2869, 1624, 1434, 1254, 1162, 992, 731.

$[\boldsymbol{\alpha}]_{\boldsymbol{D}}^{\boldsymbol{20}}$ = –104.6° (*c* = 1.0, DCM).

HRMS (ESI$^+$): m/z [M+H] calcd. for [C$_{10}$H$_{19}$N$_2$O] 183.1497, found 183.1499 Δ = 0.2 mDa.

Side-product *syn*-AB-**4.008**:

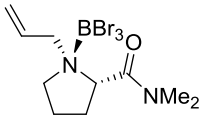

syn-AB-**4.008**

***R*$_f$** (50% acetone/heptane): 0.91 (KMnO$_4$).

^{1}H NMR (400 MHz, CDCl$_3$) δ: 6.59 (dddd, *J* = 17.1, 9.9, 9.2, 5.6 Hz, 1H), 5.56 (dd, *J* = 17.1, 0.9 Hz, 1H), 5.51–5.46 (m, 1H), 5.41–5.33 (m, 1H), 4.84 (dd, *J* = 13.5, 5.7 Hz, 1H), 4.49–4.41 (m, 1H), 4.22–4.12 (m, 1H), 3.66 (ddd, *J* = 13.4, 7.5, 6.2 Hz, 1H), 3.26 (s, 3H), 2.98 (s, 3H), 2.37–2.26 (m, 2H), 2.14–2.03 (m, 2H) ppm.

^{13}C NMR (100 MHz, CDCl$_3$) δ: 167.52, 132.16, 125.28, 100.12, 64.41, 60.59, 59.34, 38.81, 37.09, 31.25, 22.31 ppm.

^{11}B NMR (128 MHz, CDCl$_3$) δ: –3.7 ppm.

^{1}H–^{1}H NOESY (400 MHz, CDCl$_3$):

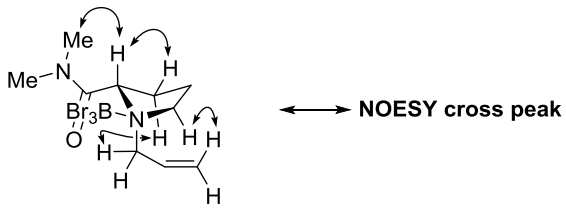

6.2.3 (*S*)-2-Allyl-1-(2-(benzo[*d*][1,3]dioxol-5-yl)ethyl)-*N*,*N*-dimethylpyrrolidine-2-carboxamide (4.020)

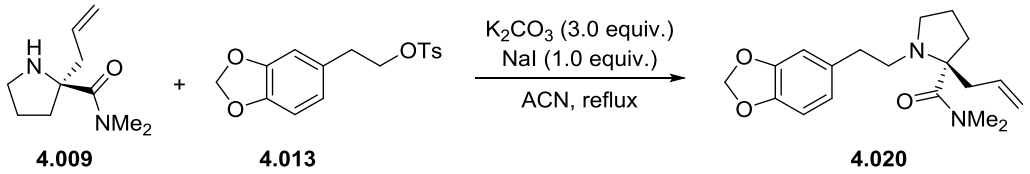

4.009 **4.013** **4.020**

To a suspension of amine **4.009** (130 mg, 0.71 mmol, 1.0 equiv.), NaI (106 mg, 0.71 mmol, 1.0 equiv.) and K_2CO_3 (295 mg, 2.14 mmol, 3.0 equiv.) in CH_3CN (5 ml) was added tosylate **4.013** (228 mg, 0.71 mmol, 1.0 equiv.). The reaction mixture was heated to reflux for 16 h, cooled to rt, diluted with DCM (5 mL), and the solid filtered off. The filtrate was concentrated *in vacuo*, and the resulting solution was washed with 5% aq. NaOH (10 ml), brine (10 ml), dried with $MgSO_4$, and concentrated *in vacuo*. The crude product was purified by flash column chromatography (50:50 EtOAc/heptane) to afford amide **4.020** as a pale-yellow oil (146 mg, 62%).

R_f (50% EtOAc/heptane): 0.50 ($KMnO_4$).

^{1}H NMR (400 MHz, $CDCl_3$) δ: 6.68 (d, *J* = 8.0 Hz, 1H), 6.61 (d, *J* = 2.0 Hz, 1H), 6.57 (dd, *J* = 8.0, 2.0 Hz, 1H), 6.99–5.90 (m, 1H), 5.87 (dd, *J* = 2.0, 1.5 Hz, 2H), 5.01–4.99 (m, 1H), 4.98–4.96 (m, 1H), 3.20 (ddd, *J* = 9.0, 8.0, 4.0 Hz, 1H), 2.86 (s, 6H), 2.82–2.74 (m, 1H), 2.75–2.60 (m, 3H), 2.57–2.49 (m, 2H), 2.08–1.94 (m, 3H), 1.88–1.78 (m, 2H) ppm.

^{13}C NMR (101 MHz, $CDCl_3$) δ: 174.08, 147.44, 145.64, 137.37, 134.70, 121.39, 116.88, 109.00, 107.97, 100.70, 71.56, 50.54, 49.86, 37.74, 36.37, 35.06, 31.24, 22.03 ppm.

6.2.4 (*S*)-2-Allyl-1-(2-(6-iodobenzo[*d*][1,3]dioxol-5-yl)ethyl)-*N*,*N*-dimethylpyrrolidine-2-carboxamide (4.025)

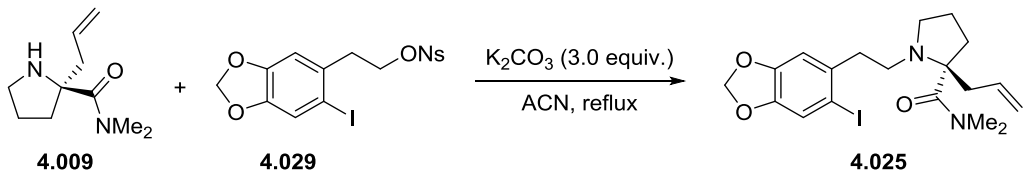

4.009 **4.029** **4.025**

A beige suspension of amine **4.009** (294 mg, 1.90 mmol, 1.0 equiv.), nosylate **4.029** (1.0 g, 2.10 mmol, 1.2 equiv.) and K_2CO_3 (790 mg, 5.71 mmol, 3.0 equiv.) in acetonitrile (10 ml) was refluxed for 13 h. The resulting mixture was cooled to rt, filtered through a fritted funnel and the filter cake washed with thoroughly with EtOAc (3 × 3 ml). The combined filtrates were concentrated under reduced pressure. The crude product was purified by flash column chromatography (35% EtOAc/heptane) to afford iodide **4.025** as a yellow oil (724 mg, 83%).

R_f (30% EtOAc/heptane): 0.31 (UV, $KMnO_4$).

^{1}H NMR (400 MHz, $CDCl_3$) δ: 7.20 (s, 1H), 6.69 (s, 1H), 6.02–5.90 (m, 3H), 5.93 (s, 2H), 5.02 (app. d, *J* = 12.6 Hz, 2H), 3.31 (td, *J* = 8.6, 3.6 Hz, 1H), 3.00 (br. s, 6H), 2.89–2.68 (m, 5H), 2.65 (dd, *J* = 16.8, 8.9 Hz, 1H), 2.61–2.53 (m, 1H), 2.08 (dd, *J* = 16.1, 11.2 Hz, 1H), 2.06–1.99 (m, 2H), 1.97–1.80 (m, 2H) ppm.

^{13}C NMR (100 MHz, $CDCl_3$) δ: 174.25, 148.51, 146.95, 137.38, 136.56, 118.62, 117.06, 109.62, 101.62, 88.04, 71.89, 50.19, 49.59, 40.30, 38.14, 36.58, 31.40, 22.14 ppm.

FTIR (film, cm^{-1}) ν: 2904, 2811, 1623, 1474, 1384, 1225, 1110, 1006, 931.

$[\alpha]_D^{20}$ = –21.4° (*c* = 0.5, DCM).

HRMS (ESI$^+$): m/z [M+H] calcd. for [$C_{19}H_{25}IN_2O_3$] 457.0988, found 457.0989, Δ = 0.1 mDa.

6.2.5 (5*S*,8*S*)-1-(2-(6-Iodobenzo[*d*][1,3]dioxol-5-yl)ethyl)-8-(iodomethyl)-7-oxa-1-azaspiro[4.4]nonan-6-one (4.032)

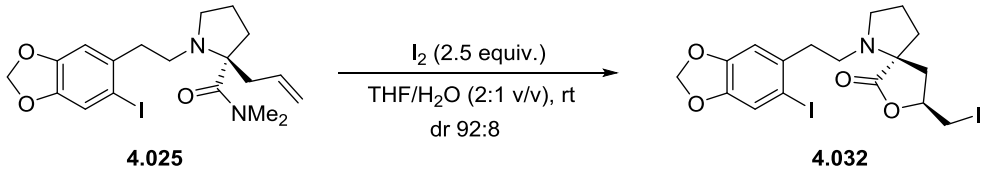

4.025 **4.032**

To a solution of amide **4.025** (1.70 g, 3.73 mmol, 1.0 equiv.) in THF (35 ml) and DI H_2O (12 ml) at rt and protected from light was added iodine (2.36 g, 9.31 mmol, 2.5 equiv.). After 16 h the reaction mixture was quenched with aq. sat. Na_2SO_3 (7 ml) and basified with 2 M NaOH (5 ml). The resulting biphasic solution was extracted with EtOAc (4 × 20 ml). The combined organic layers were washed with brine (50 ml), dried with Na_2SO_4 and concentrated *in vacuo* (bath temperature 30 °C). The resulting black residue (dr 92:8 based on ^{1}H NMR of reaction mixture) was purified using flash column chromatography (20% EtOAc/heptane to 30% EtOAc/heptane) to give *cis*-butyrolactone **4.032** as a clear oil (1.17 g, 57%).

Note: Minor diastereomer co-elutes with side-product benzyloxyethanol.

$\mathbf{R}_f$ (EtOAc/heptane) = 0.44 ($KMnO_4$, decomposes under UV).

^{1}H NMR (400 MHz, $CDCl_3$) δ: 7.21 (s, 1H), 6.74 (s, 1H), 5.94 (s, 2H), 4.31 (ddt, *J* = 10.3, 6.8, 5.3 Hz, 1H), 3.40 (dd, *J* = 10.3, 4.6 Hz, 1H), 3.26 (dd, *J* = 10.3, 7.2 Hz, 1H), 3.14 (dt, *J* = 15.7, 7.8 Hz, 2H), 2.88–2.79 (m, 2H), 2.79–2.72 (m, 2H), 2.27–2.15 (m, 2H), 2.09–1.88 (m, 4H) ppm.

^{13}C NMR (100 MHz, $CDCl_3$) δ: 177.8, 148.6, 147.1, 136.1, 118.7, 110.0, 101.7, 88.0, 75.1, 70.8, 51.7, 50.2, 40.8, 39.5, 36.8, 22.3, 7.1 ppm.

FTIR (film, cm^{-1}) ν: 2937 (br), 1768, 1475, 1248, 1153, 1039.

$[\boldsymbol{\alpha}]_{\boldsymbol{D}}^{\mathbf{20}}$ = 16.1° (*c* = 1.0, DCM).

HRMS (ESI^+): m/z [M+H] calcd. for [$C_{17}H_{19}I_2NO_4$] 555.9482, found 555.9485, Δ = 0.3 mDa.

^{1}H–^{1}H NOESY (400 MHz, toluene-d_8):

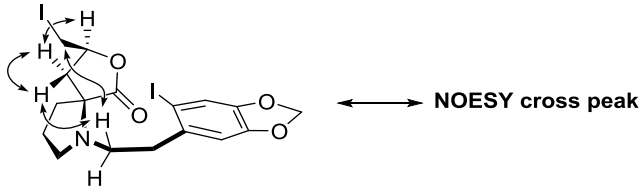

6.2.6 (*S*)-1-(2-(6-iodobenzo[*d*][1,3]dioxol-5-yl)ethyl)-8-methylene-7-oxa-1-azaspiro[4.4]nonan-6-one (4.033)

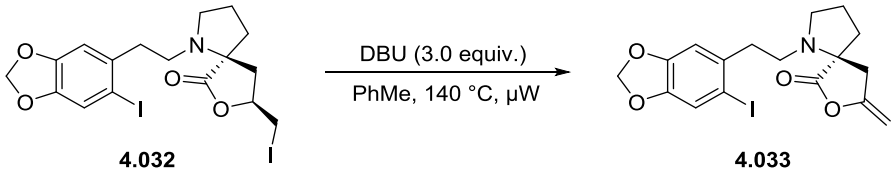

A solution of iodide **4.032** (100 mg, 0.180 mmol, 1.00 equiv.) and DBU (81 μL, 82 mg, 0.54 mmol, 3.0 equiv.) in toluene was heated in a microwave reactor (100 W, 120 °C) for 45 min. The resulting mixture of solid dark tar (presumably DBU · HI and organic decomposition products) and toluene was taken up in DCM (4 × 2 ml), concentrated and purified using flash column chromatography (50% Et_2O/pentane) to give butenolide **4.033** as a white solid (65 mg, 84%).

MP: 81.2–83.3 °C.

R$_f$ (50% EtOAc/Heptane): 0.66 (UV, $KMnO_4$).

^{1}H NMR (400 MHz, $CDCl_3$) δ: 7.21 (s, 1H), 6.72 (s, 1H), 5.95 (d, *J* = 1.4 Hz, 1H), 5.94 (d, *J* = 1.4 Hz, 1H), 4.70 (dd, *J* = 4.3, 2.2 Hz, 1H), 4.30 (dd, *J* = 4.3, 1.8 Hz, 1H), 3.23 (td, *J* = 8.6, 4.5 Hz, 1H), 3.04–2.96 (m, 1H), 2.91–2.71 (m, 3H), 2.58 (ddd, J = 11.3, 10.0, 5.0 Hz, 1H), 2.28–2.19 (m, 1H), 2.03–2.13 (m, 1H), 1.89–2.01 (m, 2H) ppm.

^{13}C NMR (400 MHz, $CDCl_3$) δ: 176.4, 153.3, 148.6, 147.1, 135.9, 118.7, 109.8, 101.7, 89.4, 88.0, 69.2, 51.6, 50.1, 40.6, 36.5, 36.4, 21.8 ppm.

FTIR (film, cm^{-1}) v: 2940 (br), 1790, 1672, 1502, 1251, 1227, 1084, 999, 844.

$[\boldsymbol{\alpha}]_{\boldsymbol{D}}^{\boldsymbol{20}}$ = +34.2° (*c* = 0.5, DCM).

HRMS (ESI$^+$): m/z [M+H] calcd. for [$C_{17}H_{18}INO_4$] 428.0359, found 428.0360, Δ = 0.1 mDa.

6.2.7 (*S*)-5,6,8,9-Tetrahydro-4*H*-[1,3]dioxolo[4',5':4,5]benzo[1,2-*d*]cyclopenta[*b*]pyrrolo[1,2-*a*]azepin-2(3*H*)-one (4.010)

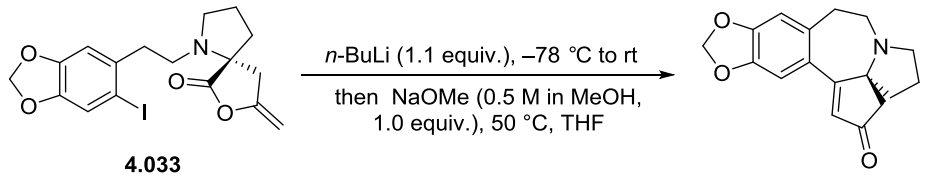

4.033 **4.010**

To a solution of iodide **4.033** (20 mg, 0.05 mmol, 1.0 equiv.) in THF (1 ml) at –78 °C *n*-BuLi (2.5 M in hexanes, 21 µL, 0.05 mmol, 1.1 equiv.) was added dropwise. The reaction mixture was stirred at –78 °C for 2 h and then allowed to slowly warm to rt. After stirring for 30 minutes, NaOMe (0.5 M in MeOH, 94 µL, 1.0 equiv.) was added and the reaction was stirred for an additional 2 h at room temperature and then heated to 50 °C for 20 minutes and then cooled to rt. The mixture was diluted with EtOAc (20 ml) and brine (10 ml). The layers were separated and the aqueous layer was extracted with EtOAc (3 × 10 ml). The combined organic layers were dried with anhydrous Na_2SO_4, filtered and concentrated. The residue was purified using flash chromatography (EtOAc) to afford **4.010** (7.7 mg, 58%) as an off-white amorphous solid.

R$_f$ (EtOAc): 0.31 (UV, $KMnO_4$).

^{1}H NMR (400 MHz, $CDCl_3$) δ: 6.70 (1H, app. s), 6.67 (1H, app. s), 6.08 (s, 1H), 6.00 (2H, dd^{AB}, $|J_{AB}|$ = 1.4 Hz, Δv = 23.8 Hz), 3.43 (1H, ddd, *J* = 4.8 Hz, 12.1 Hz, 16.4 Hz), 3.32 (1H, ddd, *J* = 2.9, 12.1, 15.0 Hz), 3.10 (app. dt, *J* = 3.6, 15.0 Hz),

2.97–2.92 (m, 3H), 2.64 (2H, distorted dd^{AB}, $|J_{AB}|$ = 18.0 Hz, Δv = 6.0 Hz), 1.95–1.81 (3H, m), 1.79–1.74 (1H, m) ppm.

^{13}C NMR (400 MHz, $CDCl_3$) δ: 205.9, 149.2, 146.4, 132.1, 131.7, 126.7, 110.1, 109.5, 101.6, 74.9, 54.2, 49.4, 44.4, 39.5, 32.8, 24.7 ppm.

$[\boldsymbol{\alpha}]_{\boldsymbol{D}}^{\mathbf{20}}$ = –72.8° (*c* = 0.006, DCM).

HRMS (ESI^+): m/z [M+H] calcd. for [$C_{17}H_{17}NO_3$] 283.1287, found 283.1286, Δ = 0.1 mDa.

HPLC: Chiralcel IA, 15% 2-propanol/hexane, 0.5 mL · min^{-1}, rt, λ=254 nm, t_R(major) = 10.9 min, t_R(minor) = 12.7 min.

6.2.8 Mosher's amide derivatization of 4.009

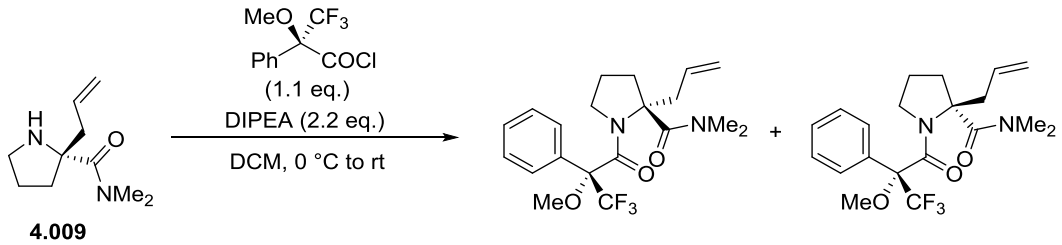

To a stirred solution of amine **4.009** (30 mg, 0.21 mmol, 1.0 equiv.) in DCM (1 ml), DIPEA (25 µL, 18 mg, 180 µmol, 2.2 equiv.) followed by (*R*)-(–)-MTPA-Cl (11 µL, 13 mg, 1.1 equiv.) was added at 0 °C. The resulting solution was warmed to 40 °C for 16 h and after full consumption of starting material allowed to cool to rt. The reaction was quenched with aqueous saturated $NaHCO_3$ (1 ml) and extracted with dichloromethane (3 × 1 ml). The combined organic layers were dried with anhydrous Na_2SO_4 and concentrated *in vacuo*. The crude product was analyzed using ^{1}H NMR.

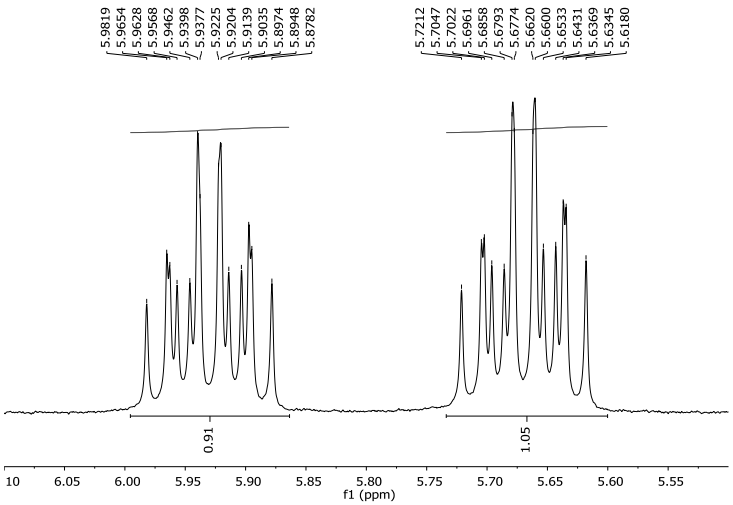

Expansion of ^{1}H NMR, diastereomeric signals from a racemic sample.

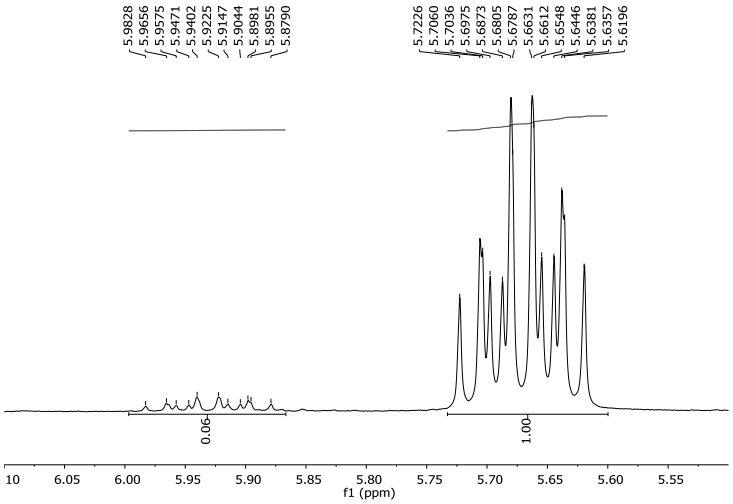

Expansion of ^{1}H NMR, diastereomeric signals from an enantioenriched sample.

6.2.9 ((5*S*,8*R*)-1-(2-(Benzo[d][1,3]dioxol-5-yl)ethyl)-8-(iodomethyl)-7-oxa-1-azaspiro[4.4]nonan-6-one (4.027)

To a stirred solution of amide **4.020** (20.0 mg, 0.60 mmol, 1.0 equiv.) in DCM (2 mL) trifluoroacetic acid (5 µL, 8 mg, 0.67 mmol, 1.1 equiv.) was added. After 15 min silver trifluoroacetate (14.7 mg, 0.67 mmol, 1.1 equiv.) and iodine (15.3 mg, 0.60 mmol, 1.0 equiv.) were added and the reaction flask protected from light. After 3 h the reaction mixture was quenched with 1 M $Na_2S_2O_3$ (1 ml) followed by 1 M NaOH (1 ml). The resulting mixture was extracted with DCM

(4 × 3 ml). The combined organic layers were dried with Na_2SO_4 and concentrated *in vacuo*. The residue was purified with flash column chromatography (30% EtOAc/Hex to 50% EtOAc/hexane) to give the lactone **4.027** as yellow oil (3.2 mg, 21%, decomposes on silica).

^{1}H NMR (400 MHz, $CDCl_3$) δ: 6.73 (d, *J* = 7.9 Hz, 1H), 6.68 (d, *J* = 1.6 Hz, 1H), 6.63 (dd, *J* = 7.9, 1.6 Hz, 1H), 5.93 (d, *J* = 3.4 Hz, 2H), 4.48 – 4.40 (m, 1H), 3.34 (dd, *J* = 10.4, 4.4 Hz, 1H), 3.24 (dd, *J* = 10.4, 7.3 Hz, 1H), 2.70-2.97 (m, 5H), 2.24-2.55 (m, 2H), 2.26-2.34 (m, 1H), 2.04-2.15 (m, 2H), 1.89-2.01 (m, 2H) ppm.

^{13}C NMR (100 MHz, $CDCl_3$) δ: 177.7, 147.7, 146.1, 133.9, 121.6, 109.3, 108.4, 101.0, 75.6, 69.3, 52.1, 51.2, 39.1, 37.6, 35.7, 22.1, 9.1 ppm.

7 COMPUTATIONAL SECTION

Systematic rotor conformer search was carried out with MMFF94 force-field as implemented in Avogadro 1.2.0. Obtained minimum energy conformers were optimized with B97D3/DEF2SVP level of theory using def2/j Weigend J auxiliary basis set and gCP BSSE correction as implemented in ORCA 4.0.0. Final single point energies were obtained using a final grid size of 5 with the verytightscf parameter.

Transition states were obtained carrying out a relaxed surface scan with N–C(Br) distance from 3.5 Å to 1.2 Å at 20 divisions. The structure closest to the saddle point was optimized using eigenvalue following algorithm. Obtained transition states were confirmed to have single imaginary vibrational frequency corresponding to the N–C–C bond breaking and forming. IRC analysis of vibrational extremes converged to starting material and product, respectively.

7.1 Diastereomer 1 (R,S,S,R)

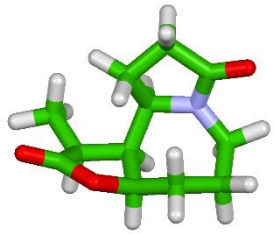

C	6.51430002324626	-0.00391880879769	1.62051952200049
C	5.17360706699375	-0.20644028665646	0.90305406819395
C	5.67334546610766	-0.70096360951693	-0.46637326052896
C	4.26582553222820	1.02769858898895	0.87948900849201
H	4.61019222477611	-1.01138060954113	1.38748140090443
C	7.42069469442220	0.46788914271199	0.48912399682537
H	6.89181301048578	-1.01264611058984	1.86056860053287
C	6.58951101995472	0.83232061322808	2.88427644229884
O	6.90581468425334	0.02421900372080	-0.69042506003317
N	3.08904913858471	0.83251698002760	0.03207960202881
C	2.66274998181860	1.97843556886141	-0.59302057951498
C	3.58310579421884	3.09933800677295	-0.12476813764253
C	4.83052353139521	2.35772957841920	0.34791755484412
H	3.75395917614067	3.81647262625653	-0.93282124679148
H	3.08858846232452	3.63626375513443	0.69823504416191
H	3.93490406737018	1.18314245110748	1.92292672517788
H	5.49110081016107	2.16846325538363	-0.50457174567954
H	5.40897552634458	2.90226491804454	1.09909375419351
O	1.73063997808488	2.05071553006557	-1.36999541887019
O	8.43074568810867	1.10848567459317	0.56001649261729
C	4.76443525924681	-0.54719954969402	-1.66950560693051
H	5.93951219935790	-1.76614240749322	-0.35924354856965
C	3.36752109677898	-1.13155030231750	-1.46833550806726
H	4.68660215725030	0.51344357846564	-1.92767722410857
H	5.24504770872806	-1.03299046577239	-2.52757647656305
C	2.56687380939041	-0.46270959903010	-0.32107594627864
H	2.81764776161245	-1.00363650216402	-2.40862152967712
H	3.42965705855951	-2.21424531030443	-1.29043567001750
H	1.52829546278953	-0.31122471682092	-0.63147565739376
H	2.54961196587569	-1.09648664041966	0.57387918386873
H	5.97143761064262	0.39944458839579	3.67971535615767
H	7.62613869613626	0.87304566342087	3.23548997811984
H	6.26554333661155	1.86420539551965	2.72092588624918

7.2 Diastereomer 2 (R,S,S,S)

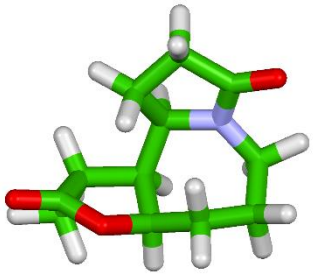

C	6.33373327977449	0.91997177226759	1.65124941980949
C	5.05571879055492	0.37600950697452	1.00567309910812
C	5.61774885566601	-0.39463148273240	-0.20781486682760
C	4.03932776133969	1.48495858777337	0.70762381604112
H	4.56674422696754	-0.34105235474765	1.67454809227740
C	7.29464993039178	1.04597904921777	0.47146477444434
H	6.19212094931027	1.91877171171915	2.07938288572509
C	6.93717725308739	0.01039797970938	2.72282752251365
O	6.83314371254331	0.29687827517946	-0.56526460311207
N	2.91577600412596	1.03070628250629	-0.10477387804330
C	2.43656064333081	1.98372247399856	-0.97019801655813
C	3.25406899852008	3.24718173670725	-0.72370237603694
C	4.52655703842372	2.72535128498476	-0.06223844047560
H	3.41100847508936	3.79025945987696	-1.66045275414516
H	2.68332238178479	3.90524762101040	-0.05193931444070
H	3.66386220291901	1.81509673114646	1.69551858657514
H	5.24791227112986	2.42736470276543	-0.83092919070334
H	5.01910024199237	3.45297663085260	0.58995726614324
O	1.53559854876179	1.81959265400267	-1.76904431627437
O	8.31907478472748	1.66501232258089	0.42011160836172
C	4.74386879349716	-0.54742266520531	-1.43751608536402
H	5.90984952558108	-1.39933941603759	0.13721547052226
C	3.37824625475261	-1.17050436749313	-1.15780566920168
H	4.61602686250091	0.43149432490316	-1.91207025162550
H	5.28664398094582	-1.16436181825335	-2.16433033155487
C	2.50306993601623	-0.34701820564709	-0.18073827802682
H	2.85411769318441	-1.26162188542853	-2.11613094639617
H	3.49681959468696	-2.19140459441911	-0.76932957811247
H	1.46119988023904	-0.35184005077361	-0.51702103049614
H	2.52183029923366	-0.77819987898836	0.82758062574264
H	7.10881171225269	-1.00365107008306	2.34048212252333
H	7.90002564210373	0.40743287164250	3.06161382618908
H	6.26671347456510	-0.06153819001000	3.58734081141826

7.3 Diastereomer 3 (R,S,R,R)

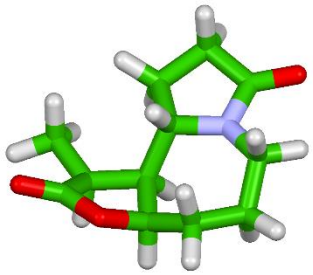

C	6.99596866054547	0.18473494062719	0.97035868516563
C	5.56601166064629	0.00002702864669	0.39689447394909
C	5.88521439935839	-1.13068026126584	-0.61246037117128
C	4.85008864004192	1.24151906942496	-0.17468533885531
H	4.89702936729551	-0.39173258426574	1.17288822519802
C	7.88664919756606	-0.06305920027615	-0.23796123025897
H	7.15250271465010	-0.71171808103857	1.59589079245331
C	7.45684716015641	1.37709507109448	1.78796889510146
O	7.20819690265149	-0.84169410398027	-1.11433121195936
N	3.43830464162788	0.98517985925955	-0.48477240865276
C	2.57778890316925	1.98226491645857	-0.06015366669224
C	3.40696241371520	3.05136931675687	0.61595565068476
C	4.74888677342565	2.38725447438002	0.85935066501763
H	3.47817183100754	3.89108122223677	-0.09032488751966
H	2.91090781413425	3.42694347102214	1.51582055433897
H	5.37778752714230	1.58461740108505	-1.08315086791382
H	5.58914819156798	3.07791936024153	0.78420083432892
H	4.76605862699725	1.95718700359520	1.86583337679662
O	1.38050968266835	2.00768056832715	-0.26409632624119
O	9.00480270936228	0.32282630591614	-0.43321601843917
C	4.99060013835301	-1.36525780239940	-1.80912428209235
H	5.95385538854075	-2.06567902820763	-0.03171608875866
C	3.50366945431667	-1.32314475402022	-1.48512391045751
H	5.22225934910319	-0.60470908962248	-2.56644009037547
H	5.27438547603108	-2.32826663634967	-2.25172858118581
C	2.95004065290786	0.08812209722643	-1.51270313576721
H	2.95194836587658	-1.90266222776227	-2.23569432512931
H	3.29448832709629	-1.80016446212867	-0.51614756408108
H	3.16316619011431	0.52513612582187	-2.50617453873523
H	1.86060369365318	0.08719548446528	-1.40118759349867
H	6.84684438600145	1.52414029375140	2.68347103208002
H	8.49048335072560	1.19862779004194	2.10254307381223
H	7.46085740955045	2.30206643093768	1.20581617885841

7.4 Diastereomer 4 (R,S,R,S)

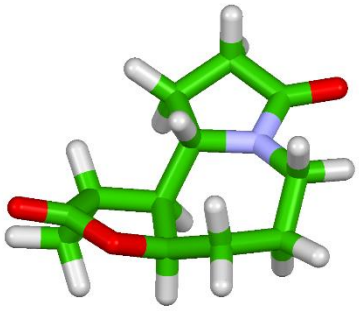

C	6.87720337181629	1.14606643060134	0.62975205330785
C	5.51109068131717	0.54049436671551	0.26609821974384
C	5.93922585311240	-0.70812320707291	-0.53776853202700
C	4.57987196086932	1.54663377203471	-0.42896754893866
H	4.97713362151057	0.21674375828121	1.16806072466893
C	7.81283340279686	0.64014593718810	-0.46109774683195
H	6.88453241129481	2.23871397145157	0.57496539306840
C	7.39937559842444	0.73131162744224	2.00593580081399
O	7.22348135602680	-0.39398013133290	-1.11031721872050
N	3.20543863486470	1.07448977217091	-0.56635509424622
C	2.25005211796084	2.00839892881544	-0.20991863703422
C	2.97473907997888	3.26308290507171	0.23895018391966
C	4.41551818110367	2.82294512870152	0.43196487812288
H	2.86546763223911	3.99837793054632	-0.57145867937815
H	2.50257780727977	3.69160861732464	1.12814979000666
H	4.99178670156068	1.80180964868120	-1.42247698453015
H	5.14607926747449	3.59066182128075	0.16244450842739
H	4.58736275182890	2.56477577580889	1.48438882279550
O	1.04929377668513	1.85527694224949	-0.30668706161667
O	8.91103441345363	1.03831621479190	-0.73005593591910
C	5.03617126579201	-1.20819807430745	-1.64515281981743
H	6.10197580163781	-1.52632663448828	0.18106558053130
C	3.57197706076586	-1.32268255336742	-1.23043795634938
H	5.12646661204886	-0.52968734804785	-2.50389111242785
H	5.42554140230259	-2.17614823454733	-1.98273933190582
C	2.79865600773307	-0.02820489035264	-1.41243829138455
H	3.07929296906666	-2.08070176007738	-1.85192694590297
H	3.48479028812928	-1.67537266040241	-0.19232076793038
H	2.87942704720743	0.27900269653415	-2.47191777954050
H	1.73188094049203	-0.17484505765586	-1.21136704504439
H	6.76074626791631	1.14107319206820	2.79716325676026
H	7.41667475492768	-0.36032763053411	2.11430230773935
H	8.41939096038197	1.10229874442674	2.15534396963987

7.5 Diastereomer 5 (R,R,S,R)

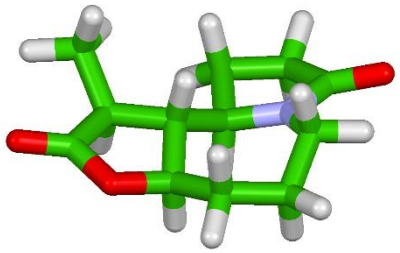

C	6.99696095750427	0.62816085012457	0.89520389654314
C	5.77892857491842	0.51219331390475	-0.02733608886141
C	5.78875857927890	-0.98981386826946	-0.34136264369759
C	4.43989087941946	0.96928841142115	0.53263941498196
H	5.99247358843568	1.07446030137224	-0.94937022637020
C	7.91283935912187	-0.47788449529412	0.36565071316656
H	6.70367681409835	0.30307539994958	1.90880894044824
C	7.72315231359951	1.95966299288156	0.98095157161807
O	7.17787496199181	-1.36118563002293	-0.35788325873380
N	3.40106697413767	1.11674517759728	-0.48645843566733
C	2.47342520196952	2.08309726629448	-0.16530994148293
C	2.92638422157402	2.71506804049301	1.14492956311575
C	4.39924771817599	2.33656690134403	1.22430203148076
H	2.72093105115442	3.78946418578282	1.14454065079286
H	2.34465778033871	2.26610340388638	1.96316265609148
H	4.12380713760562	0.20707821604594	1.27221978412662
H	4.99895345059514	3.05033585787311	0.64594864984132
H	4.80076625348676	2.29623431372711	2.24159081521586
O	1.48438882626721	2.35853731889012	-0.81532823521390
O	9.09416638741484	-0.59439499585929	0.52643553522659
C	5.11853887348394	-1.42806470808004	-1.62116637602306
H	5.31876509984560	-1.52044167464714	0.50568069377315
C	3.62524521982558	-1.11038304695835	-1.64959195959636
H	5.61988911435664	-0.93937474592717	-2.46921514578088
H	5.27691739670827	-2.50720726898938	-1.74039138229200
C	3.28954764531335	0.37484586446850	-1.72606364413599
H	3.19172718720495	-1.58736037983330	-2.53798345287839
H	3.11653258055891	-1.56379993300970	-0.78663019307506
H	3.92084534230653	0.84171923580737	-2.50163354500278
H	2.25259825671518	0.51811588050193	-2.05002745620473
H	7.14489666739087	2.71042043929334	1.52568839204844
H	8.68187134440845	1.82081759930840	1.49202326913461
H	7.93460424079359	2.35005977592321	-0.02180459258900

7.6 Diastereomer 6 (R,R,S,S)

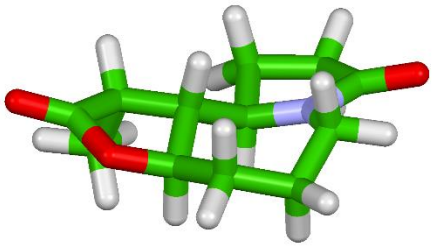

C	7.24277414576186	1.28251545291282	0.29402827695891
C	5.89538033746399	0.87731804468494	-0.31968538260193
C	6.04613604001177	-0.64654313786215	-0.36422704638631
C	4.62675041617268	1.36912412859130	0.35852930643777
H	5.88427729699922	1.24573202489651	-1.35649225332260
C	8.17638330538899	0.23151338912124	-0.30538917309609
H	7.57048303234356	2.27227168519295	-0.03923372467165
C	7.35495701588046	1.20388218757383	1.82007291853612
O	7.43983595408077	-0.85886985995762	-0.65832619841758
N	3.42600665409621	1.21014665404553	-0.46557288829981
C	2.50001386941139	2.21042412812187	-0.26692786225220
C	3.10700192194442	3.19259921607553	0.72426716878621
C	4.59333235850672	2.87293475636065	0.67127334076097
H	2.84230142326228	4.22003561114523	0.45845770241128
H	2.68030570244953	2.98961109284219	1.71788045385325
H	4.50108340949964	0.80755462973425	1.30266900026524
H	5.06797898824862	3.41702087005587	-0.15615595142292
H	5.13163851544685	3.12359225803788	1.58906881423009
O	1.40581812007825	2.27303605093185	-0.79211940298705
O	9.36633010352428	0.27842502498393	-0.42837783526483
C	5.18962946231622	-1.39564189437182	-1.35504065536385
H	5.85336207444929	-1.05122895594829	0.64403584187313
C	3.69595561676850	-1.22224869540730	-1.09286479236357
H	5.43289402151956	-1.05051681453554	-2.37019297213006
H	5.46119328202594	-2.45784227508387	-1.30977336278956
C	3.14983956524402	0.15910444471814	-1.42636278285174
H	3.15245336148228	-1.94195293610526	-1.71692388095647
H	3.45287180187978	-1.48245464359205	-0.05225643947682
H	3.52647506107330	0.45469885438478	-2.42046495794859
H	2.05756896360606	0.13133810493789	-1.51501637873539
H	7.03517755631503	0.22891425678264	2.20624292636076
H	8.39938890587796	1.35020566678937	2.11650331323168
H	6.75477171687057	1.97448067994269	2.31228487763362

7.7 Diastereomer 7 (R,R,R,R)

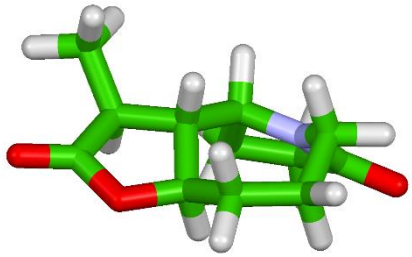

C	7.25421027964802	1.05901534779566	0.69796040077885
C	5.97450861573097	0.76014846719715	-0.07780004526838
C	5.65649528882479	-0.68957832758349	0.31604221371671
C	4.82919381478441	1.75467061757018	0.10467044322729
H	6.24079837096237	0.74560357337792	-1.14494017741033
C	7.89155614945244	-0.31987424384679	0.82301387378667
H	6.99858089830618	1.33965705745610	1.73188194236042
C	8.18564513879765	2.10527032643049	0.11593339727754
O	6.93751068424814	-1.26984577685207	0.64144006063615
N	3.54626189423942	1.21536494553166	-0.32768313570990
C	2.48072590429788	1.63454013309260	0.43363014036940
C	3.04549197966200	2.54411794926377	1.51759441363551
C	4.52940364681034	2.19742469197651	1.54540879081148
H	2.87319886566173	3.58583977842680	1.20926274273938
H	2.51631715510109	2.39439540651505	2.46378866698141
H	5.07486823117437	2.64998571807791	-0.49710197883963
H	5.17456981686168	3.02242920618631	1.86468331174080
H	4.69933043448624	1.35795182750108	2.23159995050791
O	1.31831176868330	1.33683674324488	0.24285585748892
O	9.03563859826209	-0.58537872893983	1.06015837139138
C	5.01147973727671	-1.52467169698208	-0.77572747282512
H	5.03877709488147	-0.72058611686035	1.22745990368973
C	3.57493913729018	-1.13299224641300	-1.10597415664905
H	5.64177409482615	-1.44743299275037	-1.67373463983490
H	5.04213993915582	-2.57674225472537	-0.46519014147571
C	3.36493409098643	0.33916026062102	-1.46269200921161
H	3.22686556423009	-1.75170065303354	-1.94455206830713
H	2.91272946824017	-1.36288634661650	-0.25962897902131
H	4.03579026162843	0.65057765503763	-2.27579925263071
H	2.33355632721026	0.48261572071844	-1.80468338564239
H	7.72326258878123	3.09961830357694	0.12657781224572
H	9.11596965906748	2.14623002740786	0.69178205130309
H	8.44615450043044	1.86175562759745	-0.92169690186217

7.8 Diastereomer 8 (R,R,R,S)

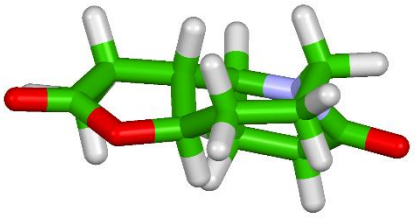

C	7.49627802253704	1.13124934601506	-0.27148171725046
C	6.02036433132381	0.79162763008446	-0.54548553387375
C	5.80756184200016	-0.58746457431135	0.10838577162347
C	4.92214712321625	1.81477225084967	-0.24064414392970
H	5.96669623753878	0.61584323816646	-1.62761060310483
C	8.10687663428524	-0.23572926121549	0.03807477025638
H	7.97589656621864	1.49451994547027	-1.18816595177403
C	7.87863285493552	2.09293704943232	0.85377241659262
O	7.12577908063651	-1.13981340947008	0.27788102219970
N	3.59558357526935	1.22993072080646	-0.43778736937174
C	2.64020689962544	1.69456329557538	0.43500957366502
C	3.32675078568612	2.69829599310008	1.34545539885336
C	4.80840762052872	2.38180649614780	1.18715656514976
H	3.08128102273690	3.70835937986127	0.98599777158884
H	2.94583754626358	2.61641258218667	2.36777702474478
H	5.06225843883380	2.65675503511278	-0.94398361160588
H	5.45163266815847	3.24998487807275	1.33786107137844
H	5.10513900473238	1.61686406502515	1.91475703959591
O	1.47153588866641	1.36027355844525	0.44157050085718
O	9.27091607308633	-0.50878815222933	0.12038767070140
C	4.99742646115648	-1.55877956479984	-0.73629393741364
H	5.36139380694827	-0.49259452952075	1.11046600834198
C	3.52806708708907	-1.19224302098775	-0.91281224386316
H	5.49024418280912	-1.62740241188519	-1.71750828808159
H	5.07477239247810	-2.55417170608303	-0.28112330682146
C	3.26381843137314	0.22472042734536	-1.42318999106123
H	3.06856779197399	-1.91005975940542	-1.60555791722344
H	2.99111910335290	-1.29860985661761	0.03950614030659
H	3.80920445681957	0.42445373690645	-2.35570385204048
H	2.19430542479101	0.33741523494007	-1.63240874026502
H	7.54456616938019	3.11323937414001	0.64286348427524
H	7.46719200520500	1.78608823265099	1.82043066470464
H	8.97048047034373	2.10412377619114	0.94443431284510

7.9 TS3.001

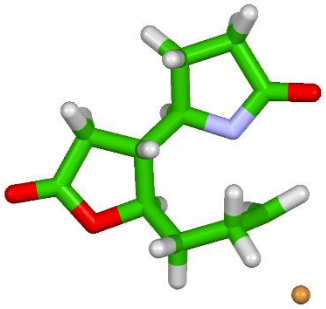

H	-1.73953627625559	-0.72384147077680	0.18045084418826
H	-0.49187588424680	0.34273172768910	-2.27099789036322
H	1.86465001850170	1.62660444633409	3.03404112701828
H	-2.73663391135614	0.61242470311498	0.98808668183799
Br	-3.79338131990409	-0.18837399900786	-1.43948008712275
C	-1.25089952082531	1.39748588449683	-0.52481872764632
C	-0.08393755264148	0.88950212030678	-1.39454207591199
O	4.30128594364118	-0.32861608716351	-1.63319118016217
O	-2.05302692320635	0.96556492779123	3.58168302709329
O	2.04447272848940	-0.25309307916289	-1.63714371821914
C	1.59569218488317	0.50676834353965	0.61633075537668
H	-0.87330750572318	2.08642369321563	0.25618333197078
H	-1.92387596420544	1.99914905459556	-1.16989593574400
H	0.47251638321140	1.76508983333273	-1.79594599918855
H	2.40852186787572	0.00648923385297	3.57207521210284
H	0.31216046106037	1.41449049978650	4.91510371466592
H	0.25616204266019	-0.36626728807810	4.76148935992197
H	0.48685718479064	-1.02348415230492	-0.49812523135789
C	-2.05945183006212	0.31926102986040	0.17725696234348
C	0.93432757585254	-0.02381707157754	-0.69019976454176
C	-0.90889534482023	0.66494839545166	3.20412268190687
C	3.26018897571415	-0.19225816494581	-1.02662212167784
N	-0.50011008234572	0.34434924732336	1.95860990521598
C	0.89891357940137	0.00498640302360	1.90616748975808
C	0.32599720264090	0.58237334338314	4.18162094503562
C	1.52507969338151	0.58347588650225	3.22153405857477
H	1.55928106943432	1.61893420349218	0.60592623205869
H	1.05331890463234	-1.11659645507051	1.90776883740325
H	3.81816489269886	0.73801079599355	0.86932724252951
H	3.21612504323100	-0.93649048453872	0.98785802491914
C	3.05611636349168	0.03938447954045	0.47374629801428

7.10 TS3.002

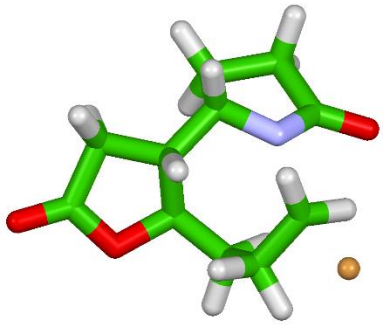

C	-6.50454095983724	1.08182691557463	-0.96918515156247
C	-5.16948185625417	0.88656985675111	-1.70563053603320
C	-7.49166505569635	0.29275573555038	-1.84593332357331
O	-6.94115370782547	0.12199527484470	-3.08461950535940
C	-5.63779015769264	0.82523217775855	-3.17509270742075
C	-4.00027884998776	1.86326225579355	-1.45830349071704
H	-4.79735106153938	-0.12696378778217	-1.44308288084834
C	-4.73825685116350	0.15749089094243	-4.22722552720377
H	-5.88171651731882	1.85115592799228	-3.53478201250269
O	-8.58873425450817	-0.13280802379161	-1.55589810590527
N	-2.94870317290834	1.55710817163674	-2.40342470008684
C	-4.30579472320204	3.39236751404524	-1.62750288923826
H	-3.67081048070978	1.69569146559180	-0.39294904627608
C	-2.97773933282013	3.92775485343400	-2.19052253594049
H	-4.63582851829160	3.87016776934997	-0.67958243636997
H	-5.11992307226043	3.54774822682229	-2.36853222121133
C	-2.34470619573796	2.66075675639309	-2.88814373813096
H	-2.29098893938651	4.26957310392910	-1.38298726295399
H	-3.08005933954321	4.76724434387783	-2.90840560097250
O	-1.43556239498370	2.73318063674494	-3.73041217223216
H	-5.41372378673727	-0.20253066101555	-5.03519513339687
C	-3.84002899079995	-1.02610807194410	-3.78113902814337
H	-4.09762494875086	0.94174377332554	-4.67246988020546
H	-3.58719915874886	-1.58945425980631	-4.70158556099051
H	-4.42108177602952	-1.73455246978264	-3.15422629248032
C	-2.52138474205793	-0.68730379535459	-3.09356269964063
H	-2.40990660038826	-0.73758849025451	-2.01003087959857
H	-1.74917833415091	-0.13578791412007	-3.63974394049800
Br	-1.36233185559421	-2.85863174799401	-3.29712801123113
H	-6.82177444546481	2.14936457951932	-0.96259067952393
H	-6.53326991961024	0.72216899196806	0.07749795024762

REFERENCES

(1) Pye, C. R.; Bertin, M. J.; Lokey, S.; Gerwick, W. H.; Linington, R. G. Retrospective Analysis of Natural Products Provides Insights for Future Discovery Trends. *PNAS* **2017**, *114* (22), 5601–5606.

(2) Whitesides, G. M. Complex Organic Synthesis: Structure, Properties, and/or Function? *Isr. J. Chem.* **2018**, *58* (1–2), 142–150.

(3) Baran, P. S. Natural Product Total Synthesis: As Exciting as Ever and Here To Stay. *J. Am. Chem. Soc.* **2018**, *140* (14), 4751–4755.

(4) Nicolaou, K. C.; Montagnon, T. *Molecules That Changed the World*, 1st editio.; WILEY-VCH Verlag GmbH, 2008.

(5) Nicolaou, K. C.; Snyder, S. A. Chasing Molecules That Were Never There: Misassigned Natural Products and the Role of Chemical Synthesis in Modern Structure Elucidation. *Angew. Chemie Int. Ed.* **2005**, *44* (7), 1012–1044.

(6) Newman, D. J.; Cragg, G. M. Natural Products as Sources of New Drugs from 1981 to 2014. *J. Nat. Prod.* **2016**, *79* (3), 629–661.

(7) Gaich, T.; Baran, P. S. Aiming for the Ideal Synthesis. *J. Org. Chem.* **2010**, *75* (14), 4657–4673.

(8) Trauner, D. The Chemist and the Architect. *Angew. Chemie Int. Ed.* **2018**, *57* (16), 4177–4191.

(9) Nicolaou, K. C.; Vourloumis, D.; Winssinger, N.; Baran, P. S. The Art and Science of Total Synthesis at the Dawn of the Twenty-First Century. *Angew. Chemie Int. Ed.* **2000**, *39* (1), 44–122.

(10) Sierra, M. A. (Miguel A.; Torre, M. C. de la. *Dead Ends and Detours : Direct Ways to Successful Total Synthesis*; Wiley-VCH, 2004.

(11) Sierra, M. A.; Torre, M. C. de la.; Cossio, F. P. *More Dead Ends and Detours : En Route to Successful Total Synthesis.*; Wiley, 2013.

(12) Dewick, P. M. *Medicinal Natural Products*, 3rd ed.; John Wiley & Sons, Ltd, 2009.

(13) Clayden, J.; Greeves, N.; Warren, S. G. *Organic Chemistry*, 2nd ed.; Oxford University Press, 2012.

(14) Moss, G. P.; Smith, P. A. S.; Tavernier, D. Glossary of Class Names of Organic Compounds and Reactivity Intermediates Based on Structure (IUPAC Recommendations 199). *PAC* **1995**, *67* (8), 1307.

(15) Dewick, P. M. *Medicinal Natural Products*; John Wiley & Sons, Ltd: Chichester, UK, 2009.

(16) Garraffo, H. M.; Jain, P.; Spande, T. F.; Daly, J. W.; Jones, T. H.; Smith, L. J.; Zottig, V. E. Structure of Alkaloid 275A, a Novel 1-Azabicyclo[5.3.0]Decane from a Dendrobatid Frog, Dendrobates Lehmanni: Synthesis of the Tetrahydrodiastereomers. *J. Nat. Prod.* **2001**, *64* (4), 421–427.

(17) Sastraruji, T.; Chaiyong, S.; Jatisatienr, A.; Pyne, S. G.; Ung, A. T.; Lie, W. Phytochemical Studies on Stemona Aphylla : Isolation of a New Stemofoline Alkaloid and Six New Stemofurans. *J. Nat. Prod.* **2011**, *74* (1),

60–64.

(18) Paudler, W. W.; Kerley, G. I.; McKay, J. The Alkaloids of Cephalotaxus Drupacea and Cephalotaxus Fortunei. *J. Org. Chem.* **1963**, *28* (9), 2194–2197.

(19) Murav'eva, V. I.; Ban'kovskii, A. I. Chemical Study of Alkaloids of Securinega Suffruticosa. *Dokl. Akad. Nauk SSSR* **1956**, *110*, 998–1000.

(20) Jacobs, W. A.; Craig, L. C. Aconite Alkaloids. IX. Isolation of Two New Alkaloids from Aconitum Heterophyllum, Heteratisine and Hetisine. *J. Biol. Chem.* **1942**, *143*, 605–609.

(21) Kam, T.-S.; Yoganathan, K.; Chuah, C.-H. Lundurines A, B and C, New Indole Alkaloids with a Novel Carbon Skeleton Containing a Cyclopropyl Moiety. *Tetrahedron Lett.* **1995**, *36* (5), 759–762.

(22) Baldwin, J. E. Rules for Ring Closure. *J. Chem. Soc. Chem. Commun.* **1976**, *0* (18), 734.

(23) Nakayama, Y.; Maeda, Y.; Hama, N.; Sato, T.; Chida, N. Total Synthesis of (–)-Stemoamide by Sequential Overman/Claisen Rearrangement. *Synthesis (Stuttg).* **2016**, *48* (11), 1647–1654.

(24) Nicolas Bogliotti; Peter I. Dalko, A.; Cossy, J. Free-Radical Approaches to Stemoamide and Analogues. *J. Org. Chem.* **2006**, *71* (52), 9528–9531.

(25) Kohno, Y.; Narasaka, K. Synthesis of (±)-Stemonamide by the Application of Oxidative Coupling Reactions of Stannyl Compounds with Silyl Enol Ethers. *Bull. Chem. Soc. Jpn.* **1996**, *69* (7), 2063–2070.

(26) Yoritate, M.; Takahashi, Y.; Tajima, H.; Ogihara, C.; Yokoyama, T.; Soda, Y.; Oishi, T.; Sato, T.; Chida, N. Unified Total Synthesis of Stemoamide-Type Alkaloids by Chemoselective Assembly of Five-Membered Building Blocks. *J. Am. Chem. Soc.* **2017**, *139* (50), 18386–18391.

(27) Martin, S. F.; Barr, K. J. Vinylogous Mannich Reactions. The Asymmetric Total Synthesis of (+)-Croomine. *J. Am. Chem. Soc.* **1996**, *118* (13), 3299–3300.

(28) Beesley, R. M.; Ingold, C. K.; Thorpe, J. F. CXIX.—The Formation and Stability of Spiro-Compounds. Part I. Spiro-Compounds from Cyclohexane. *J. Chem. Soc., Trans.* **1915**, *107* (0), 1080–1106.

(29) Lesma, G.; Sacchetti, A.; Silvani, A. Total Synthesis of 275A Lehmizidine Frog Skin Alkaloid (or of Its Enantiomer). *Tetrahedron: Asymmetry* **2010**, *21* (19), 2329–2333.

(30) Gouthami, P.; Chegondi, R.; Chandrasekhar, S. Formal Total Synthesis of (±)-Cephalotaxine and Congeners via Aryne Insertion Reaction. *Org. Lett.* **2016**, *18* (9), 2044–2046.

(31) Yasuda, S.; Yamada, T.; Hanaoka, M. A Novel and Stereoselective Synthesis of (±)-Cephalotaxine and Its Analogue. *Tetrahedron Lett.* **1986**, *27* (18), 2023–2026.

(32) Ozturk, T.; Ertas, E.; Mert, O. Use of Lawesson's Reagent in Organic Syntheses. *Chem. Rev.* **2007**, *107* (11), 5210–5278.

(33) Khim, S.-K.; Schultz, A. G. Synthesis of (−)-9,10-*Epi*-Stemoamide. **2004**, *69* (22), 7734–7736.

(34) Maryanoff, B. E.; Han-Cheng, Z.; Judith, H. C.; Turchi, I. J.; Maryanoff, C. A. Cyclizations of *N*-Acyliminium Ions. *Chem. Rev.* **2004**, *104* (3), 1431–1628.

(35) Liu, H.; Yu, J.; Li, X.; Yan, R.; Xiao, J.-C.; Hong, R. Stereoselectivity in N-Iminium Ion Cyclization: Development of an Efficient Synthesis of (±)-Cephalotaxine. *Org. Lett.* **2015**, *17* (18), 4444–4447.

(36) Srinivas, K.; Singh, N.; Das, D.; Koley, D. Organocatalytic, Asymmetric Synthesis of Aza-Quaternary Center of Izidine Alkaloids: Synthesis of (−)-Tricyclic Skeleton of Cylindricine. *Org. Lett.* **2017**, *19* (1), 274–277.

(37) Williams, D. R.; Fromhold, M. G.; Earley, J. D. Total Synthesis of (−)-Stemospironine. *Org. Lett.* **2001**, *3* (17), 2721–2724.

(38) Gyoonhee, H.; Matthew G., L.; James J., F.; Kim M., W.; Weinreb, S. M. Total Syntheses of the Securinega Alkaloids (+)-14,15-Dihydronorsecurinine, (−)-Norsecurinine, and Phyllanthine. *J. Org. Chem.* **2000**, *65* (20), 6293–6306.

(39) Weinreb, S. M. Total Synthesis of the Securinega Alkaloids. *Nat. Prod. Rep.* **2009**, *26* (6), 758.

(40) Corey, E. J.; Cheng, X.-M. *The Logic of Chemical Synthesis*; John Wiley, 1989.

(41) Šunjić, V.; Petrović Peroković, V. Rearrangements - Synthetic Reactions "Not Liable" to Retrosynthetic Analysis. In *Organic Chemistry from Retrosynthesis to Asymmetric Synthesis*; Springer International Publishing: Cham, 2016; pp 173–188.

(42) Yibin, Z.; Aubé, J. An Expeditious Total Synthesis of (±)-Stenine. *J. Am. Chem. Soc.* **2005**, *127* (45), 15712–15713.

(43) Kim, C.; Kang, S.; Rhee, Y. H. Synthesis of the Tricyclic Core in Stemonamine Alkaloids via One-Pot Gold(I)-Catalyzed Cyclization and Schmidt Rearrangement: Formal Synthesis of (±)-Stemonamine. *J. Org. Chem.* **2014**, *79* (22), 11119–11124.

(44) Chen, Z.-H.; Tu, Y.-Q.; Zhang, S.-Y.; Zhang, F.-M. Development of the Intramolecular Prins Cyclization/Schmidt Reaction for the Construction of the Azaspiro[4,4]Nonane: Application to the Formal Synthesis of (±)-Stemonamine. *Org. Lett.* **2011**, *13* (4), 724–727.

(45) Kirillova, M. S.; Muratore, M. E.; Dorel, R.; Echavarren, A. M. Concise Total Synthesis of Lundurines A–C Enabled by Gold Catalysis and a Homodienyl Retro-Ene/Ene Isomerization. *J. Am. Chem. Soc.* **2016**, *138* (11), 3671–3674.

(46) Wong, H. N. C.; Hon, M. Y.; Tse, C. W.; Yip, Y. C.; Tanko, J.; Hudlicky, T. Use of Cyclopropanes and Their Derivatives in Organic Synthesis. *Chem. Rev.* **1989**, *89* (1), 165–198.

(47) Peter A., J.; Lee, K. Total Syntheses of (±)- and (−)-Stemoamide. *J. Am. Chem. Soc.* **2000**, *122* (18), 4295–4303.

(48) Brüggemann, M.; McDonald, A. I.; Overman, L. E.; Rosen, M. D.; Schwink, L.; Scottd, J. P. Total Synthesis of (±)-Didehydrostemofoline (Asparagamine A) and (±)-Isodidehydrostemofoline. *J. Am. Chem. Soc.* **2003**, *125* (50), 15284–15285.

(49) Tsuyoshi Taniguchi, Atsuko Ishita, Masahiko Uchiyama, Osamu Tamura, Osamu Muraoka, Genzoh Tanabe, H. I. 7-Endo Selective Aryl Radical Cyclization onto Enamides Leading to 3-Benzazepines: Concise Construction of a Cephalotaxine Skeleton. *J. Org. Chem.* **2004**, *70*, 1922–1925.

(50) Taniguchi, T.; Ishibashi, H. Short Synthesis of (−)-Cephalotaxine Using a Radical Cascade. *Org. Lett.* **2008**, *10* (18), 4129–4131.

(51) Horning, B. D.; MacMillan, D. W. C. Nine-Step Enantioselective Total Synthesis of (−)-Vincorine. *J. Am. Chem. Soc.* **2013**, *135* (17), 6442–6445.

(52) Alexander Deiters; Stephen F. Martin. Synthesis of Oxygen- and Nitrogen-Containing Heterocycles by Ring-Closing Metathesis. *Chem. Rev.* **2004**, *104* (5), 2199–2238.

(53) Wipf, P.; Spencer, S. R. Asymmetric Total Syntheses of Tuberostemonine, Didehydrotuberostemonine, and 13-Epituberostemonine. *J. Am. Chem. Soc.* **2005**, *127* (1), 225–235.

(54) Peter, W.; Stacey R., R.; Hidenori, T. Total Synthesis of (−)-Tuberostemonine. *J. Am. Chem. Soc.* **2002**, *124* (50), 14848–14849.

(55) Heravi, M. M.; Vavsari, V. F. Recent Applications of Intramolecular Diels–Alder Reaction in Total Synthesis of Natural Products. *RSC Adv.* **2015**, *5* (63), 50890–50912.

(56) Kevin M. Peese; David Y. Gin. Efficient Synthetic Access to the Hetisine C20-Diterpenoid Alkaloids. A Concise Synthesis of Nominine via Oxidoisoquinolinium-1,3-Dipolar and Dienamine-Diels−Alder Cycloadditions. *J. Am. Chem. Soc.* **2006**, *128* (27), 8734–8735.

(57) Zhang, Z.-W.; Zhang, X.-F.; Feng, J.; Yang, Y.-H.; Wang, C.-C.; Feng, J.-C.; Liu, S. Formal Synthesis of Cephalotaxine. *J. Org. Chem.* **2013**, *78*, 786–790.

(58) Li, W.-D. Z.; Wang, Y.-Q. A Novel and Efficient Total Synthesis of Cephalotaxine. *Org. Lett.* **2003**, *5* (16), 2931–2934.

(59) Pilli, R. A.; Rosso, G. B.; De Oliveira, M. D. C. F. The Stemona Alkaloids. *Alkaloids Chem. Biol.* **2005**, *62*, 77–173.

(60) Greger, H. Structural Relationships, Distribution and Biological Activities of Stemona Alkaloids. *Planta Med.* **2006**, *72* (2), 99–113.

(61) Pilli, R. A.; Rosso, G. B.; Da, M.; Ferreira De Oliveira, C. The Chemistry of Stemona Alkaloids: An Update. *Nat. Prod. Rep.* **2010**, *17*, 1908–1937.

(62) Pilli, R. A.; Ferreira de Oliveira, M. da C. Recent Progress in the Chemistry of the Stemona Alkaloids. *Nat. Prod. Rep.* **2000**, *17* (1), 117–127.

(63) Bates, R. W.; Sridhar, S. Synthesis of the Stenine Ring System from Pyrrole. *J. Org. Chem.* **2011**, *76* (12), 5026–5035.

(64) Nalivela, K. S. Towards the Total Synthesis of the Stemona Alkaloids Oxyprotostemonine and 1-Hydroxyprotostemonine, University of Wollongong, 2010.

(65) Kemppainen, E. K.; Sahoo, G.; Piisola, A.; Hamza, A.; Kótai, B.; Pápai, I.; Pihko, P. M. Mukaiyama-Michael Reactions with Trans-2,5-Diarylpyrrolidine Catalysts: Enantioselectivity Arises from Attractive Noncovalent Interactions, Not from Steric Hindrance. *Chem. - A Eur. J.*

2014, *20* (20), 5983–5993.

(66) Kemppainen, E. K.; Sahoo, G.; Valkonen, A.; Pihko, P. M. Mukaiyama–Michael Reactions with Acrolein and Methacrolein: A Catalytic Enantioselective Synthesis of the C17–C28 Fragment of Pectenotoxins. *Org. Lett.* **2012**, *14* (4), 1086–1089.

(67) Li, Z.; Zhang, L.; Qiu, F. G. A Concise Stereocontrolled Total Synthesis of (±)-Stemoamide. *Asian J. Org. Chem.* **2014**, *3* (1), 52–54.

(68) Li-Gen, L.; Qiong-Xing, Z.; Tin-Yan, C.; Chun-Ping, T.; Chang-Qiang, K.; Ge, L.; Yang, Y. Stemoninines from the Roots of Stemona Tuberosa. *J. Nat. Prod.* **2006**, *69* (7), 1051–1054.

(69) Huang, S.-Z.; Kong, F.-D.; Ma, Q.-Y.; Guo, Z.-K.; Zhou, L.-M.; Wang, Q.; Dai, H.-F.; Zhao, Y.-X. Nematicidal Stemona Alkaloids from Stemona Parviflora. *J. Nat. Prod.* **2016**, *79* (10), 2599–2605.

(70) Lin, W.-H.; Ye, Y.; Xu, R.-S. Chemical Studies on New Stemona Alkaloids, IV. Studies on New Alkaloids from Stemona Tuberosa. *J. Nat. Prod.* **1992**, *55* (5), 571–576.

(71) Hitotsuyanagi, Y.; Fukaya, H.; Takeda, E.; Matsuda, S.; Saishu, Y.; Zhu, S.; Komatsu, K.; Takeya, K. Structures of Stemona-Amine B and Stemona-Lactams M–R. *Tetrahedron* **2013**, *69* (30), 6297–6304.

(72) Piisola, A. Challenges in the Stereoselective Synthesis of Allylic Alcohols, University of Jyväskylä: Jyväskylä, 2015.

(73) Sartori, A.; Curti, C.; Battistini, L.; Burreddu, P.; Rassu, G.; Pelosi, G.; Casiraghi, G.; Zanardi, F. Direct-Type Vinylogous Mukaiyama–Michael Addition Reactions Involving Pyrrolinone Donors. *Tetrahedron* **2008**, *64* (51), 11697–11705.

(74) Suga, H.; Takemoto, H.; Kakehi, A. Lewis Acid-Catalyzed Michael Addition Reactions of *N*-Boc-2-Silyloxypyrroles to 3-Acryloyl-2-Oxazolidinone. *Heterocycles* **2007**, *71* (2), 361.

(75) Marcos, I.; Redero, E.; Bermejo, F. Synthetic Studies towards (+)-Dihydroampullicin. Michael Addition of *N*-Boc-2-(*Tert*-Butyldimethylsiloxy)-3-Methyl-Pyrrole to α-Methylene Lactones. *Tetrahedron Lett.* **2000**, *41* (44), 8451–8455.

(76) Curti, C.; Ranieri, B.; Battistini, L.; Rassu, G.; Zambrano, V.; Pelosi, G.; Casiraghi, G.; Zanardi, F. Catalytic, Asymmetric Vinylogous Mukaiyama Aldol Reactions of Pyrrole- and Furan-Based Dienoxy Silanes: How the Diene Heteroatom Impacts Stereocontrol. *Adv. Synth. Catal.* **2010**, *352* (11–12), 2011–2022.

(77) Näsman, J. H. 3-METHYL-2(5H)-FURANONE. *Org. Synth.* **1990**, *68*, 162.

(78) Colomer, I.; Chamberlain, A. E. R.; Haughey, M. B.; Donohoe, T. J. Hexafluoroisopropanol as a Highly Versatile Solvent. *Nat. Rev. Chem.* **2017**, *1* (11), 0088.

(79) Liu, Y.-L.; Shi, T.-D.; Zhou, F.; Zhao, X.-L.; Wang, X.; Zhou, J. Organocatalytic Asymmetric Strecker Reaction of Di- and Trifluoromethyl Ketoimines. Remarkable Fluorine Effect. *Org. Lett.* **2011**, *13* (15), 3826–3829.

(80) Motiwala, H. F.; Fehl, C.; Li, S.-W.; Hirt, E.; Porubsky, P.; Aubé, J. Overcoming Product Inhibition in Catalysis of the Intramolecular Schmidt Reaction. *J. Am. Chem. Soc.* **2013**, *135* (24), 9000–9009.

(81) Unaleroglu, C.; Yazici, A. Gadolinium Triflate Catalyzed Alkylation of Pyrroles: Efficient Synthesis of 3-Oxo-2,3-Dihydro-1*H*-Pyrrolizine Derivatives. *Tetrahedron* **2007**, *63* (25), 5608–5613.

(82) Feofanov, M.; Anokhin, M.; Averin, A.; Beletskaya, I. The Friedel–Crafts Reaction of Indoles with Michael Acceptors Catalyzed by Magnesium and Calcium Salts. *Synthesis (Stuttg).* **2017**, *49* (22), 5045–5058.

(83) Fleming, I. *Molecular Orbitals and Organic Chemical Reactions*, Student ed.; WILEY-VCH Verlag, 2009.

(84) Gossauer, A.; Blacha-Puller, M. Synthesen von Gallenfarbstoffen, XIII. Darstellung von 3,4-Dihydro-5(1*H*)-Pyrromethenonen Aus 5(1*H*)-Pyrromethenonen Sowie 5(2*H*)-Dipyrrylmethanonen. *Liebigs Ann. der Chemie* **1981**, *1981* (8), 1492–1504.

(85) Yoshida, Y.; Sakakura, Y.; Aso, N.; Okada, S.; Tanabe, Y. Practical and Efficient Methods for Sulfonylation of Alcohols Using Ts(Ms)Cl/Et_3N and Catalytic $Me_3H{\cdot}HCl$ as Combined Base: Promising Alternative to Traditional Pyridine. *Tetrahedron* **1999**, *55* (8), 2183–2192.

(86) Staffan Torssell; Emil Wanngren, A.; Somfai, P. Total Synthesis of (−)-Stemoamide. *J. Org. Chem.* **2007**, *72* (11), 4246–4249.

(87) Kenichi, O.; Shoji, M.; Motohiro, A.; Ogura, K. Novel Synthesis of α-Trifluoromethylated α-Amino Acid Derivatives from γ-Hydroxy-α-Fluoro-α-Trifluoromethyl Carboxamides. *Org. Lett.* **2005**, *7* (4), 589–592.

(88) Gao, P.; Tong, Z.; Hu, H.; Xu, P.-F.; Liu, W.; Sun, C.; Zhai, H. Synthesis of (+)-9a-*Epi*-Stemoamide via DBU-Catalyzed Michael Addition of Nitroalkane. *Synlett* **2009**, *2009* (13), 2188–2190.

(89) Wu, A.; Cremer, D.; A. Auer, A.; Jürgen, G. Extension of the Karplus Relationship for NMR Spin−Spin Coupling Constants to Nonplanar Ring Systems: Pseudorotation of Cyclopentane. *J. Phys. Chem. A.* **2002**, *106* (4), 657–667.

(90) Neese, F. The ORCA Program System. *Wiley Interdiscip. Rev. Comput. Mol. Sci.* **2012**, *2* (1), 73–78.

(91) Alemán, C.; Maseras, F.; Lledós, A.; Duran, M.; Bertrán, J. Analysis of Solvent Effect on S_N2 Reactions by Different Theoretical Models. *J. Phys. Org. Chem.* **1989**, *2* (8), 611–622.

(92) Gandhi, V.; Plunkett, W.; Cortes, J. E. Omacetaxine: A Protein Translation Inhibitor for Treatment of Chronic Myelogenous Leukemia. *Clin. Cancer Res.* **2014**, *20* (7), 1735–1740.

(93) Gürel, G.; Blaha, G.; Moore, P. B.; Steitz, T. A. U2504 Determines the Species Specificity of the A-Site Cleft Antibiotics: The Structures of Tiamulin, Homoharringtonine, and Bruceantin Bound to the Ribosome. *J. Mol. Biol.* **2009**, *389* (1), 146–156.

(94) Robin, J.-P.; Dhal, R.; Dujardin, G.; Girodier, L.; Mevellec, L.; Poutot, S. The First Semi-Synthesis of Enantiopure Homoharringtonine via

Anhydrohomoharringtonine from a Preformed Chiral Acyl Moiety. *Tetrahedron Lett.* **1999**, *40* (15), 2931–2934.

(95) Hu, X.; Li, W.; Yuan, M.; Li, C.; Liu, S.; Jiang, C.; Wu, Y.; Cai, K.; Liu, Y. Homoharringtonine Production by Endophytic Fungus Isolated from Cephalotaxus Hainanensis Li. *World J. Microbiol. Biotechnol.* **2016**, *32* (7), 110.

(96) Garreau de Loubresse, N.; Prokhorova, I.; Holtkamp, W.; Rodnina, M. V.; Yusupova, G.; Yusupov, M. Structural Basis for the Inhibition of the Eukaryotic Ribosome. *Nature* **2014**, *513* (7519), 517–522.

(97) Cragg, G. M. L.; Kingston, D. G. I.; Newman, D. J. *Anticancer Agents from Natural Products*; CRC Press, 2012.

(98) Tuzina, P.; Somfai, P. Asymmetric Lewis Acid Mediated [1,2]-Rearrangement of Proline-Derived Ammonium Ylides. *Org. Lett.* **2009**, *11* (4), 919–921.

(99) Tietze, L. F.; Schirok, H.; Wöhrmann, M.; Schrader, K. Efficient Synthesis of Six-Membered Ring D Analogues of the Pentacyclic Alkaloid Cephalotaxine by Two Palladium-Catalyzed Reactions. *European J. Org. Chem.* **2000**, *2000* (13), 2433–2444.

(100) Gregorio, G. Di. *Asymmetric Lewis Acid Mediated [1,2]-Rearrangement Approach Towards the Formal Synthesis of Cephalotaxine*; 2016.

(101) Javier Ruiz; Nuria Sotomayor; Lete, E. Parham-Type Cycliacylation with Weinreb Amides. Application to the Synthesis of Fused Indolizinone Systems. **2003**, *5* (7), 1115–1117.

(102) Bélanger, G.; O'Brien, G.; Larouche-Gauthier, R. Asymmetric Total Synthesis of (+)-Virosine A via Sequential Nucleophilic Cyclizations onto an Activated Formamide. *Org. Lett.* **2012**, *77*, 3215–3221.

(103) Li, W.-D. Z.; Wang, X.-W. Novel Formal Synthesis of Cephalotaxine via a Facile Friedel−Crafts Cyclization. *Org. Lett.* **2007**, *9* (7), 1211–1214.

(104) Ahmed, M.; Naseer, M. M. Organolithium-Mediated Cyclization Reactions: A Practical Way to Access Hetero- and Carbocycles. *New J. Chem.* **2017**, *41* (16), 7824–7835.

(105) Kitagawa, O.; Hanano, T.; Hirata, T.; Inoue, T.; Taguchi, T. A Facile α-Iodination Reaction of Unsaturated Amides. *Tetrahedron Lett.* **1992**, *33* (10), 1299–1302.

(106) Robin, S.; Rousseau, G. Electrophilic Cyclization of Unsaturated Amides. *Pergamon Tetrahedron* **1998**, *54*, 13681–13736.

(107) Manning, C.; McClory, M. R.; McCullough, J. J. Sigmatropic Rearrangements of 1,1-Diarylindenes. Migratory Aptitudes of Aryl Migration in the Ground and Electronically Excited States. *J. Org. Chem.* **1981**, *46* (5), 919–930.

(108) O 'neal, W. G.; Roberts, W. P.; Ghosh, I.; Wang, H.; Jacobi, P. A. Studies in Chlorin Chemistry. 3. A Practical Synthesis of C,D-Ring Symmetric Chlorins of Potential Utility in Photodynamic Therapy. *J. Org. Chem* **2006**, *71* (9), 3472–3480.

(109) Eagan, J. M.; Hori, M.; Wu, J.; Kanyiva, K. S.; Snyder, S. A. Synthesis and

Applications of Hajos-Parrish Ketone Isomers. *Angew. Chemie Int. Ed.* **2015**, *54* (27), 7842–7846.

(110) Wang, Z.; Li, Z.; Wang, K.; Wang, Q. Efficient and Chirally Specific Synthesis of Phenanthro-Indolizidine Alkaloids by Parham-Type Cycloacylation. *European J. Org. Chem.* **2010**, *2010* (2), 292–299.

(111) Moreau, A.; Lorion, M.; Couture, A.; Deniau, E.; Grandclaudon, P. A New Total Synthesis of Porritoxin. *J. Org. Chem.* **2006**, *71* (8), 3303–3305.

(112) Corey, E. J.; Cho, H.; Rücker, C.; Hua, D. H. Studies with Trialkylsilyltriflates: New Syntheses and Applications. *Tetrahedron Lett.* **1981**, *22* (36), 3455–3458.

(113) Gurjar, M. K.; Reddy, D. S. Carbohydrate Based Formal Synthesis of Stemoamide Using Ring-Closing Metathesis. *Tetrahedron Lett.* **2002**, *43* (2), 295–298.

(114) Semmelhack, M. F.; Chong, B. P.; Stauffer, R. D.; Rogerson, T. D.; Chong, A.; Jones, L. D. Total Synthesis of the Cephalotaxus Alkaloids. Problem in Nucleophilic Aromatic Substitution. *J. Am. Chem. Soc.* **1975**, *97* (9), 2507–2516.